

Section 1
Barbank

SOME STATIC AND DYNAMIC PROPERTIES
OF
ELECTRON DENSITIES

SOME STATIC AND DYNAMIC PROPERTIES
OF
ELECTRON DENSITIES

by

ANDREW DIETER BANDRAUK, S.M.

A Thesis

Submitted to the Faculty of Graduate Studies
in Partial Fulfilment of the Requirements

for the Degree
Doctor of Philosophy

McMaster University

December 1967

DOCTOR OF PHILOSOPHY (1968)
(Chemical Physics)

McMASTER UNIVERSITY
Hamilton, Ontario.

TITLE: Some Static and Dynamic Properties of
Electron Densities

AUTHOR: Andrew Dieter Bandrauk, B.Sc.
(Université de Montréal, Loyola College)
S.M. (Massachusetts Institute of Technology)

SUPERVISOR: Professor R. F. W. Bader

NUMBER OF PAGES: x, 359

SCOPE AND CONTENTS:

The electron density approach in conjunction with the Hellmann-Feynman theorem is used for a systematic analysis of binding characteristics of the two isoelectronic molecular groups: N_2 , CO, BF and LiF, BeO. Electron density distributions, forces and field gradients, corresponding to static properties of electron densities, have been calculated from Hartree-Fock wavefunctions for these molecules. Force constants have been computed from polynomial fits of the forces. Correlation of the forces and field gradients are made with the static electron distributions. Correlations of the force constants are made with dynamic distributions, called relaxation densities.

ABSTRACT

The electron density approach in conjunction with the Hellmann-Feynman theorem is used for a systematic analysis of binding characteristics of the two isoelectronic molecular series: N_2 , CO, BF and LiF, BeO. Electron density distributions, forces and field gradients corresponding to static properties of electron densities, have been calculated from Hartree-Fock wavefunctions (obtained from the work of other authors) for these molecules. Correlation of these static properties with binding characteristics are presented. Covalent and ionic characteristics are made evident by an analysis of the density distributions, density difference maps obtained by subtracting atomic from molecular distributions, and the forces exerted on nuclei by these distributions. A discussion of the field gradients, as related to quadrupole polarizations of the electron densities, is presented and the relevance of these polarizations to the interpretation of nuclear quadrupole coupling constants is indicated.

Dynamic properties, as reflected by the magnitude of force constants, are analyzed in terms of functionals of the one-electron density. Force constant expressions are derived from the Hellmann-Feynman theorem. Any relation

of force constants to field gradients is shown to be not unique as a result of cancellation of static and dynamic electronic contributions to the total force constant. The total electronic contribution is shown to arise from a relaxation of density after a displacement of a certain nucleus. Relaxation of density with respect to one nucleus but which remains localized on some other nucleus in a molecule is shown to be equivalent to a field gradient. Thus, such density is separated from other density and its contribution to the force constant is treated as a field gradient. All contributions are computed from polynomial fits of the corresponding forces calculated at a number of internuclear distances. Relaxation density maps for the remaining atomic and overlap densities centered on a specific nucleus are presented. These maps are calculated as the difference between densities of the extended and equilibrium configurations of a molecule. The relaxation densities are correlated to the magnitude of the corresponding electronic force constant components. Thus, for the first time, there is demonstrated the concrete relation between covalent and ionic characteristics of electron densities in molecules and their dynamic properties which result in the magnitude of force constants.

ACKNOWLEDGEMENTS

The following thesis was accomplished during a period of about 2.5 years. Frequent railway trips between Montreal and Hamilton at the beginning of this period have been beneficial in many respects. The most important event - not related to the thesis directly - resulted in a wonderful marriage to my present wife Maria. Her constant cheerfulness and optimism after long-awaited reappearances of the writer from dark corners of the halls of academe have been an inspirational influence. Her artistic talents have resulted in an embellishment of these pages via diagrams, for which I am indebted. Many of the trips were also for the intent purpose of mountain skiing, parallelling the "relaxation" of electron densities described in this thesis. I therefore recommend wholeheartedly this recreation to any aspiring theoretic chemist. Regardless of the fact that Dr. Bader did not overly share this enthusiasm with me, in this period of association with him, I have learned to acquire his enthusiasm for the "nature of things". I would not be exaggerating if I were to say that he has strained every mental fibre to keep the author 'honest', and rescued him from tendencies towards heterodox speculation. His many critical comments, helpful

suggestions, have influenced this work in almost every development, including the subject matter itself, which was originally proposed by him as a research problem. Association with two other graduate students, Messrs. William H. Henneker and Harry J. Preston, have also added to pleasant memories. I thank Harry Preston in particular for expanding the writer's athletic interests, aside from the minor discomfiture of a broken collar bone. Many of the force calculations would have taken much more time were it not for the generous assistance in programming given so freely by William Henneker. Finally, if it appears that a not sufficient number of people have been helping the author, let me add that chief overseer of the typed preparation of this manuscript has been Miss Sybille Schonfeld. Her sacrifice of sleep (and cigarettes!) have made possible the presentation of this work on schedule. I owe thanks to Mrs. Susan Hawley for help with the appendices. In the last analysis, a great measure of tribute must be paid to the Cade's and McLean's who have persevered in the calculation of Hartree-Fock functions which are now so freely available and are helping us develop a better understanding of the nature of things.

TABLE OF CONTENTS

	<u>Page</u>
ABSTRACT	
ACKNOWLEDGEMENTS	
TABLE OF CONTENTS	
LIST OF FIGURES	
LIST OF TABLES	
I GENERAL INTRODUCTION	1
1.1 The Importance of Charge Density	1
1.2 Approximations	9
1.3 Motivation and Plan	17
1.4 N ₂ , CO, BF	24
1.5 LiF, BeO	28
II ELECTRON DENSITIES	34
2.1 The Density Distribution - A Study in Molecular Topography	34
2.2 Charge Density - ρ diagrams	39
2.3 $\Delta\rho$ Maps	49
2.4 $\Delta\rho$ Profiles	63
2.5 Concluding Remarks	64
III THE ELECTROSTATIC INTERPRETATION OF ELECTRON DENSITIES	68
3.1 Introduction and Definition	68
3.2 Chemical Binding	83
3.3 Interpretation of N ₂ , CO, BF	89
3.4 Spectroscopic Considerations	105
3.5 Interpretation of LiF and BeO	117
3.6 A Comparison of Covalent and Ionic Binding	127

	<u>Page</u>
IV MORE STATICS: FIELD GRADIENTS AND QUADRUPOLE COUPLING CONSTANTS	143
4.1 Introduction	143
4.2 The Antishielding Model	151
4.3 Interpretation of Ionic Molecules	159
4.4 Inadequacies of the Antishielding Model	165
4.5 The Townes-Dailey Theory	176
4.6 Interpretation of Covalent Molecules	183
4.7 Quadrupole Polarizations	188
V DYNAMIC PROPERTIES: FORCE CONSTANTS	195
5.1 Introduction	195
5.2 The Hellmann-Feynman or Electrostatic Approach	201
5.3 Cancellation Theorem	212
5.4 Force Constant and Quadrupole Coupling Constant	216
5.5 Platt's Model	220
5.6 Method of Calculation	229
5.7 Interpretive Scheme	238
5.8 Shielding and Dipolar Interactions	246
5.9 Characteristics of Electronic Force Constants	250
5.10 Orbital Interpretation	273
5.11 Semiempirical Considerations	278
5.12 Force Constants and Models	285
VI SUMMARY AND CONCLUSION	292
APPENDIX 1 - HARTREE-FOCK THEORY	301
APPENDIX 2 - FIELD GRADIENTS	307
APPENDIX 3 - FORCES	328
APPENDIX 4 - FORCE DERIVATIVES AND DENSITIES	339
APPENDIX 5 - ERRORS IN FORCE CONSTANT CALCULATIONS	349
BIBLIOGRAPHY	353

LIST OF TABLES

TABLE NO.		<u>Page</u>
1.1	Molecular Data	25
1.2	Orbital Energies (LiF, BeO)	30
2.1	Characteristics of Total Density Distribution	43
2.2	Increase in Charge $\Delta\rho$ (positive)	53
3.1	Orbital Energies (CO, BF)	90
3.2	Forces in N ₂	90
3.3	Forces in CO	95
3.4	Forces in BF	96
3.5	Force Changes upon Ionization	110
3.6	Forces in LiF	118
3.7	Forces in BeO	119
3.8	Total Atomic, Overlap, Shielding Forces	134
4.1	Field Gradients in LiF	157
4.2	Field Gradients in BeO	158
4.3	Derivatives of Field Gradients in LiF and BeO	172a
4.4	Field Gradients in N ₂	180
4.5	Field Gradients in CO	181
4.6	Field Gradients in BF	182
4.7	Field Gradient Components	189
5.1	Force Constants from Forces	235
5.2	Force Constants from a) Total Force b) Total Atomic, Overlap and Shielding	237
5.3	Contribution of Electron Densities to K_A^e	241
5.4	Orbital Contributions k_{iA} to Force Constant	272

LIST OF FIGURES

FIGURE NO.		<u>Page</u>
1.1	Orbital Energies in N ₂ ,CO,BF	30
2.1	Electron Density ρ	42
2.2	Density Difference $\Delta\rho$	51
2.3	$\Delta\rho$ Map (Li ⁺ F ⁻)	57
2.4	$\Delta\rho$ Map (Be ⁺ O ⁻)	59
2.5	$\Delta\rho$ Profiles	62
3.1	Fixed Electron Coordinates	71
3.2	Scaled Electron Coordinates	71
3.3	3 σ Forces - N ₂ ,CO,BF	97
3.4	4 σ Forces - N ₂ ,CO,BF	98
3.5	5 σ Forces - N ₂ ,CO,BF	99
3.6	1 π Forces - N ₂ ,CO,BF	100
3.7	3 σ Forces - LiF,BeO,C ₂	120
3.8	4 σ Forces - LiF,BeO,C ₂	121
3.9	1 π Forces - LiF,BeO,C ₂	122
3.10	Overlap Densities - N ₂ ,BeO,LiF	132
5.1	Diatomic Potential Curve E(R)	202
5.2a	Fixed Electron Coordinate System	204
5.2b	Moving Electron Coordinate System	204
5.3	Atomic and Overlap Relaxations (N ₂ ,CO,BF)	259
5.4	Atomic and Overlap Relaxations (OC,FB)	260
5.5	Atomic and Overlap Relaxations (BeO,LiF)	261
5.6	Atomic and Overlap Relaxations (OBe,FLi)	262
5.7	Total Atomic and Overlap Relaxations	268

I. GENERAL INTRODUCTION

"Si les plats que je vous offre sont mal préparés, c'est moins la faute de mon cuisinier que celle de la 'chimie' qui est encore dans l'enfance."

Anatole France

1.1 The Importance of the Charge Density

Apart from the theory of the most simple phenomena - chemical binding in small molecules, vibration and rotation of the molecule, spin and symmetry properties, - the main body of current quantum chemistry consists in model building and semiempirical methods. The models of quantum chemistry are by and large a descriptive way to summarize empirical results, whereas the semiempirical quantum chemistry does not really permit the possibility of invalidation of models. Furthermore, operationally ill-defined or non-observable parameters have played a large role in empirical chemistry. As a result, the meaning and numerical values of such concepts as orbital, resonance structure, electronegativity, hybridization, ionic character, etc., are in continuous dispute.

Beyond these objections is a fundamental objection, for chemical purposes, to the usual quantum theoretical form of the many electron wavefunction, which is defined

in a $3N$ -dimensional coordinate space for an N -electron system. But most of these coordinates are non-observable inasmuch as empirical chemical structures are 3-dimensional entities in a classical space. Empirical chemistry has emphasized for a long time the outstanding role of this 3-dimensional electron charge density and its systematic use in a rigorous quantum mechanical theory is of invaluable importance in the explanation of chemical bonds. There are but a few rigorous theorems concerning such a 3-dimensional charge density, all of them of great importance.

The first theorem enables us to derive the electronic density from the rigorous quantum mechanical treatment, i.e. solution of the Schroedinger equation. This involves a reduction of the number of coordinates required for the wavefunction via the agency of the Dirac⁽¹⁾ density matrix method. Thus, one can rigorously replace the total electronic wavefunction of a system by a density function of two positions in space - 6 space coordinates - called the density matrix or second order density matrix, to conform with the nomenclature due to Coleman⁽²⁾. In practice, the many electron wavefunction is obtained as an antisymmetric product of one electron orbital functions. Introducing this total function by the density formalism, the individual orbitals' importance becomes submerged because the density matrix is invariant to an orthogonal linear transformation

among the orbitals. It is, therefore, invariant to changes in the one-electron potential which produces a new set of orbitals expressible in terms of the old ones by such a transformation or "hybridization". Dirac showed that all the information that we can get about the individual orbitals can be summed up by giving the density matrix to which they lead. This density matrix should therefore describe all that we know about the electrons in the system. Löwdin⁽³⁾ has generalized this matrix to a transition density matrix, also in 6-coordinates, between two electronic states. The 3-space transition density or first-order density has been formulated explicitly by Longuet-Higgins⁽⁴⁾, suggesting a useful concept for summarizing and systematizing spectroscopic data on atomic and molecular assemblies. In the case of atomic and molecular systems with fixed nuclei, the diagonal elements of the first-order density matrix (which is really the kernel of an integral operator⁽⁵⁾) characterizes the electronic charge distribution, and the full first-order matrix enables one to calculate the expectation value of any one-particle operator. For an electronic Hamiltonian of a many-body system one needs the second-order density matrix in general for energy expectation values, but one can calculate the total electronic energy of an eigenstate from an exact knowledge of the first-order density matrix alone, since from the virial theorem $E = -\langle T \rangle$, the kinetic

energy T can be evaluated as a one-electron operator. At present, there is no way of finding the exact density matrix without a knowledge of the exact wavefunction, but it has nevertheless been of some interest to study the conditions a physically realizable density matrix must satisfy in order to be obtainable from an antisymmetric (symmetric) wavefunction. This is known as the N -representability condition⁽²⁾ for the density matrix. The importance of this is that one could replace the energy-variation method for the wavefunction by an energy-variation method for the density matrix. The N -body problem could be then directly reduced to a 2-body problem, or even a 1-body problem via the virial theorem. The conditions for the first-order matrix, which gives the electron density, has been recently investigated by Smith⁽⁶⁾. It is rigorously true that the 3-space electron density is the value of the 6-space density function (pair density) on the diagonal of the matrix. It is also almost equal to the sum of the orbital densities in a system (Hartree-Fock approximation), so that the individual orbital densities do not appear in the result, emphasizing the fact that the individual orbitals have no real physical significance. Chirgwin⁽⁷⁾ has even pointed out that the orbitals need not be individually time-independent in order to give a stationary total state of the system. In short, it is always possible to represent the dynamical state of a

system by its density operator⁽⁸⁾, whether that state be completely or incompletely known. The specification of this operator is sufficient to determine all physically measurable quantities which the quantum theory is in a position to furnish.

Secondly, there is the Hellmann-Feynman theorem⁽⁹⁾ which considers the force field produced by the 3-space density ρ which Feynman calls "an electron cloud prevented from collapsing by obeying the Schroedinger equation" - It is the laws of quantum mechanics which are sufficient to make matter stable. This has been shown quite generally by Dyson⁽¹⁰⁾ - Thus in a quantum mechanical system, the forces on any nucleus, considered fixed, is just the classical electrostatic interaction exerted on the nucleus in question by the other nuclei and by the charge density distribution of all electrons. This theorem was first challenged by Coulson and Bell⁽¹¹⁾ but Berlin⁽¹²⁾ proved the objection to be based upon a misunderstanding and gave further proofs of the theorem and a clear interpretation closely related to the earlier and more empirical electrostatic approach of Fajans⁽¹³⁾. The forces acting on a nucleus of a molecule as a function of the electron density provide therefore a basis for the discussion of chemical binding in classical terms. This approach has been used in a series of papers by Bader et al⁽¹⁴⁾.

Thirdly, there is a theorem due to Kato⁽¹⁵⁾, giving the cusp condition of the electron density of a Born - Oppenheimer molecule. This is related to the physical importance of the essential self-adjointness of the Hamiltonian in an N-body Schroedinger equation. These fundamental results of Kato in this area have essentially established existence of solutions for a large class of Hamiltonians in atomic (molecular) and nuclear physics. The importance of this theorem in theories based on molecular charge densities are frequently overlooked. For instance, the consequence of the coalescence of two cusps as the internuclear distance approaches zero in the united atom treatment of derivatives of electronic energies has led to inconsistencies in different authors' works⁽¹⁶⁾. If cusp conditions are not satisfied, one may have to resum infinite series as done by Levine⁽¹⁷⁾ in the united atom treatment of H_2^+ . Similarly, the average energy approximation in the perturbation calculation of force constants leads to physically inadmissible wavefunctions, due to the strong singularity of the force operator, resulting in a quadratically non-integrable perturbed function. This type of divergence also occurs in perturbation calculations of spin-spin coupling constants⁽¹⁹⁾ and correlation energies⁽²⁰⁾, for which the energy is not an analytic function, and the importance of logarithmic terms in the wavefunction has been

discussed by Pekeris⁽²¹⁾. These problems are similar to the divergences which occur in field theories as discussed recently by Dirac⁽²²⁾. They can all be related to a fundamental theorem of functions⁽²³⁾ which states that the behaviour of a function in an analytic domain is determined by its singularities outside that domain. Whenever a Hamiltonian has singularities, for instance, whenever the electron-electron and electron-nuclear distances vanish, the theorem gives rise to Kato's results, namely that the cusp conditions at these Coulomb singularities defines the form of the wavefunction and hence the electron density⁽²⁴⁾.

Finally, there is a recent theorem due to Hohenberg and Kohn⁽²⁵⁾. Using the variational principle, the above authors have shown that any property of a system in an arbitrary potential is a unique functional of the 3-dimensional charge density ρ of the ground state. The most transparent example of a functional is the number of particles in a system which is itself a simple functional of ρ . Examples of functional approaches are the Thomas-Fermi theory and its refinements⁽²⁶⁾, which departs from the usual orbital approximation in that the electron density ρ plays a central role and is assumed to behave more like a classical fluid. These theories however, because they neglect the cusp conditions demanded by Kato's theorem will not reproduce Friedel oscillations⁽²⁷⁾ (set up by a localized perturbation such as

an impurity in an electron gas) or the radial oscillations (i.e. oscillations in the radial distribution function) of the electronic density in an atom which reflect the electronic shell structure. These are manifestations of quantum effects and therefore must be incorporated in any theory involving electron density. The major part of the complexities of the many-electron problem, as always, is associated with the determination of these functionals, valid for all molecules, expressing the expectation value of any observable in terms of the electronic charge density.

Nevertheless, it appears that the density and certain of its spatial properties, such as shell structure, cusp conditions, may be quantum mechanical counterparts of the so-called classical constants of motion in a generalized density theory. Stimulated by these possibilities, there has been an attempt by Primas⁽²⁸⁾ to approach quantum chemistry using the formalism of density functional representation, wherein a canonical transformation of the quantum mechanical equations of motion raises the charge density into the fundamental role of a canonical variable. This is really an attempt at axiomatization, which is the most effective way of systematizing and therefore elucidating a body of ideas. However limited in scope, axiomatization is a stage in maturation⁽²⁹⁾. This axiomatization stems from a philosophy based on the observations that only

quantities actually accessible to precision measurements are related to the observables of the charge density, the pair density, the current density and the spin. For problems of chemical interest, it is the ground state charge density of any molecule which contains all the information necessary for discussions on the basis of quantum mechanics. This strongly suggests that a systematic analysis of electronic distributions is a powerful tool for gaining insight into numerous bond situations and deserves wider use and development. It will be one of the objectives of this work to pursue such a line.

1.2 Approximations

To make practical use of quantum theory, approximations are still necessary, because so far there is, as mentioned before, no direct differential equation nor a variational equation for either the pair density or the charge density. In the final analysis, one must always have recourse to orbital models, a feature of the independent-particle model. Although orbitals have no substantial existence, and one can argue that they are merely mathematical conveniences, they have been and still are useful as conceptual units whose characteristics are worth examining. One must hope that at least they represent a "reculer pour mieux sauter" until more sophisticated models such as those based on geminals⁽³⁰⁾

have been demonstrated to be superior in scope and tractability. The importance of the independent particle model is that it provides separable physical properties so that correlations with chemical concepts may be made. A two-electron wavefunction is not separable due to the antisymmetry requirement. We would get much lucidity if we could avoid such nonseparable quantities completely. There are several possibilities to avoid nonseparable quantities; the use of orbitals, pair functions, etc. which give separable Hamiltonians. In the case of orbitals, we obtain the independent particle model. As can best be seen from one-particle Green's function theory⁽³¹⁾, a properly independent particle model may be well represented with strong interactions between bare particles. Due to the inclusion of a self-consistent field, the particles get "dressed" and in many cases the interaction between the dressed particles (quasi particles) is drastically reduced so that an independent quasi-particle model becomes a good approximation. An extension of the Bohr atomic theory to atoms and molecules assigns these particles to their proper orbitals, which are eigenfunctions of the separable Hamiltonian. For molecules, the molecular orbital has the advantage of being conceptually based on atomic theory, due to a correlation originally used by Hund and Mulliken⁽³²⁾ with the united atom. The relationship of this theory to Hartree's atomic calculations was

pointed out by Lennard-Jones⁽³³⁾ who first derived the Hartree-Fock equations. The resulting orbitals are eigenfunctions of one-electron operators, since the Hartree-Fock (H.F.) method makes the Hamiltonian separable into effective one-electron Hamiltonians (see Appendix 1). The fact that the most important perturbation theory corrections to the solution of this separable zeroth-order Hamiltonian can be written in terms of solutions of 2-particle equations has been recently emphasized by Sinanoglu⁽³⁴⁾. Valence bond functions do not have this advantage since the solution of the first order perturbation theory is not expressible in terms of pair correlations⁽³⁵⁾.

The Hartree-Fock equations are a result of the criteria of the best energy approximation. Orbitals can also be determined by the criteria of the best approximation of the wavefunction and the criteria of the disappearance of one-particle clusters⁽³⁶⁾. The three possibilities have been discussed by Kutzelnigg and Smith⁽³⁷⁾. The energy criterion has the essential advantage that it leads directly to the powerful numerical methods for the determination of the wavefunction. Furthermore, in the general Rayleigh-Schroedinger perturbation theory, when the unperturbed Hamiltonian and the perturbation are all Hermitian, knowledge of the wavefunction corrections to order n provides the energy corrections to order $(2n+1)$ and not to the apparent order $(n+1)$,

so that one has a relative measure of the sensitivity of the wavefunction and the energy⁽³⁸⁾. The third criterion, that there are no one-particle clusters, i.e. no corrections from single excitations to all orders, is for many theoretical questions very convenient. This criterion is a necessary condition for the optimal least square approximation of the wavefunction⁽³⁹⁾. This will not necessarily imply a good approximation of all expectation values. Nevertheless, the determinant built from such orbitals is characterized by its maximum overlap with the true wavefunction⁽⁴⁰⁾. These orbitals are called Brueckner orbitals. As Sinanoglu and Tuan⁽⁴¹⁾ have shown, for any closed-shell systems the difference between Hartree-Fock and Brueckner orbitals is expected to be very small. For a closed-shell system, there is a unique Hartree-Fock method: that based on the single Slater determinant. All effects not included in the independent particle model may be referred to as correlation effects. For closed shells, the correlation is mostly of the short-range type; the long-range effects of the Coulomb repulsions are taken care of in the Hartree-Fock scheme so that residual correlation effects are not expected to affect H.F. orbitals much. As shown by Sinanoglu⁽⁴¹⁾, many electron correlations are quite unimportant for closed-shell atoms and molecules. First order corrections to the energy contain no single excitations

due to Brillouins's theorem⁽⁴²⁾ but appear only in fourth order. First order wavefunctions contain no single excitations⁽⁴¹⁾. The result is that the first-order corrections to the electron density also vanish as originally demonstrated by Møller and Plesset⁽⁴³⁾. This result holds for the expectation value of any general one-electron operator, as proved by Cohen and Dalgarno⁽⁴⁴⁾ and others⁽⁴⁵⁾. The single excitations vanish for Brueckner orbitals and not for H.F. orbitals. This difference in emphasis is due to the peculiarity of the nuclear potential. Nevertheless, the smallness of the total contribution from single excited configurations to orbital corrections along with the unimportance of many-electron correlations means that H.F. orbitals form an excellent basis for quantum chemistry. Even though correlations change the energy significantly, their effects on orbitals is slight. The Brueckner and H.F. orbitals are nearly identical. Therefore, all quantitative considerations on the shapes of molecules, electron densities, etc., can be based safely on H.F. orbitals.

Molecular orbitals (MO's), expressed as linear combinations of atomic orbitals (LCAO), are the basis of a large body of theoretical molecular structural discussion, including predictions, correlations and interpretations. All MO methods are now being viewed and judged as approximations themselves⁽⁴⁶⁾ within a definite theoretical frame-

work, the appropriate framework being the H.F. theory, spurred by the tractability inherent in Roothan's⁽⁴⁷⁾ self-consistent field (SCF) methods. There has been a very marked improvement in calculated binding energies and other molecular properties resulting from allowing for polarizations and distortions of atomic orbitals in the molecule. Experience with H.F. calculations⁽⁴⁸⁾ tends to suggest that for proper discussion of chemical binding, one must include polarization valence shell functions. These polarization functions tend to compensate for the usual lack of adequate representation of transference of electrons in the molecule. The complexity of the present functions seriously handicap a discussion of the wavefunction itself in terms of hybridization, polarities, orbital electronegativities, ionic character, etc. These are all "hangovers" of the atoms in molecules method⁽⁴⁹⁾. Although one may associate a particular atom with a particular nucleus in a molecule, the conditions of an atom in a particular molecular environment are then completely specified when the electric and magnetic potentials due to all other molecular charges, together with their successive derivatives, are given in the immediate vicinity of the atomic nucleus in question. This is the approach we adhere to in this work. It is much more difficult to generalize the descriptive terms often used by chemists by means of which

the properties of atoms in molecules may be defined. The difficulty becomes then that every molecule might need be a special case, an observation put forward by Evans⁽⁵⁰⁾ as early as 1951.

The general picture that emerges from the H.F. theory and computations retains much of the simplicity of the original "Aufbauprinzip" as used by Hund and Mulliken to identify and classify electronic states in molecules. Certain details of the theory have been brought into sharper focus as a consequence of the discovery that correlation effects in molecular ground states are rather insignificant for one-electron properties. From this fact and from the theorems of Møller and Plesset, etc., it follows that electrostatic properties of a molecule relate only to the H.F. approximation⁽⁵¹⁾, and hence that classical electrostatic molecular models can have a close empirical relationship only with an H.F. calculation. A separate empirical theory is in general needed to describe substantial contributions to dissociative energies due to correlation energies.

The fact that the first-order correction to the density and one-electron operators vanish does not mean the function satisfying the best energy criterion gives the best possible density and best expectation values for one-electron operators as pointed out previously. In connection

with the density matrix approach, an alternative set of orbitals arises which does give the best possible density. This is the set of natural spin orbitals which is defined as that orthogonal basis in terms of which the first order density matrix is diagonal. From the point of view of wavefunction analysis, these are extremely useful since they are invariants rather than artifacts of a particular basis set choice, plus as being known to optimize convergence properties of configuration interaction wavefunctions⁽⁵²⁾. On the other hand, one does not have tractable one-electron equations for the determination of the natural orbitals although attempts in this direction have been made by Bender and Davidson⁽⁵³⁾ for LiH and HF. The natural spin orbitals as well as the best overlap (Brueckner) orbitals can be obtained as solutions of coupled integrodifferential equations which differ from the H.F. equations by some additional correlation potential. Because of this, the natural spin orbitals seem to give better approximations to expectation values of one-electron operators than the H.F. orbitals⁽³⁹⁾. On the other hand, the natural spin orbitals or "best density" wavefunctions, as they are sometimes called, do not satisfy the virial theorem⁽⁵⁴⁾, whereas a "best energy" function (H.F. scheme) does. Furthermore, because of computational difficulties, the natural orbitals are usually obtained from the best

energy MO's, after which one can "boil down" the most significant features contained in a wavefunction. At this writing, it is evident that these MO's are the most useful from the point of view of calculation and interpretation as discussed above. This present work will rely on accurate Hartree-Fock wavefunctions obtained from Roothan's S.C.F. methods which have been amplified and improved in recent years.

1.3 Motivation and Plan

Energy results have relevancy to concepts of chemical bonding. However, they represent only one perspective. The numerous expectation values and molecular properties, as well as the explicit charge contours contain much more revealing information regarding the concept of bonding. An examination of the details of the disposition of the electrons in the first-row diatomics and the first-row hydrides with an accompanying interpretive analysis based on the Hellmann-Feynman forces operative in such a series of molecules and others has been recently given by Bader et al⁽⁵⁵⁾. With the appearance of another critical appraisal of such an approach by Ransil and Sinai⁽⁵⁶⁾, the present dissertation is in this respect a continuation and extension of these previous investigations.

To bring to focus the importance of electron

disposition, consider the correlation energy, a concept which has no real physical meaning but only represents a deficiency in our theoretical methods. It is the spatial correlation of electrons in atoms and molecules, as pointed out by Lennard-Jones and Pople⁽⁵⁷⁾, which has physical meaning. As emphasized recently by Cade and Huo⁽⁵⁸⁾, it is only if accurate charge densities are compared with H.F. densities in a few test cases can one correctly connect the relative dispositions of electrons in terms of correlation energy results. This relationship cannot be definitely established otherwise.

The systems analyzed in the present work comprise two isoelectronic series: a) N_2 , CO, BF; b) LiF, BeO. These cover a wide range of bonding, from triple to single bonding, from ionic to covalent. Electronic charge distributions can be obtained from accurate SCF wavefunctions obtained from Hartree-Fock calculations using extended basis sets. The functions are for N_2 from Cade et al's work⁽⁵⁹⁾, for CO and BF from Huo⁽⁶⁰⁾ and also McLean and Yoshimine⁽⁶¹⁾, for LiF and BeO from these last authors also. An effort is made to relate molecular properties to the charge distributions of these. The importance of the charge density and the accuracy of this density and other one-electron operators obtained from H.F. calculations permit an important advantage of this approach, a point we

have often stressed in this introduction.

Many properties of molecules yield information about ρ , the electron density, directly. In particular, the main part of this thesis is an attempt at relating the magnitude of force constants in diatomic molecules to the nature and properties of molecular charge distributions. The force constants of molecules are generally determined from infrared or Raman spectroscopy. In terms of the electron density, they are given by the following expression:

$$k = \int \rho \frac{\partial^2 V_{e-n}}{\partial R^2} d\tau + \int \frac{\partial V_{e-n}}{\partial R} \frac{\partial \rho}{\partial R} d\tau + \frac{\partial^2 V_{n-n}}{\partial R^2} \quad (1.1)$$

The first term is an electronic field gradient term, the classical analogue of the electronic force constant for a nuclear charge moving in a static density ρ . The last term is the nuclear field gradient. The second term measures the redistribution of charge when the molecule is stretched or contracted.

There is a direct physical connection between the spatial distribution of the electronic charge for the equilibrium configuration and the magnitude of the force constant, which determines the forces acting on the nuclei when they are displaced from their equilibrium. To what features of the electronic charge density are molecular

vibrations most sensitive will be the main objective of the present work. Whether the charge distribution is delocalized to an equal extent over the nuclei in a molecule or is localized in the region of a single nucleus, whether the distribution is diffuse or contracted, and whether it follows rigidly the nuclear displacement or relaxes in such a manner as to oppose or facilitate the nuclear motion, are the properties of primary interest in the determination of the vibrational constant.

A discussion of molecular binding is first presented which is based on a comparison of the charge distribution and the forces which it exerts on the nuclei for the molecule with that found for the separated atoms. The force constant has its origin in the same distortions which give rise to the electronic force. Thus, the interpretation of the force constant necessarily follows a discussion of the forces which are responsible for the chemical binding. The Hellmann-Feynmann approach is central in this thesis. The force expression which arises from it permits a classical interpretation of binding related to the one-electron density. The expression (1.1) for the force constant also results from this approach. This permits one to clearly isolate the different contributions - orbital, atomic, overlap and shielding - to the force constant. This has the advantage over the energy method where the sum of the orbital energies

is not equal to the total H.F. energy and hence the use of the variation of orbital energies (or ionization potentials from Koopman's theorem) is not justifiable⁽⁶⁷⁾. In correlating Walsh diagrams, the adequacy of the variation of these has been demonstrated recently by Peyerimhoff et al⁽⁶⁹⁾ as one only has to consider angular variations.

Hellmann-Feynmann expressions are functionals of the one-electron density. The density distributions, once calculated from the appropriate wavefunctions, may then be compared in terms of their relative tightness of binding, a property which determines molecular size and which ultimately must be related to the chemical reactivity of the molecule. The over-all charge distribution may be analyzed in terms of the total amount of charge which is found in different regions of space. Related to these total density maps are the density difference maps, which are obtained by subtracting from the total molecular density, the density distributions of the constituent atoms. Such maps can demonstrate redistribution of charge and serve as the basis for definitions of distinct bond types, e.g. ionic or covalent character. The physical picture provided by the one-electron density distribution may be carried even further through the use of the Hellman-Feynman theorem, which, as discussed before, relates in a rigorous manner the forces acting on the nuclei in a molecule to the one-electron density function.

Because of the essentially classical nature of the connection between the forces and the electronic charge distribution, a study of the forces can provide a physical basis for the interpretation of molecular binding. This then will be the prelude to the discussion of force constants.

In the expression (1.1) for the force constant, we have indicated the presence of two terms called field gradients. The sum of these may be determined in some cases from the quadrupole coupling constant of nuclei with quadrupole moments⁽⁶²⁾. The quadrupole coupling constants are determined by the components of the electric field gradient at the nucleus and give valuable insight into the asymmetry of the charge density distribution in the vicinity of the nucleus. Townes and Dailey⁽⁶³⁾ have laid the ground work for the theoretical understanding of these quantities but no adequate theory is yet available and much of what is written about ionic character, hybridization, etc., must be viewed skeptically⁽⁶⁴⁾. The Townes and Dailey theory is applicable to covalent molecules only. Theories first developed by Sternheimer⁽⁶⁵⁾ on the antishielding of the nuclear quadrupole moment by the electron cores of free ions are frequently used for ionic cases. These two "prescriptions" will not often explain rather subtle variations and intermediate bonding cases. For instance, an accurate appraisal of covalency effects on the quadrupole interaction must involve a

full molecular orbital treatment as Bersohn and Shulman⁽⁶⁵⁾ have recently pointed out. Refined calculations are needed to verify other points. This has been attempted by calculating field gradients from the wavefunctions for the aforementioned molecules, and analyzing the results to bring out the most important features of quadrupole coupling constants. The field gradient discussion is another prelude to the force constant dissertation, as they provide a link between static effects and the actual constant. In the discussion of the force constants, the exact connection and relevance of the field gradient to the constant itself will be further analyzed.

In concluding this introduction, we wish to remark on a point stressed by Slater⁽⁷⁰⁾ as early as 1933, namely that the study of molecular structure has been too much based on particular models rather than on general principles. Therefore, it is not surprising if certain concepts tend to disappear with more detailed functions. An exact wavefunction provides a tool for obtaining exact expectation values. These can be obtained, alternatively, from experimental data. Of importance is the fact that neither alone constitute an understanding of the electronic structure of molecules. Definitions must have meaning within a framework, providing quantitative data, obtained from either experiment or exact calculation, of a qualitative nature⁽⁷¹⁾. The importance of

symbolism in understanding the chemical bond should not be minimized. Chemistry, like atomic physics with its atomic orbits, needs not only methods of exact calculation of wave-functions, but also a justified symbolic calculus⁽⁷²⁾.

Of interest to chemistry primarily are space distributions and energy changes. The density matrix and Hellmann-Feynman theorems provide scope for definitions and data which are used and analyzed in order to obtain some correlation between molecular structures, especially various types of "bonding". It is with these views in mind that this dissertation proposes to be a contribution in that direction.

1.4 N₂, CO, BF

These three molecules make up a 14-electron iso-electronic system. Furthermore, CO is an important hetero-nuclear molecule because of the abundance of experimental data on it. Both CO and N₂ have been of some historical importance. In 1926, Birge⁽⁷³⁾ was the first to point out the energy levels of CO and N₂ presented a remarkable analogy to those of Mg. However, both molecules showed no marked analogy evident in chemical behaviour to Mg.

N₂ is inert just like argon. This was attributed by Langmuir⁽⁷⁴⁾ to the fact that the supposed 2 valence electrons were imprisoned in an octet or L shell. It was Mulliken⁽³²⁾ in 1928 who showed that the lowest ²Π state of CO⁺ was inverted; unlike the ²P state of its atomic analogue, Na, but more

Table 1.1
Molecular Data a)

Molecule	Wavefunction	Total Energy (Hartrees)	D_e (eV)	R_e (Bohrs)	k_2 (mdyn/Å)
N ₂	H.F. ⁽⁵⁹⁾	-108.9928	5.19	2.013	30.73
	Exptl.	-109.586	9.902	2.068	22.91
CO	H.F. ⁽⁶¹⁾	-112.7908	7.97	2.081	24.36
	Exptl.	-113.377	11.24	2.132	19.02
BF	H.F. ⁽⁶¹⁾	-124.1675	6.22	2.354	9.652
	Exptl.	-124.777	8.58	2.391	8.080
BeO	H.F. ⁽⁶¹⁾	- 89.4542	4.14	2.443	10.14
	Exptl.	- 89.962	6.66	2.515	7.519
LiF	H.F. ⁽⁶¹⁾	-106.9918	4.08	2.9377	2.818
	Exptl.	-107.502	5.99	2.9554	2.569

a) R_e (H.F.) and k_2 (H.F.) are from polynomial fits of the energy curve.

like a 2P of a halogen. The conclusion was, therefore, that the molecule was missing an electron of $p\pi$ character. These suggested analogies between atomic and molecular spectra showed the way to specify a definite orbit for each electron in the molecule. In the case of N_2 , its Raman spectrum led to the first determination of its moment of inertia. The intensity alternation in the rotational lines of N_2 showed that the N nucleus obeys Bose statistics, a result which Heitler and Herzberg⁽⁷⁵⁾ suggested could not be reconciled with the presence of electrons in the nucleus, the theory prevalent at that time.

In molecular orbital notation, all three molecules have the ground state electronic configuration, $1\sigma^2 2\sigma^2 3\sigma^2 4\sigma^2 1\pi^4 5\sigma^2$. The N_2 molecule is further designated by the inversion symmetry present so that its configuration can also be written $1\sigma_g^2 1\sigma_u^2 2\sigma_g^2 2\sigma_u^2 1\pi_u^4 3\sigma_g^2$. Of these molecules N_2 is the most inert, BF the most reactive. In Table (1.1) are listed some of the properties of these, both experimental and calculated with the Hartree-Fock functions indicated by the references. In Fig.(1.1), the change in orbital ordering across the series is demonstrated for the three highest orbitals in the series. The 4σ orbital is usually designated as a "lone pair" situated on the heavier nucleus and thus increases in energy as the nuclear charge decreases

when going across the series from BF to N₂. The 5σ orbital is the "lone pair" on the lightest atom and its energy decreases as one goes across from BF to N₂ due to increasing nuclear charge. The 1π orbital tends to become localized primarily on the heavier atom and therefore behaves somewhat like the 4σ orbital. It is not easy to rationalize many of the differences between these molecules from an observation of these energy levels. It is known experimentally⁽⁷⁶⁾ that the loss of an electron to form CO⁺ and BF⁺ leads to a decreased bond length and an increased vibrational frequency, whereas N₂ offers the reverse case, for the first ionization of these systems. The ionized electron is known to be from the 5σ orbital ($1_{\Sigma}^{+} \rightarrow 2_{\Sigma}^{+}$ transition)⁽⁷⁷⁾.

The central features of the empirical molecular orbital theory are the correlation diagrams and the related concepts of bonding and antibonding orbitals. The distinction of bonding and antibonding electrons is based on the criterion whether the energy level of a given electron is lowered or raised respectively, in the transition from separated atoms to the molecule⁽⁷⁸⁾. Symmetry changes also enter the evaluation of this distinction. In N₂, for example, the 3σ_g orbital would be classified as weakly bonding because of its incipient promotion to a 3s orbital in the united atom. One would infer that since for CO and BF the bond length decreased and the force constant increased

upon loss of a 5σ electron, that MO is antibonding whereas in N_2 it is bonding. From energetics alone, because of its lower energy, one would predict that in N_2 the orbital is bonding and that in CO and BF, the non-bonding situation is approached. These orbital characteristics will be analyzed via a force analysis in a more illuminating way, as it is the actual forces on the nuclei and their changes upon ionization which cause structure changes. Further insight into the varying characteristics of these molecules will be "distilled" from density and density difference maps which represent net effects, rather than orbital contributions. The force constants will also be analyzed as these represent the changes in forces in the vibrating molecule.

1.5 LiF, BeO

These two molecules are the first member of a 12-electron isoelectronic series, the others being BN and C_2 , which are all not too well understood. LiF has always been of great interest as it appears to be the prototype of an ionic molecule. BeO has always been a very perplexing case. Experimental evidence pointing to a $^1\Sigma^+$ has never been compelling. By the Wigner-Witmer correlation rules, the $^1\Sigma^+$ state cannot dissociate into ground state atoms, i.e. $Be(^1S), \alpha(^3P)$. Since it is unusual for the ground state to dissociate into excited atoms, there always remained the

possibility that the true ground state was an unobserved 3Π or $3\Sigma^+$ level. Only recent open-shell MO calculations⁽⁷⁹⁾ for these states have indeed established the $1\Sigma^+$ to be the lowest state. For this state, previous MO calculations⁽⁸⁰⁾ by Yoshimine have shown that the highest doubly occupied σ -orbital (4σ) changes character in the vicinity of R_e from mostly O basis orbitals to mostly Be basis orbitals. Since the wavefunction does not change symmetry, this change might be described as a virtual cross-over of molecular configurations. As this changes the molecular structure from what is usually thought to be $\text{Be}^{+2}\text{O}^{-2}$ to BeO , there is an abrupt change of the dipole moment function $\mu(R)$ with a maximum near R_e (slightly greater than R_e). There have been several discussions of a dipole moment function for diatomic molecules⁽⁸¹⁾. The simplest function should go to zero as $R \rightarrow 0$ and as $R \rightarrow \infty$ (united and separated atoms) and reach a maximum at some intermediate value of R . For an ionic molecule, a model of two polarizable ions is generally used⁽⁸²⁾. As the distance between the two ions increases, their polarization decreases. Both the increased separation of the ions and their reduced polarizations increase the dipole moment. Thus, the ionic model predicts a large positive slope for the $\mu(R)$ curve. For LiF , the equilibrium distance falls on the rising side of $\mu(R)$ so that its dipole moment function is in agreement

Table 1.2
Orbital Energies

Molecule	Orbitals	
	4σ	1π
LiF	-0.505	-0.479
BeO	-0.461	-0.389

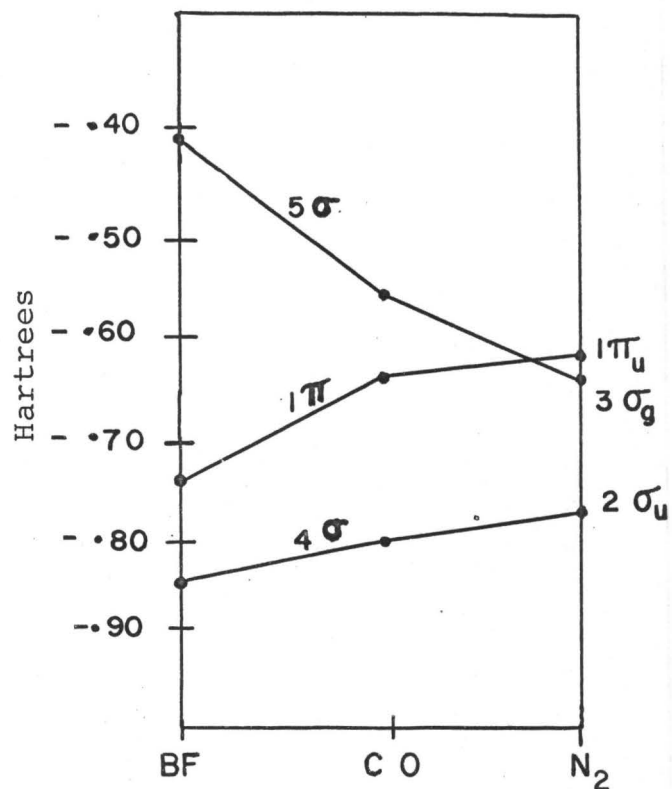


Fig. (1.1) Orbital Energies

with the ionic model. Yoshimine's calculations for BeO predict a dipole moment of 7.3 D, whereas for an undistorted Be^+O^- system at the same R, this is 6.2 D. A positive calculated $\mu(R)$ slope confirms the ionic character. The experimental dipole moment function is not known and its measurement presents considerable experimental difficulty⁽⁸³⁾. Nevertheless, of general importance has been the observation recently⁽⁸³⁾ that there is complete lack of correlation of μ and $d\mu/dR$ in SrO, an analog of BeO as these form with others the family of alkaline-earth oxides. Although there is correlation for μ and $d\mu/dR$ in BaO, μ indicates SrO is extremely ionic and yet $d\mu/dR$ is negative. This suggests that the molecule is undergoing change of configuration in spite of a large dipole moment. No model of polarizable ions can explain properly these results. Trends in the other alkaline-earth oxides suggest that BeO might be similar to SrO.

A general picture of the chemical bond in the alkaline-earth oxides can be obtained by comparing MO calculations of BeO and LiF. A reasonably adequate picture of LiF is generally thought to be that of two slightly overlapping ions Li^+ and F^- . The two highest energy occupied orbitals in LiF, $4\sigma^2$ and $1\pi^4$, are assumed to be almost entirely $2p_{\text{F}}$ because they have approximately the same energy (see Table 1.2). If BeO had the same electron

distribution, it would be described as two doubly-charged ions, Be^{++} and $\text{O}^{=}$. Comparison of the orbital energies, however, shows that in BeO the 1π orbital is considerably higher in energy than the 4σ orbital, and from the wavefunction, has become a mixture of $2p\pi_{\text{Be}}$ and $2p\pi_{\text{O}}$. The four 1π electrons are, therefore, shifted into the bond towards Be, thus tending to make the over-all dipole moment of BeO not too different from that of LiF which is 6.284 D (Debyes). The separation of equal and opposite charges at the observed LiF bond length gives a dipole moment of 7.51 D; for Be^+O^- this is 6.2 D. The calculated dipole moment for BeO is 7.3 D, indicating that the molecule is approaching the $\text{Be}^{++}\text{O}^{=}$ configuration.

On the other hand, one might expect BeO to be more covalent than LiF, since by excitation of type $s^2 \rightarrow sp$, Be becomes divalent and therefore one can expect to have a $\sigma^2 \pi^2$ configuration. This would then be the appearance of double bond character similar to ethylene except for large polarities, as pointed out by Coulson⁽⁸⁴⁾. This particular difference shows up in the crystal structures. LiF crystallizes in the simple cubic form or NaCl lattice, whereas BeO's solid conformation is wurtzite, as ZnS, which is a diamond-like structure held together by both covalent and ionic forces. A rigid-ion calculation of normal modes in solid BeO is in serious disagreement with experimentally observed

modes. A mixed valence-Coulomb force field⁽⁸⁵⁾ has to be used in order to calculate adequately phonon frequencies. It would seem that the degree of covalency is sufficiently large for directional valence forces to determine the stereochemistry of the lattice (and thus affect the phonon spectrum) were it not for the fact that closest packing criteria of the large ions O^{2-} also favor the tetrahedral crystal structure wurtzite⁽⁸⁶⁾. The question as to which characters, ionic or covalent, are prevalent will be analyzed in terms of electron densities, forces and field gradients. In a later chapter, the effect of the bonding in LiF and BeO on force constants will be also examined in order to ascertain the differences in their magnitudes as seen in Table 1.1.

II. ELECTRON DENSITIES

United we stand, divided we fall.

Atoms in molecules

2.1 The Density Distribution - A Study in Molecular Topography

A knowledge of the electron distribution in a molecule is a fundamental requirement for the understanding of the chemical behaviour of a molecule^(12,25). The calculation of the electron density in a molecule is therefore an important problem. But once the rules for defining a physically sensible wavefunction, and therefore density, have been set down, then within that framework the primary factors available for a description of molecular behaviour are the densities, the forces between particles (which are mainly coulomb forces), and whatever quantum numbers are inherent in the problem. Specifically, it is actually the distribution of the electrons within the molecular framework which determines many properties of the molecules, and particularly their chemical reactivity. Relocation of electronic charge density has always been presumed to be an important adjunct, if not cause, of chemical bond formation. The transfer of electron density into the

internuclear region of the H_2 molecule is a long-recognized phenomenon, even though the reasons for it are still the subject of considerable discussion⁽⁸⁷⁾. With scant additional illustration, the same sort of phenomenon has been assumed to occur in larger molecules. The present discussion considers the effect of chemical bond formation from the viewpoint of spatial electron distributions, in the following molecules: N_2 , CO, BF, BeO and LiF. The first three form a group of 14-electron isoelectronics; the last two are 12-electron isoelectronic analogues of each other.

From very close SCF-LCAO approximations to the true H.F. wave functions of these and of the free atoms involved in the bonding, it is possible to determine redistribution of electronic charge predicted by the H.F. calculations. It has long been held by most chemists that, in addition to "exchange effects", a chemical bond forms as a result of electronic charge density flow into the internuclear region where the potential energy is lower. Recently, Ruedenberg⁽⁸⁷⁾ has suggested that the main potential energy lowering occurs by a contraction or clustering of valence electron density about the nuclei. The concomitant and also necessary (from the standpoint of the virial theorem⁽⁷⁰⁾) increase in kinetic energy is partially offset by the effects

of delocalization. One can best gain insight into the problem of what really happens when an atom unites with another atom to form a molecule by examining the changes which the total electronic charge densities undergo in such a process of bond formation. The relevant observables are then the charge densities. To obtain a measure of such changes, one can construct a molecule which would result if the two atoms making up the molecule were united without perturbing each other, or if they were in incipient valence states arising from ground state configurations of the separated atoms. This can be done by simply superposing the electronic charge densities of these constituent atoms. One can then characterize a chemical bond by the function

$$\Delta\rho(\vec{r}) = \rho_m(\vec{r}) - \rho_A(\vec{r}) \quad (2.1)$$

where $\rho_m(\vec{r})$ is the total electronic density of the molecule M at some space point (\vec{r}) in the molecule; $\rho_A(\vec{r})$ represents the electronic charge density (at the same point) which would occur if the two constituent atoms were superposed at the molecular equilibrium distance. Thus, $\Delta\rho(\vec{r})$ is positive in regions of the molecule where charge density has accumulated and negative where charge density left. Because net charge is conserved, the integral of $\Delta\rho(\vec{r})$ over all space is zero. This function has been computed for several molecules by Roux, Daudel and co-workers⁽⁸⁸⁾, by Rosenfeld⁽⁸⁹⁾,

correlated to bond orders by Manning⁽⁹⁰⁾, and finally thoroughly discussed by Bader et al⁽⁵⁵⁾, Ransil and Sinai⁽⁵⁶⁾.

The maximum amount of chemical information is obtained from such a density difference plot when the densities of the atoms are derived from valence states which result in the overlap of singly-occupied orbitals when the atoms are brought together. This corresponds, therefore, to the valence-bond picture of chemical-bond formation. The "valence" states implied here refer to the ground states of atoms in an axial electric field. Such a field splits the p_x , p_y and p_z degeneracy, lowering the still degenerate p_x and p_y orbitals ($\rightarrow\pi$) and raising the p_z orbital ($\rightarrow\sigma$) if z is taken as the direction of the axial field. These states therefore differ from those used in the atoms in molecules method⁽⁴⁹⁾ which correspond to non-stationary states and artificial dissociations, but are nevertheless a suggestive artifice for the description of the molecule in terms of the properties of its constituent atoms. In the method advocated here, in the limit of vanishing perturbation, the averaged ground state density and the valence state density used correspond to the same energy. However, in the valence state, distinction between σ and π character is preserved in order to display the very useful picture of chemical-bond formation given by valence-bond theory. Thus, the F atoms in the molecules BF and LiF

will be considered in the "valence state" corresponding to the configuration $1s^2 2s^2 2p\sigma^1 2p\pi^4$. A spherical average over the ground-state configuration as used by other authors⁽⁸⁸⁾ for the atomic densities, would neglect the preferred direction towards the other atom. There is no difference between this valence-state density and the averaged ground-state density for Li, Be and N. B is placed in a valence state with one $p\sigma$ electron, whereas C has in addition one $p\pi$ electron. O and F are placed in states with a single $p\sigma$ electron, the remaining electrons being averaged over the π orbitals. Thus, for N_2 , CO and BF, the bond formation is visualized as overlap of $p\sigma$ orbitals on each atom and subsequent rearrangement of the densities in the molecule. This enables one to compare these three molecules systematically, and keeps four electrons in the π region as demanded by the molecular orbital representation of these molecules. For a similar comparison between LiF and BeO, it was found necessary to use the state $O(1s^2 2s^2 2p\pi^4)$ ^{a)} as the ground state for Be corresponds to $1s^2 2s^2$. The method of the function $\Delta\rho(\vec{r})$ is not without analogy with the electron population analysis devised by Mulliken⁽⁹¹⁾. The main difference between the two procedures lies in the fact that the $\Delta\rho$ method gives a local representation

a) Footnote: This corresponds to taking twice the $M_L=0$ component of the first 1D state minus the first 1S state of oxygen.

of the "bond effect" and provides information on the spatial distribution of the electrons. On the other hand, the population analysis provides a gross representation of the phenomenon and suffers from the defect that overlap populations are arbitrarily equally divided between the two nuclei. This difficulty will be circumvented in the next chapter by the use of force analyses, which clearly show any asymmetry in the distribution of the overlap region by comparing the forces the density exerts on both nuclei. The density and density difference maps can give us a pictorial and thus extremely useful interpretation of chemical bonding which will be later supplemented by the force analysis. As our ultimate goal is an analysis of force constants for the molecules N_2 , CO, BF, BeO and LiF, we discuss first some of their characteristics which can be extracted from an examination of the details of the density and density difference maps.

2.2 Charge Density- ρ diagrams

Approximating the electronic wave function for the ground state of a closed-shell molecule by a single determinant constructed from a set of occupied orthonormal orbitals $\phi_i(\vec{r})$, the one-electron probability density function associated with the wave function is given by

$$\rho(\vec{r}) = \sum_{i=1}^N n_i |\phi_i(\vec{r})|^2 \quad (2.2)$$

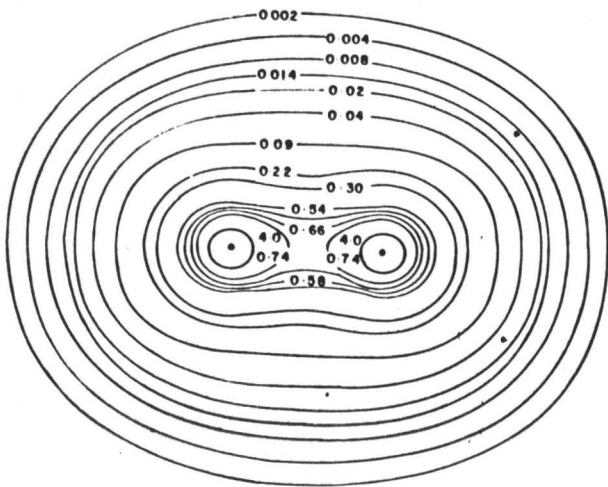
where n_i are the occupation numbers and the sum is taken over the occupied orbitals. If the functions $\phi_i(\vec{r})$ form an orthonormal set, then $\rho(\vec{r})$ represents the probability of finding an electron at the point \vec{r} in space. Although strictly speaking a probability distribution function, $\rho(\vec{r})$ may be taken as a measure of the average electronic charge density, excluding electron correlations, at point \vec{r} . In the present work, the molecular orbitals are approximated by linear combinations of atomic orbitals, $X_j(\vec{r})$ and thus equation (2.2) becomes:

$$\rho(\vec{r}) = \sum_{i=1}^N n_i \left| \sum_j C_{ij} X_j(\vec{r}) \right|^2 \quad (2.3)$$

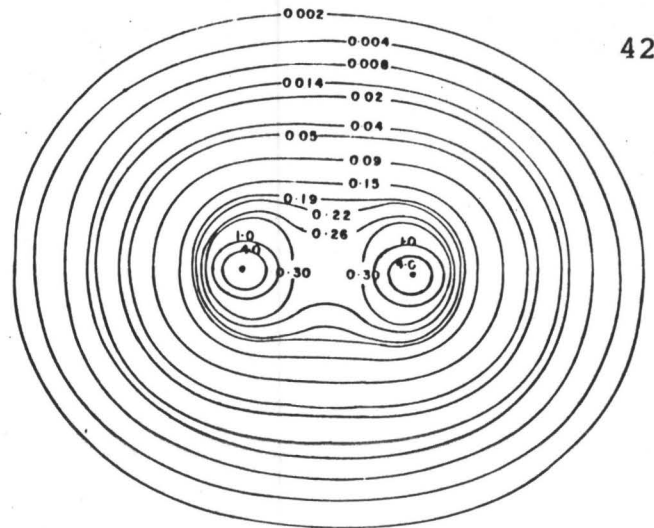
From the study of molecular charge densities, we would hope to gain insight and information about several important characteristics of molecules: their "size", "shape", their total distribution. In particular, molecular shapes are determined by the nuclear configuration and the spatial distribution of the surrounding electronic charges. The nuclear configuration parameters may be obtained from experiment, or theory, or both. Calculation of accurate charge density distributions requires accurate molecular wavefunctions.

Determination of molecular shape hinges upon the determination of molecular "size" which is complicated by the fact that the outermost charge density contours fall

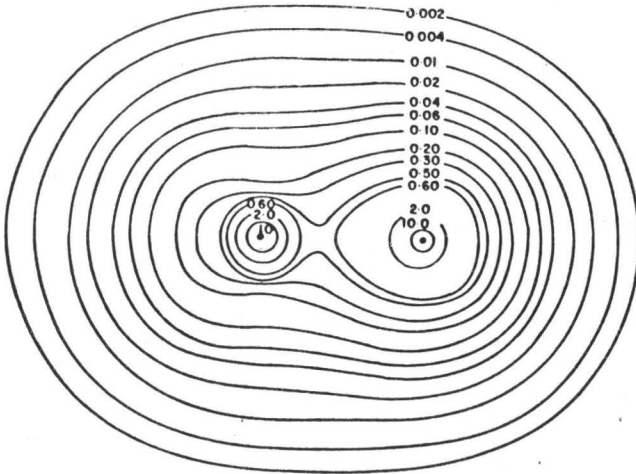
off exponentially to infinity, or at a rate which varies according to whether the molecule is in a ground state or excited state, whether it is neutral, negatively or positively charged. A cutoff contour must be defined and thus a certain degree of arbitrariness or "empiricism" probably cannot be avoided in establishing a basis upon which such definition can be made. In this work, following Bader et al⁽⁵⁵⁾, molecular size is defined with reference to a specific contour inside of which most of the charge density is contained. Arbitrariness enters when specifying the percentage of charge to be enclosed by the cutoff contour. The 0.002 contour chosen here as cutoff contour encloses about 95% of the total charge⁽⁵⁵⁾. Other criteria for definition of size, based on interaction energies, are possible and perhaps are more physically meaningful. But definition on this basis is difficult because of the wide range of interaction energies possible. A recent review⁽⁹²⁾ of quadrupole moments demonstrates the disagreements between the different experimental determinations of the same physical property, so that even here definitions are not made overly precise. There is yet no known correlation between a given range of charge density and the strength of molecular force fields. Consequently, one would not expect the size of molecules computed according to the above convention to agree necessarily with the van der Waals radii,



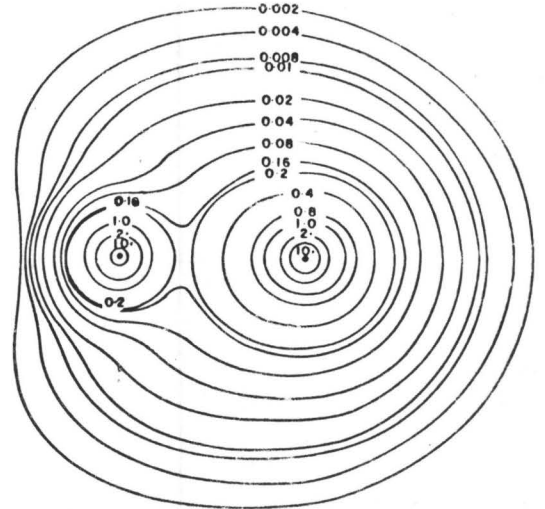
$N_2 \ ^1\Sigma^+$



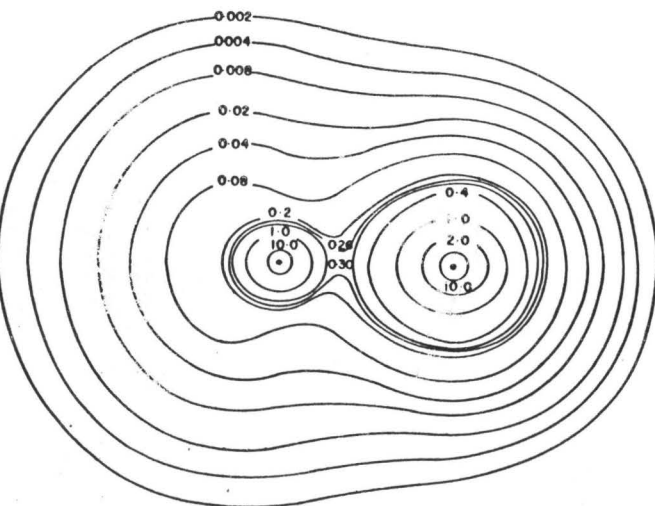
$C_2 \ ^1\Sigma^+$



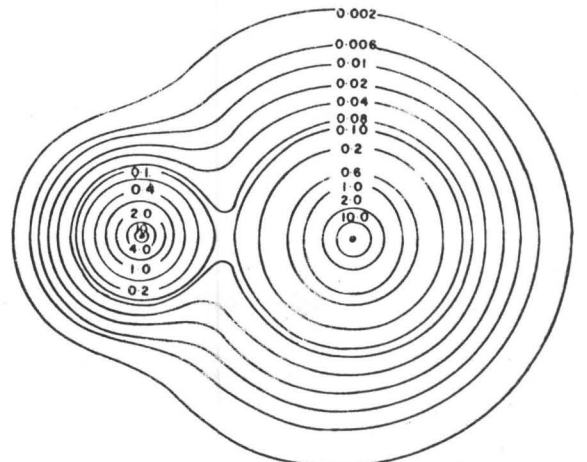
$CO \ ^1\Sigma^+$



$BeO \ ^1\Sigma^+$



$BF \ ^1\Sigma^+$



$LiF \ ^1\Sigma^+$

Fig. (2.1) Electron Density

Table 2.1

CHARACTERISTICS OF TOTAL DENSITY DISTRIBUTION

Molecule	AB	N ₂	CO	BF	C ₂	BeO	LiF
Width(a.u.) at	A	6.3	6.1	6.5	7.0	6.0	3.6
	B	6.3	6.1	5.9		6.6	6.0
	R _e /2	6.4	6.1	6.2		6.6	6.0
Length(a.u.)		8.2	8.4	8.9	8.5	7.0	7.6
R _e (a.u.)		2.068	2.132	2.391	2.348	2.50	2.8877
z-intercept of 0.002 contour (a.u.) in molecule	A	3.1	3.4	3.8	3.1	1.3	1.7
	B	3.1	2.8	2.8	3.1	3.1	3.0
in atom	A	3.0	3.2	3.4	3.2	3.6	3.3
	B	3.0	2.9	2.8	3.2	2.9	2.8
Charge Den- sity at	A	205.59	127.07	71.70	127.32	34.88	13.78
	B	205.59	310.89	447.53	127.32	310.80	447.41

or molecular diameters computed from Lennard-Jones potential data⁽⁹³⁾. But from an analytical standpoint, for different molecules a comparison is relevant and of interest.

Contour maps of the total molecular charge density distributions, all drawn to the same scale are shown in Fig.(2.1).^{a)} These projections illustrate the relative tightness of binding of these various density distributions. It is well known that the atomic charge distributions become more contracted across a row of the periodic table, a result of the increase in the effective nuclear charge. This same effect is noticeable in the density distribution at the N, O, and F nuclei in the molecular charge distributions. In Table (2.1) are listed some of the more dramatic features of the charge distributions. The distance from each nucleus to the 0.002 contour along the non-bonded axis or z-intercept as designated in Table (2.1), are listed with the radii of these same contours in the appropriate separated atoms. The diameter of the non-bonded charge densities of N, O, and F in the molecules is very close to that found in the corresponding isolated atoms. There is a greater variation in the atomic diameters across the row from N to Li. There is an increasing divergence between the atomic values and

a) Footnote: C₂, which has already been discussed by Bader et al⁽⁵⁵⁾, is included for completeness.

those found in the molecule. There is an increase in the value of the z -intercept or non-bonded radii from N to B. In particular, the value for B is significantly greater than that of the free atom. For the molecules CO and BF, this is therefore in accord with the actual dipole moments C^-O^+ , B^-F^+ . For CO this has been reassigned recently after extensive controversy about the sign⁽⁹⁴⁾. The dipole moment of BF has not been measured as yet, but has been calculated⁽⁶⁰⁾ to be 1.04 D as compared to the experimental result of 0.112 for CO. The sign and magnitude of these then follow from the nature of the dipole operator which weighs heavily charges far removed from the charge center of the system, and also from the charge distributions of these two molecules which have more charge behind the nuclei C and B than found in the free atoms. There is a sharp difference in this trend in the C_2 , BeO, LiF series. The non-bonded radii of the densities centered on the Be and Li nuclei in the molecule are considerably smaller than their corresponding atomic values. In fact, the values of the radii in the molecule are the same as the values which can be calculated for the 0.002 radius of the 1s shell densities in the ions Li^+ , Be^{++} . This is then a clear indication of charge transfer away from the light atom regions of these molecules.

In comparing N_2 and CO which are often assumed to be

quite similar in many respects except reactivity, potential parameters from viscosity data⁽⁹⁵⁾ indicate the diameters of these molecules are equal (7 a.u.). This is intermediate between our calculated lengths and widths. Such data are probably not fine enough to determine comparative molecular sizes. In fact, the polarizability of CO is greater than that of N₂⁽⁹⁶⁾, so that this may affect transport properties which generally are based on crude models. Some evidence of similarities between these two molecules comes from recent crystal structure work. The experimental results⁽⁹⁷⁾ demonstrate the same space group and same crystal parameters for the crystal forms of N₂ and CO. The question then arises as to whether size effects are very important in the structure of van der Waals lattices. Barrett et al⁽⁹⁸⁾ have recently noted the effect of dissolving N₂ and CO in solid Ar. The two molecules produce strikingly different phase diagrams. It may be that as Hillier and Rice have suggested⁽⁹⁹⁾, electron delocalization, represented in terms of the mixing of charge transfer excitation states and neutral excitation states are important contributions to the ground state binding energy of molecular crystals. In this respect, one would expect CO to differ from N₂ because of the slight decrease in binding of the electrons on the C atom as witnessed by the change in non-bonded radii. The density at 0 is slightly

more bound in the molecule. These effects increase as one goes to BF so that the high reactivity of BF can be qualitatively correlated with the decrease of binding of the density at B which has resulted in the density on B having become more diffuse than in the free atom.

A perusal of the LiF total density map shows that the molecule approximates what one can call two unequal spheres of unequal charge density coupled together. The shape of BeO approaches sphericity whereas LiF is quite elongated. The tight densities at the Li and Be ends of these molecules indicate charge transfer away from these nuclei. While the non-bonded charge density of Be has been decreased along the bond axis, the transfer is not pronounced in the regions perpendicular to the bond. Interestingly, LiF has the smallest first contour of equal density which encompasses both nuclei. As this is a rough indication of the amount of delocalized charge density, it is thus seen that LiF approaches the ideal ionic model of noncoupled spheres. In BeO, the full contour first appears at 0.16 as compared to 0.08 for LiF; for BF this is 0.26, slightly higher for C₂, and larger for CO and N₂. The observation that one can therefore make is that delocalization increases in the following order: LiF, BeO, BF, C₂, CO, N₂. Finally we notice that the F atom in LiF is nearly spherical, a somewhat surprising observation

as one would expect it to be quite polarized towards the Li nucleus. This situation also exists in the crystal. The electron density contours in the LiF crystal have been plotted by Krieg et al ⁽¹⁰⁰⁾ from x-ray data. The density around the F nucleus is almost spherical while that around the Li nucleus deviates appreciably from spherical shape, particularly in regions away from the nuclei in the crystal. Indications are that this Li density is more polarizable in the crystal LiF than for a Li⁺ ion ⁽¹⁰¹⁾ as the maximum of the radial density distribution is shifted by about 0.25Å from the Li nucleus as compared with the free ion.

In summary, in contrast to the series N₂, CO, BF where the density becomes more diffuse behind the electro-positive element, in C₂, BeO, LiF the trend is reversed, in that the density becomes tighter around the electro-positive element for these molecules. This is then in line with the tendencies of BeO and LiF to ionize first in chemical reactions because of the electron acceptor properties of the electro-positive end of these molecules,

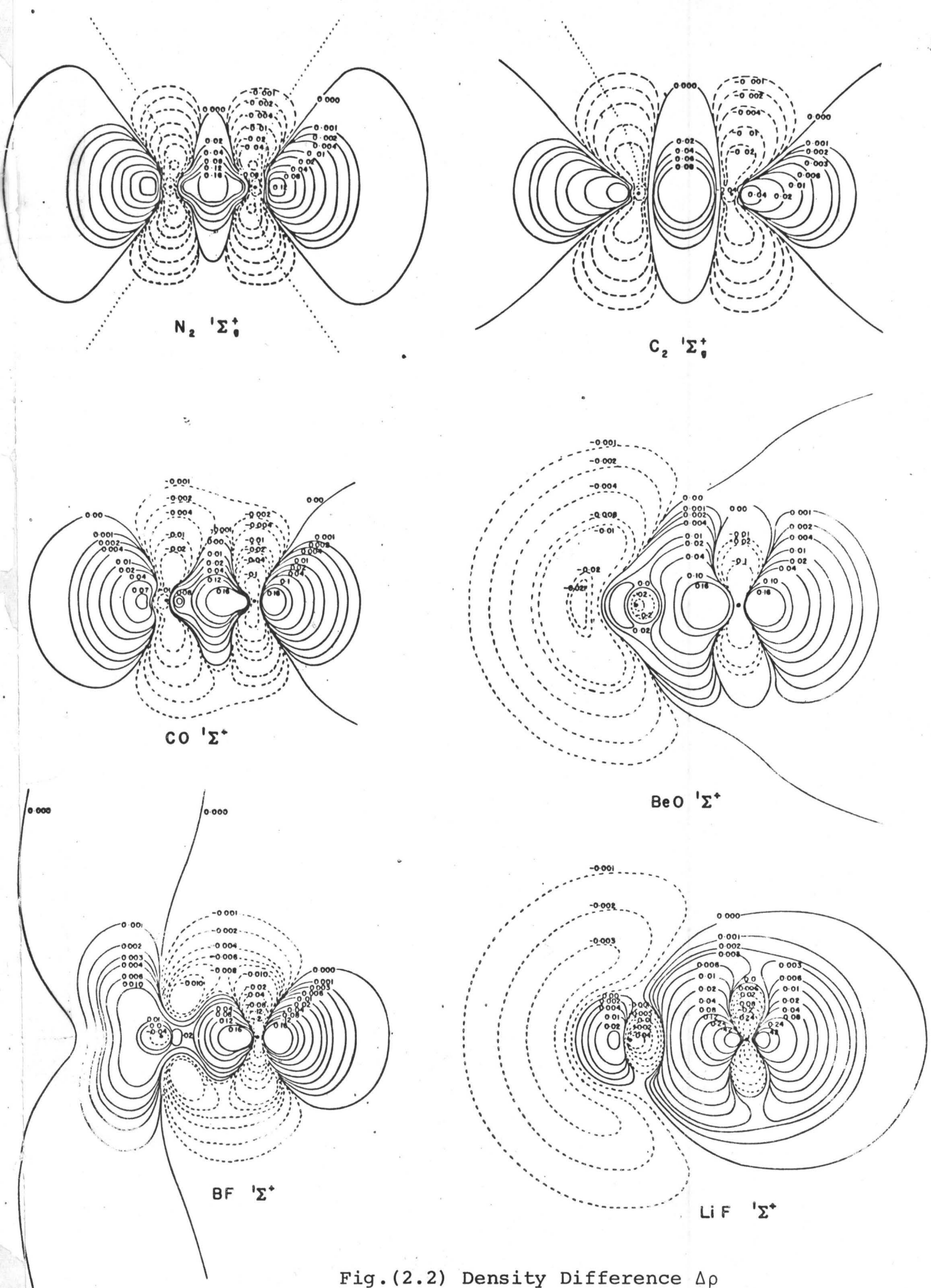
as opposed to CO which is an electron "donor" and tends to bond covalently with other elements, especially transition metals. We would thus predict that BF is a much stronger electron "donor" than CO in view of the more

diffuse density behind B. The ρ contours therefore provide structural information about molecules in terms of charge density contours and their intercepts with an appropriate set of axes. Integration of the ρ diagram can yield electron populations as a function of contour value and corresponding spatial coordinates for the entire molecule (see work of Ransil⁽⁵⁶⁾). However, the presence or absence of a chemical bond is not manifested by the appearance of the total density distributions. The features displayed by the total density map are in general gross and require further refinement. In addition, total molecular charge densities computed from wavefunctions with varying degrees of sophistication do not differ appreciably in the display of contours⁽¹⁰²⁾. This insensitivity must be somewhat superficial since striking variations are observed when one characterizes the charge density with the function $\Delta\rho$.

2.3 $\Delta\rho$ Maps

The $\Delta\rho$ diagram presents an interpretive problem because regions of positive and negative contour values are encountered. These regions do not represent absolute increase or decreases respectively, in total charge density but rather they represent an increase or decrease of probability density relative to the densities of the appropriate unperturbed dissociation products, in appropriate valence states, a distance R_e apart. By way of contrast, the ρ maps

give a time independent statistical distribution of electron charge in molecular space, whereas the $\Delta\rho$ maps tell us what regions in the molecule are electron rich or deficient compared to the hypothetical case of appropriate dissociation products. Furthermore, while there may be a net gain or deficit of electron charge density at a specified point, the net total change in density obtained by integrating over all space is zero. This density difference as defined and computed therefore reflects, strictly speaking, not charge distribution associated with formation of a chemical bond, but a difference between two scalar quantities, which may be correlated with a chemical bond only insofar as the molecular and atomic densities correlate with the accurate charge densities. The validity of these interpretations assumes the computational accuracy of the total and difference densities, and their invariance to such things as basis-set representation, relativistic and correlation effects, etc. The characteristics of $\Delta\rho$ are in general seen to depend very strongly on the quality of the approximate wavefunction, as shown by some calculations on N_2 by Smith and Richardson⁽¹⁰³⁾. For an outline of these problems, the reader is further referred to Ransil and Sinai's paper⁽⁵⁶⁾. On the basis of various diagrams, these authors conclude that the evidence so far suggests

Fig.(2.2) Density Difference $\Delta\rho$

that there are no significant major variations in the $\Delta\rho$ diagram topography in going from a limited to an extended basis set, provided molecular and atomic functions of consistent accuracy are used. We have implicitly employed such a consistent approximation perspective in what follows. Hartree-Fock wavefunctions have been employed for both the molecule and the separated atoms, the atomic functions coming from the work of Clementi⁽⁶¹⁾ which have been used as starting points in the MO calculations.

The density distribution which results from the overlap of the unperturbed atomic densities separated by R_e does not ordinarily place sufficient charge in the region between the nuclei to just balance the force of nuclear repulsion and hence result in a state of electrostatic equilibrium⁽¹⁴⁾. The density difference map $\Delta\rho$ may therefore be viewed as a picture of the change in atomic charge distribution required to balance the force of nuclear repulsion and thus obtain a stable molecule, i.e., a chemical bond. From this point of view the density difference maps provide one with a picture of the "bond density". The $\Delta\rho$ maps are given in Fig.(2.2) for $R = R_e$ (exptl.). The general characteristics of these maps is uniformly a buildup of charge between the nuclei and in the regions behind the nuclei, i.e. the region away from the bond. What is observed then, is the movement of

Table 2.2

INCREASE IN CHARGE $\Delta\rho$ (POSITIVE)

Molecule AB	$\Delta\rho$ in binding region	$\Delta\rho$ in antibinding regions behind nuclei	
		A	B
N ₂	0.25	0.13	0.13
CO	0.21	0.13	0.18
BF	0.21	0.21	0.20
C ₂ ^{a)}	0.50	0.06	0.06
BeO	0.82	0.02	0.57
Be ⁺ O ⁻	0.59	0.02	0.20
LiF	0.47	0.01	0.36

a) Ref. 55

"antibinding" electrons away and apart from "binding" electrons. A region of charge deficit of the form of $p\pi$ atomic density is evident on those nuclei where such a charge density was situated, a demonstration of the rather easy mobility of π electrons. While the original atomic densities are distorted so as to place charge in the antibinding regions, regions which pull the nuclei apart, as well as in the binding regions, regions which pull the nuclei together, in the formation of a molecule, the most important aspect is the exact disposition of the charge in the molecule, and not necessarily the amount of charge. Both of these features, the amount of charge, and its disposition can be only taken into account properly by a determination of the forces which bind the nuclei together to form the molecule, as will be done in the next chapter. An idea of the charge distribution can be roughly obtained from Table (2.2) where we list the total amount of electronic charge minus the free atom densities contained within the zero contours in the binding and antibinding regions, except in the case of BeO and LiF where we report these numbers for the total binding and antibinding regions, as one has to deal with nuclei enclosed by zero contours. In the discussion that follows, the density difference function $\Delta\rho$ is compared for the isoelectronic series N_2 , CO, BF; LiF, BeO and C_2 .

a) N₂, CO, BF

The $\Delta\rho$ map for N₂ exemplifies the reorganization of the atomic charge densities which is characteristic of the formation of a covalent bond. There is a net accumulation of negative charge, symmetrically placed between the nuclei. The large accumulation of charge density in the antibinding region behind each nucleus is also characteristic of any bond which involves the participation of p orbitals. This pattern is not found for example in H₂ or Li₂⁽⁵⁵⁾, for which the charge is concentrated almost entirely in the region between the nuclei. The large separate accumulations of charge in the antibinding region are a direct consequence of the quantum mechanical result of imposing directional properties on orbitals and hence on charge densities which possess angular momentum. The binding in CO is covalent as the difference map is very similar to that of N₂. But the charge increase is shifted towards the vicinity of the O nucleus. Simultaneously, there is apparently more charge removed in perpendicular regions at the O nucleus than at the other end of the molecule. The charge increase is still larger when one goes to F in BF. The perpendicular charge removal also follows the same trend. In fact, we see now the appearance of p π electrons situated quite diffusely at the B end of the molecule. From the numerical integration

of the various regions as reported in Table (2.2), it is evident the population numbers are all quite similar, N_2 showing slightly more charge in the binding region, i.e. between two nuclei where it exerts an attractive force on both. The difference in charges in the binding region between N_2 and CO would seem to have been put behind the O nucleus. This does not correlate with the dipole moment C^-O^+ , but the answer to this is evident from the geometry of the density difference diagrams. The density accumulated behind C is more diffuse than that behind O so that its centroid is farther away from the C nucleus. This farther displacement therefore contributes to the moment, and not the population itself. Similarly, one notes that there is more charge put behind the F nucleus, but again the effect is offset by the increased diffuseness of the charge accumulated behind the B nucleus. The maximum charge displacement behind the F nucleus is in accord with its acquiring the most $p\sigma$ character. This also correlates with Davidson's⁽¹⁰⁴⁾ recent population analysis on these same three molecules, where, contrary to popular belief, it was shown that the more electro-negative element has the larger degree of "hybridization".

b) LiF, BeO, C₂

The ionic extreme in binding is exemplified by LiF. Here the charge increase is localized on the F nucleus. The

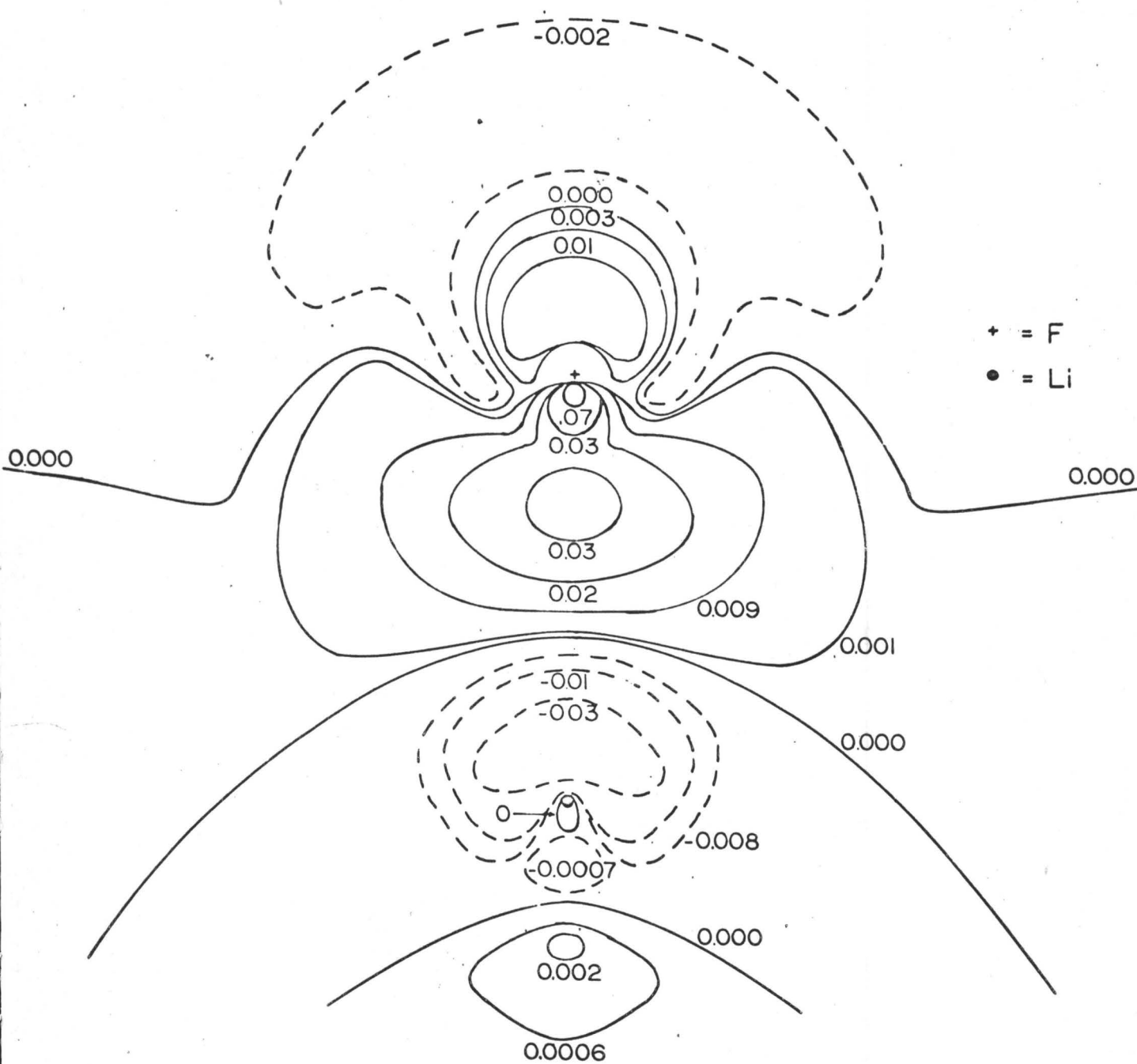
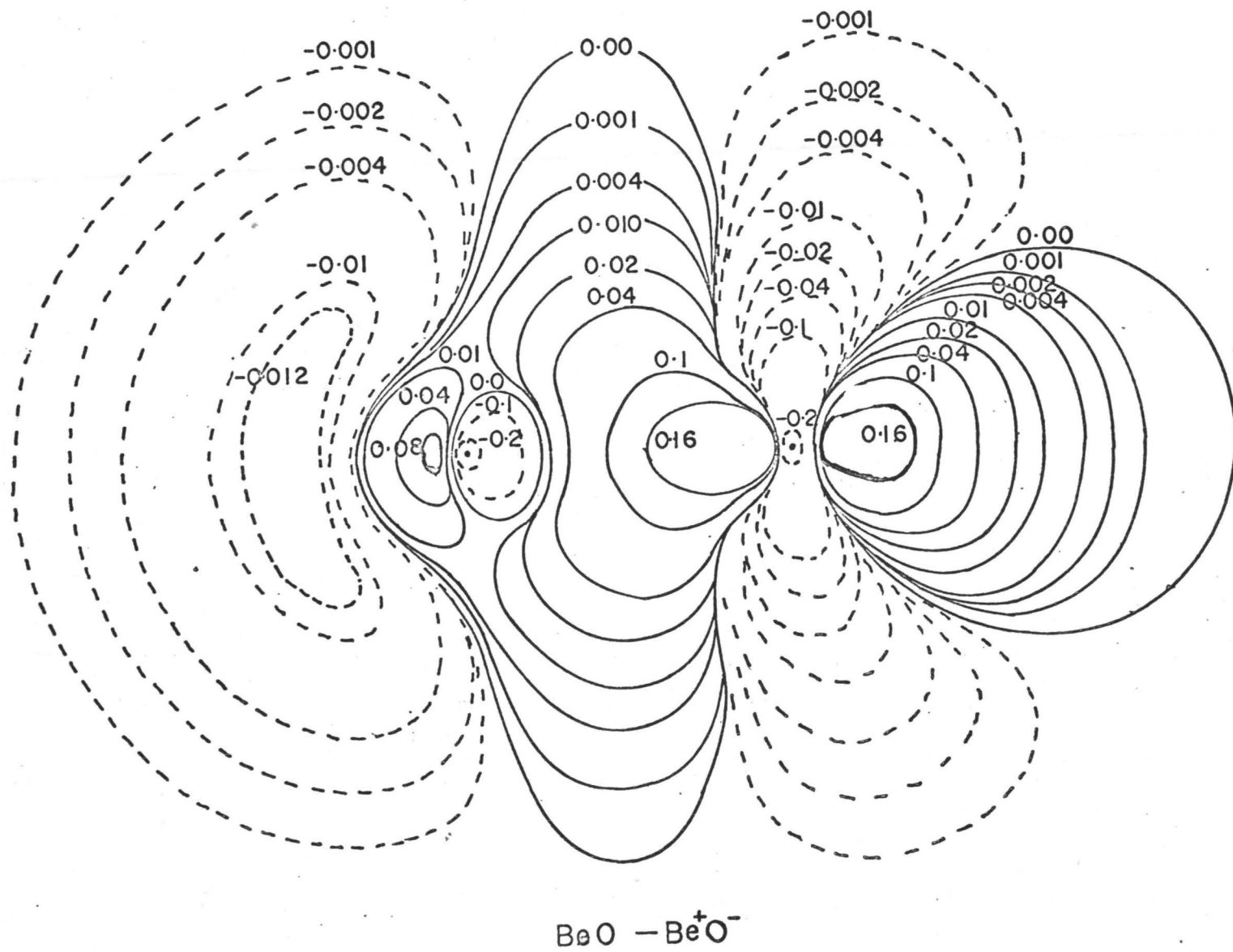


Fig.(2.3) - $\Delta\rho$ map (Li^+F^-)

small charge increase in charge density immediately behind the Li nucleus is a result of a polarization of the remaining core density of an Li^+ ion. The $\Delta\rho$ population is seen to be completely situated on the F nucleus, as it is enclosed by a zero contour with that nucleus. In view of this transfer of charge to F and the resulting negative electric field, the density on the Li nucleus must polarize away from the bond region to counter the net attractive force of the excessive density on the F nucleus. Alternatively, one can say the density on the Li nucleus is being repulsed by the accumulated charge on the other end of the molecule. In view of the clear separation of charge in two distinctive regions, it is then appropriate to speak in terms of electrostatic effects. This will be pursued further in the next chapter. The total charge increase in the zero contour encircling the F nucleus is 0.83 with 0.48 charge in front of that nucleus, a clear indication of polarization effects. A depletion of charge in a region perpendicular to the bond is suggestive of motion of $2p\pi_{\text{F}}$ density away from the F nucleus. This behaviour persists for the density difference diagrams involving the ions Li^+ , F^- , i.e. the combined densities of these ions have been subtracted from the total density of the molecule⁽¹⁴⁾. It is evident from Fig.(2.3) more

Fig. (2.4) - $\Delta\rho$ map (Be⁺O⁻)

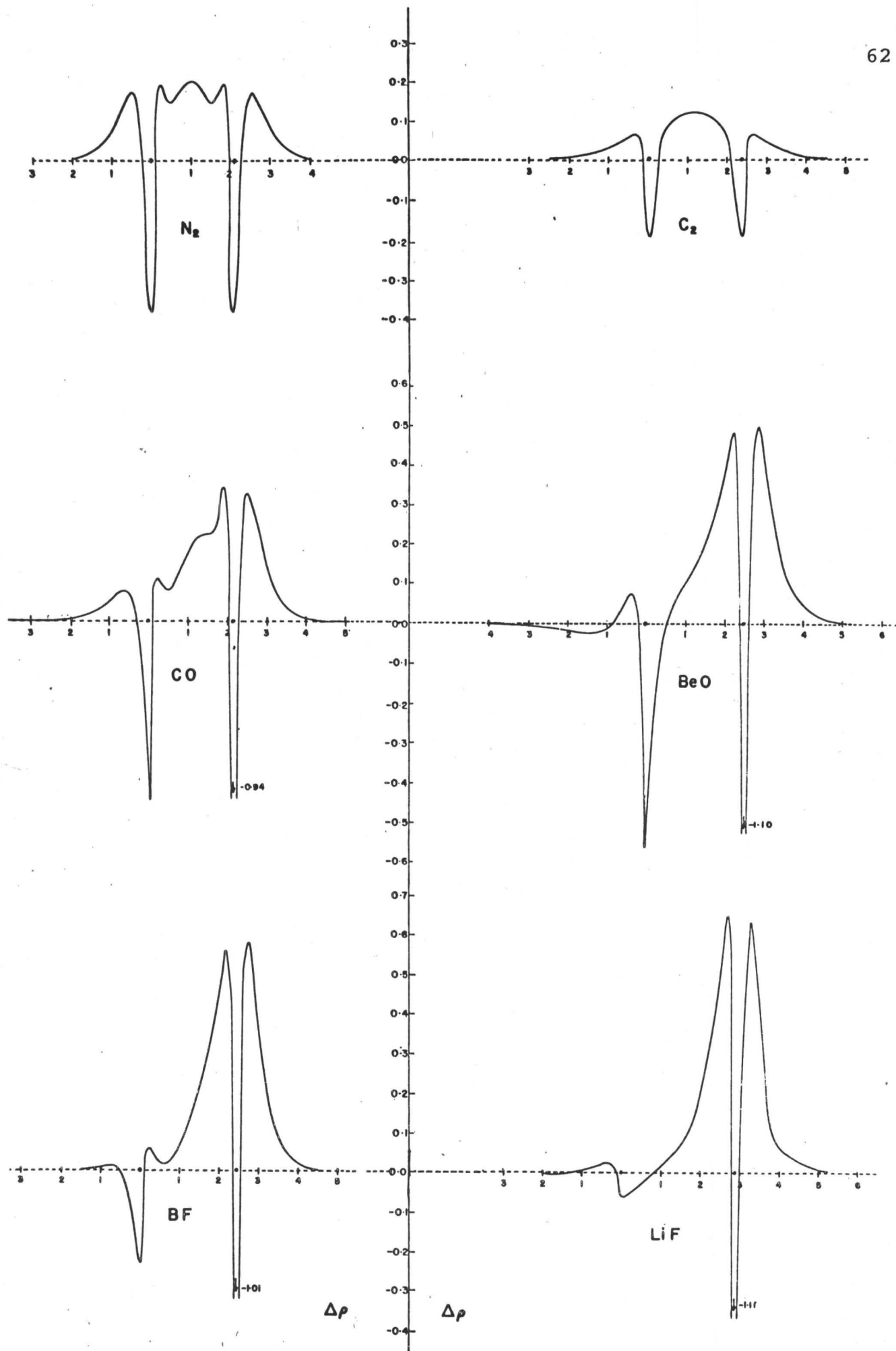
charge is placed in front of the F nucleus both along and perpendicular to the bond.

The BeO diagram shows similar features, but the transfer of charge is not as sharply defined as in the case of LiF. The positive increase in the binding region between the nuclei which is closest to the O nucleus is 0.82. The charge increase behind is 0.57. The total increase is therefore 1.39. The amount of charge lost in the perpendicular region at O is -0.55, whereas at F for LiF it is -0.19. Thus it is evident that bonding effects are more drastic in BeO. It must be remembered that the "valence-state" of the O atom is $2s^2 2p\sigma^0 2p\pi^4$ so that we have introduced a deficiency in the internuclear region. A density difference map using the constituent separated ions $\text{Be}^+ \text{O}^-$ ($2s^2 2p\sigma^1 2p\pi^4$) shows little noticeable changes as the O^- density is diffuse compared to a neutral O atom (see Fig.(2.4)). The contours around the Be nucleus for this map also show little change, indicating that the density around this nucleus must be approaching that of Be^{++} . The small values for the integrated positive $\Delta\rho$ regions behind Li and Be are effectively a result of polarizations of $1s^2$ densities. Large $\Delta\rho$ populations behind the heavy nuclei are evidence of redistribution of valence-shell densities. In fact recent work on hydrides⁽⁵⁵⁾ shows that LiH remains ionic ($\text{Li}^+ \text{H}^-$) as for this

molecule the $\Delta\rho$ population behind Li is the same as that in LiF. On the other hand, for BeH the $\Delta\rho$ population behind Be is large as a result of the promotion of the 2s valence electrons in Be to 2p σ atomic orbitals. This suggests that BeH is not to be associated with any well-defined limiting bonding case, i.e. covalent or ionic.

The negative contours which appear in front of the Li and Be nuclei in LiF and BeO and also persist in the density difference diagrams using the ions as separated constituents are reminiscent of repulsions of the Pauli exclusion type between two closed shells⁽¹⁰⁵⁾, an effect which enhances removal of charge between two separated closed shell charge densities when allowed to overlap. The net effect from the viewpoint of the density maps is a backpolarization of the densities on the Li and Be nuclei, which can be interpreted as an electrostatic repulsion of this density by the density transferred to the other end of the molecule.

C₂, which represents the covalent extreme of these two molecules, has been discussed amply by Bader et al⁽⁵⁵⁾. The small densities in the antibinding regions (see Table(2.2)) are therefore a compromise between charge decrease at the electropositive ends of the molecule and the large charge increase at the other end. They thus reflect these two

Fig. (2.5) $\Delta\rho$ Profiles

opposing tendencies, charge removal from one end and charge transfer to the other end, which by symmetry of the molecule C_2 now must happen simultaneously at one nucleus.

2.4 $\Delta\rho$ Profiles

Much of the charge density which affects the nuclei most profoundly and vice versa lies along the internuclear axis. In order to gauge clearly the effects of the charge density in regions near the nuclei it is advantageous to examine profiles of the density difference maps along the internuclear axis and in particular at the nuclei themselves. These are shown in Fig.(2.5) for all the molecules discussed above.

For all these systems, there is charge removal from the nuclear region. The relative magnitudes of these for the same nuclei in different molecules correlate also with the total charge densities at these nuclei as given in Table (2.1). In general, the charge removal is fairly constant for the same nucleus in different molecules, as can be seen from the profiles for BF and LiF, CO and BeO. There is a removal of charge in increasing order N, O, F. The tightness of the atomic densities of these increase in that same order, reflecting the increasing nuclear charge. The charge decrease at the other end is not as regular, being largest at C and Be, and smallest at B and Li in order. For those atoms which contain $p\sigma$ character, i.e. B,

C, O, F, there is evident increase in density in front and behind these nuclei, an effect which increases with nuclear charge. In other words, the profiles indicate clustering via maxima farther outward from the nuclei. This can be taken as evidence of the orbital contraction of the second principle quantum number atomic orbitals. Thus, as succinctly stated by Richardson⁽¹⁰³⁾, the clustering phenomena proposed by Ruedenberg⁽⁸⁷⁾ is indeed observed. It turns out to be synonymous with charge build up in the binding and anti-binding regions close to the nuclei. The decrease of density at the nuclei is not evident for protons such as in H_2 and HF ⁽¹⁴⁾ where there is actual charge increase. Hence, conclusions based on considerations of the H_2 molecule only must be viewed with caution, since protons are usually the exception rather than the rule, as a result of the uniquely small electron densities associated with them. It is to be noticed that Li and Be, which have no ps atomic densities, do not show clustering in the bonding region. Instead, there is charge decrease for these two in this region. It is evident that from the electropositive end, LiF and BeO are quite similar in character.

2.5 Concluding Remarks

If current notions regarding the transfer of charge in the formation of a molecule are effectively correct, one

would expect the density difference maps to show patterns which are characteristic of and distinct for limiting bond types. The density and density difference maps could then be used as the basis for definitions of distinct bond types. Up till now, the available diagrams suggest three distinctive bond types: a) the homonuclear pattern represented by N_2 and C_2 ; b) the heteronuclear pattern presented by LiF and $LiH^{(55)}$; c) a second heteronuclear pattern represented by the remainder of the first row hydrides. Both patterns a) and b) possess the most distinctive features as portrayed by our maps. Pattern a) has charge symmetrically placed between the two nuclei, in the σ -region; charge placed behind each nucleus and removal of charge at both nuclei perpendicular to the bond. In general, such a pattern, which is by definition covalent, can be qualitatively described in terms of σ -type and π -type, binding and anti-binding charge distributions, the last characteristics being derived from a force analysis pursued in the next chapter. Pattern b), termed the ionic case, has charge accumulated in two regions: around the nucleus associated with the relatively greater transfer of charge and extending a considerable distance along the internuclear axis toward the other nucleus; and to the far side of the nucleus associated with the lesser increase in charge. Pattern c) differs from pattern b) primarily in the behaviour of the

zero contour around the heavier nucleus: it either does not close upon itself or it encloses a very large volume, while the region of positive $\Delta\rho$ surrounding the lighter atom is mostly in front of it and thus binding. This pattern may be unique as a result of the presence of the proton.

N_2 , CO, BF belong to pattern a). This is a result of their isoelectronic structure and the occurrence of p σ character in the separated atom densities. The diagrams justify this classification. Nevertheless, in BF there is evidence of increasing unequal sharing of the density, and thus BF marks to some extent the transition between the examples of charge transfer (ionic character) and sharing of charge (covalent binding). LiF and BeO fall in the classification of pattern b). The BeO molecule is, however, not as clearcut as LiF. There is evident in BeO some density sharing in the regions perpendicular to the bond axis. Thus, BeO marks the beginning of a transition in the opposite direction of BF, i.e. from ionic to covalent.

The total molecular charge distributions and their properties will obviously determine the magnitude of the force constants of these molecules. One might expect that the degree to which the charge distribution relaxes during motion of the nuclei will be determined to some extent by

the tightness of the molecular charge distributions. For instance, those charges which are tightly bound to a certain nucleus will follow such a nucleus during its motion. This will particularly be true of core electrons. This effect will decrease with decreasing tightness of binding. Similarly, the $\Delta\rho$ maps which provide a detailed picture of the net reorganization of the charge density in the molecule with respect to some separated atoms, and are therefore characteristic for bonds of different type, are also of importance in the understanding of the force constants. It is to be expected that the stretching of a bond will correspond to a reversal of the direction of charge transfer shown by the $\Delta\rho$ maps. The $\Delta\rho$ maps demonstrate emphatically where charge transfer has occurred in the formation of a bond. A stretch of the bond by an infinitesimal amount will reverse the direction of this process, as the stretch corresponds to a reversal of bond formation. Similarly, contraction of the bond would cause enhancement of the $\Delta\rho$ patterns. One would thus expect that just as the $\Delta\rho$ patterns differ radically through the series from N_2 to LiF, so will the patterns of the relaxations of the charge density caused by nuclear motion demonstrate such characteristics. These anticipated results along with the nature of the binding in these molecules are further investigated in the succeeding chapters.

III. THE ELECTROSTATIC INTERPRETATION OF
ELECTRON DENSITIES

"For without a force there is no connection;
without connection, no order; without order,
no space."

Immanuel Kant

3.1 Introduction and Definition

The Hellmann-Feynman theorem, or more appropriately the electrostatic theorem to emphasize its application, offers another operational viewpoint from the usual tyranny of the energy representation of quantum mechanics. In essence it states that all forces on atomic nuclei in a molecule can be considered as purely classical interactions involving Coulomb's law. This implies the conclusion that the force on any nucleus in any system of nuclei and electrons is just the classical electrostatic attraction of other nuclei and the electron charge density $\rho(\vec{r})$. The theorem appears, therefore, as a powerful tool for researches in quantum chemistry. For if once the electronic density is known accurately, the forces acting on the different nuclei can be determined exactly and the energy for a given nuclear configuration follows by integration.

The proof of this theorem is quite simple. Consider

a system of n electrons and N nuclei, the latter fixed, i.e. the limit of zero nuclear momentum (adiabatic or Born-Oppenheimer approximation). Let $\vec{\nabla}_a$ be the gradient operator with respect to the coordinates of nucleus A . The Schrodinger representation gives the following equation of motion of the electrons:

$$H\Psi = E\Psi \quad (3.1)$$

where $H \equiv T_{el} + V$ is the Hamiltonian operator, E the energy of the system, and Ψ the electronic wave function. The force acting on nucleus A is:

$$\vec{F}_A = -\vec{\nabla}_a E = -\vec{\nabla}_a \left(\int \Psi^* H \Psi d\tau_1 \dots d\tau_i \dots d\tau_n \right) \quad (3.2)$$

where $d\tau_i$ implies integration of the volume coordinates of electron i . The operation (3.2) gives:

$$\begin{aligned} \vec{F}_A = & - \left(\int \vec{\nabla}_a \Psi^* H \Psi d\tau_1 \dots d\tau_n + \int \Psi^* H \vec{\nabla}_a \Psi d\tau_1 \dots d\tau_n \right) \\ & - \int \Psi^* (\vec{\nabla}_a H) \Psi d\tau_1 \dots d\tau_n \end{aligned} \quad (3.3)$$

The term in parentheses vanishes for an exact wavefunction because it is equal to:

$$E \vec{\nabla}_a \left(\int \Psi^* \Psi d\tau_1 \dots d\tau_n \right) = E \vec{\nabla}_a (1) \equiv 0 \quad (3.3a)$$

Furthermore, the kinetic energy operator T_{el} of the electrons is independent of nuclear coordinates for fixed electron coordinates. Therefore:

$$\vec{F}_A = -\vec{\nabla}_a E = -\int \Psi^* (\vec{\nabla}_a H) \Psi d\tau_1 \dots d\tau_n = -\int \Psi^* (\vec{\nabla}_a V) \Psi d\tau_1 \dots d\tau_n \quad (3.4)$$

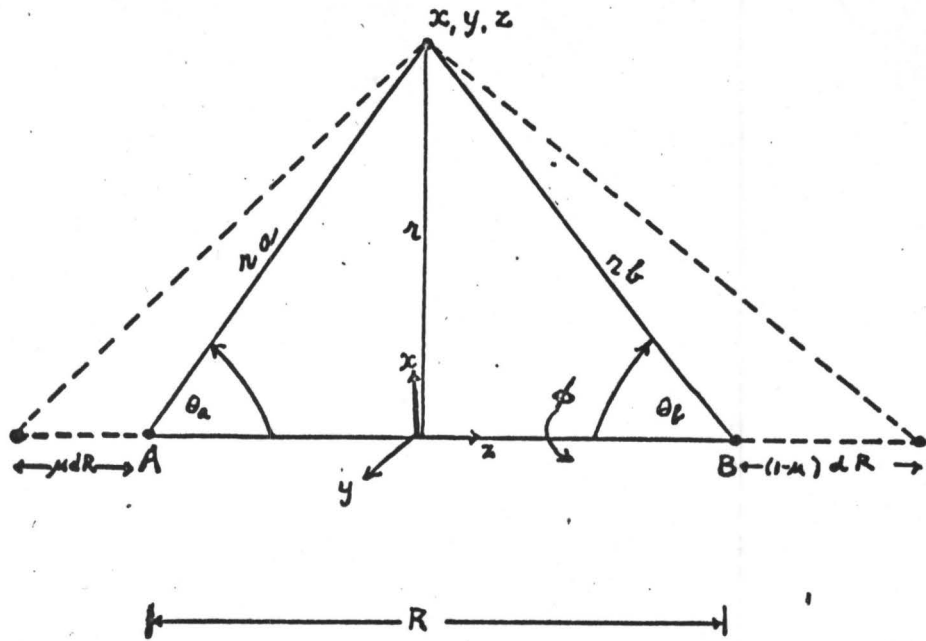
where V is the potential energy operator of the system.

The expression (3.4) is the fundamental equation of Hellmann and Feynman. The operator V is comprised of three parts: the electrostatic interaction between nuclei V_{nn} , the electron-nuclear interaction V_{en} , and the interaction between the electrons themselves V_{ee} . This last part is independent of the nuclear coordinates for fixed electron coordinates, a point further discussed below, and its contribution to (3.4) vanishes. The interaction between the nuclei is independent of the electronic coordinates and hence can be immediately integrated out. The detailed operator V_{en} is:

$$V_{en} = - \sum_{i=1}^n \sum_{a=1}^N \frac{Z_A e^2}{|\vec{R}_a - \vec{r}_i|} \quad (3.5)$$

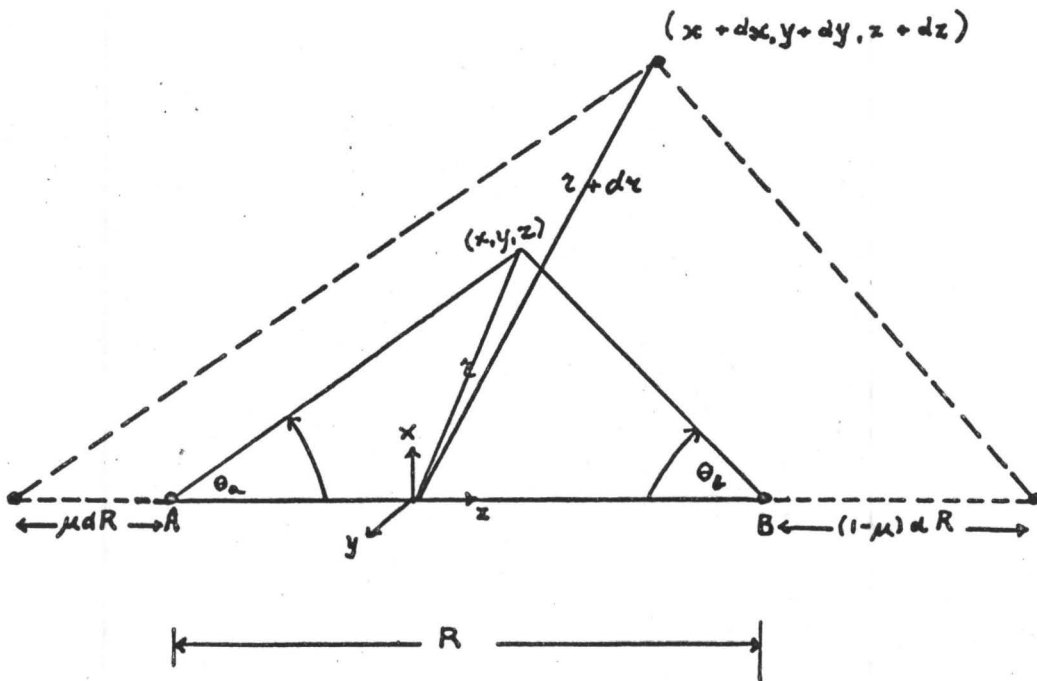
where \vec{R}_a is the coordinate vector of nucleus A and \vec{r}_i is the electronic coordinate vector with respect to some common origin. Z_A is the nuclear charge of A . Since V_{en} is a one-electron operator, the integral (3.4) can be easily transformed into an integral involving the 3-dimensional electronic density (1st order density matrix) of the system, i.e.

$$\int \psi^* (\nabla_a V_{en}) \psi d\tau_1 \dots d\tau_n = \sum_{i=1}^n \int \rho_i(\vec{r}_i) \nabla_a \left(\frac{-Z_A}{|\vec{R}_a - \vec{r}_i|} \right) d\tau_i \quad (3.6)$$



Fixed Electron Coordinates

Fig. (3.1)



Scaled Electron Coordinates

Fig. (3.2)

where ρ_i is the electron density of electron i , i.e.

$$\rho_i = \int \Psi^* \Psi \, d\tau_1 \dots d\tau_{i-1} d\tau_{i+1} \dots d\tau_n$$

Summing over i , we obtain

$$\int \Psi^* (\vec{\nabla}_a V_{en}) \Psi \, d\tau_1 \dots d\tau_n = Z_A \int \rho(\vec{r}) \vec{\nabla}_a \left(-\frac{1}{|\vec{R}_a - \vec{r}|} \right) d\tau \quad (3.7)$$

where ρ is the total electronic density of the system.

Therefore, the force acting on nucleus A is given by

$$F_A = -\vec{\nabla}_a V_{nn} - Z_A \int \rho(\vec{r}) \vec{\nabla}_a \left(-\frac{1}{|\vec{R}_a - \vec{r}|} \right) d\tau \quad (3.8)$$

The theorem can be generalized to degenerate electronic states (Hall⁽⁴⁵⁾). We therefore see that all distortion energies, dissociation energies, etc., can be functionals of ρ alone. For instance, for a diatomic molecule, $\vec{\nabla}_a = -d/dz_a = +d/dz_b = +d/dR$ (see Fig.(3.1)), then

$$D = E(\infty) - E(R) = - \int_R^\infty F \, dR \quad (3.9)$$

so that for an exact ψ the interelectronic term $1/r_{ij}$ would not enter the computation. The approach has been pursued by Hurley⁽¹⁰⁶⁾ in a series of papers and also by Bader⁽¹⁰⁷⁾.

For an exact wavefunction since from (2.3a):

$$2 \int \psi H \frac{\partial \psi}{\partial R} d\tau = \int H \frac{\partial \rho}{\partial R} d\tau = 0$$

and for space fixed electron coordinates

$$\frac{\partial T_{el}}{\partial R} = \frac{\partial V_{ee}}{\partial R} = 0$$

this implies that

$$\int H \frac{\partial \rho}{\partial R} d\tau = \frac{\partial \langle T_{el} \rangle}{\partial R} + \frac{\partial \langle V_{ee} \rangle}{\partial R} + \int V_{e-n} \frac{\partial \rho}{\partial R} d\tau = 0 \quad (3.10)$$

Therefore, the electron correlations affect ρ but do not affect the forces directly as they do also the energy calculations.

One can see, therefore, that the Hellmann-Feynman approach has many advantages, in particular giving rise to alternative ways of getting at energy differences of iso-electronic processes besides also giving the forces. These methods have been studied recently by Epstein et al⁽¹⁰⁸⁾ giving rise to the integrated and integral Hellmann-Feynman formulae. Time-dependent extensions of the approach can be also found in the works of Hayes and Parr⁽¹⁰⁹⁾, and also Epstein⁽¹¹⁰⁾.

Unfortunately, the variational principle does not apply to these methods. Little progress has been made with the applications of the Hellmann-Feynman theorem since its discovery of some thirty years due to a further difficulty that the theorem does not always hold for approximate wavefunctions and can, in fact, lead to absurd results in cases where sufficient care is not taken in the choice of an approximate wavefunction. Consider as an example the molecule H_2^+ and let R be the internuclear distance. The derivative dE/dR is then the slope of the potential energy

curve. If the wavefunction for the ground state is taken to be a simple linear combination of $1s$ orbitals centered on the two protons, the slope calculated is from the Hellmann-Feynman theorem negative at all internuclear distances⁽¹¹¹⁾. This corresponds to a completely repulsive curve. On the other hand, if the same wavefunction is used to calculate the energy directly, one obtains a reasonably satisfactory potential energy curve. The source of the difficulty lies in the approximate wavefunctions's failure to allow for charge polarization. This case has been discussed at length by Hurley⁽¹⁰⁶⁾. He gives methods of modifying the approximate wavefunctions in order that the Hellmann-Feynman theorem may be brought into agreement with direct calculations of the energy. If one realizes that any function may be expanded in terms of a fixed set of functions (i.e. which do not depend on the nuclear configuration), then only if all the variational parameters are chosen by the Ritz variational method do the electrostatic and conventional, i.e. dE/dR , method coincide. In particular, a wavefunction which does not vary at all with the nuclear configuration will give the same results by the conventional and electrostatic methods, a rather impractical but yet instructive example. Furthermore, Heitler-London functions as in the H_2^+ example above, which depend explicitly on nuclear coordinates if expressed in

terms of a single fixed set of Cartesian coordinates because the functions are built up of atomic orbitals rigidly attached to one of the nuclei of the molecule, will not give the same results by both methods. To remedy this deficiency, Hurley has introduced "floating functions" because of the treatment of the internuclear distance as a variable parameter. Such functions, determined by the variational principle satisfy the Hellmann-Feynman theorem. In general, as seen from Eq.(3.3) for a wavefunction to obey the theorem we must have

$$\int \frac{d\Psi^*}{dR} H\Psi d\tau + \int \Psi^* H \frac{d\Psi}{dR} d\tau = 0 \quad (3.11)$$

Wavefunctions which satisfy this equation are called stable⁽⁴⁵⁾. If the variation of the wavefunction with R is described in terms of a set of parameters α_k , then for a stable function

$$0 = \frac{dE}{dR} - \left\langle \frac{\partial H}{\partial R} \right\rangle = \sum_k \left(\frac{\partial E}{\partial \alpha_k} \right)_R \frac{d\alpha_k}{dR} \quad (3.12)$$

A floating function is defined by the vanishing of each term in the sum over k⁽¹¹²⁾, so that any stable function may be expressed as a floating function by a suitable choice of parameters. The theorem is satisfied if either the parameters are independent of R so that $d\alpha_k/dR = 0$ or else parameters are optimized so that $\partial E/\partial \alpha_k = 0$. Hirschfelder and Coulson⁽¹¹³⁾ have discussed the use of certain hypervirial relations for the construction of

stable wavefunctions.

Floating functions, however, do not lead to an accurate estimate of the atomic polarizability⁽¹¹⁴⁾ or good energies⁽¹¹⁵⁾. There are valid objections to floating functions. Firstly, as Longuet-Higgins and Brown⁽¹¹⁶⁾ have shown, it requires much energy to detach the center of a charge density from a nucleus. Secondly, it has been shown⁽¹¹⁷⁾ for H_2^+ , by Miller and Lykos that a maximum distortion of bonding atomic orbitals occurs at the equilibrium internuclear distance (- they also point out that this does not correspond to maximum overlap, a condition usually invoked for strongest bonding). The important first order effect in the distortion of atomic orbitals in molecule formation is the polarization of the atomic orbital. This polarization phenomenon can be understood as arising from external fields of neighbouring charges. This sort of example has been considered by Salem and Wilson⁽¹¹⁸⁾. A neutral atom in an external field does not move. The force on the nucleus due to the polarized electronic charge cancels out exactly the effect of the external field. This was pointed out among others, by Sternheimer⁽¹¹⁹⁾, in terms of shielding and antishielding concepts, later extended to the interpretation of quadrupole coupling constants.

It is evident that in all the cases where the

applications of the Hellmann-Feynman theorem to approximate functions gives physically unacceptable results, the difficulty may be traced to a clearcut physical deficiency in the wavefunction, which is intrinsically related to the parameter undergoing variation. In general, calculations of dE/dR by means of the theorem leads to errors which are of 1st order in ϵ if ψ differs from the true wavefunction by terms of order ϵ as shown by Salem and Wilson. This is in contrast to the calculation of E and therefore dE/dR , for which errors are of second order in ϵ ⁽³⁸⁾. However for stable functions, which Hall has shown includes Hartree-Fock functions, the Hellmann-Feynman theorem leads to errors which are only second order in ϵ , as the conventional method. The Hartree-Fock functions belong to the category of stable functions since they are stationary solutions of the type (3.11), as can be seen from the Hartree-Fock equations (see Appendix 1). This is the essence of Brillouin's theorem. This has also been considered generally by Stanton ⁽¹²⁰⁾ and is implicit in a paper by Allen ⁽¹²¹⁾. For variational functions, the success of this method, i.e. the magnitude of the correction ϵ , depends on how well the parameters chosen to minimize the ground-state energy can represent the operator one wishes to calculate. This provides a more subtle test than Brillouin's theorem. For example, the diamagnetic shielding $\langle 1/r_a \rangle$ is usually in

good agreement with experiment since it is an operator that plays a significant role in the energy of the molecule (in V) and therefore is favoured by the variational determination of the energy of the molecule.

For dispersion phenomena, Salem and Wilson have shown that the complete density to second-order is necessary to obtain the forces by the electrostatic theorem as opposed to the variational method where the first-order wavefunction yields the energy to 3rd order. On the other hand Yaris⁽¹²²⁾ obtains the 2nd order force using the first order density only. This result is not in contradiction with the results of Salem and Wilson. The difference is due to the way the systems have been divided. Yaris uses a relative electronic coordinate system centered on each of the two nuclei, i.e. functions which follow the nuclei. Thus in zeroth order, if nucleus A moves a distance dR , its electronic charge moves with it and hence $\partial H_0/\partial R = \partial \psi_0/\partial R = 0$, where H_0 and ψ_0 are the zeroth order Hamiltonian and wavefunction. Salem and Wilson used a space fixed electronic coordinate system and considered that moving nucleus A a distance dR leaves the zeroth order electronic charge unchanged. Thus in their method of dividing up the total Hamiltonian and wavefunction, $\partial H_0/\partial R$ and $\partial \psi_0/\partial R$ do not vanish, and the second-order wavefunction is necessary. Yaris's method involves an effective charge

model, or what Epstein et al⁽¹¹⁰⁾ call a complete orbital following model and only works for nonoverlapping shells but not for valence electron which are a case of incomplete orbital following, requiring knowledge of the exact wavefunction. Nevertheless, this example brings out one important point, namely, that the validity of the Hellmann-Feynman theorem and the stability of Ψ depend on the fundamental choice of integration variables. The value of dE/dR is independent of the choice. The precise form of the operator in the integrand, Eq.(3.2), depends upon the electronic coordinates fixed during the differentiation and in particular on the coordinate origin⁽¹²³⁾. For Cartesian or spherical polar coordinates arbitrarily centered, (see Fig.(3.1)) one can write (Berlin, Feynman):

$$\frac{dE}{dR} = -\frac{Z_A Z_B}{R^2} + Z_A \int \rho \frac{\cos \theta_a}{r_a^2} d\tau \quad (3.13)$$

where ρ is the electron density (diagonal element of first-order density matrix), Z_A is the nuclear charge of A, θ_a and r_a are defined in Fig.(3.1). Secondly, any orbital centered on nucleus A which completely follows that nucleus will contribute nothing to the force as shown by Yaris. This will be of importance in force constants where the nonorbital following becomes a "relaxation".

The electrostatic or Hellmann-Feynman theorem results when the electron is held fixed with respect to a

space fixed axis system during differentiation, thereby giving expressions (3.8). There is still some ambiguity since the nuclei may move in a number of ways during the differentiation. The nuclear motion may not be a pure vibration and, if movement is allowed only along the z-axis, it is possible for some translation of the molecule to occur. We will consider first, the case where there is no molecular translation, i.e., as R changes, the center of mass remains fixed with respect to the space fixed axis system. For a diatomic molecule with masses m_a and m_b , the center of mass is a distance uR from center A with $u = m_b/(m_a+m_b)$. If the center of mass is to remain fixed, nucleus A must move by an amount $u dR$ and nucleus B by $(1-u)dR$ (see Fig.(3.2)). For this fixed electron method, $\partial H/\partial R = \partial V/\partial R$, as discussed at the beginning of the introduction. Using the spherical coordinates shown in Fig.(3.1), which are the most convenient for our purpose, then:

$$\frac{\partial V}{\partial R} = -\frac{Z_A Z_B}{R^2} + \frac{\partial V}{\partial r_a} \frac{\partial r_a}{\partial R} + \frac{\partial V}{\partial r_b} \frac{\partial r_b}{\partial R}$$

It is easy to show that

$$\frac{\partial r_b}{\partial R} = (1-u) \cos \theta_b \quad \frac{\partial r_a}{\partial R} = u \cos \theta_a$$

Therefore

$$\frac{\partial V}{\partial R} = -\frac{Z_A Z_B}{R^2} + u Z_A \frac{\cos \theta_a}{r_a^2} + (1-u) \frac{Z_B \cos \theta_b}{r_b^2} \quad (3.13)$$

Now translation has no effect on the energy, i.e. $dE/dR_T=0$

where d/dR_T implies translation (isotropy of space),
i.e. moving both nuclei by amount dR in the same direction,

$$\frac{dE}{dR_T} = \int \rho \left[Z_A \frac{\cos \theta_a}{r_a^2} - \frac{Z_B \cos \theta_b}{r_b^2} \right] d\tau = 0 \quad (3.14)$$

which merely expresses the fact that the electronic forces on each nucleus are equal and opposite. Therefore, we can add any multiple of Eq.(3.14) to (3.13) without changing the resulting force at all. The result will be that we can obtain different expressions for the same equation⁽¹²⁴⁾. If we choose to keep nucleus B fixed and allow nucleus A to move, then

$$\left(\frac{\partial V}{\partial R} \right)_{z_b} = - \frac{Z_A Z_B}{R^2} + \frac{Z_A \cos \theta_a}{r_a^2} \quad (3.15)$$

which implies that the center of mass moves by $u dR$, i.e.,

$$\langle \Psi | \left(\frac{\partial V}{\partial R} \right)_{z_b} | \Psi \rangle = \langle \Psi | \frac{\partial V}{\partial R} | \Psi \rangle - u \frac{dE}{dR_T}$$

One can easily show by integrating the electron density ρ over (3.15) that keeping nucleus B fixed gives Eq.(3.13), the expression originally derived by Feynman and Berlin.

For scaled coordinate systems with scale factors dependent on R , it is not possible to reduce dE/dR to a one-electron integral. For example, for a diatomic molecule and trial functions constructed from confocal elliptic coordinates $\lambda = (r_a+r_b)/R$, $\mu = (r_a-r_b)/R$ and ψ , see Fig.(3.2), $1/R$ plays the role of a scale factor. The

Hellmann-Feynman relation in that case for exact and stable functions becomes identical to the quantum mechanical virial theorem⁽⁷⁰⁾, i.e.

$$RdE/dR + 2\langle T \rangle + \langle V \rangle = 0 \quad (3.16)$$

This comes about because now one has another choice of independent variables, λ and μ , and the electrons move during the differentiation. The movement is such that the internal angles θ_a and θ_b describing the electronic position remain fixed as R changes, as shown in Fig.(3.2). This is exactly equivalent to keeping the ratios r_a/R and r_b/R fixed. It is easy to see then that:

$$T(R,r) = \frac{T(l,r')}{R^2} \quad (3.17)$$

since T is a homogeneous function of second degree.

$$V(R,r) = V(l,r')/R$$

since V is homogeneous of first degree. The notations $T(l,r')$ and $V(l,r')$ indicate that these three quantities are now independent of R , and $r' = r/R$. Therefore

$$\left(\frac{\partial T}{\partial R} \right)_{r'} = \frac{-2T(l,r')}{R^3} = \frac{-2T(R,r)}{R} \quad (3.18)$$

$$\left(\frac{\partial V}{\partial R} \right)_{r'} = \frac{-V(l,r')}{R^2} = \frac{-V(R,r)}{R}$$

$$\left(\frac{\partial H}{\partial R} \right)_{r'} = \frac{-2T-V}{R} \quad (3.19)$$

or that $\frac{dE}{dR} = -\frac{1}{R} \langle \psi | 2T+V | \psi \rangle$ which is equivalent to (3.16).

The failure of approximate wavefunctions, eg. Heitler -

London functions, constructed from atomic orbitals rigidly attached to more than one nucleus to satisfy the electrostatic theorem was due to the fact that they were a complete orbital following model and hence required "floating" to remedy the deficiency. Nevertheless, they satisfied the virial theorem and hence showed binding. The equivalence of these two theorems demonstrates the close connection between the Hellmann-Feynman and virial theorems for scaled coordinate systems. In general, one can obtain conditions different from optimum scaling that lead to approximate wavefunctions for which the virial relationships are valid⁽¹²⁵⁾. These conditions will not lead to good approximate wavefunctions just as floating functions which satisfy the Hellmann-Feynman theorem give poor energies. As Löwdin⁽¹²⁶⁾ has shown, the validity of the virial theorem is not a sufficient condition for testing the accuracy of a wavefunction. Only for exact and stable wavefunctions is the condition to satisfy the virial and Hellmann-Feynman theorems both necessary and sufficient.

3.2 Chemical Binding

We have shown on the basis of wave mechanics that the electric forces exerted on the nuclei by the molecular electronic distribution can be interpreted from the electrostatic viewpoint when the molecule is in a stationary state, even though the charge distribution is dependent on the

electronic motion in as much as the electrons have kinetic energy.

Berlin⁽¹²⁾ has made an interesting subdivision of the space around a diatomic molecule into "binding and antibinding regions", according to whether negative charge in a given region tends to push the nuclei together electrostatically or to pull them apart. The binding region is of course between the two nuclei, but in a diatomic molecule it extends out at each end to a conical boundary making an angle of 125° with the bond line for a homonuclear. This angle decreases with increasing disparity in nuclear charge at both ends of the molecule so that in ethane, for example, even the electrons of the C-H bonds have a net antibinding effect on the carbon nuclei. This sort of observation has been used by Bader and Preston⁽¹⁰⁵⁾ to criticize the usual notions of hybridization in determining geometries in three and four-center molecules. In an attempt to give precise meaning to the covalent and ionic bond concepts, the approach was also extended to diatomic molecules, LiF, LiH, and HF⁽¹⁴⁾. The interpretation made in these papers and fully expanded in an analysis of the first-row diatomics⁽⁵⁵⁾ makes use of the electrostatic point charge model concepts of shielding and antishielding in addition to polarization and overlap contributions to forces. This differs from the Berlin treatment, primarily

because of the L.C.A.O. approximation inherent in the Hartree-Fock functions used, whereby one can associate each molecular orbital with distinct separated-atom atomic orbitals. This enables one to see how the forces in a molecule change upon formation of a bond between the separated atoms and correlate these with the types of bonding present.

The force exerted on nucleus A in a diatomic molecule A-B is as we have seen above

$$F_A = \frac{Z_A Z_B}{R^2} - Z_A \int \rho(\vec{r}) \frac{\cos \theta_a}{r_a^2} d\tau \quad (3.20)$$

When each molecular orbital is occupied the electron density is

$$\rho(\vec{r}) = \sum_i n_i \phi_i^2(\vec{r}) \quad (3.21)$$

where n_i is the occupation number of orbital ϕ_i , and the orbitals are assumed orthogonal so that one has the advantage of the additivity evident in (3.21). It is convenient to define a quantity f_{iA} for each MO as the force exerted on nucleus A by the density in the i th MO multiplied by R^2/Z_A . This gives a dimensionless number, and the total force on nucleus A becomes:

$$F_A = \frac{Z_A}{R^2} (Z_B - \sum_i f_{iA}) \quad (3.22)$$

The force on each nucleus is zero for large values of R

and for the equilibrium internuclear separation R_e . Thus at these two values of R , $Z_B = \sum_i f_{iA}$ (or $Z_A = \sum_i f_{iB}$ for Z_B). For large values of R each f_{iA} value reduces to the orbital occupation number of the atomic orbital with which the i th MO correlates. This is a result of the fact that at this limit the charge density on atom B exerts a field at A equal to that obtained from an equivalent number of point charges located at the B nucleus, irrespective of the symmetry of the atomic orbital. Each electron thus effectively shields one unit of nuclear charge and for a molecule which dissociates into neutral atoms, $\sum_i f_{iA} = Z_B$ and F_A becomes zero. For smaller values of R , however, the exact disposition of the charge density in each orbital determines its f_{iA} value. An increase in the f_{iA} value over its value for large R implies that the formation of the molecule has resulted in a transfer of charge density to the region between the nuclei where it exerts a binding force on the nuclei in excess of the simple shielding of an equivalent number of nuclear charges. Such an MO is defined binding. The f_{iA} value may remain unchanged, in which case it is termed non-binding as it plays the same role in the molecule as it did for large values of R where the density simply shielded an equal number of nuclear charges. The f_{iA} value may decrease at R_e , in which case it is termed antibinding.

Each f_i value is the sum of three contributions which

are determined by the atomic and overlap populations. The force on A due to the density situated on A is termed an atomic force. This force is zero unless the atomic density on A is polarized. The overlap forces provide separate measures of the binding of both nuclei by the density resulting from the overlap of orbitals situated on A and B. Any inequality in the sharing of the overlap density by the two nuclei is made evident by differences in their overlap forces. The atomic density on B will shield some fraction of the nuclear charge on B from A. Thus the contribution to the force on nucleus A from the density situated solely on B is called the shielding force (or screening force as used by Bader et al).

Using these definitions, one can qualitatively analyze the working concepts, ionic and covalent bond. An ionic bond resulting from the transfer of one electronic charge between the atoms has the following characteristics⁽¹⁴⁾ in terms of the forces acting on the nuclei: the shielding of the cationic nucleus should be decreased by unity and the shielding of the anionic nucleus increased by units corresponding to the transfer of charge from one center to the other. The forces exerted by the overlap density should be ideally zero, or at least small and unequal for the two nuclei, as the transferred charge is centered on the anion as an atomic density and not in the overlap region. This

transfer of charge will result in the cationic nucleus experiencing a net electric field of $-1/R^2$. Thus, the remaining atomic density on the cation must polarize away from the anion to overcome the net attractive force. The atomic force term for the cation will thus be negative. The anionic nucleus will experience a force of repulsion due to the net positive charge centered on the cation. Thus the atomic density on the anion must be polarized toward the cation (positive atomic force) to achieve electrostatic equilibrium. A covalent⁽⁵⁵⁾ bond, on the other hand, is the result of the transfer of charge density from each atom to the region between the nuclei where it is equally shared by both nuclei. Thus for a covalent bond the shielding forces exerted on both nuclei should be decreased, and by the same amount. The resulting repulsive forces should then be balanced by large and equal overlap forces. Ionic character will be made evident by inequalities in the shielding and overlap forces exerted on the two nuclei.

The density distributions of N_2 , CO, BF, BeO, LiF are analyzed in the light of the above definitions in an endeavour to determine the nature of their bonding. A comparison of the forces as a result of these density distributions for these five molecules should allow us to gain insight into their types of bonding which range from the purely covalent N_2 to the nearly ionic LiF. The

next step will then be to analyze the changes of these forces as a nucleus undergoes an infinitesimal displacement. This will bring us into the realm of force constants.

3.3 Interpretation of N₂, CO, BF

In the density chapter, we have pictured the formation of a chemical bond for these molecules along the lines of simple valence bond theory. This was considered from the viewpoint of the overlap of singly occupied orbitals ($p\sigma$ orbitals) of atomic densities derived from ground state valence states, with additional rearrangement of charge as put in evidence by the density difference maps. In the force analysis which follows now, this method allows one to correlate the various molecular orbitals with the appropriate atomic orbitals in the separated atoms as represented by their valence states. For N₂ and CO, a straightforward correlation is also possible from the orbital energies of the ground state free atoms listed in Table 3.1. Some difficulty is encountered with BF, since both the $2s_F$ and $2p_F$ orbitals are all lower in energy than the corresponding B atomic orbitals. This would mean that upon dissociation of this molecule, according to the MO picture, one would end up with the B atom in a 2P state ($2s_B^2 2p\pi_B^1$) and the F atom with the configuration ($2s_F^2 2p\sigma_F^2 2p\pi_F^3$) also in a 2P state. In order to keep continuity of discussion, we assume that each valence state, corresponding to the slightly perturbed

Table 3.1

ORBITAL ENERGIES

Orbital	Energies			
	B	C	O	F
2s	-0.495	-0.706	-1.244	-1.573
2p	-0.310	-0.433	-0.632	-0.730

Table 3.2

FORCES ON N^{a)} IN N₂ R = 2.068 a.u.

a.o.	MO	f _i (R=∞)	f _i (R _e)	A	O	S
1s ¹	1σ _g	1.000	1.160	0.152	0.008	1.000
1s ¹	1σ _u	1.000	1.085	0.074	0.014	0.997
2s ¹	2σ _g	1.000	2.682	-0.042	1.842	0.882
2s ¹	2σ _u	1.000	-0.463	-0.775	-0.167	0.470
2pσ ¹	3σ _g	1.000	0.150	-1.766	1.221	0.696
2pπ ²	1π _u	2.000	2.433	0.416	0.935	1.082
Totals		7.000	7.046	-1.943	3.853	5.136

a) Calculated from Cade et al's function Ref. 59

ground state atoms, has one singly occupied $p\sigma$ orbital. By this artifice, the 5σ MO is always correlated with a $p\sigma$ atomic orbital on each separated atom. The 3σ MO correlates with the $2s$ atomic orbital on the heavy atom, whereas the 4σ MO correlates with the $2s$ orbital of the light atom. We demonstrate the interpretation firstly for N_2 , following the account of Bader et al⁽⁵⁵⁾.

a) N_2

In this homonuclear case, each molecular orbital correlates with an atomic orbital on nucleus A and one on B. Of the pair of electrons in the i th molecular orbital, the one which correlates with atom A contributes zero to the value of f_i at large R and the one which correlates with atom B contributes a value of unity (except π 's which give 2). Table 3.2 gives a breakdown of the orbital forces. The calculations are for $R_e = 2.068$, i.e. the experimental distance. At the Hartree-Fock minimum, $R_e = 2.013$, the total f_i 's are 6.986. This is an assurance that the wavefunctions are indeed accurate and will reproduce one-electron properties to a high degree of accuracy, probably to within 1% of the true value, as suggested previously by Goodisman and Klemperer⁽⁴⁵⁾. The individual f_i 's do not differ significantly between those for the experimental R_e and Hartree-Fock R_e . (see Appendix 3)

One can obtain a quantitative measure of the binding

or antibinding nature of each MO by comparing its f_i value with unity. The $1\sigma_g$ and $1\sigma_u$ are slightly binding due to what is termed innershell polarization, the polarization being towards the nuclei. This can be seen from the atomic contribution to the force. The near zero overlap contributions indicate that no amount of charge has been transferred from either atom in the formation of the "core" orbitals. The $2\sigma_g$ is a strongly binding orbital as its electron density exerts an attractive force on the nuclei which is almost three times greater than the simple shielding or nonbinding value of unity. $f_{2\sigma_u}$ is negative so that the $2\sigma_u$ orbital is strongly antibinding in the sense that it not only deshields the nuclear charges, but tends to increase the repulsion between the nuclei by pulling them apart. The total density in the $2\sigma_g$ and $2\sigma_u$ orbitals gives a small net binding (2.22). This is slightly greater than the nuclear charge of 2, which is to be shielded. The strong binding force exerted by the $2\sigma_g$ density may be interpreted as the result of two effects: the accumulation of charge in the overlap region and an inward polarization of the remaining atomic densities on each nucleus. The transfer of charge to the binding region is reflected in the shielding value being less than unity. This disposition of the $2\sigma_g$ density is characteristic of all first-row homonuclears⁽⁵⁵⁾ except for C_2 and N_2 for

which the atomic force contribution is small and negative. This would then mean that some of the density is back-polarized and thus would also be responsible for the under-shielding. In such a case an actual population analysis performed by integrating could only settle the issue as to how much charge is actually present. However, for binding purposes it is the electric field experienced by the nucleus which is of importance and not the real population. The distinction between effective populations based on a field effect and real population numbers arises from the fact that we are looking at different moments of the density. The forces, corresponding to the $\langle r^{-2} \rangle$ moment, are in this work emphasized because they are what produces stability of molecules. The net populations corresponding to the zeroth moment of the density are not as significant from an operational standpoint. The large amount of charge density which is accumulated in the antibinding region by the $2\sigma_u$ orbital may be interpreted as the result of both an overlap and a polarization effect. A transfer of charge behind the nuclei results in a negative overlap and a considerable antishielding relative to the separate atoms. In addition, the atomic densities are strongly polarized outwards and exert a fairly large atomic force drawing the nuclei apart. The resultant feature of the density in the $2\sigma_g$ and $2\sigma_u$ molecular orbitals are a net attractive force from the

overlap density (the $2\sigma_g$ orbital placing more density in this region than the $2\sigma_u$ removes) and a net antibinding force from the atomic densities.

The surprising fact that the $3\sigma_g$ orbital shows antibinding (as opposed to the MO theory classification of it as a weakly bonding orbital) can be explained from the sign of its atomic force contribution. The charge density transferred into the binding region as the result of the overlap of $2p\sigma$ atomic orbitals is seen to be very contracted along the internuclear axis where it exerts a correspondingly large binding force on the nuclei (see Fig. 6 in Bader et al⁽⁵⁵⁾). Ruedenberg⁽⁸⁷⁾ has suggested that the main potential energy lowering of the electrons in a molecule occurs by such a contraction or clustering of valence electron density. There is also a very strong back polarization of the atomic density in that orbital, which results in an atomic force term which more than negates the large positive overlap contribution to the force. The $1\pi_u$ orbital, density is typical of a π -bond. There is considerable antishielding of the nuclei relative to the separated atoms, indicating that a substantial amount of charge is transferred to the overlap region. This overlap density is not particularly effective in binding the nuclei due to the presence of a nodal surface along the internuclear axis. It is the sum of the overlap and shielding contributions for the $1\pi_u$

Table 3.3

Forces on C in CO

 $R_e = 2.132$ a.u.

a.o.	MO	$f_i(R=\infty)$	$f_i(R_e)$	A	O	S
$1s^2_o$	1σ	2.000	2.000	0.000	0.000	2.000
$1s^2_c$	2σ	0.000	0.266	0.257	0.009	0.000
$2s^2_o$	3σ	2.000	2.527	-0.495	1.198	1.824
$2s^2_c$	4σ	0.000	1.271	-0.152	0.396	1.027
$2p^1_{\sigma c} + 2p^1_{\sigma o}$	5σ	1.000	-1.009	-2.334	0.788	0.536
$2p^1_{\pi c} + 2p^3_{\pi o}$	1π	3.000	3.056	0.216	0.762	2.078
Totals:		8.000	8.111	-2.508	3.154	7.466

Forces on O in CO

a.o.	MO	$f_i(R=\infty)$	$f_i(R_e)$	A	O	S
$1s^2_o$	1σ	0.000	0.319	0.319	0.000	0.000
$1s^2_c$	2σ	2.000	2.002	0.000	0.002	2.000
$2s^2_o$	3σ	0.000	2.346	0.955	1.178	0.213
$2s^2_c$	4σ	2.000	-1.295	-2.786	1.167	0.324
$2p^1_{\sigma c} + 2p^1_{\sigma o}$	5σ	1.000	0.962	0.524	-0.528	0.966
$2p^1_{\pi c} + 2p^3_{\pi o}$	1π	1.000	1.739	0.589	0.768	0.382
Totals:		6.000	6.072	-0.398	2.586	3.884

Table 3.4

Forces on B in BF $R_e = 2.391$ a.u.

a.o.	MO	$f_i(R=\infty)$	$f_i(R_e)$	A	O	S
$1s^2_F$	1σ	2.000	2.000	0.000	0.000	2.000
$1s^2_B$	2σ	0.000	0.352	0.336	0.016	0.000
$2s^2_F$	3σ	2.000	2.256	-0.310	0.408	1.999
$2s^2_B$	4σ	0.000	2.016	-0.347	0.727	1.636
$2p\sigma^1_B + 2p\sigma^1_F$	5σ	1.000	-1.042	-1.348	0.015	0.291
$2p^4_{\pi F}$	1π	4.000	3.490	0.059	0.349	3.082
Totals:		9.000	9.072	-1.451	1.515	9.008

Forces on F in BF

a.o.	MO	$f_i(R=\infty)$	$f_i(R_e)$	A	O	S
$1s^2_F$	1σ	0.000	0.325	0.323	0.027	0.000
$1s^2_B$	2σ	2.000	2.003	0.000	0.003	1.999
$2s^2_F$	3σ	0.000	1.569	0.991	0.533	0.045
$2s^2_B$	4σ	2.000	-0.834	-2.806	1.793	0.179
$2p\sigma^1_B + 2p\sigma^1_F$	5σ	1.000	0.914	0.672	-0.732	0.972
$2p^4_{\pi F}$	1π	0.000	1.062	0.632	0.367	0.064
Totals:		5.000	5.037	-0.189	1.966	3.259

B
(2)

C
(2)

N
(1)

O
(0)

F
(0)

3.0
2.4
1.8
1.2
0.6
0.0
-0.6

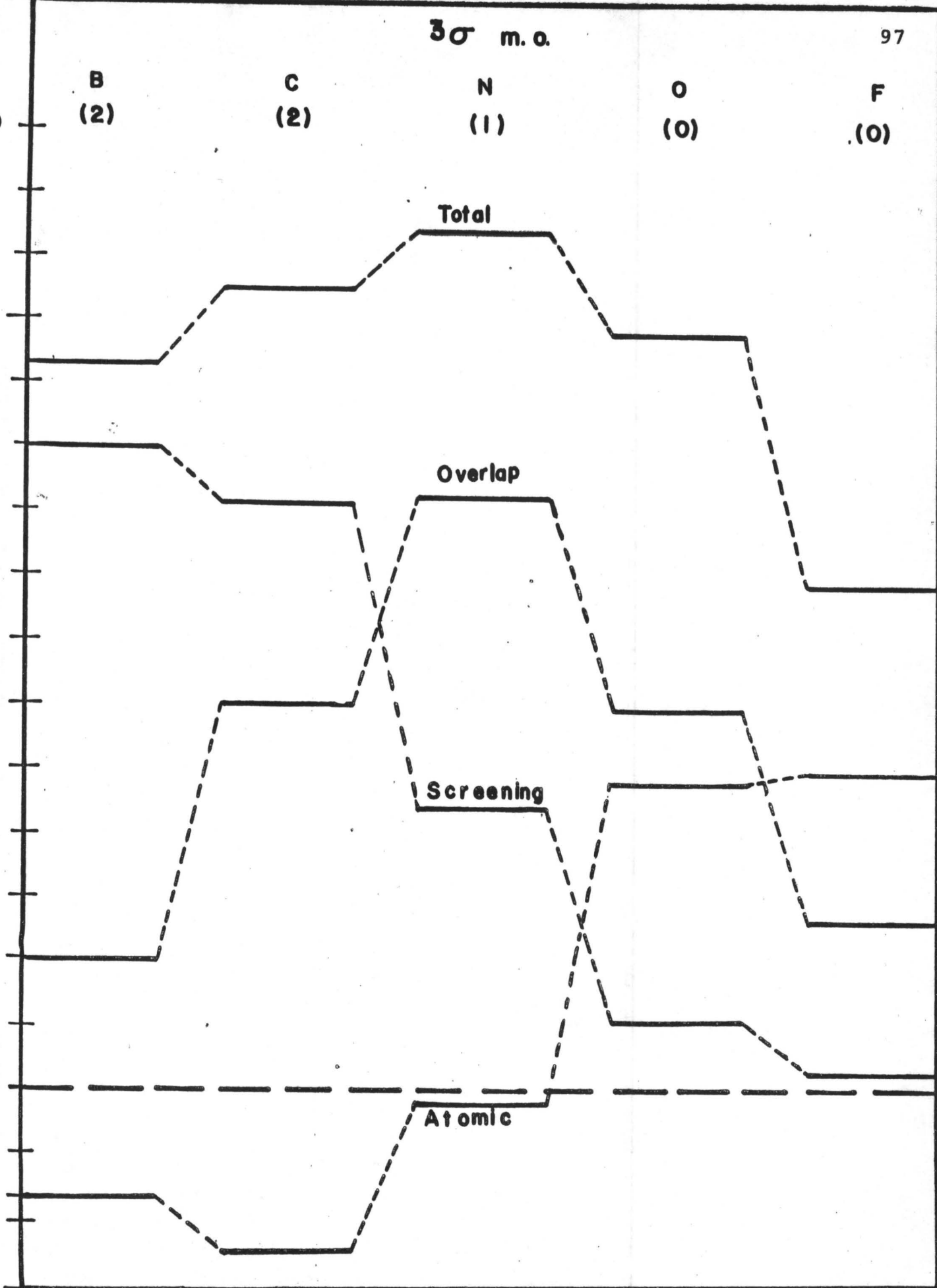


Fig.(3.3)

Footnote: In the diagrams, screening is shielding,

B
(0)

C
(0)

N
(1)

O
(2)

F
(2)

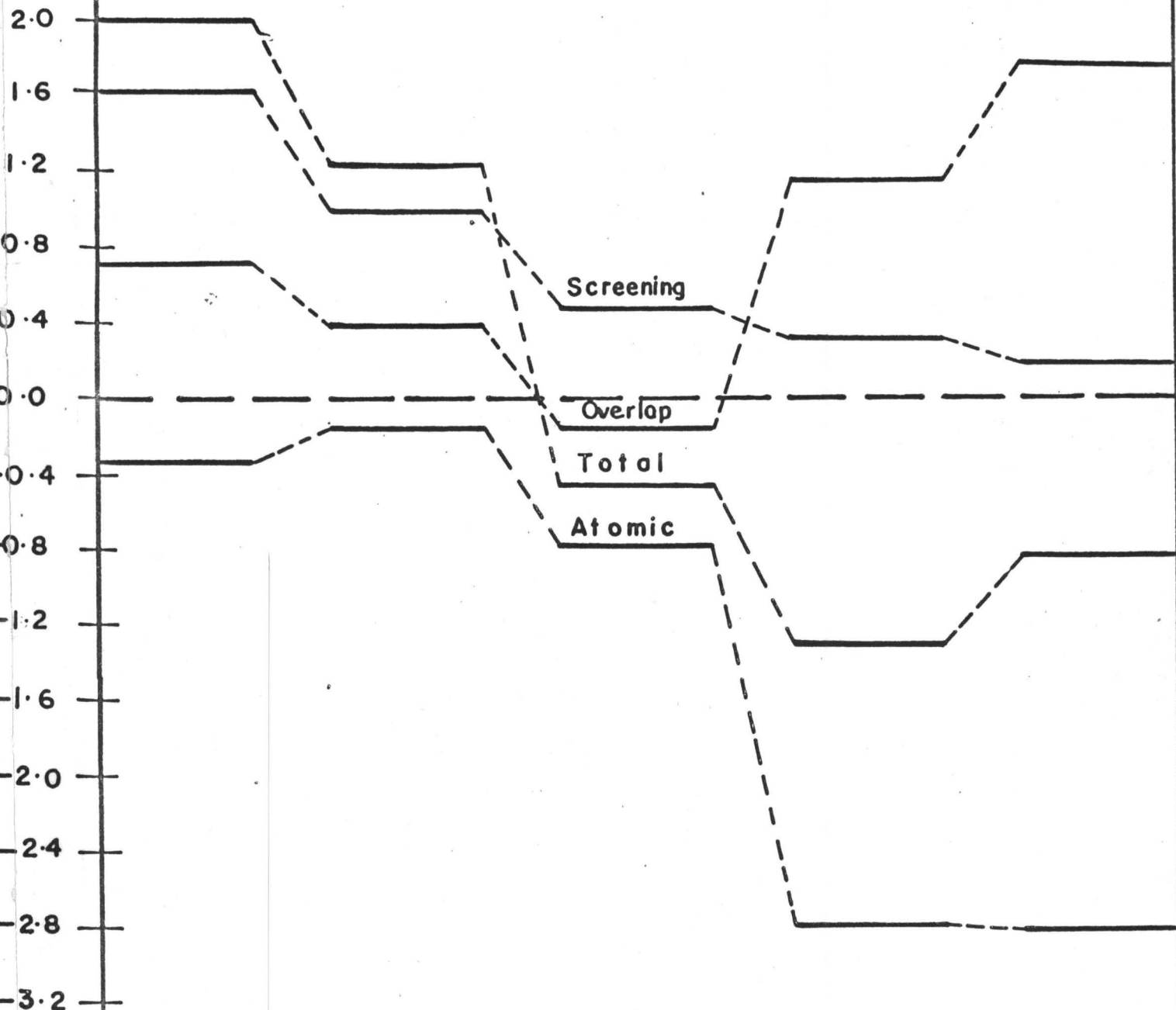
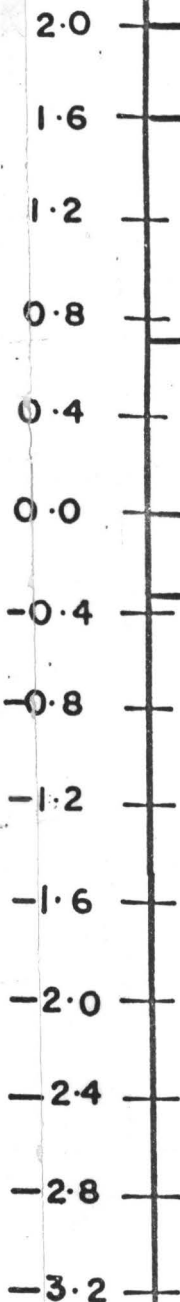


Fig. (3,4)

50 σ mo.

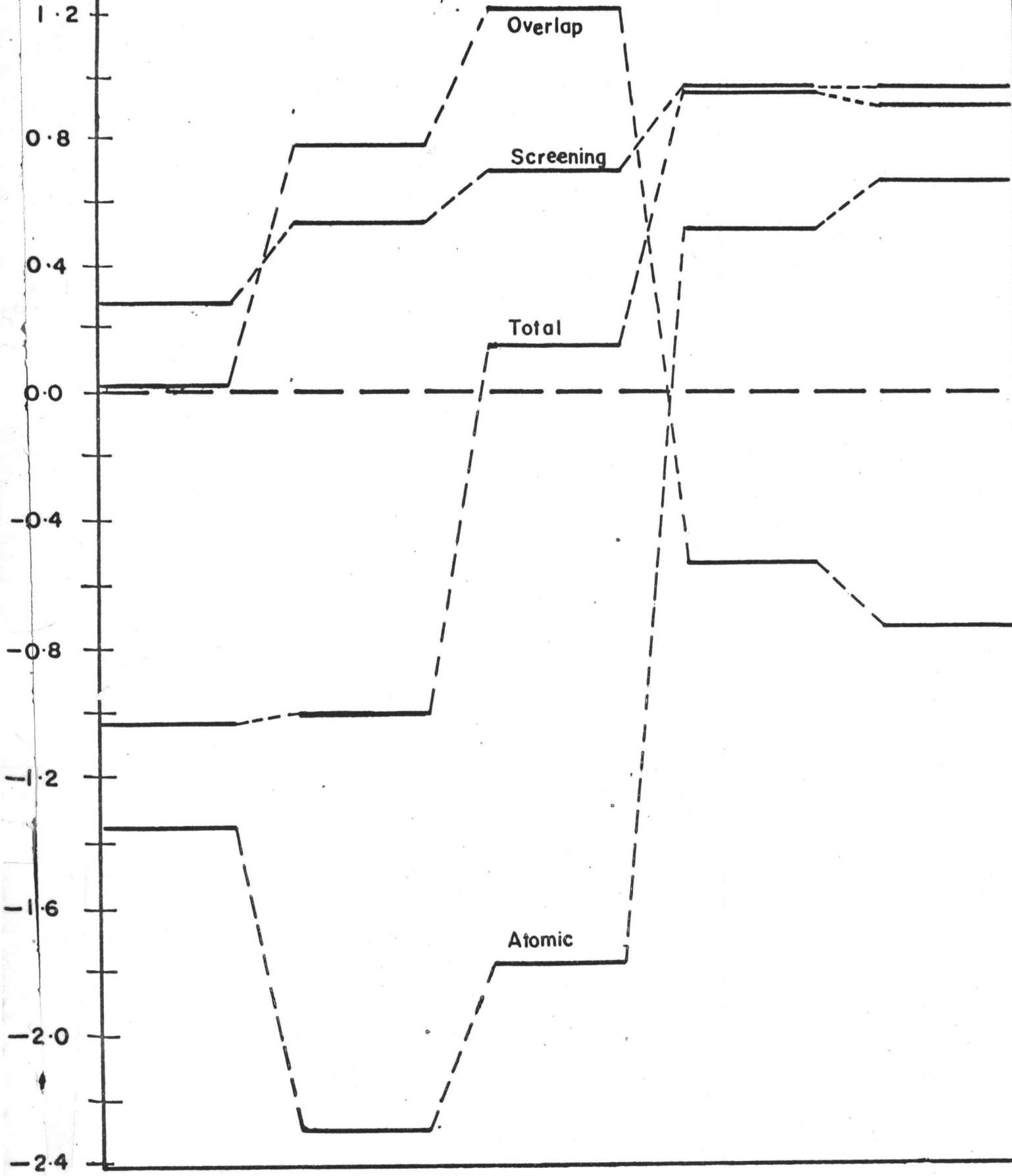
B
(I)

C
(I)

N
(I)

O
(I)

F
(I)



Fig, (3.5)

B
(4)

C
(3)

1π
N
(2)

O
(1)

F
(0)

3.6

3.0

2.4

1.8

1.2

0.6

0.0

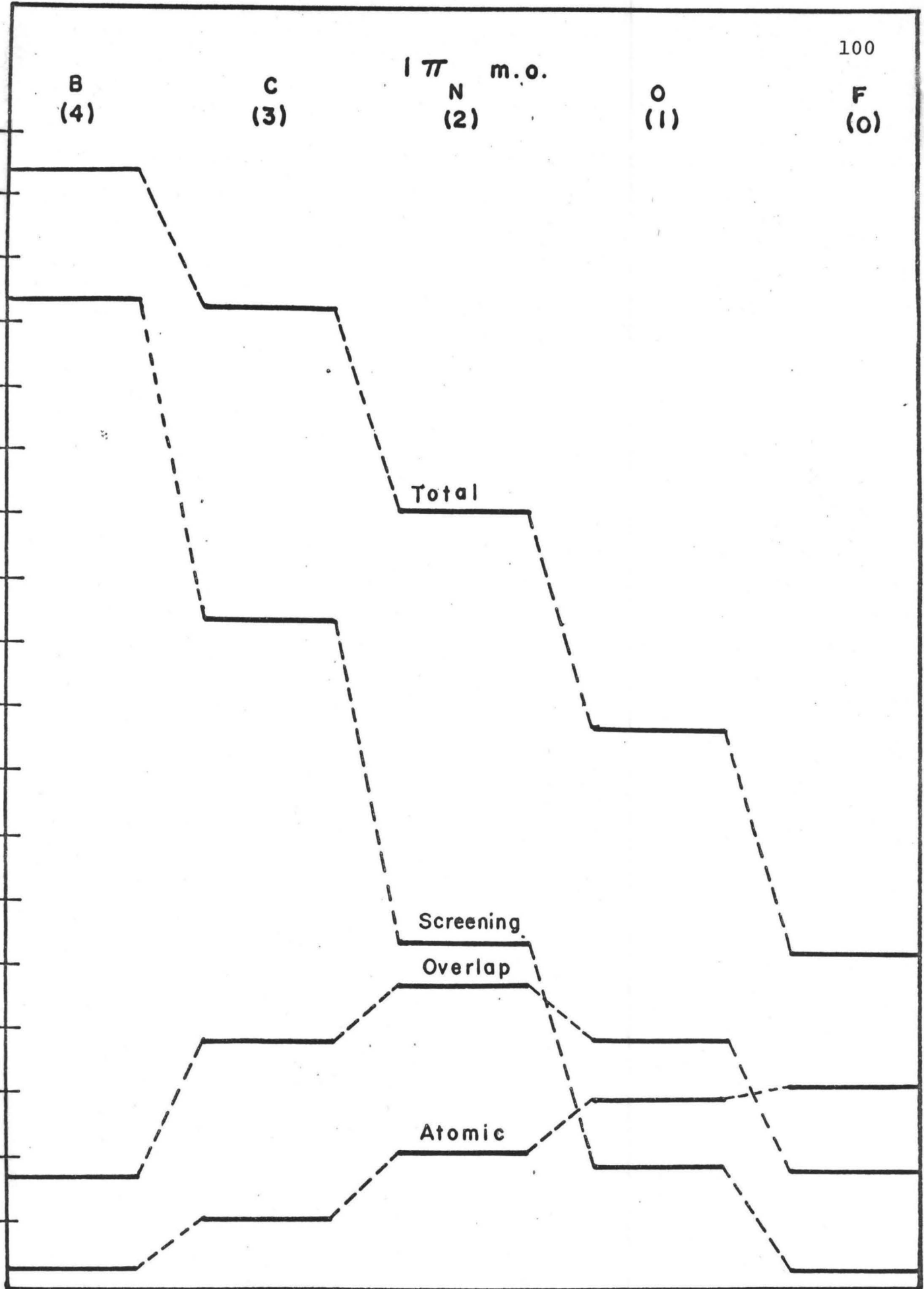
Total

Screening

Overlap

Atomic

Fig. (3.6)



orbital which is equal to unity, the nonbinding value. Thus the result of antishielding of the nuclei and transferring the charge density to the overlap region does not in itself, in the case of a pi-bond, result in any significant net binding.

b) CO, BF

In approaching these two molecules, we must now deal with a proliferation of numbers pertaining to the various orbital contributions to the forces. As the aim of this discussion is of comparative nature, it is more appropriate to demonstrate graphically comparative features. In Figures (3.3) to (3.6) are plotted the atomic, overlap and shielding components of the forces for the orbitals 3σ , 4σ , 5σ and 1π respectively. This is done for each atom, for which, in parenthesis, are listed the total forces corresponding to infinite separation, namely $f_i(\infty)$ (see Table 3.2). A zero $f_i(\infty)$ indicates charge centered on the nucleus considered whereas a non-zero value measures the shielding population of charge situated on the other nucleus. The 1σ and 2σ orbitals require little discussion as they are the inner $1s$ shells of each atom. These are all slightly polarized into the bond as in N_2 , and show negligible overlap effects as expected for such tightly-bound densities (see Tables 3.3 and 3.4 for the actual forces).

The 3σ orbital density as seen from a density map⁽⁶⁰⁾

is known to have the most density over all the other orbitals in the binding region. This is confirmed by the larger overlap forces for it as compared to other orbitals. The maximum force occurs for N_2 and is smallest at F, as a result of it being mainly $2s_F^2$. This localization of charge on the heavy nucleus is portrayed by the drastic decrease in shielding force from B to F. The localization is further indicated by the increase of atomic polarization, in the forward direction, at the heavier nucleus. The negative polarizations at B and C indicate some delocalization of the orbital density behind these nuclei. The overlap forces increase from both extremes B and F towards N. This suggests therefore that delocalization of this orbital is least for BF and largest for N_2 . In terms of net binding characteristics as delineated in the previous discussion, there is net binding at all nuclei, since for all cases the total force exceeds that predicted for the separated atoms. This is in keeping with the usual strong bonding characteristics of that orbital.

The 4σ orbital is characterized for N_2 by a node in the middle of the bond in view of the ungerade symmetry inherent. Thus, one would expect it to reflect characteristics quite different from that of the 3σ orbital. In fact, the overlap force is smallest at N and increases towards B and F, in opposite direction to that of the 3σ orbital. The

overlap force is maximum at the F nucleus. However, this is offset by a large backpolarization of the density on that nucleus, an indication of large $p\sigma$ character of that density. This backpolarization causes the orbital to be extremely antibinding. Maximum binding occurs at the other end of the BF molecule, i.e. at B, as a result of a large shielding force from the density on F. In fact, because of the way we have correlated this orbital with the separated atoms, this would suggest that charge has been transferred from B to F. The orbital is evidently delocalized in the bond region, as seen from the overlap forces, being the least so for N_2 because of the nodal property of a $2\sigma_u$ orbital. In the present scheme, the orbital is net binding at B and C, and net antibinding at N, O, F. For the latter three nuclei, the total forces are negative and therefore fall short of the non-binding shielding value of 2.0 (1.0 for N).

The 5σ orbital is the "mirror image" of the 3σ orbital as much of the charge is now localized on the light nucleus. Therefore, the shielding increases in going from B to F. The overlap force is maximum at N and minimum at F, where it is in fact negative. A negative overlap force is also exhibited at O. The reason for this behaviour can be found in the large backpolarizations of atomic densities on B and C. In the density discussions, we have already indicated that for these two nuclei, the atomic densities in the molecule are

more diffuse behind the nuclei than in the free atoms. Thus charge removal must occur in the bond region, especially near the heavier nuclei, via the agency of overlap in order to enhance expansion of density behind the nuclei at the other end of the molecule. This is then reflected in the signs of the overlap forces. There is charge delocalization, nevertheless, onto the heavy nuclei. The shielding forces at B and C indicate the delocalization is actually larger than for the 3σ orbital. For this latter orbital, the charge density was atomic $2s^2$ situated mainly on O and F, so that one would not expect it to be appreciably delocalized. The 5σ orbital must involve $p\sigma$ atomic character of density on the light nuclei as indicated by the large negative atomic forces for these. As a result of these, the orbital is anti-binding at B, C and N. At O and F the orbital is essentially non-binding, the principal contribution to the force being from shielding effects of density at the other nuclei. The orbital is therefore considerably less binding than the 3σ orbital, which has most of the charge situated on the opposite end of the molecule.

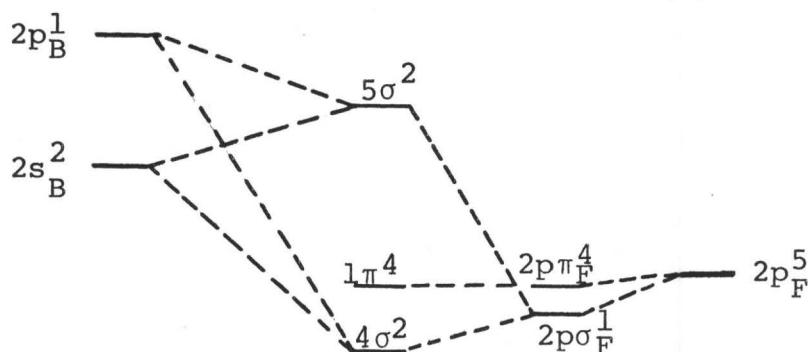
The 1π orbital is distinguished from the σ orbitals by a nodal plane in which lies the internuclear axis. This has the effect of introducing undershielding of π densities which are by symmetry requirements situated perpendicular to the internuclear axis. The maximum total force occurs at B,

decreases to a minimum at F. The principal cause of this trend is portrayed by the shielding force, which although is undershielding because of the geometrical nature of π densities, nevertheless contributes mostly to the force at the light nuclei. The overlap and atomic forces are small compared to these. Maximum overlap occurs at N_2 . The overall picture is then of a density distribution which becomes polarized towards the more electronegative element. Yet the overlap forces are equal at both ends of the molecule. Finally, the orbital is slightly antibinding at B, essentially non-binding at C and binding at the other nuclei, the net binding increasing in the direction towards F.

3.4 Spectroscopic Considerations

The above attempt at an orbital force analysis runs into some difficulty whenever an absolute correlation of molecular orbitals with separated atoms is not feasible, BF being one example. We have made it a point to retain the simple valence-bond picture of bond formation, by insisting on single occupancy of the $p\sigma$ orbitals of the separated atoms. In the case of BF, dissociation of the molecule as seen from the atomic orbital energies in Table 3.1 would predict the separated atoms to be in the configurations $B(2s^2 2p\pi^1)$ and $F(2s^2 2p\sigma^2 2p\pi^3)$. This corresponds to the $M_L = \pm 1$ components of the $2P$ atomic ground state of these, as opposed to the $M_L = 0$ component of that same state inherent in the valence-

bond picture. In order for this last picture to be operative, one would have to invoke crossing of the $2p\sigma_B$ and $2s_B$ components of the 4σ and 5σ orbitals as shown in the following diagram:



Since we adhere to the valence-bond picture in correlating the molecule with the separated atoms, some degree of arbitrariness is therefore imposed on the assignment of net binding properties of the MO's, properties defined with respect to the separated atoms. One might have expected this arbitrariness since using orbital f_i values in an interpretive scheme violates a desirable tenet of any acceptable interpretive approach, namely invariance to orthonormal transformations. The usefulness of the MO's resides nevertheless in the fact that when they are calculated by the Hartree-Fock method, the orbital energies are to a first approximation the ionization energy (Koopman's theorem⁽¹²⁷⁾). One can also on qualitative grounds, assign bonding powers to these^(78,128). Such facility in correlating spectroscopic features is not displayed by localized

equivalent orbitals⁽¹²⁹⁾ since removal of an electron from a molecule, for instance, comes from all over the molecule and not from a particular localized region of space⁽¹³⁰⁾. In order to pursue any possible correlation between orbital forces and spectroscopic properties of these for a molecule such as BF, an approach will be tried which puts less emphasis on the correlation with the forces from separated atoms. The previous analysis is still quite meaningful for N₂ and CO where the correlations derived from both the MO and valence-bond methods can be made to coincide without the difficulty of level crossing, by virtue of the relative energies of the atomic orbitals of the separated atoms being just right for such a correlation.

Concerning the usual bonding powers of these higher orbitals, we have noted before that upon ionization of a 5σ electron, BF and CO undergo a bond length decrease of 3.3% and .9% respectively whereas N₂ upon loss of the equivalent electron, namely 3σ_g, undergoes a bond length increase of 2.7%. Before remarking on the significance of this, it must be realized that the ions, other things being equal, are expected and observed to have usually shorter bond lengths than the uncharged molecules due to the contraction of the orbitals by the excess nuclear charge, i.e. due to less shielding. Robinson⁽⁷⁶⁾ has used a standard

arbitrary 4% correction due to this ion effect in the study of bonding powers of MO's in isoelectronic series. Thus he is able to show that the bonding ability of the 5σ orbital decreases as the electronegativity difference or polarity increases, and furthermore, that the bonding power of the $2\sigma_u$ orbital in N_2 is approximately half of that of the 4σ orbital in CO. The general conclusion is that for homonuclear molecules 5σ is more strongly bonding than 4σ but as the electronegativity difference between the atoms increases, 4σ becomes more strongly bonding. A knowledge of the orbital forces should allow for an even more direct physical interpretation of the ionization process. The removal of an electron from an orbital whose electron density exerts a force drawing the nuclei together should result in a decrease in the total attractive force in the ion and thus to an increase in R_e . The use of orbital forces in this way was first suggested by Berlin and applied by Clinton and Hamilton⁽¹³¹⁾ and by Hurley⁽¹³²⁾. These authors made the assumption that the forms of the orbitals remain unchanged during the ionization process. This simplification termed the rigid orbital hypothesis by Hurley is appealing as the net force of repulsion or attraction resulting from a vertical ionization will be simply one-half of the original force exerted by the pair of electrons in the i th MO.

Within the rigid orbital approximation, one can define a net force change, resulting from such an ionization, more explicitly. This will thus give us a measure of the change of the binding effect of an orbital. The definitions of bonding and antibonding, which are derived from energetic considerations and nodal characteristics of the molecular orbitals correlate remarkably well with the empirical definition regarding observed changes in bond length which accompany the removal of an electron in a diatomic molecules.⁽¹²⁸⁾

In order to compare binding characteristics and see if these correlate with bonding characteristics we define a Δf_i , corresponding to the change of force arising from the removal of an electron out of a possible n_i electrons in the orbital i . The net force which will tend to pull the nuclei together or apart is the result of the sum of the forces operative at each nucleus. If the forces at both nuclei are positive, i.e., pointing into the bond, then they will pull the nuclei together. The net force is defined by $(Z_A f_i^A + Z_B f_i^B)$, where Z_A and Z_B are the nuclear charges at A and B, f_i^A and f_i^B are the force per unit charge experienced by these nuclei respectively. The definition has meaning with respect to some arbitrary fixed point from which one views the motion of both nuclei at the same time (the point could be the center of mass as an example). Ionization reduces this net force by the factor $1/n_i$, since we are ionizing one

Table 3.5

FORCE CHANGES UPON IONIZATION
(RIGID ORBITAL APPROXIMATION)

Molecule	State	Orbital Ionized	Δf_i	$\Delta R_e/R_e$ (predicted)	Exptl. $\Delta R_e/R_e$ (%)
N ₂	X ² Σ _g ⁺	3σ _g	-1.05	+	+1.9
	A ² Π _u	1π _u	-8.516	+	7.2
	B ² Σ _u ⁺	2σ _u	+3.241	-	-2.0
CO	X ² Σ ⁺	5σ	-0.821	+	-0.9
	A ² Π	1π	-8.062	+	9.6
	B ² Σ ⁺	4σ	+1.367	-	+3.4
BF	X ² Σ ⁺	5σ	-1.508	+	-3.3 ^{a)}
	A ² Π	1π	-6.752	+	-
	B ² Σ ⁺	4σ	-1.287	+	-

a) This result is somewhat questionable in view of the experimental uncertainties (see Ref. 76). We thank Dr. P. E. Cade for pointing out this uncertainty.

electron out of n_i . Δf_i therefore becomes

$$\Delta f_i = \frac{-1}{n_i} [Z_A f_i^A + Z_B f_i^B] \quad (3.23)$$

If the net force is positive, then the resulting force upon ionization has been reduced by the amount Δf_i . A negative Δf_i therefore implies a decrease in force, and hence a bond lengthening; a positive Δf_i implies an increase in force and therefore a bond shortening, since positive forces are defined as being attractive. The Δf_i 's and the ΔR_e 's in Table (3.5) agree well with the experimental ΔR_e 's for N_2 . In the case of CO and BF, the 4σ and 5σ orbitals do not agree as well. As Bader et al⁽⁵⁵⁾ have shown, there is considerable reorganization of the charge density in orbitals other than the ones involved in the ionization process. This problem they have nicely discussed for some of the ions, both positive and negative, of N_2 and O_2 . Contraction of the orbitals and hence bond shortening occurs, but not regularly for each orbital. This is demonstrated by an increased binding of the remaining skeleton for positive ions as compared to the neutral molecule. The 5σ orbitals in CO and BF indicate that this contraction occurs for the ion as seen from their Δf_i 's. The 4σ orbital in CO is predicted to decrease the bond length upon loss of one electron, whereas experimental results indicate the opposite effect. As this loss comes from an orbital the

density of which is extremely backpolarized at the oxygen (atomic force of -2.8), the experimental result suggests considerable reorganization of charge which will tend to pull the nuclei apart even more than such an orbital density did in the neutral molecule. The π orbital Δf_i 's correlate very well with the experimental results. As is well known by diatomic spectroscopists⁽¹³³⁾ but not generally appreciated among chemists, 1π is a more effective bonding orbital than 5σ . This has been discussed theoretically in terms of overlap populations, as a bonding criterion, which in the last analysis Mulliken admits has no theoretical foundation and is fallible in extreme cases⁽¹³⁴⁾. The Δf_i 's demonstrate the binding characteristics to be in agreement with the experimental predictions, and therefore support the bonding properties of this orbital. In the ionization of a π electron there is considerable increase of the bond distance and this is fairly independent of bond polarity. This independence of polarity may be understood if one remembers that the π -bond behaves like a covalent bond as far as the overlap forces are concerned, as seen from the equality of these forces at both nuclei in the same molecule (Fig.(3.6)). The increased polarity of the 1π orbital is evident from the shielding forces. However, the increasing nuclear charge in going from N to F enhances any forces resulting from polarizations and overlap densities situated at these nuclei,

and thus equalizes to a large extent the Δf_i 's. The result is that orbital polarities as defined from population analyses⁽¹⁰⁴⁾ which reflect integrated charge densities associated with a particular atom, are not able to interpret the insensitivity to polarities of the bonding powers of the 1π orbital. It is the forces operative in the molecule from which one can predict Δf_i 's (preferably with non-rigid orbital wavefunctions of the ionized molecule also), which are a cause for the similarities of the binding (and bonding) characteristics of the 1π orbital.

The usual picture of localized "lonepairs" is not so evident using a force analysis. Energy considerations seem to indicate the existence of such isolated entities. For instance, Mulliken⁽¹³⁵⁾ long ago pointed out that discrepancies between free atom ionization potentials and "lone pair" ionization potentials in molecules can be reconciled simply by invoking electrostatic interactions (dipolar and charge transfer). Absence of vibrational structure on some Rydberg series and in photoionization has been often cited as evidence⁽¹³⁶⁾ for the presence of such nonbonding electrons. The force analysis suggests that such entities do not exist as isolated in view of the presence of sizable contributions from overlap and shielding, indicating delocalization. The largest backpolarization seems to come with largest overlap. This appears at F and O

in the 4σ orbital, implying significant hybridization in the chemical sense but also a fair amount of delocalization. This is consistent with the recent population analysis done by Davidson⁽¹⁰⁴⁾ on these same molecules, where it was shown that more electronegative element has the larger degree of hybridization in each case. Although the back-polarizations are large for the heavy nuclei, the exact disposition of these charges can best be inferred from the density and density difference diagrams. In fact, it was shown in the previous chapter, that for the heavier nuclei, atomic radii for densities situated on them are virtually identical to the radii of free atoms. This then demonstrates that the charge accumulated behind the heavy nuclei resides in a region close to these. The increase in charge in that region is slightly larger for F than for O. The relative position as gauged by the magnitude of the atomic and overlap forces suggests that for O the displacements of charge occur much closer to that nucleus. The amount of charge displaced behind the two nuclei O and F which is 0.18 and 0.20 respectively is not in accord with the usual large displacements associated with isolated "lone pairs".

At the other end of the molecules CO and BF, the densities indicated also charge transfer behind the nuclei C and B, the magnitude of which was equal for N, C: 0.13 and is at B: 0.21. The difference in disposition of these is

characterized by the increased diffuseness of these charges, thus correlating with the decreasing nuclear charge as one goes from N to B. For C and B, the "lone pair" is normally associated with the 5σ orbital. Interestingly enough, at B, for this orbital there is less overlap and less back-polarization as measured by the forces. Furthermore, the overlap force at F for this orbital is more negative than at O, indicating more charge removal from near the F nucleus as compared to O. This therefore substantiates the information obtained from the density maps, that the charge accumulated behind B is placed farther away behind that nucleus than behind C for CO. Thus, in this series, the lightest nucleus has the most diffuse backpolarized charge and is disposed farthest away from the binding region. This sort of behaviour is further substantiated by a recent calculation of Huo⁽¹³⁷⁾ on some excited states of BeO where it is shown that the 5σ orbital displacement away from the nucleus is strongest in this molecule because of the largest ratio $\langle z \rangle_{5\sigma}/R_e$ as compared to CO, BF, NO and CN. This is most likely due to BeO being the most hetero-nuclear of the series. Such "lone pair characteristics" of the 5σ orbital is also predicted by qualitative MO theory⁽¹³⁸⁾. The density map analysis shows that this latter approach exaggerates the amount of charge placed behind the nuclei. The importance of this backpolarization depends on

the nuclear charge at which this occurs. For in terms of forces, the larger the backpolarization force f_i and the larger the nuclear charge, the greater is the antibinding of the 5σ orbital. This will then influence the stability of a molecule considerably. For LiF, for instance, one can predict the 5σ density to be still more diffuse behind Li than behind Be in BeO. However, in view of the small nuclear charge of Li, there probably will be little effect on the stability or instability of the molecule. The more important aspect to be considered then, will be the previous localization of this density.

In summary, a comparison of the partial forces on A and B for a particular orbital can provide a quantitative comparison of the effectiveness of this orbital density in binding the nuclei. From Table (3.5), the 4σ orbital can be seen to be more binding as one goes from N_2 to BF. This is supported by the decrease in the Δf_i values for that orbital in going to BF. The 4σ orbital, therefore, although strongly antibinding for N_2 as seen from Fig.(3.4), changes binding characteristic at BF. For this molecule, ΔR_e should be quite large upon loss of one 4σ electron. The 5σ orbital is more difficult to characterize. The localization of density on the light nuclei B and C is not complete, less so than for the 3σ orbital for instance. The 5σ orbital is

always strongly antibinding with respect to nucleus A but goes from moderately antibinding in N_2 to essentially nonbinding at O and F. Thus one may classify the orbital as being totally an antibinding orbital. This would agree with the experimentally observed bond length decrease for CO and BF upon loss of such an electron through ionization. The 1π orbital is seen to be in general binding both from the Δf_i 's in Table (3.5) and the orbital forces in Fig.(3.6). It appears to be a characteristic of this orbital that the π density is polarized in a direction counter to the direction of charge transfer in the σ distribution as demonstrated by positive atomic forces and nearly equal overlap forces at both nuclei in the molecules for the π density. This is, therefore, the primary cause for its binding character being prevalent in these molecules.

3.5 Interpretation of LiF and BeO

In the previous chapter on densities, these two molecules were shown to have quite different density distributions as compared to N_2 , CO and BF. Trends displayed by this latter series were found to go the opposite way for LiF and BeO. The distinctive features for these were the tightening of density at Li and Be, small regions of charge transfer behind these nuclei in addition to some charge removal in front of these. Charge transfer to the heavy

Table 3.6.

Forces on Li in LiF

 $R_e = 2.8877$ a.u.

a.o.	MO	$f_i(R=\infty)$	$f_i(R_e)$	A	O	S
$1s^2_F$	1σ	2.000	2.000	0.000	0.000	2.000
$1s^2_{Li}$	2σ	0.000	-0.338	-0.418	0.076	0.004
$2s^2_F$	3σ	2.000	1.955	-0.071	0.038	1.987
$2s_{Li} 2p^1_F$	4σ	1.000	1.994	-0.297	0.095	2.197
$2p^4_F$	1π	4.000	3.503	0.019	0.251	3.233
Totals:		9.000	9.115	-0.766	0.460	9.421
ionic case (Li^+F^-)		10.000		-1.000	0	10.000

Forces on F in LiF

a.o.	MO	$f_i(R=\infty)$	$f_i(R_e)$	A	O	S
$1s^2_F$	1σ	0.000	0.185	0.184	0.000	0.000
$1s^2_{Li}$	2σ	2.000	2.006	0.007	0.030	1.969
$2s^2_F$	3σ	0.000	0.595	0.468	0.115	0.014
$2s_{Li} 2p^1_F$	4σ	1.000	-0.378	-1.141	0.753	0.044
$2p^4_F$	1π	0.000	0.602	0.412	0.171	0.019
Totals:		3.000	3.045	-0.070	1.069	2.046
ionic case (Li^+F^-)		2.000		1.000	0	2.000

TABLE 3.7

FORCES ON Be IN BeO		Re = 2.50 a.u.				
a.o.	m.o.	fi(R=∞)	fi(R _e)	A	O	S
1s _O ²	1σ	2.000	2.000	0.000	0.000	2.000
1s _{Be} ²	2σ	0.000	-0.722	-0.769	0.046	0.000
2s _O ²	3σ	2.000	2.059	-0.240	0.323	1.976
2s _{Be} ²	4σ	0.000	1.684	-0.455	0.569	1.570
2p _O ^{π 4}	1π	4.000	3.019	0.072	0.550	2.396
Totals		8.000	8.040	-1.391	1.488	7.943
ionic (Be ⁺² O ⁻²)		10.00		-2.000	0.000	10.000
FORCES ON O IN BeO						
a.o.	m.o.	fi(R=∞)	fi(R _e)	A	O	S
1s _O ²	1σ	0.000	0.320	0.320	0.000	0.000
1s _{Be} ²	2σ	2.000	1.994	0.000	0.013	1.981
2s _O ²	3σ	0.000	1.306	0.835	0.427	0.045
2s _{Be} ²	4σ	2.000	-0.815	-2.768	1.784	0.168
2p _O ^{π 4}	1π	0.000	1.235	0.521	0.536	0.178
Totals		4.000	4.041	-1.092	2.760	2.372
ionic (Be ⁺² O ⁻²)		2.00		+2.000	0.000	2.000

Li
(2)

Be
(2)

C
(1)

O
(0)

F
(0)

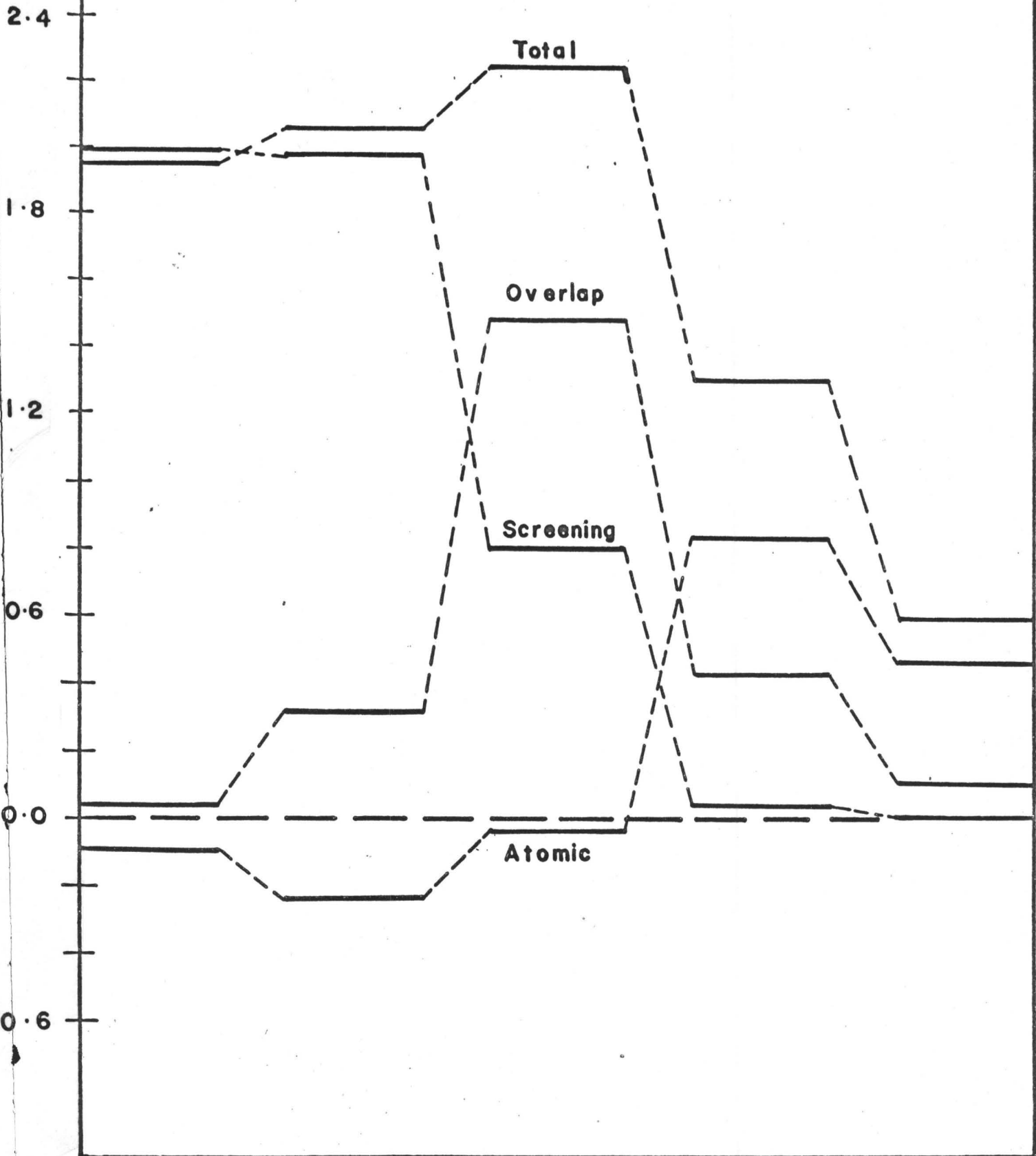


Fig. (3,7)

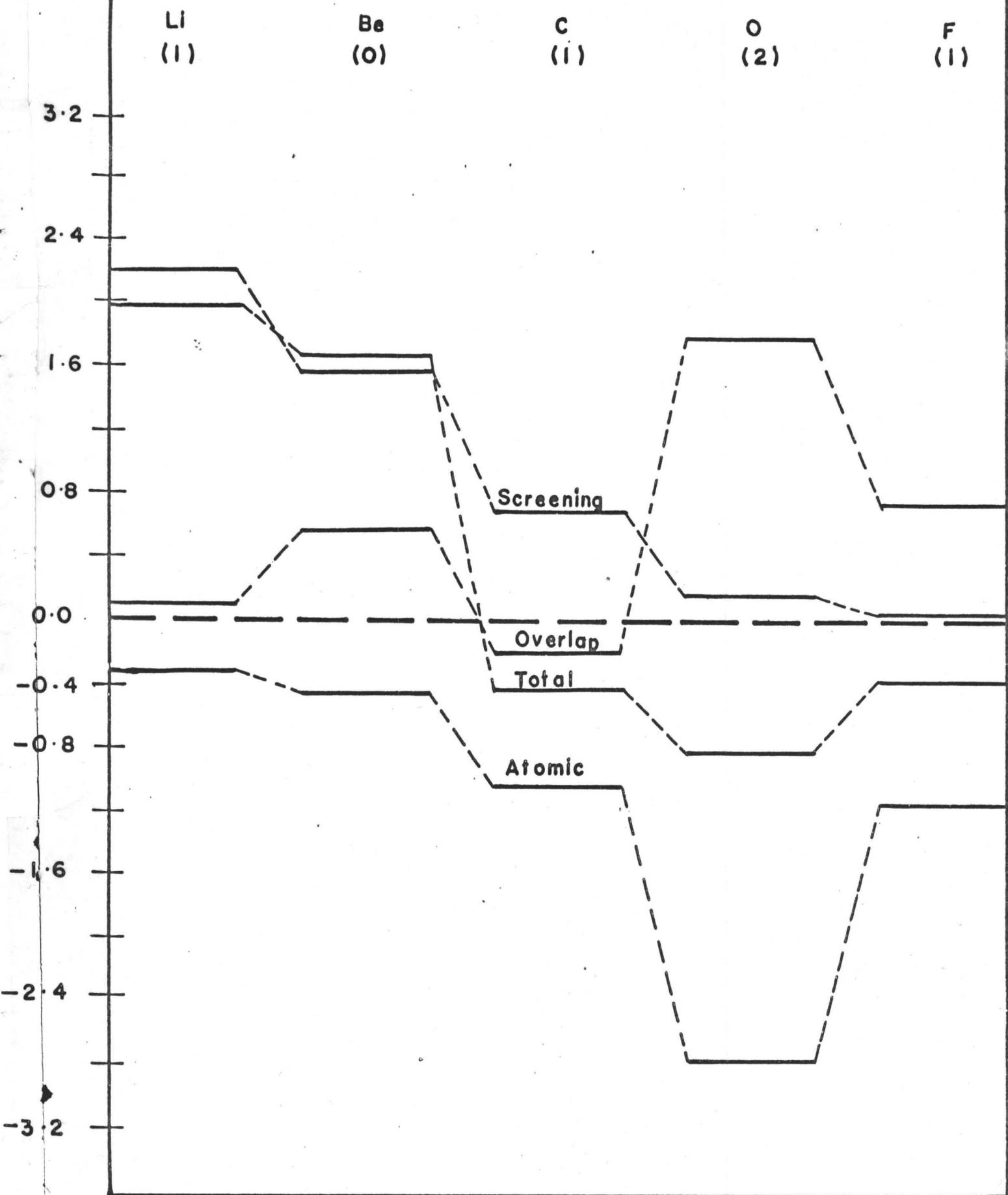
4σ m.o.

Fig. (3.8)

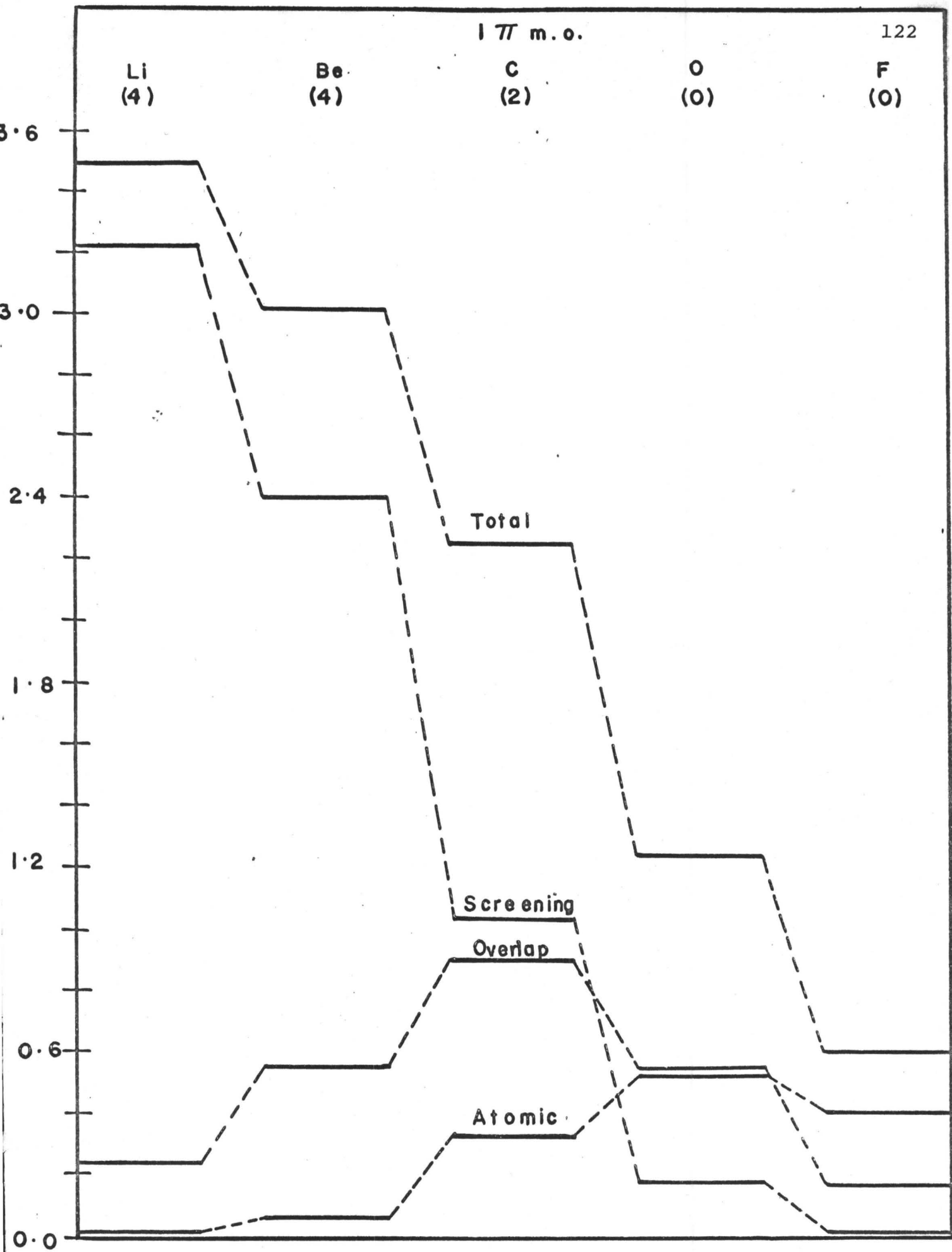


Fig. (3,9) .

nuclei O and F was also put in evidence by the $\Delta\rho$ maps, the transferred charge being distinctively separated from its original nucleus for LiF but less so for BeO. In view of these features, one can expect that a force analysis will further accentuate these charge transfer effects, for instance, by deshielding or overshielding of nuclei, small and large overlap forces, and finally back and forward polarizations arising from transferred charge.

In Tables (3.6) and (3.7) are listed the orbital contributions to the forces, with further subdivision into atomic, overlap and shielding components. The appropriate correlations of the MO's with the various separated atom orbitals are indicated, with their corresponding $f_i(\infty)$, the effective electronic charge seen from one nucleus, for the separated case. The orbital contributions are further displayed graphically in Fig.(3.7) to (3.9) in which has also been included the forces for the covalent isoelectronic analogue C_2 . The discussion of this molecule via density and force analyses has been reported previously by Bader et al⁽⁵⁵⁾. The forces have also been discussed for LiF⁽¹⁴⁾ before. LiF is reconsidered here along with C_2 for completeness and also more extensively, as emphasis will eventually be put on force constants and field gradients. The 1σ and 2σ orbitals, corresponding to $1s^2$ density on the heavy and light nuclei respectively as seen from the shielding forces

(see tables), demonstrate new features of the atomic polarizations at Li and Be. The $1s^2$ atomic densities are polarized behind these nuclei whereas at the heavy nuclei O and F, these are polarized into the bond. In the series N_2 , CO, BF, all inner shells are polarized forwards. The backpolarizations of atomic densities at Li and Be are greatest for the $1s^2$ density, which is in the 2σ orbital. These correlate with the increase in charge behind Li and Be as displayed by the density difference maps, using both neutral and ionic species as the separated constituents.

The 3σ orbital, as seen from Fig.(3.7) indicates large localization of the charge at the heavy nuclei, corresponding to $2s$ densities from the orbital correlations. The shielding f_i 's at Li and Be are very close to the separated atom value of 2.0. The magnitude of these decreases to zero at F, indicative of nearly complete localization of this density in the heavy nucleus. The overlap contribution is maximum for the most covalent molecule, C_2 , decreasing to zero in LiF. There is a small overlap contribution at both nuclei in BeO. The charge localization is thus less perfect for BeO as compared to LiF. Delocalization is maximum for C_2 . The characteristics of the 3σ orbital for the series N_2 , CO, BF were the same as for C_2 . In passing to BeO and LiF, this characteristic

of maximum delocalization and concentration into the bond region is reversed by virtue of the high electrostatic field of the nuclei O and F. The 3σ density therefore acquires 2s atomic character centered on the heavy end for the molecules BeO and LiF. The orbital as a result of this is most binding for C_2 , binding at O and F, and essentially non-binding at the light nuclei Li and Be.

The 4σ orbital demonstrates increased shielding of the heavy nuclei when viewed from the light nuclei, and decreased shielding of the light nuclei when viewed from the heavy end of the molecule. C_2 , which is the limit of the average of these two tendencies, indicates slight deshielding of the nuclei. Overlap effects are largest at the heavy nuclei, being negative only for C_2 . Large atomic backpolarizations of density situated at O and F is indicative of the presence of $p\sigma$ atomic character. This effect is largest at O for which the largest shielding changes occurred also. The overall picture for this orbital is that for the unsymmetrical molecules LiF and BeO, there has been large transfer of charge from the electropositive end of the molecule to its electronegative end. The transfer is most complete for LiF for which one has nearly vanishing shielding and overlap contributions from density on the Li nucleus. At Be, there is still some charge left as indicated by its small overlap and shielding effects.

In the case of C_2 , the trend is motion of charge away from the internuclear region and motion behind the nuclei. As a result of this, the 4σ orbital is strongly antibinding for the C_2 molecule. The binding character increases dramatically at Li and Be, and decreases in the same fashion at O and F, as a result of charge transfer having occurred from one end to the other.

The 1π orbital, as in the previous group of molecules N_2 , CO, BF, puts in evidence the typical undershielding of its charge density. The shielding contributions to the binding change drastically in going from Li, through Be and O, to F. The asymmetry in charge disposition is thus displayed effectively by this trend, so that one concludes that the π bond is most polar in LiF but less so in BeO. The overlap f_i 's arising from this density is equal at both nuclei in the same molecule, a feature displayed by the 1π orbital of the previous group of molecules studied. At Li, the atomic and overlap densities are vanishingly small as they contribute little to the corresponding f_i 's. The atomic f_i at Be is also negligible but there is a larger overlap contribution, about half of that in C_2 . This indicates transfer of π density from the O atom towards Be, as further amplified by the rather large undershielding of the O nucleus by its own density. The effect of this transfer or "back-donation" of π density was made evident

in the total density map for the BeO molecule, in which it was noticed that a tight Be core was engulfed in a very diffuse envelope of density. We thus see again the easy correlation one can make with density distributions and the forces binding a molecule. These correlations will also enter force constant discussions, in which the response of these densities to nuclear displacements will determine the magnitude of these constants via changes in the forces.

3.6 A Comparison of Covalent and Ionic Binding

The concept of the ionic character of a bond is rooted in the language of valence-bond theory, the percent ionic character being related to the relative weighting of the wavefunction for the ionic structure to that for the covalent structure. Relating this concept to the parameters in an approximate wavefunction makes it difficult to give an exact mathematical or physical interpretation to it. The inadequacies of past definitions of partial ionic character have been detailed by Shull (139). The original purpose in defining ionic and covalent character and the closely related concept of electronegativity was to obtain by empirical methods some crude estimate of how the valence electrons were distributed or shared in a molecule. In this sense the use of the words ionic and covalent was predictive in nature. Since the electron density can now be calculated with some precision, it might be argued

that the concept of the relative ionic-covalent character of a bond could be discarded. The physical property of interest is, after all, the electron density and not the wavefunction. However, the terms ionic and covalent are still useful in a descriptive sense when they are defined in terms of the density distribution and its dependent properties. In what follows, we define the terms ionic and covalent via the density distributions and the $\langle r^{-2} \rangle$ moment of these, corresponding to the forces which the density exerts on the nuclei. These definitions will parallel to some extent previous definitions based on observables which are determined by the one-electron density. For example, the first moment $\langle r \rangle$ partitioned into components along appropriate axes gives the dipole moment of the charge distribution and thus offers another definition of ionic character based on the ratio of the observed to the ideal dipole moment⁽⁸⁶⁾. These same definitions will obviously exclude any definition of ionic character which does not result in an actual asymmetry in the calculated charge distribution. For example, our approach would not consider H_2 as partially ionic, as opposed to the valence-bond theory where one introduces structures such as H^+H^- . The problem of defining partial ionic character directly in terms of the orbital components of a wavefunction has been considered by Shull⁽¹⁴⁰⁾. His analysis is in terms of the natural orbitals, which as pointed out in the general

introduction, have invariant properties for a given system, independent of the basis set. This method is absolute in the sense that no comparison is made between the molecule and its constituent atoms. One still has the problem of partitioning the electron space via weight factors in order to correlate diverse phenomena such as bond energies, force constants, etc. Our weight factor in this discussion is the force operator which helps characterize the densities and density differences in a systematic way.

The regions of charge increase in the $\Delta\rho$ maps are the regions to which charge is transferred to obtain a state of electrostatic equilibrium in the formation of a chemical bond. As pointed out in the previous chapter, they may be regarded as providing pictures of the "bond density". Thus, it is natural to characterize the bond according to the location, relative to the nuclei, of the charge increase which binds the nuclei. The $\Delta\rho$ maps (see Fig.(2.2)) for the homonuclear diatomic molecules N_2 and C_2 exhibited an increase in the charge density symmetrically placed in the binding region. It is the force exerted by this shared density which binds the nuclei in these molecules as it represents the increase in the density relative to a distribution which does not place sufficient density in the binding region to balance the force of nuclear repulsion. Thus the definition of a covalent

bond is one for which the $\Delta\rho$ map exhibits a density increase which is shared equally by both nuclei. The nature of the charge increase in the binding region found in the $\Delta\rho$ maps for CO and BF were very similar in appearance to that of N_2 , except for a more diffuse charge relocation behind the C and B nuclei. In the case of CO, this diffuse density behind C as opposed to the tighter density behind O will make it easier for the C end of the molecule to donate density to some other atom such as a transition metal. Because of the still more diffuse charge density behind BF, on the basis of the density diagrams, one would predict that BF would be a stronger ligand than CO. As stated succinctly by Moffit⁽¹⁴¹⁾, this means that this density is therefore nicely suited, sterically, for combining with groups which approach the molecule. The rearrangement of the CO system after loss of a 5σ electron results in a configuration which has a shorter bond length than the ground state, as discussed previously. As much of the diffuseness of the density comes from this orbital, then donation of such an electron to some other nucleus will be assisted by the rearrangement, as there is a reduction in "activation energy" for the "transition state", i.e. the incipient polyatom, made evident by the rearrangement of the CO skeleton. For loss of the $5\sigma(3\sigma_g)$ electron in N_2 , there is bond lengthening, so that the rearrangement is not quite favourable for electron donation.

For BF, the rearrangement is in the same direction as CO but even greater so that this would tend to increase the stability of a ligand-metal complex with BF as the ligand. This prediction for BF is however incomplete as the density difference maps indicate there is a tendency for the B nucleus to also attract charge to it (notice the appearance of π density at B). These two effects therefore support the experimentally known fact that BF is the most reactive of the series N₂, CO, BF.

The nature of the charge increase in the binding region found in the $\Delta\rho$ map for LiF is distinct from that found for the homonuclear diatomic molecules, in addition to CO and BF. The $\Delta\rho$ map for LiF exhibits the characteristics of ionic binding as defined by: (1) a transfer of charge from one atom to the other, the charge increase being localized on one atom as indicated by the fact that the positive contours are approximately centered on one of the nuclei and the region of increase is bounded by a zero contour which encompasses only a single nucleus, (2) a polarization of the density increase localized on the anion and of the density remaining on the cation in a direction counter to the direction of the charge transfer. This last characteristic is a direct consequence of the extreme localization of the valence charge density on a single nucleus, which exerts a net attractive force on the other

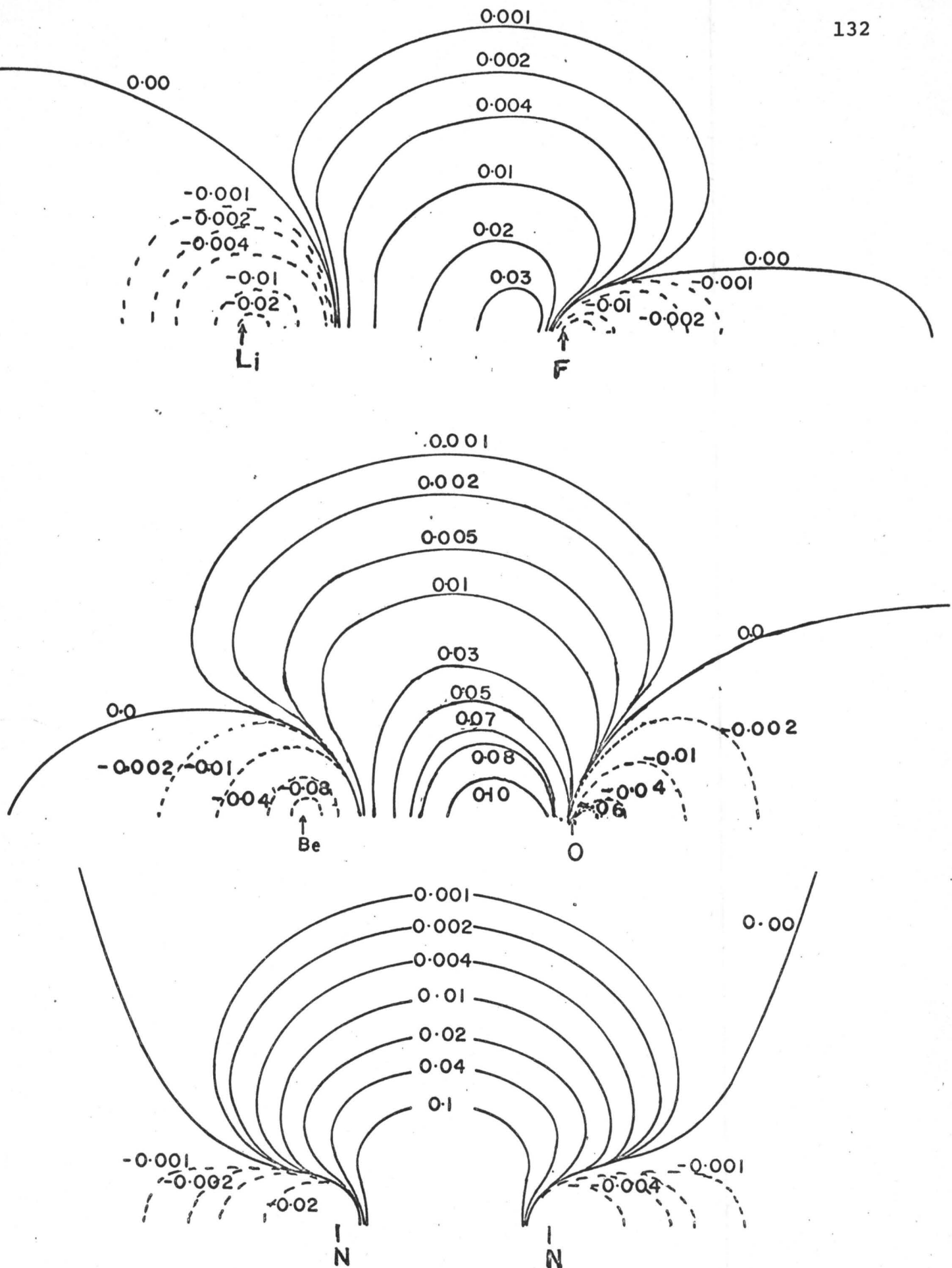


Fig. (3.10) Overlap Densities

nucleus. Thus, the density in the immediate vicinity of the Li nucleus must be polarized away from the F nucleus to counterbalance the net force of attraction exerted by the density transferred to F. These polarizations are evident in the $\Delta\rho$ maps for LiF and BeO. BeO is somewhat different than LiF since the complete separation of charge is not as evident. The reason for this difference is the delocalization of the 1π density from O to Be as discussed in the forces for that orbital.

The distinction between the characteristic of ionic and covalent binding may be made more quantitative by comparing the nature and magnitude of the contributions to the electronic forces in the two limiting cases. If we make a tentative identification of the localized and shared charge of the density difference maps with the atomic and overlap populations, respectively, we may restate the definitions of covalent and ionic binding in terms of the atomic, overlap and shielding contributions to the forces. In the formation of a covalent bond the buildup of a large overlap population or shared density between the nuclei results in a deshielding of both nuclei. This deshielding results in a net force of repulsion acting on the nuclei, a force which is counterbalanced by the attractive force exerted by the overlap density. In Fig. (3.10), we present the overlap density for N_2 . One sees that the effect of overlap is to concentrate

TABLE 3.8

Total atomic, overlap and shielding contribution to the forces

AB	Atomic $\sum_i f_i$ (AA)	Overlap $\sum_i f_i$ (AB)	Shielding $\sum_i f_i$ (BB)	Unshielded Nuclear Charge (BB) $Z_A - \sum_i f_i$	Totals ^{a)} $\sum_i f_i$
NN	-1.943	3.853	5.136	1.864	7.046
CO	-2.508	3.154	7.466	0.534	8.112
BF	-1.451	1.515	9.008	-0.008	9.072
B ⁺ F ⁻	-1.000	0.000	10.000	-1.000	
C C	-0.735	2.198	4.523	1.477	5.986
BeO	-1.391	1.488	7.943	0.057	8.040
Be ⁺⁺ O ⁼	-2.000	0.000	10.000	-2.000	
LiF	-0.766	0.460	9.421	-0.421	9.115
Li ⁺ F ⁻	-1.000	0.000	10.000	-1.000	
N N	-1.943	3.853	5.136	1.864	7.046
O C	-0.398	2.586	3.884	2.116	6.072
F B	-0.189	1.966	3.259	1.741	5.036
F ⁻ B ⁺	+1.000	0.000	4.000	1.000	
C C	-0.735	2.198	4.523	1.477	5.986
O Be	-1.092	2.760	2.372	1.628	4.040
O ⁼ Be ⁺⁺	+2.000	0.000	2.000	2.000	
F Li	-0.070	1.069	2.046	0.954	3.045
F ⁻ Li ⁺	1.000	0.000	2.000	1.000	

a) The small deviations of these numbers from Z_B values are indicative of the degree of accuracy of the Hartree-Fock wavefunctions.

charge symmetrically in the bond region and also aid removal of charge from behind the nuclei. In a covalent bond, it is the force exerted by this overlap or shared density which binds the nuclei together. To determine how closely the density in a covalent bond meets the above requirements we have assembled in Table (3.8) the total atomic, overlap and shielding contributions to the forces for the molecules considered in this work. In the case of the separated atoms, the total shielding contribution is equal to Z_A , the nuclear charge, and the atomic and overlap contributions are zero. The difference between Z_A and the total shielding which is also listed is a measure of the amount of nuclear charge present in the molecule which is no longer shielded by the atomic density distributions. The deshielding of the nuclei is a result of the distortion of the atomic charge distributions and of the migration of charge to the region of overlap. There is, in fact, a correlation between the amount of descreening and magnitude of the overlap contribution to the force. Both of these quantities increase to a maximum at N_2 and then decrease through CO , BF when the light nucleus is considered. The same trend holds for C_2 , BeO and LiF . When considered at the heavy nucleus, slight anomalies in the shielding at O in CO and BeO occur (there is more deshielding of the electropositive nucleus than the trend would suggest). In

the series N_2 , CO, BF, the overlap is smallest in BF, suggesting decreasing covalency for that molecule. The total increased shielding of the F nucleus supports this conclusion. On the other hand, the near equality of overlap contributions at both nuclei in this series is further evidence that N_2 , CO, BF are to be considered covalent. The atomic contributions provide a quantitative measure of the antibinding effect exerted by the nonbonded density increase. In every case except LiF, the overlap contribution is greater than the deficit created by the deshielding of the nuclei and the excess attractive force exerted by the overlap density is balanced by the negative atomic force contributions. The net force of attraction which binds the nuclei is exerted by the overlap or shared density for the molecules N_2 , CO, BF, C_2 and BeO, so that these would be considered covalent.

In an idealized model of an ionic bond, there is no overlap or shared density and no corresponding force contribution. Instead, the complete transfer of charge will increase the shielding contribution of the anion and decrease that of the cation. These values are listed for the bracketed ionic structures of the molecules BF, BeO and LiF. The increased shielding of the anionic nucleus exerts a net force of attraction on the cationic nucleus. As noted earlier, this force is balanced by a negative atomic force which arises from a polarization of the density remaining on the

cation. The net force of repulsion acting on the anionic nucleus because of the charge transfer is in turn balanced by a positive atomic force term. Ideally, one would wish to calculate the contributions to the forces based on a partitioning of the charge in the manner indicated by the density difference diagrams, rather than by an orbital population analysis. The partitioning of the charge as suggested by the density difference diagram is determined by the total distribution of the charge in the molecule, while the partitioning based on a population analysis will change with a change in the orbital basis set. If the density distributions employed are Hartree-Fock densities, i.e., correct to second order⁽¹⁴²⁾, then the density difference diagrams should remain unchanged regardless of the nature of the basis set used in the expansion. We can obtain an estimate of the force contributions as determined by the density difference maps for the ionic case by using the information contained in these maps to reassign the force contributions obtained from the population analysis. The density difference map suggests that the valence charge density is transferred in the formation of LiF is localized on F within the zero contour enveloping the F nucleus. Thus in this case the overlap population should be added to the atomic population on F and the forces exerted on the nuclei by this combined density equated to that exerted

by the density localized on F in the density difference map. The overlap forces are relatively small in any event for LiF and are larger for F than Li, reflecting the fact, as shown by the overlap density map in Fig.(3.10) that the density lies within the charge increase localized on F. Thus the sum of overlap and atomic contributions at F is indeed 1.00 in accord with the atomic value for the ionic structure. At Li the overlap is not enough to override the atomic backpolarization. In fact, since the overlap density map indicates nearly symmetrical charge removal around Li, then much of this contribution at Li must come from the overlap density closer to F. Thus, one could add the overlap and shielding forces at Li, the result being 9.88 which approaches the ionic value of 10.00. The signs of the atomic force term at Li and that of the sum of overlap and atomic forces at F indicate the densities on both Li and F are polarized in a direction counter to the direction of the charge transfer as required for electrostatic equilibrium. In the case of BeO, the distinction between covalent and ionic character is not as clear cut, as a result of the zero contour encompassing both nuclei. The reason for this large delocalization has already been noted in the discussion of the 1π orbital forces for that molecule, where it was shown that the overlap force was equal at both nuclei, an indication of

equal sharing of the orbital density. In fact, this behaviour was found for the 1π orbitals of all the molecules considered in this work, but the magnitude of the 1π overlap forces for LiF were small compared to the other molecules. The total overlap density for BeO is illustrated in Fig.(3.10) It can be seen that there is delocalization of this density in the π region of the Be nucleus. However, the major part of the density is localized on the O nucleus, with strong $p\sigma$ character evident. This suggests that one should consider this density localized on O, the same as was done for F in LiF. The force resulting from adding this overlap density to the atomic density is 1.67. The expected force contribution for the ionic case Be^{++}O^- is 2.00 at O, i.e., the amount of polarization force in the forward direction required to counter the nuclear repulsion from the net positive force of 2.00 experienced by the O nucleus from Be^{++} . We can similarly add the overlap and shielding contributions at Be. This gives a total force of 9.43 as compared to 10.00 for the ionic case. Although we are somewhat short of the proposed structure Be^{++}O^- , the $\Delta\rho$ map along with the overlap density map and the forces suggest that the overlap density is better considered as being localized on O. Such an association is not easily done for BF, but since many of the features of this molecule as seen from the $\Delta\rho$ map parallel those of BeO, it is evident

that ionic character is present to a large extent. The electropositive ends of the molecules BeO and BF are also quite similar from a force analysis standpoint. There is nearly complete shielding of the heavy nuclei O and F. The binding at Be and B come from the overlap force, which can be considered as mostly charge situated on the heavy nuclei. The increased shielding of the heavy nuclei is an indication these are approaching electrostatic binding which is associated with ionic character. The main difference between the two resides in the fact that the B atomic density contains p character and there is a tendency to attract π density towards B from the other end of the molecule, more so than Be in BeO. The large region of charge depletion behind Be is very similar to Li and LiF, hence reinforcing the ionic status of Be in BeO.

Thus, in ionic binding both nuclei are bound by the charge localized on one of them. This is clearly exemplified by LiF. For BeO, the case is not as clear cut, but from the density difference maps, it is evident much of the charge increase is to be associated mainly with the O nucleus. Therefore, BeO is largely ionic in character by the above definition. In covalent binding, as represented by the homonuclears N₂ and C₂, the nuclei are bound by a density increase in the bond region which is shared equally between them. For CO, this density increase is slightly polarized

towards the O nucleus, as seen by the slight asymmetry displayed by the $\Delta\rho$ map. Nevertheless, it is still this same density which binds the nuclei, so that CO must be classified as distinctly covalent. BF represents the intermediate case, as a result of incomplete charge transfer to one end of the molecule. The density transferred towards the F nucleus is essentially localized on it. This is demonstrated by the increased shielding of that nucleus by this density. For a covalent molecule, deshielding would have been expected. There is also a fair amount of charge placed behind the B nucleus. This is, therefore, indicative of covalent behaviour. Thus, we have the result for BF that the electropositive end of the molecule shows covalent tendencies, whereas the electronegative end indicates ionic tendencies.

It can be argued that the breakdown of a total electronic force into atomic, overlap and shielding contributions is not unique, nor fundamental. This partition was made feasible by the separation inherent in the L.C.A.O. approximation of Hartree-Fock wavefunctions. In the case of LiF, it is possible to associate the charge transferred with the F atom from the $\Delta\rho$ map. Although for BeO, the association was not made as definite by the $\Delta\rho$ map, association was still possible with the O nucleus by examining the magnitude of contours. Thus, it was concluded

most of the charge transferred was indeed situated on the O nucleus. In the case of covalent molecules, there is a clear separation of charge in the binding region from the charge in the antibinding region. The overlap density diagram for N_2 (see Fig.(3.10)) indicates that the charge increase in the binding region as portrayed in $\Delta\rho$ maps is indeed mostly an overlap density. Therefore, one can consider this density as a separate entity. The increase in the antibinding regions reflect a change essentially in the atomic densities as a result of bond formation; therefore, a consideration of the forces exerted by this density is also appropriate. In the final analysis, these force components should not depend on the properties of basis sets employed. In view of this uncertainty, it is the density and density difference maps which must be emphasized, by which one can therefore form the correct partitions of the forces. In the case of BF, such a partition was not easily obtained, as a result of the complex nature of the $\Delta\rho$ diagram. The somewhat arbitrary dissection of the force into atomic, overlap and shielding components is nevertheless instructive and of operational value in correlating the various bonding characteristics in a systematic way.

IV. MORE STATICS: FIELD GRADIENTS AND
QUADRUPOLE COUPLING CONSTANTS

"On a souvent besoin d'un plus petit que soi"
La Fontaine

4.1 Introduction

In atoms and molecules, nuclei are embedded in an electronic distribution. When such a distribution outside a particular quadrupolar nucleus is nonspherical, there is an interaction between the nuclear moments and the external fields from this distribution. This interaction is responsible for hyperfine structure of rotational lines. A nuclear-quadrupole coupling constant eQq can be calculated from this hyperfine structure when both Q , the nuclear quadrupole moment, and q , the external field gradient, are finite. Effectively, q is a measure of the departure from spherical symmetry of the charge distribution, at the nucleus, of the electrons and other nuclei present in the same molecule. The quantity depends on the environment of the quadrupolar nucleus in the molecule and is therefore intimately connected with the types of valence bonding in the molecule. In the region of the nucleus, wavefunctions, which otherwise have proved satisfactory, have not previously been tested. Simple molecular orbital

theory is open to the objections discussed in the previous chapter, namely that correctly polarized and scaled wavefunctions must be used for quantities involving the electron density. For example, a wavefunction which does not obey cusp conditions at $r = 0$ will yield an inferior value for field gradients, even though this has little effect on the energy⁽¹⁴³⁾. Furthermore, the r^{-3} dependence of the field gradient means that ideas drawn from properties that depend on r^{-1} , such as the energy, must be used with caution.

The significance of nuclear quadrupole coupling constants in relation to the theory of chemical bonding has been emphasized by Townes and Dailey⁽⁶³⁾. In general, the direct determination of the electronic distribution in chemical bonds is difficult since most bond parameters, such as length and dipole moment are properties of the whole molecule. If it were possible to insert a charged probe at different points within a molecule, then the charge distribution could be studied. As Dailey has pointed out, quadrupolar nuclei act as built-in probes, the only disadvantage being that since their positions are fixed, they give information about the electron distribution at one point only. Thus, nuclear electric quadrupole moments can function as a probe of the electronic environment in much the same way that the proton magnetic moment can, one

of the most popular probes of the chemist. This great interest in correlating the magnetic resonance frequency shifts with charge distribution in molecules, as opposed to the use of quadrupole coupling constants, however, has only achieved partial success because the chemical shifts depend not only on the charge distribution of the ground state but also on how the ground state wavefunction is deformed in the presence of an external field. Quadrupole coupling constants have theoretical simplicity in that they depend only on the ground state charge density. This is because the interaction between a nuclear moment and the molecular charge distribution is such that first-order perturbation theory is quite adequate for the calculation⁽¹⁴⁴⁾.

Nuclear quadrupole coupling constants offer, therefore, in principle a promising means of obtaining useful information on charge distributions. Recent advances in experimental methods make routine measurements of quadrupole resonance frequencies a practical possibility⁽¹⁴⁵⁾. Mossbauer spectroscopy in conjunction with applied external magnetic fields allow a determination of the quadrupole interactions for various nuclear states. To date, the most useful information has been obtained from the temperature dependence of the quadrupole interactions and from the correlation of quadrupole coupling data with

crystal-field and chemical bonding theories. In discussing the theory of the origin of nuclear quadrupole interactions in free molecules, we shall make use of data obtained from microwave and molecular beam spectroscopy, the first being applicable for molecules with permanent electric dipole moments; the second where this is not so, but the molecules have magnetic moments either electronic or nuclear or both.

From the theoretical or interpretive side, chemists have depended almost exclusively upon the basic considerations and relationships concerning the connection between chemical bonding and quadrupole coupling constants put forward by Townes and Dasley. This theory deals with the covalent structure of the molecule. These authors emphasize that all contributions to q may be neglected except those arising from the valence electron densities in the orbitals of the lowest eccentric atomic state, usually p orbitals. In the simplest form of the theory as applied to halogen atoms, the valence shell consists of one valence electron in an $np\sigma$ orbital and four nonbonding electrons in $np\pi$ orbitals, which is equivalent to a "hole" in $np\sigma$: $q_{cov} = -q_{n\sigma}$. Values of $q_{n\sigma}$ are derived from spectra of free atoms. In an ionic molecule, the halogen ion is considered to have an undistorted spherical shell of electrons: $q_{ion} = 0$. If i is the fraction of ionic structure, then

$$q = (1-i) q_{cov} \quad (4.1)$$

This can be refined to include further factors such as hybridization, resonance, etc., as amplified by Das and Hahn⁽¹⁴⁵⁾. In general, however, work followed along such lines is not definitive, reflecting a remark made by Dailey in 1955⁽¹⁴⁶⁾: "Obviously personal preference plays an important role in the task of evaluating three parameters from one experimentally determined constant." Only rigorous calculations performed with accurate wavefunctions can settle the validity of the interpretations usually made.

The second interpretive approach is invariably tied in with the realm of solid state physics, in particular with the study of ionic crystals. The distortion of the electron shells of ions due to external point charges in ionic crystals, was first considered by Foley, Sternheimer, and Tycko⁽¹⁴⁷⁾ as a contribution to the field gradients at the nuclei. They estimated for a number of ions, the factor $(1-\gamma^\infty)$, by which the field gradient due to the external charge was altered by this shell distortion, and then used these values of $(1-\gamma^\infty)$ for discussing nuclear quadrupole coupling constants in a number of ionic diatomic molecules. Van Kranendonk⁽¹⁴⁸⁾ showed the importance of γ^∞ in determining nuclear magnetic relaxation times in ionic crystals. γ^∞ is called the antishielding factor and is therefore pivotal in the Sternheimer antishielding theory, which is in effect a point charge model.

Both theories have been hybridized to explain experimental data, especially on nuclear-quadrupole interactions in alkali halides and nuclear spin-lattice relaxation times in ionic crystals. Wikner et al⁽¹⁴⁹⁾ conclude that the charge transfer covalent bond model is inadequate in explaining observed relaxation times, and that the theory of the ionic model modified to include antishielding and induced dipole polarization is better established than the covalent model. The covalent model is very poor for the metal nucleus. On the other hand, Bersohn and Shulman⁽⁶⁶⁾ would rather bury this approach, as they emphatically state that the model of an 1S_0 ion in an electric-field gradient coming from external point charge is inadequate. For transition-metal halides, they prefer the Townes and Dailey approach which seems to agree better with transferred magnetic hyperfine interactions results. For anions, higher-order polarizabilities introduce non-converging terms into the calculated field gradients. Evidently not all is well in the land of the ions. Das and Karplus⁽¹⁵⁰⁾ have given a hint to the problem, namely that for the alkali halides, orbital overlap is important and consequently the ionic model is inadequate. In a recent calculation on the diatomic molecule KCl ⁽¹⁵¹⁾, they have shown that overlap affects the field gradient significantly in the direction required to explain discrepancy between

theory and experiment. Covalency would seem to lead to effects in the opposite direction, suggesting that covalent binding can play only a small role.

It appears now that neither the Townes and Dailey theory nor the Sternheimer antishielding theory, nor a combination of these two theories can account for experimental data of the alkali halides. This discrepancy has been tentatively resolved by DeWijn⁽¹⁵²⁾ by considering effects of the ionic chemical bond on the polarizations of the ions. We have already noticed a partial quenching of the atomic polarization forces in LiF. This was also manifested in the density difference diagrams by a removal of charge from between the bond region, typical of a Pauli exclusion effect between two closed shells. Clearly, this demonstrates the limitation of the non-overlapping charge model. An accurate charge distribution is necessary in order to obtain the observed field gradients. The antishielding phenomena is a result of trying to extend the point-charge model. If the correct wavefunction of the crystal or molecule were available, the correct field gradient could be obtained without any antishielding factor.

The inadequacies of the Townes and Dailey and the antishielding theories will be delineated below by a discussion of these and their applications. Field gradients

have been calculated using the Hartree-Fock wavefunctions used in the force analysis. The relevant formula for the field gradient q_A at nucleus A is

$$q_A = \frac{2Z_B}{R^3} - \langle \psi | \sum_{i=1}^n \frac{3 \cos^2 \theta_{a_i} - 1}{r_a^3} | \psi \rangle \quad (4.2)$$

where Z_B is the charge of nucleus B, R the internuclear distance and ψ the total electronic wavefunction. The operator in the bracket is a one-electron operator and hence the integral can be reduced to a functional of the one-electron density ρ , as for the forces. This thus permits partitioning of the electronic field gradient into orbital contributions:

$$q_A = \frac{2Z_B}{R^3} - \sum_{j=1}^k n_j \langle \phi_j | \frac{3 \cos^2 \theta_{a_j} - 1}{r_a^3} | \phi_j \rangle \quad (4.3)$$

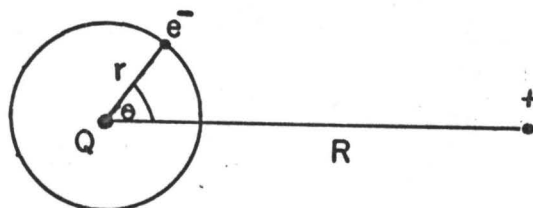
where ϕ_j is the j 'th MO and n_j its occupation number. For certain wavefunctions, the field gradient integrals are conditionally convergent because of a singularity in the integrand at the nucleus. Since the value of the integral depends on the treatment employed in the neighbourhood of the singularity, some care is required to obtain the physically correct value⁽¹⁵³⁾. For instance, in confocal elliptical coordinates, one must add a correction equal to $\frac{4}{3}\pi$ times the electron density at the nucleus⁽¹⁴⁴⁾. This corresponds to the limiting process of first excluding a spherical volume element, centered on the nucleus, in the

integration over all coordinates, and then permitting the radius of the excluded sphere to go to zero⁽¹⁵⁴⁾. Thus, for a spherical S shell, one would obtain zero for the integral, which reflects the physically obvious fact that such a spherical shell cannot contribute to an observable electric quadrupole interaction since all nuclear orientations in such a charge distribution have the same energy. The methods of integration and formulae for the various orbital contributions are given in Appendix 2.

4.2 The Antishielding Model⁽¹⁵⁵⁾

The problem to be considered is an ion with a nuclear quadrupole moment in the field of an external positive point charge. We have to find the factor $(1-\gamma^\infty)$ by which the direct interaction between the external charge and the nuclear quadrupole moment of Q , i.e. $2Q/R^3$, is affected by the deformation that the presence of this charge causes in the closed shells of the ion. If the distorted electron distribution opposes the field gradient due to the positive charge, then γ^∞ is positive and there is a shielding effect, while if the distorted distribution enhances the field gradient, then γ^∞ is negative and there is an antishielding effect.

Consider an electron at the position r, θ as shown below.



The electron interacts with both the quadrupole moment Q of the nucleus and with the distant charge. We have, therefore, a system with a ground state Hamiltonian H_0 which is subjected to the above two perturbations described respectively by the Hamiltonians H_2 and H_1 . In terms of ordinary perturbation theory, there can be three types of second-order perturbations: (1) second order in H_1 alone; (2) second order in H_2 alone; or (3) a second-order interaction arising from first-order perturbations due to both H_1 and H_2 . The latter is the one which is of interest. Physically it corresponds to a deformation in the ground state wavefunction by H_1 and a subsequent interaction of H_2 with the deformed wavefunction. The perturbation could be applied, of course, in reverse order. The final results obtained by either procedure can be shown in general to be equivalent. Let u_1 , and u_2 represent the first-order perturbations in the ground state wavefunction u_0 of the electrons, due to H_1 and H_2 .

The Schroedinger equation becomes

$$(H_0 + H_1 + H_2)(u_0 + u_1 + u_2) = (E_0 + E_1 + E_2)(u_0 + u_1 + u_2)$$

where E_0, E_1, E_2 are expectation values over u_0 of H_0, H_1, H_2 respectively. Separating the terms of first order in H_1 and in H_2 , we obtain

$$\begin{aligned} (H_0 - E_0)u_1 &= -(H_1 - E_1)u_0 \\ (H_0 - E_0)u_2 &= -(H_2 - E_2)u_0 \end{aligned} \quad (4.4)$$

Now in atomic units

$$\begin{aligned} H_0 &= -\frac{1}{2}\nabla^2 + V_0 \\ H_1 &= -\frac{1}{R} - \frac{r \cos \theta}{R^2} - \frac{1}{2} \frac{r^2(3 \cos^2 \theta - 1)}{R^3} \dots (4.5) \\ H_2 &= -Q \frac{1}{2} \frac{3 \cos^2 \theta - 1}{r^3} \end{aligned}$$

Only the third term in H_1 is of interest. The first term cannot distort the electron distribution and the second term is responsible for the ordinary dipole polarization. There is a possibility of having an indirect interaction between the nuclear quadrupole moment and the external charge by way of a second order perturbation with the second term in H_1 and the first order in H_2 but Foley et al⁽¹⁴⁷⁾ have shown it to be less than ten per cent of the interaction of first order in both the third term in H_1 and the first term in H_2 . The net energy E of the electron is given by

$$E = \frac{\langle u_0 + u_1 + u_2 | H_0 + H_1 + H_2 | u_0 + u_1 + u_2 \rangle}{\langle u_0 + u_1 + u_2 | u_0 + u_1 + u_2 \rangle}$$

Expanding to first order, we obtain

$$\begin{aligned}
 E = E_0 + E_1 + E_2 + & \frac{\langle u_1 | H_0 - E_0 | u_1 \rangle}{\dots} + \frac{\langle u_2 | H_0 - E_0 | u_2 \rangle}{\dots} + \frac{2\langle u_0 | H_1 | u_1 \rangle}{\dots} \\
 & + \frac{2\langle u_0 | H_2 | u_2 \rangle}{\dots} + 2\langle u_0 | H_1 | u_2 \rangle + 2\langle u_0 | H_2 | u_1 \rangle + 2\langle u_1 | H_0 - E_0 | u_2 \rangle + \dots
 \end{aligned}
 \tag{4.6}$$

The underlined terms represent second-order perturbation from H_1 and H_2 separately. From Eq.(4.4) it follows that

$$\langle u_0 | H_1 | u_2 \rangle = \langle u_0 | H_2 | u_1 \rangle = -\langle u_1 | H_0 - E_0 | u_2 \rangle \tag{4.7}$$

Thus, it is only a matter of convenience whether $\langle u_0 | H_1 | u_2 \rangle$ or $\langle u_0 | H_2 | u_1 \rangle$ is calculated. Sternheimer⁽⁶⁵⁾ solves this by using only the quadrupole terms of the interaction H_1 by a numerical procedure. However, as Dalgarno⁽¹⁵⁶⁾ has pointed out, the presence of singularities in self-consistent field potentials, which is related to cusp conditions discussed in Chapter I, introduces some arbitrariness into the derived values of shielding factors. Bersohn has employed a variational method for the problem⁽¹⁵⁷⁾.

One may thus calculate either (a): the electronic distortion due to the electric field gradient and thence the interaction of this distorted distribution with the nuclear quadrupole moment Q ; or (b): the electronic distortion due to Q and in turn its interaction with the external field. Both approaches give identical results within second-order

perturbation theory as can be seen from equations (4.6) and (4.7); but the situation would become more complicated if one were to go beyond it. The Sternheimer method is a perturbation method of type (b) on restricted Hartree-Fock functions (RHF). Recent investigations have shown that the relaxation of these constraints leads to a new way of calculating electric quadrupole polarizabilities and Sternheimer antishielding factors, so that the distortions induced in the inner shells by distorted outer closed shells are thus included in a natural way. By comparison with the results of the perturbation method (which normally does not take these distortions of outer shells into consideration) these are found to be significant for large ions. An extensive review of these investigations has been given by Freeman and Watson⁽¹⁵⁸⁾. This approach, the unrestricted Hartree-Fock method (UHF) (see Appendix 1), is also pertinent to any distortion of an ion by a crystalline field. In all investigations to date and (by definition) in all γ^∞ estimates, a most serious shortcoming has arisen in the unrealistic electrostatic fields which have been used. The problem is more acute for unclosed aspherical shells. An UHF wavefunction should already, therefore, include a contribution from the polarized core so that no correction for core-shielding effects of the type considered by Sternheimer should be

necessary.

In a molecule, there is no clear distinction of valence shells as such because of charge transfer and overlap effects. Furthermore, any density associated with a particular nucleus will take on polarization components with the symmetry of the field. To separate the density into atomic or ionic entities in order to calculate, by perturbation theory, the effect of the external remaining charges on one of these entities would be quite impractical. In such a case, one uses the unrestricted Hartree-Fock approach in calculating the total wavefunction of the system and thus replaces the standard perturbation theory which is used in either method (a) or (b). Thus, an exact wavefunction will take into account polarizations to all orders, polarizations which have mainly the symmetry of the field, axial for a diatomic molecule. In terms of Eq.(4.7), this means that u_1 is exact as far as H_1 , the perturbation from external charges, is concerned. In fact, the exact wavefunction also includes, therefore, the perturbation of the distorted inner and valence shells on the external charge. One can therefore calculate the electric field gradient using the external field perturbation method, since one knows u_1 exactly. Sternheimer⁽¹⁵⁹⁾ has shown that the two ways of calculating the field gradient, by considering the internal nuclear or the external field perturbation, are completely equivalent for second-order perturbation theory

Table 4.1

Field Gradients at Li in LiF at $R_e = 2.8877$ a.u.

a.o.	MO	$g_{2p}(R=\infty)$	$g_i(R=\infty)$	$g_i(R_e)$	A	O	S
$1s^2_F$	1σ	<u>+0.373</u>	2.000	2.000	0.000	0.000	2.000
$1s^2_{Li}$	2σ		0.000	-0.010	-0.098	0.083	0.004
$2s^2_F$	3σ		2.000	2.041	-0.013	0.053	2.001
$2s^1_{Li} + 2p^1_F$	4σ		1.000	2.682	0.068	0.217	2.397
$2p\pi^4_F$	1π		4.000	2.919	-0.021	0.122	2.818
Totals:			9.000	9.633	-0.064	0.475	9.221

Field Gradients at F

a.o.	MO	$g_{2p}(R=\infty)$	$g_i(R=\infty)$	$g_i(R_e)$	A	O	S
$1s^2_F$	1σ	<u>+72.690</u>	0.000	0.001	0.001	0.000	0.000
$1s^2_{Li}$	2σ		2.000	2.046	0.042	0.042	1.962
$2s^2_F$	3σ		0.000	0.312	0.226	0.073	0.013
$2p^1_F + 2s^1_{Li}$	4σ	72.690	1.000	126.787	125.963	0.784	0.039
$2p\pi^4_F$	1π	-145.380	0.000	-122.941	-122.006	-0.935	0.000
Totals:		-72.690	3.000	6.206	4.226	-0.036	2.014

a) Underlined $g_{2p}(\infty)$'s are $+\frac{R^3}{2} \times q_{210}$

Table 4.2 a)

Field Gradients at Be in BeO at $R_e = 2.50$ a.u.

a.o.	MO	$g_{2p}(R=\infty)$	$g_i(R=\infty)$	$g_i(R_e)$	A	O	S
$1s^2_O$	1σ	<u>+1.094</u>	2.000	2.001	0.000	0.000	2.001
$1s^2_{Be}$	2σ		0.000	0.058	0.016	0.042	0.001
$2s^2_O$	3σ		2.000	2.494	0.119	0.393	1.982
$2s^2_{Be}$	4σ		0.000	2.595	0.395	0.653	1.547
$2p\pi^4_O$	1π		4.000	1.312	-0.483	-0.049	1.844
Totals:			8.000	8.420	0.045	1.039	7.334

Field Gradients at O

$1s^2_O$	1σ	<u>+30.779</u>	0.000	0.006	0.006	0.000	0.000	
$1s^2_{Be}$	2σ		2.000	1.994	0.003	0.015	1.976	
$2s^2_O$	3σ		0.000	1.222	0.830	0.348	0.043	
$2s^2_{Be}$	4σ		2.000	46.922	44.914	1.859	0.149	
$2p\pi^4_O$	1π	-61.558	0.000	-40.440	-39.955	-0.569	0.084	
Totals:			-61.558	4.000	9.704	5.798	1.654	2.252

a) Underlined $g_{2p}(\infty)$'s are $+\frac{R^3}{2} \times q_{210}$

and has noted that on physical grounds, one expects the equivalence to be complete, i.e., correct to all orders of the nuclear quadrupole and the electronic perturbation. If one uses an exact wavefunction (without nuclear interaction), one has then summed the electronic perturbation to all orders. The question then becomes, is an RHF wavefunction, as we have used in the force analysis, accurate enough to calculate field gradients. For closed-shell molecules, the RHF orbitals are internally consistent eigenfunctions of the H-F equations and therefore Brillouin's theorem applies to them. Since the main perturbations on the atomic densities are of axial symmetry as a result of bond formation, perturbations from nuclear moments can be safely disregarded. Thus, we can confidently surmise that the field gradients obtained from the RHF functions used in this work will be quite accurate; the quadrupolar energy as calculated using second-order perturbation theory (first order in H_1 and H_2) should be thus reliable.

4.3 Interpretation of Ionic Molecules

In Tables (4.1) and (4.2), there are presented field gradients for the two molecules LiF and BeO, with an orbital breakdown of the various contributions, in addition to atomic, overlap and shielding components. These have all been multiplied by $R^3/2$ in order to transform them into

effective charges, i.e.,

$$q_A = \frac{2}{R^3} [Z_B - \sum_{i=1}^N g_i] \quad (4.8)$$

where

$$g_i = \frac{R^3}{2} n_i \langle \phi_i | \frac{3 \cos^2 \theta_a - 1}{r_a^3} | \phi_i \rangle$$

Also listed is $g_{2p}(\infty)$ which represents the field gradient of the 2p electrons on the free atom in question. These have been calculated from Hartree-Fock atomic functions used in the density difference diagrams. Shielding corrections for these valence electrons have been neglected due to their smallness and the inherent difficulties discussed previously. For Li and Be, $g_{2p}(\infty)$ is taken from spectroscopic data. (see ref. 145, pp.131).

a) LiF

A comparison with the forces in Table (3.6) shows only correlation with the shielding charges. In particular, the atomic polarizations at Li indicate little or no parallel behaviour as the forces. This is due to the fact that much of this polarization is of p character. Such polarization only contributes to the field gradient in second order, as compared to first order for the forces, because of the different symmetries of the operators involved. The net atomic contribution at Li is antishielding. This is not in accord with that obtained by the Sternheimer theory

which predicts $g_{\text{Li}}(\text{atomic}) = \gamma^\infty = 0.249^{(160)}$, since $q_{\text{Li}} = -\frac{2}{R^3}(1-\gamma^\infty)$. On the other hand, the Li nucleus does not see a fully negative fluoride ion. In fact, adding the overlap and shielding contributions, one gets 9.696. For the forces at Li, this sum was 9.881. One thus sees that higher negative moments involve larger undershielding phenomena. This undershielding comes about because of the factor $(3 \cos^2 \theta_B - 1)$ which favours charge placed on the internuclear axis much more than the factor $\cos \theta_B$ operative in the forces. Thus, the σ shielding contributions are larger than in the forces, but this factor is overwhelmed by a large undershielding from the π electrons.

The net field gradient at Li is $-0.0526 e/a_0^3$. From the Sternheimer theory, $q_{\text{Li}} = -2(1-\gamma^\infty)/R^3$ with $\gamma^\infty = +0.249$. Using $R_e = 2.8877$ a.u., our calculation predicts $\gamma^\infty = +0.367$. The quadrupole coupling constant in LiF^7 has been measured by Braunstein and Trischka⁽¹⁶¹⁾ for which they report eq $Q = 412$ kc/sec. From the quadrupole moment $Q_{\text{Li}^7} = -4.3 * 10^{-26} \text{cm}^2$ as calculated by Browne and Matsen⁽¹⁶²⁾ with an accurate wavefunction of LiH, one can calculate the experimental q_{Li} in LiF to be $-0.041 a_0^{-3}$. This would imply a still larger shielding factor γ^∞ . However, in view of the fact that Braunstein et al obtained very poor spectroscopic constants (error of 20%), their quadrupole constant is probably not very accurate either. At $R = 2.9877$ a.u., we

calculate $\gamma^\infty = +0.300$ (see Appendix 3). The experimental equilibrium value of LiF is 2.9554 a.u.⁽¹⁶³⁾, so that γ^∞ at this distance will be between 0.300 and 0.367. This variation of γ^∞ with internuclear distance is indicative of bonding effects on the polarizations of the ion.

At the fluorine nucleus, the shielding from the Li density indicates the presence of essentially an Li^+ ion, just as the force analysis predicted. The positive π overlap field gradient at Li definitely shows this density is quite far away from the Li nucleus, a point not exactly accentuated by the forces, where it was found the π overlap forces were about equal at both nuclei. The π overlap field gradient at F is negative, hence really behaving as an atomic density. Interestingly, it completely negates the positive σ -overlap contribution. The atomic g 's at F show up something quite important, namely, that the $p\pi$ electrons are more polarized than their $p\sigma$ counterpart. Much of the contribution to the total electronic field gradient comes from this difference. A perusal of the density difference diagrams of LiF using neutral and ionic separated atoms (see Chapter II), show a removal of $p\pi$ electrons around the F nucleus and accumulation of this density along the bond, more so in front of the F nucleus. A density difference map for the σ density only, by Bader and Henneker⁽¹⁴⁾ showed that some of this perpendicular

charge removal was due to a contraction of the σ density along the bond, i.e., a polarization effect arising from the presence of Li^+ . It is evident that chemical bonding has profound effects on the polarizations of densities.

The total field gradient at F is $+2/R^3(-3.206)$ which corresponds to $\gamma^\infty = +4.206$. The Sternheimer value for γ^∞ is -22.0 ⁽¹⁶⁴⁾. In other words, the point charge model predicts a value of completely wrong sign. A recent H.F. calculation of q_F in NaF by Matcha⁽¹⁶⁵⁾ also predicts a negative field gradient, whereas the anti-shielding model predicts a large positive q_F . The overlapping of Li^+ and F^- densities has obviously considerably altered the field gradient contributions at F, from that of a point charge model. The delinquents in this state of affairs are the $2p\sigma$ and $2p\pi$ electrons at F, which have individually different polarizations. The field gradient at Li on the other hand, is governed by a substantial undershielding of the $2p\pi$ electrons on F.

b) BeO

In the force analysis, it has already been indicated that this molecule was intermediate between Be^+O^- and $\text{Be}^{++}\text{O}^{=}$. One feature of this molecule distinct from that of LiF was a larger delocalization of the π density towards Be. The π overlap forces indicated equal sharing of this density. This is no longer true for the

field gradients which weight regions closer to the nucleus more than the forces. Nevertheless, the negative contribution of the overlap field gradient at Be indicates that this density is beginning to behave as an atomic charge, so that the π density is indeed more polarized towards Be than towards Li in LiF. There is again a significant difference between the σ and π atomic field gradients. This disparity, just as in LiF, contributes largely to the total field gradient. This difference is in the same direction as that in LiF, contributing to shielding, rather than antishielding as predicted by the Sternheimer theory.

At Be, there is the usual large undershielding of the π electrons from O. Adding the overlap and shielding contribution, the net result is 8.373, whereas the result for the forces was 9.430. The 1π shielding force at Be was 2.396, whereas the 1π shielding field gradient is 1.844. It is evident that the smaller the internuclear distance, the more severe is the undershielding by π electrons. The Sternheimer shielding factor for Be^{++} is $\gamma^\infty = 0.189$ ⁽¹⁶⁶⁾. Assuming the ionic model $\text{Be}^{+2}\text{O}^{-2}$, i.e. $q_{\text{Be}} = -\frac{4}{R^3}(1-\gamma^\infty)$, using $R = 2.50$ a.u. and $q_{\text{Be}} = -\frac{2}{R^3}(0.420)$, one obtains $\gamma^\infty = 0.81$. The calculated γ^∞ is thus too high, since in the molecule the net charges on the nuclei are smaller as a result of incomplete charge transfer. In order to reproduce our calculated field gradient with the Sternheimer γ^∞ ,

we would have to assume a structure $\text{Be}^{+0.5}\text{O}^{-0.5}$. This is not realistic in terms of the large charge transferred from Be (shielding at O is 2.252). Thus, the Be density as seen from O behaves very much like Be^{+2} . For O^- , Burns and Wikner⁽¹⁶⁷⁾ report $(1-\gamma^\infty) = 29.22$, i.e., antishielding. Our calculation gives $q_0 = +\frac{2}{R^3} (-1.704)$ so that $(1-\gamma^\infty) = -0.852$. This is therefore of opposite sign to the antishielding model. The main source of these theoretical disagreements as in LiF are a result of the different contributions of $2p\sigma$ and $2p\pi$ electrons situated at the heavy nuclei, a reflection of the influence of the bonding process on the polarizations of densities.

4.4 Inadequacies of the Antishielding Model

To gauge the reasons for the above discrepancies, one must look into the assumptions which are inherent in the antishielding model. Firstly, no distinction is made between $p\sigma$ and $p\pi$ orbitals. The Li^+F^- density difference map shows that there is a more concentrated $2p\sigma$ density along the bond on both sides of the F nucleus, thus increasing the shielding. Furthermore, there is an increase of π density in front of the F nucleus. This also increases the shielding factor at F as the antishielding of the π atomic density is reduced. The fact that the atomic contribution of the π electrons at F is less in magnitude than that of the σ electrons indicates a strikingly different

polarization of these. The second assumption is made that the electrons on one ion are almost external to the other, i.e., there is very little overlap. The picture of the molecule as being two spherical balls of charge touching each other is an oversimplification. If one looks at the density difference diagrams for LiF and BeO, one notices "exchange" distortions at the electropositive elements, with radial excitations which expand the electron density of the positive ion in directions perpendicular to and also along the internuclear axis behind these ions. The net result of these distortions at Li and Be does not produce appreciable atomic field gradients for these nuclei. At Be, the σ polarizations are actually cancelled by π density which has been transferred from O. The exchange distortions also affect the polarization of the σ density of the F^- ion or F atom as seen by the rather abrupt cutoff of the positive $\Delta\rho$ region near Li, with accompanying backpolarization. The total overlap force added to the atomic force at F gives a value of 1.00, as expected for the ionic model. On the other hand, the field gradient, which measures regions closer to the nucleus, indicates that the $2p\sigma$ electrons at F contribute more than the $2p\pi$ electrons in magnitude. This increased shielding by the $2p\sigma$ electrons can be partly understood in terms of the clustering of density around the heavy nuclei as

demonstrated by the profiles of the $\Delta\rho$ map along the internuclear axis (see Fig.(2.5)). Furthermore, there is obvious loss of π electrons from the vicinity of these nuclei. This substantiates the assumption made by DeWijn⁽¹⁵²⁾ that in alkali halide molecules the polarizations of the orbitals of the halogen ions along the internuclear axis are quenched by overlap with the alkali core. This quenched polarization may not be noticeable in the forces, but will affect field gradients by virtue of prohibiting radial excitations, i.e., motion of more density towards the positive ion via orbitals of higher principal quantum numbers centered on F. Assuming that it is the $p\pi$ orbitals which are freely polarizable, DeWijn is thus able to present a theory which has the advantage of being applicable by means of simple semi-empirical calculations. These same effects are operative in BeO. The $\Delta\rho$ diagrams using both neutral and Be^+ , O^- , atomic densities indicate the increase of charge along the internuclear axis on both sides of O and polarization of π electrons into the bond region. In view of the diffuseness of O^- density, one therefore concludes that with respect to the F^- and O^- ions, polarization of the $p\pi$ electrons and some depolarization of the $p\sigma$ electrons tend to contribute to a shielding of the heavy nuclei F and O, with the result that one has negative field gradients

rather than positive ones as predicted by the anti-shielding theory. The situation at the positive ions is that both Li and Be see less $p\pi$ electrons on the other nucleus than predicted by the ionic model, since the nature of the disposition of such a density contributes significantly to undershielding.

One therefore has the result that the field gradients predicted by the antishielding model is an order of magnitude larger and of wrong sign for the F^- and O^- ions, while the results for the positive ion are predicted to be larger by a factor of two. The introduction of covalency, which amounts to introducing the Townes-Dailey theory, does not help the situation⁽¹⁵⁵⁾. This results in a deficiency in the $p\sigma$ orbital of a halogen atom which contributes a positive amount to the atomic q at the halogen nucleus (see next section). On the other hand, a point forgotten by many authors, a deficiency of the $p\pi$ density will create the opposite effects, i.e., reduce the antishielding contribution of these at the halogen nucleus. Our observation has been that in all the molecules we have studied so far, it is the π -bond which demonstrates covalent characteristics, whereas the ionic character is predominant in the σ -region. Thus it becomes now clear that the simplification of considering the $p\pi$ electrons as point charges located at the more electronegative nucleus is not totally justifiable.

For the molecule KCl , Das and Karplus⁽¹⁵¹⁾ showed that the inclusion of overlap effects between the ions K^+ and Cl^- alters the field gradient in the right direction to improve the agreement with the observed field gradient at the halogen nucleus. Charge-transfer covalency on the other hand, increases the discrepancy with experiment. This would not be so if one considers covalency of the π electrons also, whereas these authors consider only $p\sigma$ covalency. Introduction of overlap, they show, enhances the potassium field gradient by a factor of two. The discrepancy may well come from the undershielding of $p\pi$ electrons on the Cl nucleus. Although the internuclear distance is 5.04 a.u., the Cl^- ion will be very diffuse, so that a small undershielding of the halogen nucleus by the $p\pi$ electrons will counter any overlap effects which are also small.

These effects are probably larger in LiF because of the smaller internuclear distance. DeWijn⁽¹⁵²⁾ has, in fact, pointed out that the discrepancy is always largest at the smallest cation, the presence of which results in a shorter bond distance. This enhances the undershielding of the $p\pi$ electrons and thus is a primary source of the decreased antishielding at the alkali ion. In the case of BeO , the internuclear distance is smaller than in LiF . It has been stated by Das⁽¹⁶⁸⁾ that in spite

of the diffuseness of the O^- charge distribution, the compactness of positive ions as manifested by their small radii argues against the possibility of much covalent bonding. This is certainly questionable, since the electropositive ion tends to draw to itself the π electrons from the electronegative ion. We have also seen, moreover, that the electronic configuration was intermediate between Be^+O^- and $Be^{++}O^-$. Thus, at Be, one must deal with undershielding of the O nucleus, whereas at O, larger covalency of the π electrons will introduce a greater disparity in magnitude between σ and π contributions.

The paradox extends, as discussed by DeWijn⁽¹⁵²⁾, to the dependence of the antishielding effect on molecular vibrations. For $q(v)$, i.e., the increase of q with increase of the vibrational quantum number by one unit, calculated with antishielding theory, there is quite good agreement at the alkali site. At the halogen ion there again is a large discrepancy. The antishielding model predicts $q(v)$ to be negative. The observed $q(v)$'s, although of equal order of magnitude, have opposite signs. An effect other than antishielding must therefore be operative. Since q arises from all charges other than that of the nucleus under consideration, q will be affected by the change of charge distribution caused by molecular

vibrations. Assuming q to be a function of internuclear distance R , it will vary with R during the course of molecular vibration as follows: ⁽¹⁶⁹⁾

$$q(R) = q^{(0)} + q^{(1)} \zeta + q^{(2)} \zeta^2 + \dots \quad (4.9)$$

where $\zeta = (R - R_e)/R_e$ and R_e is as before the equilibrium internuclear distance. The wavefunction for an anharmonic potential can be obtained by solving a harmonic oscillator problem and the average values of the above expansion are obtained from this wavefunction. $q(R)$ is then approximately expressed as ⁽¹⁷⁰⁾

$$q(R) = q^{(0)} + q^{(2)} (v + \frac{1}{2}) + \dots$$

where (4.10)

$$q^{(v)} = 3Be/\omega_e (1 + \alpha_e \omega_e / 6B_e^2) q^{(1)} + 2Be/\omega_e q^{(2)}$$

The first term is the average of ζ over the anharmonic molecular vibrations; the last, the average of ζ^2 over the harmonic vibration. Be is the rotational constant, ω_e the vibrational frequency, α_e the rotation vibration constant. Using the recent experimental data of Gordy ⁽¹⁶³⁾ for LiF and Herzberg's ⁽⁷⁷⁾ tables for BeO, the resulting $q^{(v)}$'s are:

$$\begin{aligned} q_{\text{LiF}}^{(v)} &= .012 q^{(1)} + .003 q^{(2)} \\ q_{\text{BeO}}^{(v)} &= .009 q^{(1)} + .002 q^{(2)} \end{aligned} \quad (4.11)$$

These effects are quite small and include second order effects $q^{(2)}$. Using calculated values of $q(R)$ at seven

different points (see Appendix 2) we have made a best fit of these values to a 4th order polynomial. In Table 4.3, we present the first and second derivatives of the field gradient, and not $q^{(v)}$ as this would only obscure what we wish to show. We have transformed the first derivatives into effective charges so that

$$dq_A/dR = - 6/R^4 (Z_B - Z_{\text{eff}}) \quad (4.12)$$

Also included are contributions from the $p\sigma$ (4σ orbital) and $p\pi$ electrons (1π orbital) on the electronegative element.

The first thing one notices is that the $p\pi$ electrons at F and O are less sensitive to molecular vibration than the $p\sigma$ electrons. This suggests that the polarization of σ electrons at the electronegative nucleus is much more dependent on vibrations than the π electrons. This does not agree with DeWijn's semi-empirical theory, which considers only the polarization of the π electrons. The overlap contributions are negligible compared to the polarization contributions. The Li and Be charge densities behave again as point charges Be^{+2} and Li^+ as seen from their shielding contributions. Thus, at the more electronegative nucleus, the main contribution to $q^{(v)}$ comes from the restoration of polarization of $p\sigma$ electrons, i.e., an increased antishielding. The $p\pi$ electrons as they become more localized on the electronegative nucleus with

Table 4.3

DERIVATIVES OF FIELD GRADIENT IN LiF & BeO

	q	dq/dR	d ² q/dR ²	$-\frac{R^4}{6} \frac{dq}{dR}$							Total Electronic
				Nuclear(Z_B)	p σ	p π	A	O	S		
Li	-0.053	+0.008	-0.033	9.0	-2.528	-2.358	-0.003	-0.307	-8.781	-9.091	
F	-0.266	1.102	-0.756	3.0	-11.589	-2.915	-15.220	+0.224	-2.020	-17.016	
Be	-0.058	-0.023	+0.024	8.0	-2.388	-0.708	-0.283	-0.781	-6.738	-7.802	
O	-0.883	2.595	1.105	4.0	-14.105	-3.357	-19.021	-0.220	-2.040	-21.277	

increasing internuclear distance, also enhance the antishielding since they always contribute a net positive field gradient. However, their effect is only $\frac{1}{4}$ of that of the $p\sigma$ electrons. The net result is an increasing field gradient at F and O. On the other hand, the antishielding model would predict a decrease since $dq/dR = -6/R^4(1-\gamma^\infty)$ and $(1-\gamma^\infty)$ is 23 and 29 respectively for F^- and O^- . At the electropositive nuclei, namely Li and Be, the field gradients are very small, so are their changes. There is the usual undershielding of $p\pi$ electrons offset by an overlap and a slight overshielding of the $p\sigma$ electrons. These small changes are not in exact agreement with the shielding models which predict larger positive effects, i.e., $dq/dR = +6/R^4(1-\gamma^\infty)$ where $\gamma^\infty < 1$.

In all classical models such as the antishielding model, no attempt is made to portray directly the intramolecular electronic charge distributions. Terms are introduced to represent the polarization energy, but whether these are applicable in the inhomogeneous electric field occurring within the molecule is open to question. Buckingham⁽¹⁷¹⁾ has introduced such inhomogeneous fields in order to preserve the classical simplicity of the ionic model. However, this requires the knowledge of hyperpolarizabilities, second order polarizabilities which are not easily calculated with reliability⁽¹⁶⁴⁾. Benson

and van der Hoff⁽¹⁷²⁾ were probably the first to point out that orthogonalization of Li^+ 1s orbitals to F^- 2p orbitals gave backpolarizations at F^- due to Pauli repulsions between two closed shells. They concluded that although LiF is usually considered to be an ionic molecule, the inclusion of some covalent character was an essential feature. Similarly in the crystal, in order to explain properly nuclear quadrupole relaxation times, it has become evident⁽¹⁵⁵⁾ that any effective theory should include simultaneously the Van Kranendonk ionic model and the Yoshida-Moriya covalent model⁽¹⁷³⁾. The latter model enables one to calculate transition probabilities for nuclear spins in ionic crystals assuming that the transitions are induced mainly by a distortion of the residual covalent binding between neighbouring ions by the lattice vibrations. The Van Kranendonk model considers a point-charge ionic crystal where the transitions are induced by fluctuating field gradients from lattice vibrations. In view of the fact that the work of Watson and Freeman⁽¹⁷⁴⁾ suggests that the Sternheimer procedure underestimates $|\gamma^\infty|$, certainly modification of the negative ion structure by its environment must be a major source of the discrepancies. For systems with axial symmetry, it is now clear that binding affects the polarizations of the π and σ electrons differently. At

the electronegative site, shielding is increased as a result of depolarization of the σ electrons and an opposite polarization into the bond of π electrons. At the lighter atom, there is very little polarization of the core, or if there is any, it is effectively cancelled by back-donated π electrons. There is, furthermore, substantial undershielding of the π electrons situated at the electronegative site. There is thus a decrease in magnitude of the total field gradient, which one would misconstrue for a shielding effect on the part of the cation density itself due to externally induced polarizations. In highly symmetric systems such as alkali halide crystals, distortions from cubic symmetry by lattice vibrations will define directions along which polarizations will become asymmetric, so that densities along the internuclear distances will have different polarizations as those away from these regions. This will then affect field gradients at the halogen nuclei as in the axially symmetric cases. Furthermore, undershielding of the heavy nuclei by the electron densities which are situated on these will also be a factor contributing to smaller field gradients at the alkali sites. It is unfortunate that there is no long-lived quadrupolar isotope of F (F^{19} , the most abundant isotope has no nuclear quadrupole moment). Otherwise, the negative field gradients

as predicted by our calculation would have indicated the failure of the antishielding model and the possible deficiencies would have been brought to light sooner.

4.5 The Townes-Dailey Theory

The standard semi-empirical theory of field gradients and quadrupole constants is due to Townes and Dailey⁽⁶³⁾. Other general discussions have been given by Gordy⁽¹⁷⁵⁾, Das and Hahn⁽¹⁴⁵⁾, Orville-Thomas⁽¹⁷⁶⁾ and Lucken⁽¹⁷⁷⁾. Townes and Dailey related q_A for a molecule to the atomic field gradients q_{at} for a p electron, outside closed shells at nucleus A. The closed shells are assumed to be spherically symmetrical and to make no contribution to q . Other electrons give contributions that decrease rapidly with n and l . Thus, $q_A = f q_{at}$, where f depends on the electronic structure of the molecule. The calculation of q_{at} from experimental results in many cases is possible from hyperfine splitting of atomic beam spectra⁽¹⁷⁸⁾ which involves transitions between the energy levels of the free atom in a magnetic field. These quantities are also less accurately determined from the hyperfine splitting of optical spectra. For N, with a spherically symmetric configuration which gives zero interaction with the quadrupole moment of the nucleus, one can still obtain approximate values of $\langle 1/r^3 \rangle$ for the p electrons from the fine structure of optical

lines due to spin-orbit coupling⁽¹⁷⁹⁾. One can also calculate these from atomic Hartree-Fock wavefunctions such as those used for the density difference diagrams. However, there are quadrupolar deviations from spherical symmetry of atomic cores due to distortions from polarization of the electronic charge distribution by the nuclear quadrupole, and also by valence electrons, as we discussed in the previous sections. There is also a second order effect on the valence electrons themselves which is only taken into account by UHF calculations. These effects have been recently discussed by Sternheimer⁽¹⁵⁹⁾. By introducing the shielding factor γ_A , the total field gradient of the valence electrons should be regarded as altered to $q_{at}(1-\gamma_A)$. For the first row atoms these are small. For B, $\gamma_A = .142$; F, $\gamma_A = .11$, which represents a shielding effect in both cases⁽¹⁸⁰⁾. In general, as discussed before, calculations coupled with known theoretical difficulties indicate enough uncertainties in the calculated correction factors due to shielding that their present general use for evaluating nuclear quadrupole moments does not seem justified. Furthermore, in molecules, since the charge distributions that produce the various contributions to the field gradient are disposed differently with respect to the core electrons, the different contributions will all, in general, be subject to different antishielding factors and hence

more ambiguity exists⁽¹⁸¹⁾. In what follows, we have shunned this approach due to its uncertainties.

In a molecule, then, q_A is primarily dependent on the way in which valence electrons fill the lowest energy p-type orbitals. Contributions to q_A come from several different sources.

1) valence electrons associated with the nucleus in position

2) other charges associated with adjacent atoms

3) distortion of nonbonding closed shells of electrons around the nucleus.

Type (2) is usually considered not important, depending on $1/R_e^3$. However, these external charges produce changes in the wavefunction of other electrons in the atom. These contribute primarily to (3). For instance, if there is a nearby negative charge, the atomic electrons including those in closed shells tend to move away from this charge, partially cancelling its effect or shielding the nucleus. The effects of type (2) and (3) presumably cancel to a very large extent. It is generally assumed that the contribution to q of an external charge is reduced by a factor of 10. Estimates as discussed before show that distortions of the closed shell of electrons surrounding the nucleus will produce contributions to q less than 1% of the value due to a single electron of the valence shell.

It is also argued that the $p\pi$ electrons are perturbed and hence will cancel such polarization effects.

Quadrupole coupling constants are usually assumed to be sensitive only to charge near the nucleus, and not to outer regions of the molecule. Hence, Townes and Dailey expand the wavefunction near the nucleus in terms of atomic configurations. The question becomes then how these configurations are related to the nature of the chemical bond. Furthermore, both Dailey⁽¹⁴⁶⁾ and Gordy⁽¹⁷⁵⁾ reject overlap, which implies that neither valence bond nor MO methods provide adequate link between atomic and molecular wavefunctions. The chief argument against inclusion of overlap has been that normalization changes the electron density near the nucleus whereas the major effects of bonding should occur only in the outer regions of the atom - Our density difference maps certainly strongly vitiate any such arguments - Alternatively, the interpretation becomes that other configurations such as valence states and ionic configurations will change the charge density at the nucleus. The role of overlap has thus been puzzling. Inclusion of overlap in crude calculations may lead to errors since the wavefunction of the neighbour atom is far from being the correct solution to Schroedinger's equation in regions near the nucleus considered. That is why hybridization has always seemed a more reasonable

Table 4.4^{a)}Field Gradients on N in N₂ at R_e = 2.068 a.u.

a.o.	MO	$g_{2p}(R=\infty)$	$g_i(R=\infty)$	$g_i(R_e)$	A	O	S
1s ¹	1σg	<u>10.964</u>	1.000	1.009	-0.002	0.010	1.000
1s ¹	1σu		1.000	0.988	-0.012	0.004	0.997
2s ¹	2σg		1.000	5.011	2.286	1.800	0.926
2s ¹	2σu		1.000	2.551	2.244	-0.017	0.323
2p ^o ¹	3σg	10.964	1.000	11.517	9.626	1.289	0.602
2p ^π ²	1πu	-10.964	2.000	-8.051	-8.325	-0.453	0.727
Totals:		0.000	7.000	13.026	5.817	2.634	4.575

a) Underlined $g_{2p}(\infty)$ is $+\frac{R^3}{2} \times q_{210}$

Table 4.5^{a)}Field Gradients on C in CO at $R_e = 2.132$ a.u.

a.o.	MO	$g_{2p}(R=\infty)$	$g_i(R=\infty)$	$g_i(R_e)$	A	O	S
$1s_O^2$	1σ	<u>6.324</u>	2.000	2.001	0.000	0.000	2.001
$1s_C^2$	2σ		0.000	0.084	0.077	0.007	0.000
$2s_O^2$	3σ		2.000	4.029	0.828	1.350	1.851
$2s_C^2$	4σ		0.000	1.559	0.277	0.436	0.845
$2p\sigma_C^1 + 2p\sigma_O^1$	5σ	6.324	1.000	6.841	5.291	0.992	0.558
$2p\pi_C^1 + 2p\pi_O^3$	1π	-3.162	3.000	-0.837	-2.192	-0.167	1.522
Totals:		3.162	8.000	13.677	4.281	2.619	6.777

Field Gradients on O

a.o.	MO	$g_{2p}(R=\infty)$	$g_i(R=\infty)$	$g_i(R_e)$	A	O	S
$1s_O^2$	1σ	<u>19.089</u>	0.000	0.018	0.018	0.000	0.000
$1s_C^2$	2σ		2.000	2.003	0.000	0.002	2.000
$2s_O^2$	3σ		0.000	4.057	2.585	1.229	0.243
$2s_C^2$	4σ		2.000	22.116	20.241	1.564	0.311
$2p\sigma_O^1 + 2p\sigma_C^1$	5σ	19.089	1.000	6.204	5.725	-0.075	0.554
$2p\pi_O^3 + 2p\pi_C^1$	1π	-28.634	1.000	-24.873	-24.515	-0.603	0.244
Totals:		-9.545	6.000	9.524	4.054	2.118	3.353

a) Underlined $g_{2p}(\infty)$'s are $+\frac{R^3}{2} \times q_{210}$

Table 4.6 a)

Field Gradients at B in BF at $R_e = 2.391$ a.u.

a.o.	MO	$g_{2p}(R=\infty)$	$g_i(R=\infty)$	$g_i(R_e)$	A	O	S
$1s_F^2$	1σ	<u>4.238</u>	2.000	2.000	0.000	0.000	2.000
$1s_B^2$	2σ		0.000	0.051	0.036	0.015	0.000
$2s_F^2$	3σ		2.000	2.693	0.119	0.512	2.062
$2s_B^2$	4σ		0.000	3.061	0.468	0.916	1.678
$2p_B^1 + 2p_F^1$	5σ	4.238	1.000	2.555	1.983	0.244	0.329
$2p\pi_F^4$	1π		4.000	2.320	-0.281	0.055	2.546
Totals:		4.238	9.000	12.680	2.325	1.741	8.615

Field Gradients at F

a.o.	MO	$g_{2p}(R=\infty)$	$g_i(R=\infty)$	$g_i(R_e)$	A	O	S
$1s_F^2$	1σ	<u>41.763</u>	0.000	-0.007	-0.009	0.002	0.000
$1s_B^2$	2σ		2.000	2.004	0.000	0.004	2.000
$2s_F^2$	3σ		0.000	1.969	1.417	0.502	0.050
$2s_B^2$	4σ		2.000	64.245	61.813	2.244	0.189
$2p_B^1 + 2p_F^1$	5σ	41.763	1.000	4.063	3.936	-0.385	0.513
$2p\pi_F^4$	1π	-83.526	0.000	-71.448	-71.012	-0.477	0.041
Totals:		-41.763	5.000	0.827	-3.855	1.889	2.793

a) Underlined $g_{2p}(\infty)$'s are $+\frac{R^3}{2} \times q_{210}$

approximation to Schroedinger's equation. As Gordy has explicitly stated, it is necessary to assume hybridization or to treat bonding in terms of delocalized MO's. The recent trends would seem to favour the latter approach, as exemplified by Harris and Cotton's⁽¹⁸²⁾ recent work on metal complexes. In the final analysis, as we have seen for the ionic case, although overlap may not contribute to a particular property, it will significantly alter other domains of the electron density which will thus affect expectation values considerably. This is the rule rather than the exception and as Davies⁽¹⁸³⁾ pointed out, may well be the explanation of the difficulty found in the interpretation of eQq and of the injunction to ignore overlap.

4.6 Interpretation of Covalent Molecules

In Tables (4.4) to (4.6), there are presented the electronic field gradients in terms of effective charges for the series N_2 , CO and BF. Orbital breakdowns as well as atomic, overlap and shielding contributions of each orbital are given. In addition, free atom values of the contributions from 2p electrons are given as $g_{2p}^{(\infty)}$.

As seen from these tables, the shielding contributions correlate quite well with the shielding forces (see Chapter III). Atomic densities, which show back-polarization in terms of atomic forces, are found to be

less shielding for field gradients because of the $1/r^3$ dependence, than for the forces which have a $1/r^2$ dependence. The largest disagreement is found with the 1π electrons. These electrons only shield about 1/3 of the corresponding nuclear charge in N_2 because of their spatial distribution, whereas the forces show a shielding of $\frac{1}{2}$ of these nuclear charges. The discrepancy in shielding diminishes as one goes to larger internuclear distances such as in BF. It has been remarked by Kolker and Karplus⁽¹⁴⁴⁾ that as the wavefunction becomes more accurate, the contribution of the π electrons decreases as a result of orbital expansion. The difference between screening coefficients for σ and π orbitals was first noted by Mulliken⁽¹⁸⁴⁾, although it is often forgotten in approximate MO calculations⁽⁴⁶⁾. We have already remarked on the contraction of the σ -density in connection with the density diagrams, as a result of contraction of the $2p\sigma$ orbitals in the molecule. The disparity in $2p\sigma$ and $2p\pi$ contributions, as noted earlier for N_2 by Richardson⁽¹⁸⁵⁾, results in a noncancellation of these contributions. In the valence state for N ($2p\sigma^1 2p\pi^2$) there is a complete cancellation since $q_{2p\sigma} = -2q_{2p\pi}$. The total contributions from the overlap and shielding add up to give a net shielding charge of 7.21, which effectively cancels the nuclear charge. Hence, for N_2 , most of the field gradient

contribution comes from the atomic density, in agreement with the Townes-Dailey theory. The polarization of the π electrons into the bond complicates any discussion in terms of hybridization. However, one can express the net atomic field gradient in terms of effective atomic populations, making use of $g_{2p}^{(\infty)}$, the field gradient value of the free atom $2p\sigma$ orbital. For N_2 , this is 10.964. Then by adding the total σ atomic field gradient, one obtains an atomic population for N_2 of $2p\sigma^{1.25} 2p\pi^{1.50}$.

In the case of CO, the total shielding contribution at C due to O density is undershielding by about 1.2 charges, most of the deficiency coming from the π electron distribution. However, the sum of the overlap and shielding charges exceed the oxygen nuclear charge by 1.40 charges. A comparison of π overlap field gradients indicate that the density is unequally shared in contrast to the force analysis which predicted equal sharing. The total shielding at O due to C density is less than the O nuclear charge by 2.65 as compared to 2.12 from the force analysis. Much of this undershielding is therefore a result of backpolarization of atomic charges, also indicated by the forces. The field gradients thus accentuate the effect. The sum of shielding and overlap g 's at O is 5.47, somewhat less than the C nuclear charge of 6. In terms of the free atom field gradients, one obtains the following populations:

$2p\sigma_C^{1.0} 2p\pi_C^{0.70}$, $2p\sigma_O^{1.50} 2p\pi_O^{2.55}$. For BF, the sum of overlap and shielding field gradients at B indicates an overshielding of the F nuclear charge by 1.35, similar to the situation of C in CO. At F, this sum is 4.7, nearly completely shielding the 5 nuclear charges on B. In terms of free atom field gradients, the atomic populations are: $2p\sigma_B^{0.51} 2p\pi_B^{0.13}$, $2p\sigma_F^{1.62} 2p\pi_F^{3.45}$.

The field gradients in covalent molecules are not easily correlated by the Townes and Dailey theory with electronic structure. The first difficulty is that invariably one has to deal with the polarization of π electrons, which, as we have discussed in connection with the forces, go counter to electron transfer which occurs in the σ -region. Furthermore, the theory underestimates the contribution of overlap and shielding densities at light nuclei, and overestimates these at the heavy nuclei. These two contributions do not cancel out the nuclear charges for the last case. In the case of the light nuclei, the smaller $p\sigma$ gradients seriously limit any conclusion of the amount of "hybridization" present as a result of the overshielding of the nuclear charge at the other end of the molecule by the total overlap and shielding densities. The symmetric molecule N_2 shows best cancellation of nuclear charge and overlap plus shielding densities ($Z_N = 7.0$, $Q+S = -7.21$). For the other nuclei, one therefore

has the problem of partitioning the overlap density. In the next section, these will be discussed together with the atomic contributions in connection with certain features of the density.

A general comparison of the atomic densities of these molecules indicates increasing $p\sigma$ character and also $p\pi$ character in the order B(.51,.13), C(1.0,.70), N(1.25,1.50), O(1.50,2.55), F(1.62,3.45), where the bracketed values are $p\sigma$ and $p\pi$ net atomic populations referred to the free atom field gradients. Since the contribution of a simple $p\pi$ electron to field gradients is $-\frac{1}{2}$ that of a $p\sigma$ electron, we see that in all cases except F is there a preponderance of $p\sigma$ contribution, so that F would be termed as having a "p-electron defect"⁽¹⁴⁵⁾ of about $0.10 = (\frac{3.45}{2} - 1.62)$. This small defect would indicate a large amount of ionic character were it not for the fact that the atomic $p\pi$ population of F has decreased by about .5 charge due to transfer and polarization into the bond region. One might be tempted to obtain the ionic character i by linear interpolation of q from the equation

$$q = i q_{\text{ion}} + (1-i) q_{\text{cov}}$$

as done for a compound similar to BF , I_nCl by DeWijn⁽¹⁸⁶⁾. This necessitates the use of an antishielding factor for

the ion F^- or depolarization of the $p\sigma$ density and polarization of the $p\pi$ as discussed before. As all these are difficult to get at in practice, the best one can say is that the atomic field gradients are obtainable from the above net atomic populations. The π population must be obtained a priori from MO calculation in order to have meaningful results, due to their polarizations. The important suggestion of independent or even opposed σ and π polarizations has been previously discussed by various authors⁽¹⁸⁷⁾. Extended Hückel theory calculations for heterocyclic rings suggest pronounced and independent σ and π electron polarizations also⁽¹⁸⁸⁾. Simple electronegativity considerations, while giving a reasonable guide to the σ -polarization may lead to erroneous conclusions for the π -polarization. Nuclear quadrupole resonance studies interpreted in terms of the Townes-Dailey theory have thus always predicted large total electron excesses on electronegative atoms⁽¹⁸⁹⁾. It is therefore obvious that SCF-MO treatments will give lower values for the π -electron density, hence suggesting a need for refinements in the interpretation of quadrupole resonance data, a refinement which necessarily depends on the knowledge of the exact electron distribution.

4.7 Quadrupole Polarizations

The forces provide a measure of the axial dipole polarizations of the charge distributions. In particular,

TABLE 4.7

Field Gradient Components

A	q_A (total) a.u.	q_A (electronic)* $R^3/2$	$-(A+O)*R^3/2$	$\frac{\%(\Delta q_{el})}{-q_{210}}$	$q_{val.}(q_{210})$
Li	-0.053	-9.633	-0.411	+110	(0)
Be	-0.058	-8.420	-1.084	+ 99	(0)
O	-0.883	-9.704	-7.452	+224	(+2)
F	-0.266	-6.206	-4.230	+106	(+1)
B	-0.538	-12.680	-4.066	- 4	(-1)
C	-1.172	-13.677	-6.900	+ 59	(-½)
N	-1.365	-13.026	-8.451	+ 77	(0)
O	-0.728	-9.524	-6.172	+ 82	(+½)
F	+0.611	-0.827	+1.966	+ 95	(+1)

the atomic forces provide a measure of the extent of this polarization at each nucleus. These are related to dipole shielding factors β_∞ ⁽¹⁹⁰⁾ which are defined as the ratio of the change in the electric field at the nucleus, due to an atomic charge distribution, to the electric field at the nucleus from some external charge alone. The most characteristic rearrangement of the charge distribution is, however, its quadrupole polarization. The field gradient operator, $(\frac{3 \cos^2 \theta_a - 1}{r_a^3})$, provides a measure of this very polarization at nucleus A. Negative charge on the axis contributes $-2/r_a^3$ to the field gradient while charge on the perpendicular axis contributes $+1/r_a^3$ ($\theta = \pi/2$). A polarization of the charge along the axis at the expense of the perpendicular component in the region of the nucleus results in a negative field gradient and the magnitude of the gradient provides a measure of the quadrupole polarization. The electronic field gradients calculated from the H-F wavefunctions at the indicated R_e 's are given in Table 4.7. They are negative in every case. These figures, however, include the contribution from the atomic density distribution centered on the second nucleus in the molecule. This second atomic contribution exerts a field gradient equivalent to some number of point charges situated at the position of the second nucleus and is, therefore, large and negative. The contribution to q_A by a pair of inner shell electrons

on nucleus B is for example simply $-2(2/R_e^3)$. To obtain a measure of the quadrupole polarization which reflects the polarization of the density in the region of each nucleus independent of the changing contribution of the atomic density on the second nucleus, we have subtracted this latter contribution from the total electronic field gradients, as listed in Table (4.7). This results in a field gradient which is the sum of the contributions from the atomic and overlap populations for a given nucleus and is a measure of the quadrupole polarization in the region of a single nucleus as depicted in the $\Delta\rho$ maps. To make the relationship between this partial field gradient and the $\Delta\rho$ map complete, we have calculated the fractional increase in the field gradient relative to that for the separated atoms, using the same valence state for the atom as that employed in the construction of the $\Delta\rho$ maps. For example, the valence state of the F atom used in the $\Delta\rho$ maps is the $M_L = 0$ component of the 2P state which corresponds to the 2p subshell configurations of $2p\sigma_F^1 2p\pi_F^4$. The field gradient for the valence state of the F atom thus equals $-1+4(\frac{1}{2}) = (+1)$ times the magnitude of the field gradient of a single 2p electron. The same atomic values $g_{2p}^{(\infty)}$ for the 2p electrons, as in Tables 4.1 to 4.6, corresponding to the $\Delta\rho$ valence states, were used to calibrate the partial field gradients in the molecule. Table 4.7 lists the change

in the number of $2p\sigma$ electrons required to produce the calculated change in the partial field gradients. They are, therefore, measures of the extent of quadrupole polarizations. The bracketed values in the table are the field gradients for the appropriate valence states of the separated atoms also expressed relative to the $2p$ atomic values: a contribution of -1 for a single $2p\sigma$ electron and of $+1$ for simultaneous single occupancy of the $p\pi_+$ and $p\pi_-$ orbitals.

The spherical charge symmetry of the N atom in its $4S$ ground state is greatly distorted in the nuclear regions in the N_2 molecule. The σ component of the charge density is increased by 77% at the expense of the π charge component. This quadrupole polarization is even larger at the O nucleus in CO. The partial field gradient at F in BF is positive but the excess π component of the charge density in the free atom is halved by the process of bond formation. The increase in the σ component of the charge density found for the O nucleus in BeO and F in LiF exceed the values expected on the basis of the filling of the double and single $2p\sigma$ orbital vacancies found in the separated O and F atoms. This, as we have already discussed, was one of the reasons for the failure of the Sternheimer antishielding theory when applied to negative ions. Thus, the cationic charge distribution in an ionic

bond exhibits both dipolar and quadrupolar deviations from spherical symmetry. The dipole polarization is necessary for the establishment of electrostatic equilibrium and the quadrupole polarization results in an enhancement of the σ component of the charge density at the expense of the π component.

The asymmetry of the valence state of atomic carbon resulting from the configuration $2p\sigma_C^1 2p\pi_C^1$ is enhanced by 60% in the formation of the CO molecule. While the partial field gradient of the charge density in the vicinity of the boron nucleus in BF is negative in value, it represents a small decrease in the σ charge component derived from the valence state atomic charge density with a single σ electron in the 2p subshell. As noted previously, the charge increase in the region of boron nucleus is predominantly perpendicular rather than axial as in C, N, O or F, and the region of charge removal is not centered about the boron nucleus. The slight decrease in the quadrupole polarization noted for the boron reflects the partial transfer of charge to the vacant $2p\pi$ orbitals of the boron atom in the formation of BF. The charge density in the molecule in the vicinity of boron is still predominantly quadrupolarized.

The partial gradients for Be and Li are small and negative, the values being -0.140 and -0.034 a.u. respectively. Using the $g_{2p}(\infty)$ from atomic data (see section 4.3)

yields approximate increases of 110% and 100% in the σ over π components of the charge densities. Thus, even the cationic charge distribution in an ionic molecule exhibits both dipole and quadrupole polarizations, although the latter is small in magnitude.

The total field gradients in atomic units are listed as q_A in Table 4.7. N has the largest negative q_A . This is due to a large $p\sigma$ electron excess and also an increasing $p\sigma$ atomic field gradient. All q_A 's are negative except at the fluorine nucleus in BF. The situation for this nucleus is different in the molecules LiF and BF. Standard ionic polarization theory (Sternheimer antishielding) would predict the field gradients to be positive at F in LiF and still more positive in BF as a result of covalency of the $2p\sigma_F$ electrons in that molecule. q_F in LiF is negative whereas in BF it is positive. The signs follow from excess $p\sigma$ density at F in LiF and a defect of ~ 0.05 $p\sigma$ electrons in BF. In conclusion, it is evident the quadrupole polarizations are strongly affected by chemical bonding. Thus, caution must be used in interpreting these polarizations, as measured from quadrupole coupling constants. Models which do not take into account rearrangement of charge as a result of bonding will not predict adequately the quadrupole polarizations.

V. DYNAMIC PROPERTIES: FORCE CONSTANTS

La vérité, pour l'un, fut de bâtir -
elle est, pour l'autre, d'habiter.
A. de Saint-Exupéry

5.1 Introduction

From many points of view, the most interesting properties of molecules involve displacements of their nuclei. An essential step in the analysis of such effects is the expression of the electronic eigenfunctions in terms of the internuclear distance. In many cases, of which the treatment of reaction kinetics is perhaps the most important, this step involves formidable difficulties that only diligent computations can cope with. As a result, it has most frequently been handled phenomenologically⁽¹⁹¹⁾. In other cases, however, where the associated nuclear motions are of small amplitude, as for example vibrations, the problems are more tractable⁽¹⁹²⁾. In this chapter, we shall be concerned with intramolecular properties and therefore with vibrations. The subject of this section deals with the magnitude of vibrational frequencies, and hence force constants of diatomic molecules. The importance of further work in the latter context has been underlined recently by Parr⁽¹⁹³⁾, in an attempt to correlate molecular

potential energy functions to theoretical ideas regarding chemical bonding.

To a surprisingly good approximation, a potential function composed only of quadratic terms in the nuclear displacements may be made to fit the vibrational spectrum of most molecules. Furthermore, the potential energy constants for isotopic molecules are the same as in normal molecules, depending therefore on the electronic structure rather than on the nuclear structure of the isotope. This identity of force constants is a fortunate circumstance for polyatomics where otherwise it becomes impossible to calculate the constants uniquely. The force constants, determined from the vibrational frequencies, directly reflect the electronic structure of the molecule. Stretching force constants (our subject) although sensitive to molecular environment exhibit a fairly straightforward qualitative relationship. Their magnitude is to a good approximation inversely proportional to the bond length, which is in turn a measure of the bond order, and they are in general transferable among similar molecules⁽¹⁹⁴⁾. The empirical relationships between vibrational force constants and bond lengths which hold for a very wide variety of molecules, such as Badger's rule⁽¹⁹⁵⁾ and other rules⁽¹⁹⁶⁾, and between force constants, bond lengths and dissociation energies⁽¹⁹⁷⁾, have encouraged theoretical attempts to find

a practical way of calculating force constants. These include calculations of (d^2E/dR^2) ⁽¹⁹⁸⁾, of (dT/dR) ⁽¹⁹⁹⁾ which can be related to the force constant by the virial theorem, calculation of the force on an atomic nucleus in the molecule and use of the Hellmann-Feynman theorem ⁽²⁰⁰⁾, perturbation theory ⁽²⁰¹⁾ and an electrostatic approach ⁽²⁰²⁾. The principles of these methods have been reviewed from time to time. However, their application to a wide range of actual many-electron diatomic molecules has not been particularly successful. The simplicity of the empirical relationships has not been matched by the theory, and underlying regularities cannot easily be discerned. It is evident that exact force constant calculations are, therefore, of importance for a better understanding of molecular binding.

In particular, little attention has been paid to ab initio calculations of molecular force constants. Although the force constant operator involved has been stated in a form which could, in principle, facilitate calculation, those features of the electronic charge density to which the force constant is most sensitive have not been systematically investigated. In 1950, Platt ⁽²⁰²⁾ derived an approximate theoretical expression for the force constant of a diatomic molecule and applied it with some success to diatomic hydrides. Pauling had previously ⁽²⁰³⁾ (in 1927)

predicted internuclear separations for hydrogen halides employing the same underlying model, namely the united atom electron distribution. Platt's result was criticized by Clinton⁽¹⁹⁹⁾, who noted that Platt's derivation ignored the explicit variation of the electronic charge density with internuclear distance. In addition, by differentiation of the virial theorem with respect to the internuclear distance R , Clinton concluded that the explicit variation of the electronic-charge density with internuclear distance is a necessary condition for the molecule to have a non-vanishing force constant. Platt's impressive numerical results were interpreted as due to approximate cancellation of higher correction density terms. The fact that the force constant involves the derivative of the electronic charge density with respect to R was shown earlier by Byers Brown⁽²⁰¹⁾, through differentiation of the Hellmann-Feynman theorem. He then proceeded to express the force constant in terms of infinite perturbation sums. Salem⁽²⁰⁴⁾ employed certain sum rules to arrive at various alternative expressions for the force constant, related to the perturbation sums, and also derived the force constant expressions from the Hellmann-Feynman theorem.

The primary purpose of the present study is to investigate further the mathematical forms which the force constant can assume and use of these for interpretive purposes.

The form depends upon whether the virial theorem or the Hellmann-Feynman theorem is used to define the first energy derivative and what coordinate representation is employed to describe the wavefunction. These points have been emphasized in chronological order by Salem⁽²⁰⁴⁾, Phillipson⁽²⁰⁵⁾, Schwendeman⁽²⁰⁶⁾, Benston and Kirtman⁽²⁰⁷⁾. The choice of coordinate representation is an important factor as this can change the form of the force constant expression and its possible interpretation. As in the force analysis, we will find that the Hellmann-Feynman approach is the most advantageous method which permits one to isolate the different contributions to force constants. This hopefully puts one in a better position to explicitly analyze the role which the electronic-charge distribution plays in the vibrations of atomic nuclei. One question which may be asked is, for example, to what features of the electron-charge density are molecular vibrations most sensitive? Also, how important are the effects of electron correlation, and the related question of how reliable are Hartree-Fock wavefunctions, and their best approximations, in providing the ambient charge density in which the nuclei move?

It is to these and related questions that this chapter purports to be an introduction. In general, for a diatomic molecule, the force constant is the second

derivative of the total molecular energy with respect to R , evaluated at the equilibrium distance R_e . The nature of the differentiation process is investigated. Consideration of the first energy derivative, yielding the mathematical formulation of the Hellmann-Feynman theorem has already been discussed in a previous chapter in connection with the force analysis of chemical binding. The differentiation process is applied again to arrive at the second energy derivative, and hence the force constant. Employing a space fixed coordinate system in which one of the atoms is fixed, one can visualize the relative importance of the various terms involved so that one can get more insight into the relationship between chemical binding and the force constant. The scheme adopted here was thus designed to allow calculation of the force constants for any molecule, and in such a way as to show up those features of the electronic structure which have the most influence. To obtain the best accuracy of prediction in any particular case, the data employed should be restricted to a series of molecules in which the bond character is similar, or at least suffers no abrupt change along the series⁽²⁰⁸⁾. The two series N_2 , CO , BF and LiF , BeO , fit the above criteria. A calculation of the forces at a number of internuclear distances, curve fitting these to obtain derivatives and hence furnishing force constants, anharmonic constants, etc., use of field

gradients and the Hellmann-Feynman expression of the force constants will enable us to compare results for correlation schemes. The result of this will be to show that regularities reflect the extent to which the repulsive forces between the nuclei of the bonded atoms are reduced by electronic shielding and electronic relaxation effects. These relaxation effects will be pictorialized via the use of actual electron density diagrams representing the density differences between the extended and normal molecule.

5.2 The Hellmann-Feynman or Electrostatic Approach

We assume the validity of the Born-Oppenheimer approximation, according to which⁽²⁰⁹⁾ nuclear and electronic motions are separable. Specifically, we consider the nuclei to be subject to an effective potential energy function $E(R)$ which is the eigenvalue of the electrons for the nuclei fixed in each instantaneous configuration. The electrons are taken to remain during nuclear motion in the same quantum state, the characteristics of which adapt continuously to the shifting of the nuclei. The effective potential $E(R)$ for the nuclei is thus defined by

$$[T_{e1}(\vec{r}_i) + V(R, \vec{r}_i)]\psi_{e1}(R, \vec{r}_i) = E(R)\psi_{e1}(R, \vec{r}_i) \quad (5.1)$$

In this equation as in (3.1), \vec{r}_i refers to the electronic coordinates, T_{e1} is the electronic kinetic energy operator, and V is the total electrostatic potential energy operator. The nuclear coordinates are understood to have been written

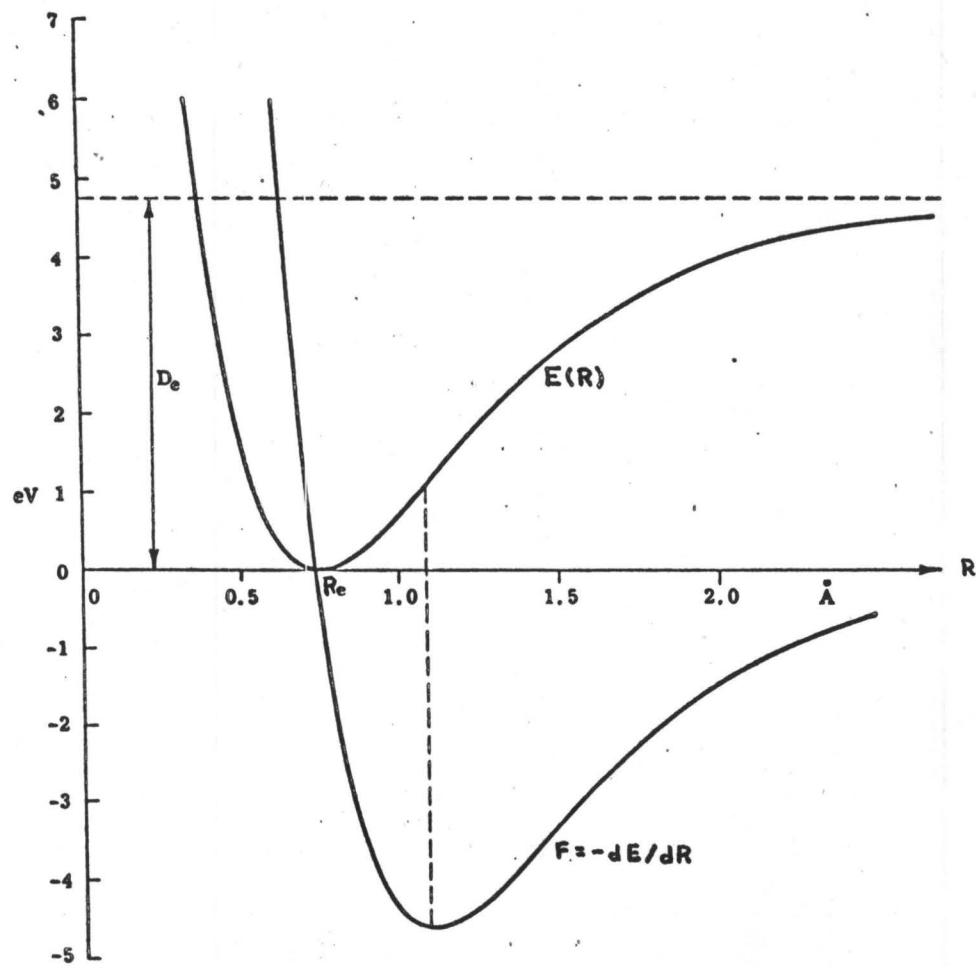


FIG 51. General form of a diatomic potential curve, $E(R)$, and of its derivative, $F = -dE/dR$ (to scale for H_2 molecule).

in terms of R and of the coordinates of some fixed point O , preferably on the molecular axis. In the equation, R appears only as a parameter. One can plot $E(R)$ and dE/dR as in Fig.(5.1). For bound states, as considered here, the function $E(R)$ has a minimum at R_e , with $(dE/dR)_{R_e} = 0$. The force constant k_2 of the molecule in the state represented by ψ_{e1} is defined by approximating $E(R)$ near R_e by a parabolic function (harmonic oscillator) and obtaining thereby

$$k_2 = (d^2E/dR^2)_{R_e} \quad (5.2)$$

where the differentiation occurs with respect to R only. Alternatively, we can express the force constant as

$$k_2 = \left[\frac{d}{dR} (dE/dR) \right]_{R_e} = - \left(\frac{dF}{dR} \right)_{R_e} \quad (5.3)$$

i.e. the differentiation of the force curve. The force only has meaning in so far as it operates on a certain nucleus, so that one must differentiate with respect to a nuclear displacement, eg., z_a ,

$$k_2 = + \left(\frac{dF_A}{dz_a} \right)_{R_e} = + \left(\frac{d^2E}{dz_a^2} \right)_{R_e} = \left(\frac{d^2E}{dR^2} \right)_{R_e} \quad (5.4)$$

This follows from the Hellmann-Feynman force on nucleus A ,

$$F_A = - \frac{dE}{dR} = + \frac{dE}{dz_a} = -Z_A \left[\int \frac{\cos \theta_a}{r_a^2} d\tau - \frac{Z_B}{R^2} \right] \quad (5.5)$$

where from Fig.(5.2) one has $-dz_a = dR$.

Before deriving the force constant expressions, we

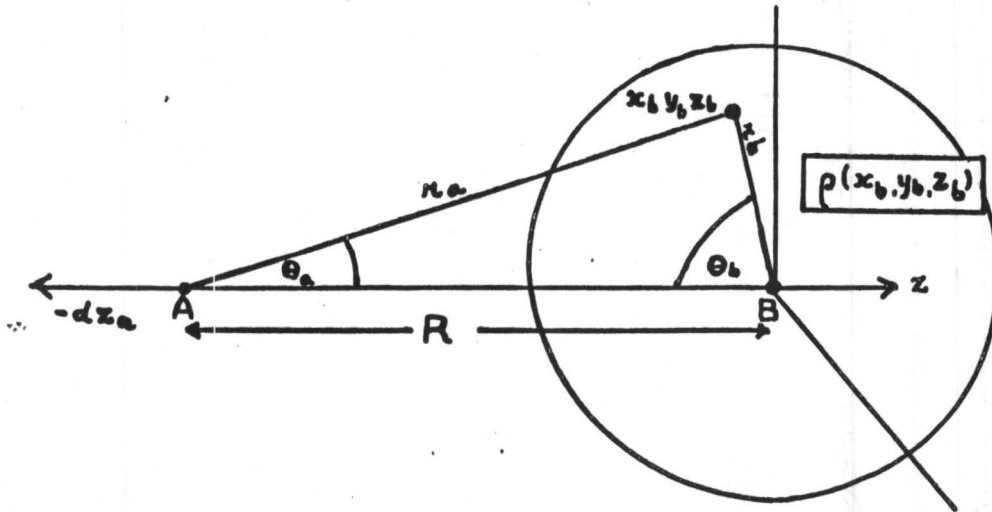


Fig.(5.2a) Fixed Electronic Coordinates Centered on B

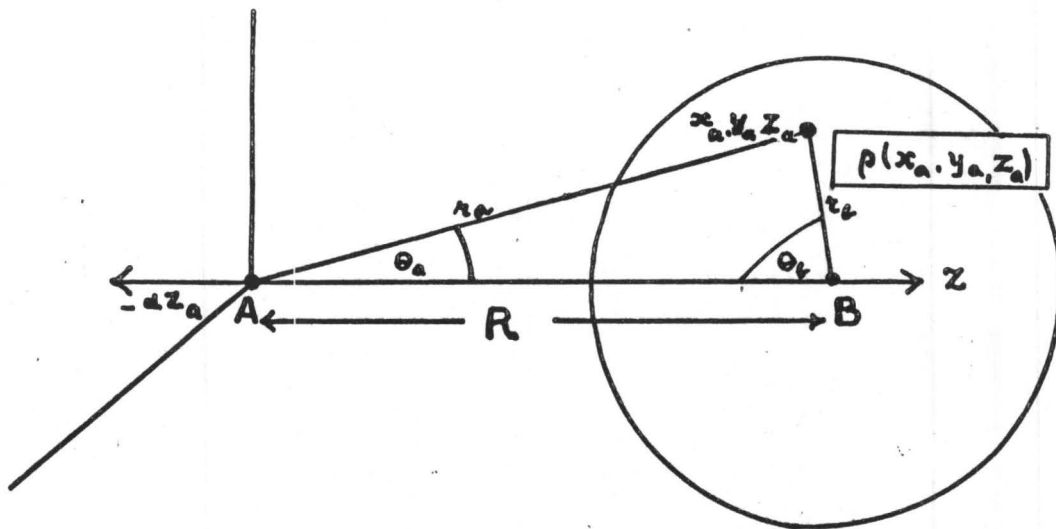


Fig.(5.2b) Moving Electronic Coordinates Centered on A, and B Fixed

wish to digress upon the real physical meaning of the force expression in order to clarify some points not discussed before and which are of relevance to the interpretation of force constants. Firstly, if we had expressed H and ψ in terms of Cartesian coordinates centered on nucleus B, the z axis being directed as indicated in Fig.(5.2), then in this representation, the only quantities in H and ψ which depend on R are the distance r_{a_i} of the electrons from nucleus A in addition to R itself and other variational parameters in ψ . For this case (1), see Fig.(5.2a), the expression for ψ would be (132)

$$\psi(\alpha, \vec{r}_a, \vec{r}_b) = \psi(\beta, [x_b^2 + y_b^2 + (z_b - R)^2]^{1/2}, [x_b^2 + y_b^2 + z_b^2]^{1/2}, \arctan y_b/x_b) \quad (5.6)$$

where $\arctan y_b/x_b = \phi$, and β represents all parameters including R . Furthermore we would have

$$-\frac{\partial \vec{r}_a}{\partial z_a} = +\frac{\partial \vec{r}_a}{\partial z_b}, \quad \frac{\partial \vec{r}_b}{\partial z_a} = 0$$

where this last relationship depends on the fact that the function ψ is fixed at z_b and does not depend on z_a . In fact, we see from the right-hand side of Eq.(5.6) that ψ depends on z_a (since $-dz_a = dR$) only through the parameters β (and R itself)

$$\text{i.e.}; \quad -\frac{d\psi(\beta, \vec{r}_b)}{dz_a} = -\frac{\partial \psi}{\partial \beta} \frac{\partial \beta}{\partial z_a} = -\frac{\partial \psi}{\partial z_a'}(\beta, \vec{r}_b) \quad (5.7)$$

where the primed superscript on z_a indicates differentiation

of parameters only, including R . For this case, then

$$\frac{dE}{dR} = -\frac{dE}{dz_a} = -\int \psi^* \frac{\partial H}{\partial z_a} \psi d\tau - \int \frac{\partial \psi^*}{\partial z_a} H \psi d\tau - \int \psi^* H \frac{\partial \psi}{\partial z_a} d\tau \quad (5.8)$$

The point to be underlined is that for this space fixed function, there has been a change in the density $\rho = |\psi|^2$ due to the nuclear motion, i.e. $d\psi/dz_a = \partial\psi/\partial z_a' \neq 0$.

However, the integral $\int \frac{\partial \rho}{\partial z_a} H d\tau = 0$ for stable wavefunctions, so that we retain the classical electrostatic interpretation.

On the other hand, for case (2), see Fig.(5.2b), ψ is expressed in terms of cartesian coordinates centered on nucleus A, so that

$$\psi(\alpha, \vec{r}_a, \vec{r}_b) = \psi(\alpha, [x_a^2 + y_a^2 + z_a^2]^{\frac{1}{2}}, [x_a^2 + y_a^2 + (z_a - R)^2]^{\frac{1}{2}}, \arctan y_a/x_a) \quad (5.9)$$

This function therefore depends explicitly on z_a and R , so that

$$\begin{aligned} \frac{d\psi}{dz_a} &= \frac{\partial\psi}{\partial r_a} \frac{\partial r_a}{\partial z_a} + \frac{\partial\psi}{\partial(\cos\theta_a)} \frac{\partial(\cos\theta_a)}{\partial z_a} \\ &+ \frac{\partial\psi}{\partial\alpha} \frac{\partial\alpha}{\partial r_a} + \frac{\partial\psi}{\partial R} \frac{\partial R}{\partial z_a} \end{aligned} \quad (5.10)$$

If α and R are constant, then we have rigid orbital following, or more precisely, just translation of the system. If the function remains centered on A, there is no change in ψ and H for this rigid following, so that $\partial\psi/\partial z_a = \partial H/\partial z_a = 0$, since r_a is constant⁽¹²²⁾. Thus the only change in ψ comes from nonrigid following with respect to A, i.e.

$$\frac{d\psi}{dz_a} = \frac{\partial\psi(\alpha, \vec{r}_a)}{\partial z_a'}$$

where α represents all parameters including R , for ψ centered on A. The same result could have been obtained had we moved nucleus B by $dz_b = dR$, keeping A fixed. Since $\psi(\alpha, \vec{r}_a)$ only depends on z_b through α , then

$$\frac{\partial \psi(\alpha, \vec{r}_a)}{\partial z_b} = - \frac{\partial \psi(\alpha, \vec{r}_a)}{\partial z'_a} = \frac{\partial \psi(\alpha, \vec{r}_a)}{\partial \alpha} \frac{\partial \alpha}{\partial z_b} \quad (5.11)$$

Furthermore, since $-d/dz_a = +d/dz_b = d/dR$, then

$$\frac{d\psi(\alpha, \vec{r}_a)}{dz_a} = - \frac{d\psi(\beta, \vec{r}_b)}{dz_b} = \frac{\partial \psi(\alpha, \vec{r}_a)}{\partial z'_a} \quad (5.12)$$

where in the equation, we have transformed (α, \vec{r}_a) into (β, \vec{r}_b) . This is permissible as long as one takes total derivatives of ψ , and can be checked using simple Slater orbitals. The importance of (5.12) will appear when we deal with the force constant expression. As the force constant is a measure of the changes in the forces, rigid following must contribute nothing since for such a case there is no change in force. The force changes will come from changing or relaxing densities $\partial \psi(\alpha, \vec{r}_a) / \partial z'_a$, which do not follow nucleus A.

The Hellmann-Feynman force expression is derived from a space-fixed electronic system, i.e. case (1), so that one thus eliminates interelectronic coordinates. Furthermore, mathematical operations such as differentiation is necessarily done with respect to a fixed coordinate system.

Therefore, whenever we shall use the Hellmann-Feynman formulae, we shall imply that the functions to be differentiated are expressed in terms of some space fixed coordinate. Coordinates will be introduced as variables in order to indicate a specific coordinate system other than some arbitrary space fixed system.

Differentiating expression (5.5) with respect to R , we have:

$$\frac{d^2E}{dR^2} = \frac{2Z_A Z_B}{R^3} + Z_A \left[\int \rho \frac{d}{dR} \left(\frac{\cos \theta_a}{r_a^2} \right) d\tau + \int \frac{d\rho}{dR} \frac{\cos \theta_a}{r_a^2} d\tau \right]$$

In fixed electronic coordinates,

$$\frac{d}{dR} \left(\frac{\cos \theta_a}{r_a^2} \right) = \frac{d^2}{dR^2} \left(\frac{-1}{r_a} \right) = \frac{1-3 \cos^2 \theta_a}{r_a^3} + \frac{4\pi}{3} \delta(r_a=0)$$

(see next section), and using the relation $dR = -dz_a$, we have:

$$k_2 = \frac{d^2E}{dR^2} = \frac{2Z_A Z_B}{R^3} + Z_A \left[\frac{4\pi}{3} \rho(A) - \int \rho \left(\frac{3 \cos^2 \theta_a - 1}{r_a^3} \right) d\tau - \int \frac{d\rho}{dz_a} \frac{\cos \theta_a}{r_a^2} d\tau \right] \quad (5.13)$$

where ρ is expressed in a space fixed system.

Equation (5.13) corresponds to the more general equation given earlier by Hornig⁽⁶⁴⁾

$$k_2 = \int \rho \frac{d^2V}{dR^2} d\tau + \int \frac{d\rho}{dR} \frac{dV}{dR} d\tau \quad (5.14)$$

The first integral, comprised of the first three terms in (5.13) is the force constant analogue of classical electrostatics for point charges (nuclei) immersed in a fixed

charge distribution of density ρ . This, by definition is a field gradient term. The second integral which is equivalent to the last term of (5.13) has no classical analogue⁽²⁰¹⁾, and expresses the change in the charge distribution due to the movement of the nuclei. This corresponds to a reaction of the system upon the field, a condition usually ignored in classical field theories but not in quantum field theories.

The field gradient term, which corresponds to moving the nuclei while holding the electrons fixed is positive and quite large because as one moves the nuclei, the initial electronic configuration does not correspond to a very low energy situation. The reason for this can be seen in expression (5.13) first derived by Salem⁽⁶⁷⁾. The electronic field gradient term requires the correction $\frac{4\pi}{3}\rho(A)$, which we have omitted in the previous chapter, as it does not affect the energy of the rotational states of a nucleus if ρ is spherical about it. However, if one moves a nucleus of charge Z_A from the center of such a distribution by an amount dR , one can easily calculate that the restoring force is $Z_A \frac{4\pi}{3} \rho(A) dR$. Consider a small volume element $d\tau = \frac{4\pi}{3} (\Delta R)^3$ at A . Then the charge Q in that volume is $\frac{4\pi}{3} \rho(A) (\Delta R)^3$ in the limit $\Delta R \rightarrow 0$. If one displaces the nucleus Z_A from the centre of this charge distribution by the

distance ΔR , then the restoring force is $\Delta F = Z_A Q / (\Delta R)^2 = Z_A \left(\frac{4\pi}{3} \rho(A) \Delta R \right)$ in the limit $\Delta R \rightarrow 0$. Therefore, the force constant $\Delta F / \Delta R$ for such a displacement is $Z_A \left(\frac{4\pi}{3} \rho(A) \right)$. We see then, that the larger $\rho(A)$ is, the larger is the force constant so that it becomes energetically more difficult to displace a nucleus from the center of a charge distribution with high density. This is the basis of the objection to floating functions as introduced by Hurley in order to satisfy the Hellmann-Feynman theorem. The term $\frac{4\pi}{3} \rho(A)$ is positive and thus usually exceeds any electronic field gradient terms which are sometimes negative. For the F nucleus, $\frac{4\pi}{3} \rho(A)$ is of the order of 1300 a.u., so that it is quite inconvenient in an analysis using equation (5.13). As shown explicitly later, much of this is cancelled by the relaxation component of the force constant $\int \frac{d\rho}{dR} \frac{dV}{dR} d\tau$. This can be shown using perturbation theory to be always negative, following an argument first given by Byers Brown⁽²⁰¹⁾. Expanding $\partial\psi_0/\partial R$ in terms of the complete set of equilibrium wavefunctions ψ_n ,

$$\frac{\partial\psi_0}{\partial R} = -\sum_{n \neq 0} \frac{(\partial H / \partial R)_{0n}}{E_n - E_0} \psi_n \quad (5.15)$$

where $(\partial H / \partial R)_{0n} = \langle \psi_0 | \partial V / \partial R | \psi_n \rangle$, the sum excluding the state $n = 0$, and since $\rho = \psi_0^* \psi_0$, we have

$$\int \frac{d\rho}{dR} \frac{dV}{dR} d\tau = -2 \sum_{n \neq 0} \frac{|\langle \psi_0 | \partial V / \partial R | \psi_n \rangle|^2}{E_n - E_0}$$

Since $E_n > E_0$, the integral is obviously always negative. This term then has the effect of reducing the energy of the system by a rearrangement of the density. The field gradient plus $4\pi/3 \rho(A)$ is the static part of the force constant, i.e., the electron density is kept fixed. The relaxation term $\int \frac{d\rho}{dR} \frac{dV}{dR} d\tau$ represents a dynamic effect, i.e., a response of the electronic system to nuclear motion, which thus helps reduce the energy of the total system and hence, the force constant. The magnitude of these two terms, the static and dynamic terms, depend on the choice of center kept fixed⁽⁶⁷⁾ during the infinitesimal extension or contraction of the internuclear distance by R . In most cases, the force constant appears as the difference of two very large terms.

The center of mass is not fixed in the derivation of equation (5.13). In as much as we have indicated that detachment of orbitals is not too likely, there will be some translation of the electronic density with the nucleus being considered. This translation must contribute nothing to the total force constant. This can be avoided by starting from equation (5.5) and differentiating it with respect to $dz_b = dR$. Thus, one obtains

$$\frac{d^2E}{dR^2} = \frac{d^2E}{dz_b dz_a} = \frac{2Z_A Z_B}{R^3} + Z_A \int \frac{\partial \rho}{\partial z_b} (\alpha, \vec{r}_a) \frac{\cos \theta_a}{r_a^2} d\tau \quad (5.16)$$

where ρ has been expressed in terms of coordinates centered on nucleus A so that $\partial \vec{r}_a / \partial z_b = 0$. In this method, which corresponds to Murrell's original approach⁽²⁰¹⁾, translation effects have been avoided by moving nucleus A by $dR/2$ and then nucleus B by the same amount. From (5.11) we have further that

$$\frac{d^2 E}{dR^2} = \frac{2Z_A Z_B}{R^3} - Z_A \int \frac{\partial \rho}{\partial z'_a}(\alpha, \vec{r}_a) \frac{\cos \theta_a}{r_a^2} d\tau \quad (5.17)$$

where dz'_a implies differentiation with respect to parameters only (see equations (5.9), (5.10)). The significance of this is that the electronic contribution to the force constant depends only on "relaxation" effects when ρ is expressed in terms of coordinates centered on A. This has the advantage that it avoids the calculation of contributions from rigid orbital following, since the only force changes occur for non-following for such a coordinate system. This approach has been advanced by Schwendeman⁽²⁰⁶⁾. We see that it is equivalent to Murrell's method, as one would expect from Galilean relativity. The disadvantage is that all effects are lumped together as relaxation, including density, which is fixed at B and therefore follows nucleus B. From the electrostatic viewpoint, this is equivalent to a field gradient contribution.

5.3. Cancellation Theorem

We have commented that translation effects must

cancel out in the force constant calculation as these do not contribute to actual force changes. The nullification of these contributions are a general result of translational invariance of the energy. From equations (5.13) and (5.17)

we must have

$$\int \frac{d\rho}{dz_a} \frac{\cos\theta_a}{r_a^2} d\tau + \int \rho \left(\frac{3 \cos^2\theta_a - 1}{r_a^3} \right) d\tau - \frac{4\pi}{3} \rho(A) = \int \frac{\partial\rho}{\partial z_a} \frac{\cos\theta_a}{r_a^2} d\tau$$

now

$$\int \frac{d\rho}{dz_a} \frac{\cos\theta_a}{r_a^2} d\tau = \int \frac{\partial\rho}{\partial z_a} \frac{\cos\theta_a}{r_a^2} d\tau + \int \frac{\partial\rho}{\partial z_a} \frac{\cos\theta_a}{r_a^2} d\tau$$

where $\frac{\partial\rho}{\partial z_a}$ implies differentiation of r_a and $\cos\theta_a$ only, i.e. differentiation of coordinates only. This is then the rigid orbital approximation (see Eq.(5.9)). We thus have the result that

$$\int \frac{\partial\rho}{\partial z_a} \frac{\cos\theta_a}{r_a^2} d\tau + \int \rho \left(\frac{3 \cos^2\theta_a - 1}{r_a^3} \right) d\tau - \frac{4\pi}{3} \rho(A) \equiv 0 \quad (5.18)$$

for rigid following. For a spherical charge density centered on A, the electronic field gradient is zero and we thus obtain the special case

$$\int \frac{\partial\rho_{\text{sph}}}{\partial z_a} \frac{\cos\theta_a}{r_a^2} d\tau - \frac{4\pi}{3} \rho(A) = 0 \quad (5.19)$$

This special case had been enunciated as a theorem by Salem but he failed to recognize its wider generality, i.e. a nonspherical charge distribution which follows a nucleus rigidly will always demonstrate cancellation of field

gradient and relaxation term. This can be easily verified by using Slater atomic orbitals of any symmetry centered on A and performing the operation indicated in Eq.(5.18). Much of the interpretive scheme of Salem is thus invalidated because of the omission of this important aspect. Schwendeman's and Murrell's expressions are thus seen to be a simplification arising from this cancellation.

One can derive this result in a much more general fashion. A system which moves through space without undergoing spatial distortions corresponds to a translationally invariant system, and because of the isotropy of space suffers no change in energy, force, etc. Thus we must have

$$\vec{\nabla} E = \vec{\nabla}^2 E = \vec{\nabla}^n E = 0 \quad \text{for } n > 0$$

By starting with the Hellmann-Feynman expression for the force, we have for $n = 2$,

$$\int [\rho \vec{\nabla}_a^2 (-1/r_a) + \vec{\nabla}_a \rho \vec{\nabla}_a (-1/r_a)] d\tau = 0 \quad (5.20)$$

In order to obtain meaningful results as the first integral is singular, one must first omit a small sphere of radius ϵ about A and integrate over angular variables, as discussed in the field gradient calculations of the fourth chapter. Then a correction obtained from Poisson's equation $\vec{\nabla}^2 (1/r_a) = -4\pi \delta(A)$ must be added (see Appendix 2) for the excluded sphere. This is all a matter of convention to ensure that a spherical charge distribution gives no field gradient. The second

part of the integral is absolutely convergent if ρ is made up of Slater functions since for the worst case, a 1s function, we have in the small excluded sphere

$\int_{\epsilon \rightarrow 0} \frac{de^{-r}}{dz} \frac{\cos\theta}{r^2} 4\pi r^2 dr$ which goes to zero as $\epsilon \rightarrow 0$. We thus have

$$\int_{r_a > \epsilon} \rho \hat{\nabla}_a^2 (-1/\vec{r}_a) d\tau + \int \hat{\nabla}_a \rho \hat{\nabla}_a (-1/\vec{r}_a) d\tau = 4\pi \rho(A) \quad (5.21)$$

For translation along the z-axis only, by symmetry

$$\int_{r_a > \epsilon} \rho \frac{3 \cos^2 \theta_a - 1}{r_a^3} d\tau + \int \frac{\partial \rho}{\partial z_a} \frac{\cos \theta_a}{r_a^2} d\tau = \frac{4\pi}{3} \rho(A) \quad (5.22)$$

which is the result (5.18) and proves our theorem,

namely that the density which follows rigidly nucleus A cannot contribute to the force constant, so that in a fixed coordinate representation the result (5.22) holds true.

This cancellation will also hold for higher derivatives by successively differentiating the equality (5.22). The result is that only relaxation effects contribute to all higher derivatives of the energy. To show this generally, we differentiate the force on nucleus A with respect to z_b and remember that $\partial \vec{r}_a / \partial z_b = 0$, then

$$\frac{dE^n}{dR^n} = \frac{d^n}{dR^n} \left(\frac{z_A z_B}{R} \right) + z_A \int \frac{\partial^{n-1} \rho(\alpha, \vec{r}_a)}{\partial z_b^{n-1}} \frac{\cos \theta_a}{r_a^2} d\tau$$

Furthermore, from Eq. (5.11) $\frac{\partial}{\partial z_b} = -\frac{\partial}{\partial z_a}$, therefore

$$\frac{dE^n}{dR^n} = \frac{d^n}{dR^n} \left(\frac{z_A z_B}{R} \right) + (-1)^{(n-1)} z_A \int \frac{\partial^{n-1} \rho(\alpha, \vec{r}_a)}{\partial z_a^{n-1}} \frac{\cos \theta_a}{r_a^2} d\tau \quad (5.23)$$

a result reported previously by Schwendeman⁽²⁰⁶⁾.

5.4 Force Constant and Quadrupole Coupling Constants

In the fixed electronic coordinate method, i.e. Hellmann-Feynman method, we saw that only H depended explicitly on the coordinates of nucleus A. In these so-called "one-center" coordinates, the derivative of the wavefunction with respect to R involves only the derivative with respect to the variational parameters, including R. Defining these parameters by β_i , we have (ψ centered on B)

$$\psi = \psi(x_b, y_b, z_b; \beta) ; \frac{d\psi}{dR} = \frac{\partial \psi}{\partial R} = \sum_i \frac{\partial \psi}{\partial \beta_i} \frac{\partial \beta_i}{\partial R}$$

The electronic force constant in this representation we have seen is (from (5.13) and (5.5))

$$k_2^{el} = \left[\int \psi^* \frac{d^2 V_{en}}{dR^2} \psi d\tau - \sum_i \frac{\partial \langle F_{el} \rangle}{\partial \beta_i} \frac{\partial \beta_i}{\partial R} \right]_{R_e} \quad (5.24)$$

On the other hand, in the moving coordinate representation, the electronic force constant is given by the following equivalent expression from (5.17)

$$k_2^{el} = - \sum_i \frac{\partial \langle F_{el} \rangle}{\partial \alpha_i} \frac{\partial \alpha_i}{\partial R} \Big|_{R_e} \quad (5.25)$$

where the α_i 's are now the parameters obtained after expanding the density onto nucleus A. The second term of (5.24) appears formally to be identical with the equality (5.25), yet there is no contradiction. The dependence of

the parameters β_i on R is different from the R dependence of the parameters α_i , the difference arising from the transformations from one nucleus to the other (Eq. (5.6) and (5.8)). In particular, Schwendeman's expression is a special case of the confocal elliptical representation of Phillipson⁽²⁰⁵⁾ where now the density is centered simultaneously on A and B to avoid translation of the system as a whole. Phillipson prefers to call the field gradient contribution a "quadrupole" correction to the force constant. He emphasizes the fact that the appearance of the quadrupole operator in the force constant expression is contingent upon the choice of coordinate representation and thus appears to rule out the possibility of assigning an invariant connection between the force constant k_2 and the quadrupole coupling constant q . This view is also supported by Schwendeman who shows that different symmetries of the electron density are involved in the force constant and the field gradient. For instance, the electronic contribution to the force constant is

$$k_2^{el} = -Z_A \int \frac{\partial \rho(\alpha, \vec{r}_a)}{\partial z'_a} \frac{\cos \theta_a}{r_a^2} d\tau \quad (5.26)$$

which Schwendeman equates to

$$k_2^{el} = -Z_A \left(\frac{4\pi}{3}\right)^{\frac{1}{2}} \int \frac{\partial \rho_{10}}{\partial z'_a}(\alpha, \vec{r}_a) d\tau \quad (5.27)$$

This is permissible as can be easily shown by considering a 1s orbital $\psi_{1s}(\vec{r}_a) = e^{-Zr_a}$. Then $\frac{\partial \psi_{1s}}{\partial z'_a}(\vec{r}_a) = -\frac{dz}{dz_a} r_a e^{-Zr_a}$, so that upon performing this operation, the angular symmetry of the function has not changed. However, in the next section, in connection with Platt's model, we will show that a spherical charge density centered on nucleus B, to which are applied equations (5.26) and (5.27) when this density is expanded onto A, will give a field gradient contribution to the force constant. This is also true for any density of other symmetry centered on nucleus B, as can easily be verified by using simple Slater orbitals. The result is that Eq.(5.27) is equivalent to a field gradient for a fixed charge density. For density which follows nearly completely nucleus A, then (5.27) also gives a field gradient which is a measure of the effect from that charge which does not follow that nucleus rigidly, but relaxes with respect to it. It is evident, therefore, that with respect to nucleus A, any density fixed on B will represent a relaxation. However, as the contribution of this "fixed" relaxation is equivalent to a field gradient, it will be more convenient to treat it as such. These ideas will be further pursued in the analysis of the density contributions to the force constant.

The relationship between force constants k_2 and field

gradients q_A' defined by $q_A = 2Z_B/R^3 - \int \rho \frac{3 \cos^2 \theta_a - 1}{r_a^3} d\tau$

depends on which nucleus one is considering. Use of a linear relationship in order to attain some empirical correlation has been made for C-H bonds⁽²¹⁰⁾. The detailed expression relating the force constant to the quadrupole constant of either nucleus involves a certain amount of cancellations, as was shown in the previous section. A previous attempt to relate these two quantities is due to Hornig⁽⁶⁴⁾. The explicit relationship was analyzed by Salem⁽⁶⁷⁾ using Eq.(5.13) in order to account for an apparent correlation for a series of molecules, ionic hydrides specifically. Although he indicated evidence that the partial force constant for moving a proton along with a $2p_z$ orbital was zero, the reason was not made clear. Furthermore, for those molecules which have negative field gradients, as those considered in this work (see Table (4.7)), there is obviously no linear relationship between the force constant and the field gradient, since k_2 by definition is a positive quantity. These negative field gradients cancel to a large extent in the total force constant expression as they arise from p_z orbitals which mainly follow the nuclei on which they are situated. It is that density, which does not follow the nucleus considered, which will contribute a field gradient to the force

constant. The separation of this fixed part of the density from the total is by no means simple. It can be done for that charge fixed on nucleus B. The remaining density, atomic and overlap must be considered as relaxation. Thus, no general relationship between the force constant and the field gradient of the total density is possible in view of cancellation phenomena.

5.5 Platt's Model

We now present an instructive example to demonstrate the equivalence of field gradients and relaxations of densities fixed with respect to some center other than A. The Hellmann-Feynman expression was used for the force as a result of the advantage derived from its exclusion of the requirement of any knowledge of $\partial\psi/\partial R$, i.e. the adiabatic change in the electronic wavefunction with nuclear motion. In the force constant expression, one therefore has to cope with this factor, or rather $\partial\rho/\partial R$, the change in density. The center of gravity of the distribution $\partial\rho/\partial R$ thus enters the force constants. It also determines infrared intensities⁽²¹¹⁾, since the change in dipole moment with vibration is

$$\frac{\partial\mu}{\partial R} = \int \frac{\partial\rho}{\partial R} z \, d\tau \quad (5.29)$$

In the force constant calculations, the term one must consider is

$$k_2^{el} = -Z_A \int \frac{d\rho}{dz_a} \frac{\cos\theta_a}{r_a^2} \, d\tau \quad (5.30)$$

As we have mentioned before, this is a quantal term expressing the reaction of a particle on a field, thus giving rise to a second order correction to the energy of the total system. This is by no means negligible as it must cancel with the classical electrostatic terms when the molecule is uniformly translated. By expanding the perturbed (1s) density $\partial\rho/\partial R$ for an H atom using the expression (5.15),

$$\frac{\partial\psi_0}{\partial R} = - \sum_{n \neq 0} \frac{\langle 0 | \partial H / \partial R | n \rangle}{E_n - E_0} \psi_n$$

Byers Brown and Steiner⁽²¹²⁾ have shown by summing over discrete states that 93.2% of the contribution to the relaxation (5.30) comes from continuum states, whereas the resulting polarizability of the displaced charge only had an 18% contribution to the total from continuum states. This corresponds to pulling a spherical charge distribution, undistorted, a distance R from the nucleus. One way of circumventing this problem is to use floating functions à la Hurley, which follow the nucleus. This approach has indeed been used by Liehr⁽¹⁹²⁾ in the calculation of vibronic effects on transition probabilities. For certain systems, it is possible to omit these variations in charge density and assume that there is no orbital following. This approximation will hold well for protons, the electrostatic field of which are small because of the small

charge of the proton. This approximation has been successfully used by Platt⁽²⁰²⁾ and by Longuet-Higgins and Brown⁽¹¹⁶⁾ in calculations on molecular hydrides.

Let us therefore consider a hydride M^-H^+ . A typical compound of this class would be FH. In a first approximation we may consider such a molecule as built out of a negative ion M^- , consisting of a nucleus M surrounded by a charge density of Z_M+1 electrons, and of the proton buried in this density at its equilibrium position. Hence, from (5.13),

$$k_2 = Z_H [q_H + \frac{4\pi}{3} \rho(H) - \int \frac{d\rho}{dz_H} (\vec{r}_M) \frac{\cos\theta_H}{r_H^2} d\tau] \quad (5.31)$$

and

$$q_H = \frac{2Z_M}{R^3} - \int \rho \frac{3\cos^2\theta_H - 1}{r_H^3} d\tau .$$

If the total charge density in our model is chosen to be spherical, then for electrostatic equilibrium

$$\frac{Z_M}{R_e^2} = \int \rho(\vec{r}_M) \frac{\cos\theta_H}{r_H^2} d\tau \quad (5.32)$$

which means that the charge density inside the sphere of radius R_e must equal Z_M in order to completely shield the nuclear charge, and thus give $F_H=0$. Since q_H is the negative derivative of F_H , it will also be zero, i.e. complete screening of the nucleus, except for a singularity at $Z_H=0$, which contributes an additional $\frac{8\pi}{3} \rho(H)$. This

additional contribution comes about because the electric field or force must be continuous in the x and y directions, considering the sphere with radius R_e as a boundary. The discontinuity in the field occurs along the normal, i.e. the z axis, and the magnitude of it is $4\pi\rho$ ⁽²¹³⁾. Our result for a spherical charge distribution centered on M, then is:

$$k_2 = z_H \left[4\pi\rho(H) - \int \frac{d\rho(\vec{r}_M)}{dz_H} \frac{\cos\theta_H}{r_H^2} d\tau \right] \quad (5.33)$$

We obtain Platt's formula $k_2 = 4\pi\rho(H)$ if we assume that the charge density is fixed on nucleus M and follows only that nucleus in addition to being rigid, for then $\rho(\vec{r}_M)$ is independent of z_H completely and the integral vanishes since $d\rho/dz_H \equiv 0$.

Alternatively, one could have started from Eq.(5.17) and using Eq.(5.12):

$$k_2 = z_H \left[\frac{2z_M}{R^3} + \int \frac{d\rho(\vec{r}_M)}{dz_M} \frac{\cos\theta_H}{r_H^2} d\tau \right] \quad (5.34)$$

which represents the relaxation method of Murrell and Schwendeman. In other words, we measure the change in force resulting from a change in density at the proton as nucleus M carries with it the density $\rho(\vec{r}_M)$. We assume for simplicity that we are dealing with a 1s density centered on M, so that $\rho(\vec{r}_M) = e^{-r_M}$. Using the results -

$$\frac{\partial}{\partial z_M} e^{-r_M} = -\cos\theta_M e^{-r_M}$$

$$\frac{\cos\theta_H}{r_H^2} = \begin{cases} \frac{2r_M}{R^3} P_1(\cos\theta_M) & r_M < R \\ -\frac{\cos\theta_M}{r_M^2} & r_M > R \end{cases}$$

(see Pitzer et al (154) or Appendix 2)

we obtain

$$\int \frac{d\rho}{dz_M}(\vec{r}_M) \frac{\cos\theta_H}{r_H^2} d\tau = \begin{cases} \frac{8\pi}{3} e^{-R_e} - \frac{2}{R^3} \int_0^{R_e} e^{-r_M} 4\pi r_M^2 dr_M & r_M < R_e \\ \frac{4\pi}{3} e^{-R_e} & r_M > R_e \end{cases}$$

For $r_M < R_e$, we then have the field gradient of all the charge inside the radius R_e . The resulting force constant is then

$$k_2 = z_H \left[\frac{2z_M}{R_e^3} + 4\pi\rho(H) - \frac{2}{R_e^3} \int_0^{R_e} e^{-r_M} 4\pi r_M^2 dr_M \right]$$

For electrostatic equilibrium the first and third terms are equal, i.e. complete shielding. We thus obtain again Platt's equation

$$k_2 = 4\pi\rho(H) \quad (5.35)$$

This simple example therefore demonstrates the equivalence between field gradients and relaxation effects. The Murrell-Schwendeman-Phillipson interpretation includes field gradient effects as relaxation. For charge distributions localized on a particular nucleus, the electrostatic inter-

pretation indicates these should be more appropriately considered as field gradient effects.

We have seen that $q_H = \frac{8\pi}{3} \rho(H)$, so that $k_2 = \frac{3}{2} q_H$. For HF, HBr and HI, Salem has discussed this correlation. The experimental data suggests that q_H is 85% of the force constant on the average, rather than the predicted 67%. The agreement can be improved by assuming the complete following of the proton by an added spherical charge density. This would increase $\rho(H)$ but would not affect k_2 since orbital following would contribute nothing. The addition of polarization at H in the form of $p\sigma$ character would decrease q_H since $p\sigma$ contributes a negative field gradient. If this polarization remained rigid and followed the proton, k_2 again would be unaffected. However, if one assumed that this polarization changed upon vibration, as it most certainly does, then $\rho(H)$ would have to be increased, since the relaxation term due to the changing polarization is positive ($q_H < k_2$) but the field gradient contribution of $p\sigma$ electrons would reduce q_H . The question as to which charge density to use has thus always been in dispute. Hall and Rees⁽²⁰²⁾ have pointed out that a separated ion wavefunction would give improved results for Platt's model, which originally depended on united atom wavefunctions. More recently, using Hartree-Fock atomic wavefunctions, McDugle and Brown⁽²¹⁴⁾ have shown that cal-

culated equilibrium distances and force constants are in much better agreement with experiment for the united-atom model. Platt's treatment is least accurate for the lighter molecules, for which the electron density will become significantly perturbed by motion of the proton. Introduction of polarization will, as we have discussed above, alleviate any discrepancy. Relaxation or orbital following will then have to be considered explicitly.

It must be pointed out that nucleus M is not in equilibrium but sees a repulsive force from a single positive charge, the unshielded proton. Thus, polarization must be introduced at M to achieve electrostatic equilibrium. Similarly, the force constant at M is equal to $2Z_H Z_M / R^3$, i.e. the field gradient produced by the proton at nucleus M, since $\rho(\vec{r}_M)$ completely follows that nucleus and hence contributes nothing to the force constant. In actuality, the electronic field gradients are not negligible since the bonding involves mostly $p\sigma$ electrons in molecules such as HF and HCl. Thus their magnitudes and the change of polarization of $p\sigma$ and $p\pi$ electrons, which we have seen in the previous chapter can be quite different, must be taken into account.

At the proton, Platt's model violates another tenet of rigorous quantum chemistry, namely the virial theorem. The assumption that $\partial\rho/\partial z_H=0$ implies constant scale. Satis-

faction of the virial theorem requires optimum scale which minimizes the energy. On the other hand, the above assumption ensures validity of the Hellmann-Feynman theorem, which requires only that $\int \frac{\partial \rho}{\partial z_H} H d\tau = 0$, a condition satisfied by Platt's assumption. The violation of the virial theorem requirements was pointed out by Clinton. The objection has been removed by a scaling technique proposed by Hall and Rees⁽²⁰²⁾. However, we now see that the success of Platt's model is more a result of its satisfying the Hellmann-Feynman theorem, even though somewhat artificially, and less a spurious result because of its violation of the virial theorem.

In extending the model to polyatomic molecules as done by Longuet-Higgins and Brown⁽¹¹⁶⁾, satisfactory results are again obtained. The reason for this is that for the particular case of bending and twisting modes, the electronic contributions diminish considerably. We have commented before that electrostatics requires the tangential component of the force on a boundary surface to be continuous. For a spherical distribution, the force is constant on the sphere and hence perpendicular modes will have vanishing electronic force constants. This sort of reasoning has been used by Bader in a discussion of proton transfer reactions⁽²¹⁵⁾. One can extend these ideas to potential barriers, where if as in ethane one assumes as a first approximation the charge

density to have cylindrical symmetry about the C-C bond, then the twisting modes will be hardly affected by the electronic field gradient because of the continuity of the perpendicular force components on the protons. Clinton⁽²¹⁶⁾ was one of the first to point out that much of the barrier to internal rotation comes from nuclear-nuclear interactions. Our considerations would seem to indicate that a large part of the remaining contribution comes from electronic relaxation effects. One important factor is orbital following at the protons, which must be included. That orbital following does occur is reflected in the low values of interaction force constants. The assumption of orbital following corresponds to quite a sizable value of $\partial\rho/\partial r_H$ which drastically reduces the nuclear repulsion contribution in C-H bonds⁽²¹⁷⁾. In fact, it is impossible to get a nonvanishing electronic contribution to the interaction constants of stretching-stretching type if the wavefunctions are not allowed to follow the nuclear motion^(88b). This is because of the result that no molecular integrals then depend simultaneously on two different bond distances: $d^2E(\text{el.})/dRdR'$ is necessarily zero (R and R' are two different bond lengths). The electronic term therefore measures the electronic rearrangement during vibration. The negative signs of interaction constants in some molecules are precisely the result of the

preponderance of this electronic relaxation⁽²¹¹⁾ over nuclear terms. Bader⁽²¹⁸⁾ has used perturbation theory and certain simplifying assumptions about the "transition density" to evaluate these effects. In conclusion, we can state that relaxation is the rule rather than the exception.

5.6 Method of Calculation

The relaxation terms are in general much too difficult to calculate from ab initio functions. In the case of Cade's function for N_2 , the parameters do not vary with R in any systematic way, thus making it impossible to evaluate $d\alpha/dR$ in any consistent manner. The method we have adopted in this present work is a calculation of forces at different internuclear distances, followed by a polynomial fit of these, so that one can easily obtain the derivatives one is interested in. This has advantage over an energy fit, since in general the forces are smaller and much more sensitive functionals of the density. Moreover, this permits one to partition the derivative into orbital contributions. One can show this for the force constant by considering the derivative of the force expression:

$$\begin{aligned} \frac{d}{dR} \int \rho F d\tau &= \int \frac{d\rho}{dR} F d\tau + \int \rho \frac{dF}{dR} d\tau \\ &= \sum_i 2n_i \langle \phi_i | F | \frac{d\phi_i}{dR} \rangle + \sum_i n_i \langle \phi_i | \frac{dF}{dR} | \phi_i \rangle \end{aligned}$$

where the ϕ_i 's are orbitals, and the second equality comes about by writing the force F as a sum of orbital terms $n_i \langle \phi_i | F | \phi_i \rangle$. The relaxation is therefore separable into orbital contributions by comparing the two equalities by term, i.e.,

$$\int \frac{d\rho}{dR} F d\tau = 2 \sum_i n_i \langle \phi_i | F | \frac{d\phi_i}{dR} \rangle$$

In the case of the energy, the sum of the individual orbital energies is not equal to the total energy in Hartree-Fock theory. The sum of orbital energies counts the pair interactions twice. Thus, one cannot easily calculate any relationship between variations of orbital energies and orbital force constant (or for that matter, force) contributions. The first derivative of the force curve gives the force constant. The orbital field gradients have already been given in the previous chapter. The densities at the nuclei are also easily calculated from the known wavefunctions. Hence, using equation (5.13), one can work back to obtain the numerical values of the relaxation terms in addition to analyzing the force constant orbital by orbital, and also in terms of atomic, overlap and shielding contributions.

The force curve is expanded in the Dunham form used by molecular spectroscopists, i.e.,

$$F(R) = F_1 + F_2 \zeta + F_3 \zeta^2 + F_4 \zeta^3 + \dots$$

where $\zeta = (R - R_e)/R_e$. This was fitted to the forces calculated at seven regularly spaced points, as listed in Appendix 3. Curve fitting was done for net forces and also for the individual orbital electronic forces. The wavefunctions used are claimed to be close to Hartree-Fock functions by the authors who calculated them. However, as optimization is not complete in general, the force curves obtained are not ideally smooth, so that poor results for higher derivatives are obtained if one fits a polynomial through all the given points. These difficulties in polynomial fits have been discussed by Cade et al for energy derivatives, for which scaling of the energies should be done as per McLean⁽²¹⁹⁾. To ensure rapid convergence of a power series, one should not use too wide a range of R ⁽²²⁰⁾. On the other hand, if the range is too narrow, higher order terms in the polynomial become negligible and prevent the exact determination of the coefficients of these terms. The best fit was obtained when more points were used than the minimum required by the degree of the polynomial. For the seven points available, a fourth order polynomial was found to give, in general, best agreement for the force constant k_2 , the anharmonic constant k_3 and 3rd order constant k_4 . Because of the unevenness of the optimization of certain functions and the sensitivity of the forces to these, two methods of curve fitting were used in order to ascertain consistency

of the results. A Tchebycheff polynomial best fit was used first. In this method, a polynomial is chosen which will go through the best set of a given number of points, the procedure being one of iterative testing of each point and discarding the worst ones. This method was at all times checked against a least square fit of the polynomial of the same degree. The least square method has been studied by Pliva et al for various potential energy curves⁽²²¹⁾. Best results are obtained by an overdetermination of the polynomial, i.e., using more points than the minimum required. In all cases, the best fit and least square method agreed to two or three significant figures. The N_2 wavefunction was the most reoptimized of all the wavefunctions used, especially at the Re(exptl.) where all exponents were all optimized twice⁽⁵⁹⁾. At internuclear distances other than this, reoptimization was not as complete or was interpolated. Nevertheless for this molecule, we had eleven points to work with since wavefunctions for all these points, (forces for these are listed in Appendix 3) had been made available by Cade. This permitted a check on possible limitations in using only seven rather than more points. Varying the number of points and reasonable distributions of these, it was possible to obtain nearly identical results with a seven and eleven point fit to the same order polynomial, namely fourth order. In order to present consistency

of the method, we cite as an example the results obtained from the Tchebycheff and least square fits, for the molecule N_2 . Using the least square method, the values for k_2 , $k_3/3$, $k_4/12$ were in order: 1.51879, -2.20817, 1.80996;^{a)} and for the Tchebycheff method: 1.52348, -2.20654, 1.74976. Extending the degree of the polynomial gave poorer results for k_4 in general, with some change in k_3 and little or no change in k_2 . One unpleasant aspect was the observation that the distribution of points for N_2 sometimes affected the magnitudes and even signs of some of the components of k_3 and k_4 , even though the sum of these components always were nearly the same for the different distributions. However, these in no way affected visibly the components of k_2 , such as the orbital, atomic, etc., components. In view of this difficulty with k_3 and k_4 , we have declined to include any discussion of these. This problem was not noticed with the molecules CO and BF when McLean's functions were used. For these, at distances other than R_e , only the coefficients of the basis orbitals were reoptimized whereas the exponents were those of R_e , which had been properly optimized. As the optimizations were therefore more consistent or even for the range of R values considered, less difficulty was observed in the polynomial fit. Uneven optimization can thus be troublesome. A previous calculation of the forces at different values of R and curve fitting

a) Footnote: See Table (5.2) for units.

these for wavefunctions of Huo⁽⁶⁰⁾ for CO and BF presented the same difficulty as N₂, even more so. Huo's wavefunctions had also been partially optimized or interpolated at some R values other than R_e. However, some irregularities were found in the atomic forces. In fact, at 0 for CO, k₂ was found to be below the experimental value, whereas using the C forces, the same result was obtained as with the McLean function. In view of the fact that the McLean functions gave better energies than Huo's for CO and BF as a result of larger basis set expansions, these were used in the calculation of the forces. The same authors' functions were used for BeO and LiF.

The question as to whether one should have expanded the Dunham series for the force about the point where the net force is zero, as done by Goodisman for H₂⁽²⁰⁰⁾, must be answered in the negative. For N₂, the force is zero at R = 2.025 a.u., whereas R_e(exptl.) = 2.068 a.u. and R_e(H.F.) = 2.0132 a.u. At R = 2.025 a.u., k₂ was 1.857, and k_{3/3}:-2.197. The reason for the higher k₂ can be found in the inadequacy of the H.F. potential curves at large distances, as they rise to ionized or excited states for most cases. This usually means that the H.F. minimum must occur at an R_{min.} < R_e(exptl.) since the H.F. curve must rise faster than the experimental curve for large R⁽²²²⁾. The result is that k₂ is larger than the experimental value

Table 5.1

FORCE CONSTANTS FROM FORCES^{a)}

AB	R_e (exptl.)	k_2 (exptl.)	k_2 (calculated)	R_e (H.F.)	k_2 (calculated)
NN	2.068	1.472	1.519	2.0132	1.864
CO	2.132	1.222	1.379	2.081	1.652
OC			1.546		1.822
BF	2.391	0.519	0.532	2.354	0.610
FB			0.701		0.796
BeO	2.515	0.483	0.530	2.4377	0.670
OBe			0.674		0.824
LiF	2.955	0.165	0.161	2.9377	0.170
FLi			0.147		0.155

a) See Table 5.2 for units.

if calculated at the H.F. minimum. Evaluation of these quantities at R_e will give results closer to experimental values, in view of the fact that R_e is closer to the inflexion point of the curve, at which $k_2 = 0$ (see Fig.(5.1)). These problems and others related to the accuracy of the force constants are further discussed in Appendix 5.

In Table (5.1) are listed results for k_2 at R_e (experimental) and R_e (Hartree-Fock) calculated from the total forces and compared with the experimental values. The H.F. R_e is smaller than R_e (exptl.) . The force constants are all considerably higher at the H.F. R_e whereas k_2 calculated at R_e (exptl.) is in much closer agreement with the experimental result. In Table (5.2) are also listed values of k_2 , $k_3/3$ and $k_4/12$ calculated by two different methods. The first method (a) involved a polynomial fit of the net total forces, nuclear and electronic. Method (b) consisted of a polynomial fit of the individual atomic, overlap and shielding electronic forces. The results from these electronic forces were then added to the nuclear contributions. As can be seen from the table, both methods were consistent with each other. The overall agreement between k_2 , k_3 and k_4 , as calculated from the forces, with the experimental results was an indication of the accuracy of the method of polynomial fits. For the force constants, best agreements are

Table 5.2^{c)}

FORCE CONSTANTS FROM: a) CURVE FITS OF TOTAL FORCES

b) CURVE FITS OF ATOMIC, OVERLAP, SHIELDING FORCES

AB	R_e	k_2			$k_{3/3}$			$k_{4/12}$		
		Exptl.	(a)	(b)	Exptl.	(a)	(b)	Exptl.	(a)	(b)
NN	2.068	1.472	1.519	1.503	-1.959	-2.208	-2.114	1.630	1.810	1.717
CO	2.132	1.222	1.379	1.383	-1.548	-1.640	-1.653	1.216	1.315	1.224
OC			1.546	1.552		-1.628	-1.628		1.365	1.261
BF	2.391	0.519	0.532	0.544	-0.572	-0.660	-0.635	0.318	0.452	0.476
FB			0.701	0.711		-0.774	-0.712		0.588	0.520
BeO	2.500	0.483	0.567	0.554	-0.489	-0.602	-0.579	0.291	0.311	0.325
OBe			0.711	0.698		-0.636	-0.603		0.332	0.338
LiF	2.8877	0.165	0.198	0.199	-0.152	-0.198	-0.195	0.124	0.133	0.118
FLi			0.174	0.184		-0.185	-0.177		0.144	0.126

c) Units used throughout

$$R(a_0) = 1 \text{ bohr} = 0.529167 \text{ \AA}$$

$$E = 1 \text{ hartree} = 4.35942 \times 10^{-11} \text{ erg}$$

$$F = 1 \text{ hartree/bohr} = 8.2377 \times 10^{-3} \text{ dyne}$$

$$k_2 = 1 \text{ hartree/bohr}^2 = 15.5684 \times 10^5 \text{ dyn/cm}^2$$

$$k_3 = 1 \text{ hartree/bohr}^3 = 29.4205 \times 10^{13} \text{ dyn/cm}^2$$

$$k_4 = 1 \text{ hartree/bohr}^4 = 55.5978 \times 10^{21} \text{ dyn/cm}^3$$

found for the calculation from the forces at the lighter nucleus in the molecule. This is understandable if one remembers that the heavy atom has the larger atomic charge density. It is then more difficult to variationally optimize this density as it contributes much more to the energy than the lighter atom, and is thus relatively insensitive to small energy changes. In what follows, the force constant components obtained as the derivative of the corresponding forces are used in an analysis which is correlated with densities to elucidate the nature of these force constants.

5.7 Interpretive Scheme

The degree to which the force constant depends upon explicit variation of the wavefunction with R via the parameters is as we have indicated dependent upon the differentiation process (see section 5.4). Consequently, there arises the general problem of the relative importance, in the force constant expression, of the parameter derivatives $\frac{\partial \alpha_i}{\partial R}$ for moving coordinates centered on A, or $\frac{\partial \beta_i}{\partial R}$ for fixed coordinates centered on B. Their qualitative and quantitative roles are far from clear in the two-center representation, i.e., confocal elliptical, which makes use of the virial theorem. Only equation (5.25), which results from this approach, has a one-electron character to it. Other equivalent expressions involve the potential

energy operator (see Phillipson⁽²⁰⁵⁾) and thus make it difficult to reduce the problem to one-electron integrals. For exact wavefunctions, both the Hellmann-Feynman approach and that of Schwendeman and Phillipson give the same result for the value of the force constant.

From the interpretive aspect, one encounters certain differences. In the electrostatic approach, one keeps the total density fixed with respect to some arbitrary point, for example nucleus B, and then one moves nucleus A. If the total density remains rigid with respect to nucleus B, then the contribution to the force constant is the field gradient of the total density. This density then relaxes. From the cancellation theorem, all the density which follows nucleus A rigidly cancels its field gradient contribution via the relaxation term

$$\int \frac{d\rho}{dz_a}(\beta, \vec{r}_b) \frac{\cos\theta_a}{r_a^2} d\tau = \int \frac{\partial\rho}{\partial z_a}(\beta, \vec{r}_b) \frac{\cos\theta_a}{r_a^2} d\tau$$

The working equation for the electrostatic approach is from Eq.(5.13)

$$k_2 = Z_A \left[\frac{2Z_B}{R^3} - \int \rho(\beta, \vec{r}_b) \left(\frac{3 \cos^2\theta_a - 1}{r_a^3} \right) d\tau + \frac{4\pi}{3} \rho(A) - \int \frac{d\rho}{dz_a}(\beta, \vec{r}_b) \frac{\cos\theta_a}{r_a^2} d\tau \right] \quad (5.36)$$

In view of the linear dependence on ρ in this expression,

one may decompose ρ into a sum of terms

$$\rho = \rho_A + \rho_{AB} + \rho_B$$

where ρ_A and ρ_B are charge densities centered on nuclei A and B, and ρ_{AB} is the overlap density. The contributions from the electronic terms to the force constant in the limiting case of rigid following of nucleus A by ρ_A and of nucleus B by ρ_B are:

atomic: $k_2^{(AA)} = 0$

overlap: $k_2^{(AB)}/Z_A = \frac{4\pi}{3} \rho_{AB}(A) - \int \rho_{AB} \frac{3\cos^2\theta_a - 1}{r_a^3} d\tau - \int \frac{d\rho_{AB}}{dz_a} \frac{\cos\theta_a}{r_a^2} d\tau$

shielding: $k_2^{(BB)}/Z_A = \frac{4\pi}{3} \rho_B(A) - \int \rho_B \frac{3\cos^2\theta_a - 1}{r_a^3} d\tau$ (5.37)

The null contribution from the atomic density rigidly following nucleus A follows from the cancellation of the field gradient and relaxation terms by the cancellation theorem. The shielding term $k_2^{(BB)}$ for rigid following of nucleus B, i.e., ρ remains fixed on B, contributes a field gradient term in addition to a density contribution which we showed before was the force constant for a nucleus on which this density was completely localized. The electronic overlap constant always contains a relaxation term, even for rigid densities which follow the nuclei. If there were no orbital following of nucleus A, then this relaxation would be zero. However, as a result of the L.C.A.O. approximation, where the densities are centered on A and B,

Table 5.3

AB	CONTRIBUTIONS OF ELECTRON DENSITIES TO K_A^e								
	$K_A^{(AA)}$	$K_A^{(AB)}$	$K_A^{(BB)}$	Total	$Z_B - K_A^{(BB)}$	$K_A^{(D)}$ $(K_A^{(AA)} + K_A^{(AB)})$	$F_A^{(Z-S)}$	Δ_{AB}	Δ_B
NN	-1.208	3.143	4.115	6.051	2.885	1.935	1.864	-5.644	-0.242
CO	-2.989	3.366	6.507	6.884	1.493	0.377	0.534	-3.760	+0.140
BF	-1.926	1.904	8.285	8.262	0.715	-0.022	-0.008	-2.040	-0.099
BeO	-1.931	1.365	7.458	6.892	0.670	-0.523	+0.057	-4.521	+0.350
LiF	-0.977	0.170	9.007	8.201	-0.007	-0.807	-0.421	-1.166	-0.094
NN	-1.208	3.143	4.115	6.051	2.885	1.935	1.864	-5.644	-0.242
OC	-0.584	2.407	3.237	5.060	2.763	1.823	2.116	-1.307	-0.050
FB	-0.524	2.333	2.650	4.460	2.882	1.809	1.741	-0.880	-0.069
OBe	-0.177	1.364	2.118	3.306	1.921	1.187	1.628	-2.077	-0.086
FLi	+0.098	0.570	2.089	2.757	0.911	0.668	0.954	-1.166	+0.079

the overlap density is continuously changing with nuclear motion.

If one defines the total relaxation in terms of an effective charge by

$$\Delta_D = R^3/2 \int \frac{d\rho_D}{dz_a} \frac{\cos\theta_a}{r_a^2} d\tau \quad (5.38)$$

where $\rho_D = \rho_B(\beta, \vec{r}_B)$ and $\rho_{AB}(\beta, \alpha, \vec{r}_A, \vec{r}_B)$ respectively, one can calculate these using Eq.(5.36) for components $k_2^{(BB)}$ and $k_2^{(AB)}$ using the previously calculated density $\rho(A)$ (see Appendix 4), the field gradients (see Chapter 4) and the values of the k_2 's which have been obtained by polynomial fits of the forces, as described previously. The Δ 's are listed in Table (5.3). Perusal of this table shows Δ_B is small in all cases, as one would expect since this charge density is far from nucleus A, and sits quite rigidly on nucleus B. The signs of Δ_B fluctuate from nucleus to nucleus. Ideally, one would like this to be positive so that this relaxation would cancel the small density term $\frac{4\pi}{3} \rho_B(A)$ at nucleus A. For this cancellation to occur, this small density would have to follow nucleus A completely. This is quite reasonable as this density is far away from nucleus B, albeit centered on it, and is mainly perturbed by A. The values for the relaxations Δ_B are small and depend on $\rho_B(A)$, the accuracy of which is difficult to assess from Hartree-Fock theory, as it is only a part of the total density. It

is probably much more realistic to view this relaxation term as being positive and cancelling the density term.

The overlap relaxations Δ_{AB} are much more problematic as they involve a certain amount of charge following of nucleus A as well as following nucleus B since

$\rho_{AB} = \psi_A^*(\vec{r}_a) \psi_B(\vec{r}_b)$. From the tables, it is evident the overlap relaxations are much larger than the Δ_B 's. The values of the Δ_{AB} 's are negative, the sign being just right

to cancel the density correction $\frac{4\pi}{3} \rho_{AB}(A)$ which is negative for all nuclei (see Appendix 4). For N_2 ,

$R^3/2(\frac{4\pi}{3} \rho_{AB}(A))$ is -6.153 as compared to Δ_{AB} which is -5.644. It is thus evident that much of the overlap density follows the nuclei. One can further show this by calculating the integral (5.38) using simple Slater orbitals centered on A and B.

It is thus seen that the total relaxation effects as calculated by the space fixed method involve large quantities which cancel field gradient contributions. One way to avoid these is to view these relaxations from the nucleus which is being moved, for example nucleus A. This, as we have seen, is also equivalent to the motion of nucleus B with respect to A. We then have from (5.16)

$$k_2^{el} = -Z_A \int \frac{\partial \rho}{\partial z_a}(\alpha, \vec{r}_a) \frac{\cos \theta_a}{r_a^2} d\tau = Z_A \int \frac{\partial \rho}{\partial z_b}(\alpha, \vec{r}_a) \frac{\cos \theta_a}{r_a^2} d\tau \quad (5.39)$$

In this equation, explicit dependence on the field gradient does not appear, which is as it should be since we have previously indicated there is no definite relationship between these two. We have already demonstrated in connection with Platt's model that for any density $\rho_B(\beta, \vec{r}_b)$ which remains rigidly fixed on nucleus B, the integral (5.39) is a field gradient contribution of the form

$$\begin{aligned} k_2^{(BB)} &= z_A \left[\frac{4\pi}{3} \rho_B(A) - \int \rho_B \frac{3 \cos^2 \theta_a - 1}{r_a^3} d\tau \right] \\ &= z_A \int \frac{d\rho}{dz_b}(\beta, \vec{r}_b) \frac{\cos \theta_a}{r_a^2} d\tau \end{aligned}$$

where differentiation of coordinates r_b only occurs.

The density term $\frac{4\pi}{3} \rho_B(A)$ is best considered with the relaxation of this density for which we have indicated cancellation will occur. The total $k_2^{(BB)}$ including relaxation, i.e. $z_A \int \frac{\partial \rho}{\partial z_b}(\beta, \vec{r}_b) \frac{\cos \theta_a}{r_a^2} d\tau$, is best considered as a field gradient. From (5.39) with respect to nucleus A any density fixed on B is moving with B and therefore relaxing. We thus have that the relaxation of density on B with respect to A can be evaluated as a field gradient term, in view of the equivalence of these two. We can, therefore, consider the density on B as shielding that nucleus from A. In terms of effective charges, we define

$$K_A^{(BB)} = \frac{R^3}{2} \left[\int \rho_B \frac{3 \cos^2 \theta_a - 1}{r_a^3} d\tau - \frac{4\pi}{3} \rho_B(A) - \int \frac{\partial \rho_B(\beta, \vec{r}_b)}{\partial z_b} \frac{\cos \theta_a}{r_a^2} d\tau \right] \quad (5.40)$$

as the shielding contribution per unit charge to the force constant expression. If ρ_B is expressed in terms of coordinates centered on A, this is then equivalent to

$$K_A^{(BB)} = \frac{R^3}{2} \left[\int \frac{\partial \rho_B}{\partial z'_a} (\alpha, \vec{r}_a) \frac{\cos \theta_a}{r_a^2} d\tau \right]$$

where primes indicate differentiation of parameters only.

The overlap density $\rho_{AB}(\alpha, \beta, \vec{r}_a, \vec{r}_b)$ can be considered in a similar fashion, i.e., as a relaxation effect if one expands it onto center A completely so that $\rho_{AB} = \rho_{AB}(\alpha, \vec{r}_a)$. This avoids the appearance of large cancellations of relaxation and field gradient effects which occur if this density is kept fixed with respect to nucleus B, i.e. by expanding it completely in terms of coordinate \vec{r}_b . We have already seen that density which follows nucleus A, such as ρ_A , to a very large extent, is best considered as relaxing with respect to nucleus A. It is precisely for ρ_A and ρ_{AB} , as we have discussed above, that most of the cancellation of field gradient and relaxation terms occur in the space fixed approach. It is therefore much more convenient to consider these two together. We therefore define

$$K_A^{(D)} = \frac{R^3}{2} \left[\int \frac{\partial \rho_D}{\partial z'_a} (\alpha, \vec{r}_a) \frac{\cos \theta_a}{r_a^2} d\tau \right] \quad (5.41)$$

where $\rho_D = \rho_A(\alpha, \vec{r}_a) + \rho_{AB}(\alpha, \vec{r}_a)$, as the electronic contri-

bution from these densities. Our final expression for the force constant becomes

$$k_2 = \frac{2Z_A}{R^3} [(Z_B - K_A^{(BB)}) - K_A^{(D)}] \quad (5.42)$$

The first term, $(Z_B - K_A^{(BB)})$ is the total unshielded charge on nucleus B and therefore, following our previous discussion, is a net field gradient. The last term represents the sum of atomic and overlap relaxation effects with respect to nucleus A.

5.8 Shielding and Dipolar Interactions

The working equation (5.42) for the interpretation of force constants involves one-electron operators only, as seen from the general expression for the K's (Eq.(5.41)). The force constants are therefore ultimately related to the one-electron density. In the force analysis, we have emphasized the importance of the exact disposition of the charges in the molecule as depicted by the density difference diagrams. Our task is, therefore, to relate in a similar qualitative fashion the electron densities to the various quantitative factors in Eq.(5.42), which influence the force constants.

The shielding term $k_2^{(BB)}$ contributes a field gradient term and is therefore easily handled. From (5.42), we have

$$k_2^{(BB)} = -2Z_A K_A^{(BB)} / R_e^3$$

where $K_A^{(BB)}$ is an effective charge producing the calculated electric field gradient. If this were the only contribution, we would have for the force constant

$$k_2 = 2Z_A(Z_B - K_A^{(BB)})/R_e^3$$

and for the anharmonic constant

$$k_3 = -6Z_A(Z_B - K_A^{(BB)})/R_e^4$$

To test the assumption, we note that $k_3/k_2 = -3/R_e$. From a Dunham analysis⁽²⁰⁶⁾ one can show $k_3/k_2 = 3a_1/R_e$, where for most diatomic molecules $-2 > a_1 > -4$. For N_2 , a_1 is -2.75 , and for LiF -2.72 . Since $R_e > 2$ for N_2 and LiF , one sees that shielding is not the only contribution and relaxation effects must be considered from the rest of the density, i.e., atomic and overlap.

The expression which summarizes the atomic and overlap relaxation effects is Eq. (5.41), i.e.,

$$\begin{aligned} K_A^{(D)} &= \frac{R^3}{2} \left[\int \frac{\partial \rho_D(\alpha, \vec{r}_a)}{\partial z'_a} \frac{\cos \theta_a}{r_a^2} d\tau \right] \\ &= -\frac{R^3}{2} \int \frac{\partial \rho_D(\alpha, \vec{r}_a)}{\partial z_b} \frac{\cos \theta_a}{r_a^2} d\tau \end{aligned} \quad (5.43)$$

This integral represents the interaction of the change in electron density $\partial \rho / \partial z'_a$ with a point dipole at the point $z_a = 0$, i.e., nucleus A, directed along the internuclear axis. By this method, one can visualize force constants as the change in force components on one nucleus (A) exerted by the change in charge distribution resulting from

a small unit displacement of the other nucleus (B). This is, of course, equivalent to moving nucleus A instead of B. The relaxation effects are, however, measured with respect to A, for which nucleus B appears to be moving. The equivalent of these two approaches is summarized by the two integrals in Eq.(5.43). White⁽²²³⁾ used a similar approach in calculating atomic force constants for the case of solid copper, but the formalism was never developed explicitly. His treatment considers the total dipole effect from nuclear and rigid core charge movements, which as we have indicated, are more easily treated as field gradients. In addition, the relaxation of the conduction electrons is treated in a crude fashion as a perturbation by the virtual displacements of the nuclear and core charges. The dipole interaction has been extensively used also as a model in calculating transition intensities in electronic spectra, an example being some calculations of Jones on benzene⁽²²⁴⁾. In this approach, the nuclei and atomic orbitals are assumed not to move together so that the resulting dipole field is, in part, responsible for vibrational interaction terms⁽¹⁹²⁾. Such a model has been discussed in detail by Liehr⁽²²⁵⁾, who gives a careful analysis of the errors which arise from different approximations. The methods used in most of these calculations overemphasize non-orbital following and so do not allow the atomic orbitals, and therefore

densities, to move at all with the nuclei. If we displace a certain nucleus in a molecular configuration from its equilibrium position, then there will be some tendency for the valence electrons to remain in their equilibrium positions instead of being carried away by the atom with which the atomic orbital is associated. The actual amount of following or non-following which then is a relaxation, can be judged from the values of the K's. Our later discussion would certainly suggest that orbital following is quite large.

One can visualize the relaxation effects most clearly by the use of density diagrams. In particular, by considering the total atomic and overlap densities centered on one atom, i.e. $\rho_D(\alpha, \vec{r}_a) = \rho_A(\alpha, \vec{r}_a) + \rho_{AB}(\alpha, \vec{r}_a)$, and seeing how this changes with nuclear vibration, one can hopefully get a true picture of these relaxation effects. Keeping nucleus A fixed and displacing nucleus B, we have subtracted ρ_D^{eq} from ρ_D^{ext} i.e., the sum of equilibrium atomic and overlap densities from the sum of their extended counterparts. These then represent the change in density $\partial \rho^{(D)} / \partial R$ which interacts with an imaginary dipole $Z_A dR$ at A. It will be shown how these density differences can be qualitatively correlated with the trends in the force constant contributions from the relaxation terms. One need not consider the relaxation of

ρ_B in terms of densities, as such densities are small near A. The contribution from ρ_B is best treated as a field gradient term. Inclusion of ρ_B in the density diagrams would only obscure the overlap effects which are predominant in the bond region.

5.9 Characteristics of Electronic Force Constants

A comparison of the contributions to the total force from charge density in different spatial regions of the molecules in the two series N_2 , CO, BF; C_2 , BeO, LiF, demonstrated that the manner in which a state of electrostatic equilibrium is reached is characteristic of the binding found in each of these molecules. The general nature of the variation in the spatial distribution of the charge density through these two series of molecules is also evident from ρ and $\Delta\rho$ maps as discussed previously. In particular, it was found that for the 14-electron isoelectronic group N_2 , CO, BF, the charge density became more diffuse at the electropositive end of the molecules. This was the result of the presence of a 5σ orbital which contributes appreciably to density accumulation behind the light nucleus. This is in sharp contrast to the 12-electron group LiF, BeO, which has no 5σ orbital. Thus the charge density becomes very tight at the electropositive end, indicative of charge transfer to the electronegative atom in the molecule. The contribution of the overlap charge

density to the binding in the molecules decreased in the order N_2 , CO, BF. In CO, the shared density exerts a larger force on C than on O, while in BF it binds the F nucleus more than B. The atomic forces exerted on the N, O, and F nuclei in N_2 , CO and BF decrease sharply through the series, an indication of an increasingly symmetrical arrangement of the charge density in the immediate neighbourhood of these nuclei. In the ionic molecules BeO and LiF, the direction of the atomic polarizations and their forces which are exerted on the nuclei O and F are reversing to counter the net positive field which results from the transfer of charge to O and F. The charge increase is more symmetrically localized on F.

These contrasting tendencies in the two series should therefore result in quite different relaxation effects during nuclear vibration. The force constant components should parallel the forces to some extent as they represent the change in forces. On the basis of the density (ρ), density difference ($\Delta\rho$) and force discussions one would expect maximum deshielding of the nuclei and maximum overlap contributions to prevail in the force constant of the covalent prototype, N_2 . At the other extreme of bonding character, the presence of charge transfer should manifest itself in overshielding of the heavy nuclei, deshielding of the light nuclei by an amount equivalent to the magnitude

of the charge transferred, negligible overlap contributions. In view of the fact that as the molecule is extended, dipole moment functions for BeO and LiF indicate increasing ionic character as a result of depolarization effects, one might expect the densities centered on the heavy nuclei to become more symmetrical. This conjecture is further supported by the dynamics of alkali metal plus halogen molecule reactions, in which the notion of long-range electron transfer to the halogen by stripping seems to be well established⁽²²⁶⁾. We can thus anticipate that the density situated at O and F will follow these nuclei and perhaps even facilitate nuclear motion via a decrease in polarization in the internuclear region. In the field gradient analysis, we have already indicated the different polarizations of $p\sigma$ and $p\pi$ densities. Thus we might expect the changes in these polarizations to show up in the density difference maps advocated in the previous sections. Inasmuch as bond stretch is the undoing of molecular bonding, it is to be anticipated that in the group N_2 , CO, BF, density difference maps of the extended and equilibrium densities will indicate a reversal to the valence states of the separated atoms for these molecules. In these molecules, accumulation of density behind the nuclei was manifested by the $\Delta\rho$ diagrams. On extension of the nuclear configuration, these charge accumulations will reverse and flow back into the bond region

in order to attain the more symmetrical electron distribution of the valence states. This relaxation effect should show up in the atomic force constant contributions as impeding nuclear motion.

a) Atomic, Overlap, Shielding K_A^e 's

In order to exemplify and validate these predictions, we present in Table (5.3) the numerical values of the derivatives of the atomic, overlap and shielding forces, obtained from polynomial fits of these forces as described in section 5.6. The derivatives correspond to K_A^e 's representing the integral (5.41)

$$K_A^{(x)} = \frac{R^3}{2} \int \frac{\partial \rho_x(\alpha, \vec{r}_a)}{\partial z_a} \frac{\cos \theta_a}{r_a^2} d\tau = -\frac{R^3}{2} \int \frac{\partial \rho_x(\alpha, \vec{r}_a)}{\partial z_b} \frac{\cos \theta_a}{r_a^2} d\tau$$

and x is generally representative of the atomic density (AA), the overlap density (AB), and the shielding density (BB).

The shielding $K_A^{(BB)}$ is best treated with the nuclear field gradient, thus giving a measure of the relative undershielding of the nuclei by the atomic densities situated there. The total unshielded charge ($Z_A - K_A^{(BB)}$) is therefore included in the table, with the corresponding $F_A^{(Z-S)}$, the unshielded charge which appears in the force analysis. This last quantity has been correlated with dissociation energies of homonuclear diatomics by Bader et al⁽⁵⁵⁾. It is seen from the table that maximum undershielding in the force constants occurs at N₂. Minimum deshielding

occurs in LiF. At Li, there is actually complete shielding of the F nucleus, whereas at F, there is deshielding of the Li nucleus by 0.91 charge. The overlap K_A^e 's, i.e. $K_A^{(AB)}$, are maximum at N_2 and minimum in LiF. In fact, for Li $K_A^{(AB)}$ is vanishingly small (0.17). The atomic K_A^e 's, i.e. $K_A^{(AA)}$ differ appreciably for these two limiting cases of bonding, i.e. covalent in N_2 and ionic in LiF. $K_A^{(AA)}$ for N_2 is negative, indicating that the density changes are opposing the nuclear motion as predicted before. In LiF, the two ends of the molecule behave differently. At Li, the density relaxes in such a way as to also oppose nuclear motion, the magnitude of $K_A^{(AA)}$ being comparable to that for N_2 . This means that charge must be leaving regions behind the Li nucleus and accumulating in front of it, annihilating the "hole" which was evident in the $\Delta\rho$ diagram for that molecule. At F, $K_A^{(AA)}$ is positive, hence implying the electronic relaxation is aiding nuclear motion. There must then be charge removal from the binding region in the vicinity of the F nucleus. The magnitude of this effect would indicate that charge removal is very small or symmetric about the F nucleus. The $K_A^{(AA)}$'s become more negative at the heavy end, i.e. oppose motion of the heavy nucleus more and more as one goes from LiF, through BeO, BF, CO and N_2 . This is indicative of increased charge

restoration into the binding region, which in the bonding process are asymmetrically disposed in the covalent molecules but are more symmetrically relocated at the heavy nuclei in the more ionic cases. Thus the decrease in magnitude and eventual reversal in sign of $K_A^{(AA)}$ at F in LiF as one goes from N_2 to LiF reflects this characteristic of the equilibrium densities. The overlap contributions to the force constant decrease from N_2 to LiF at the heavy nuclei, reflecting the increase of p density and decrease of s density in the bonding of these nuclei. At the electropositive nuclei, Li to N, the atomic contributions always oppose nuclear motion much more than at the heavy nuclei. At B and C, we have noted in the previous chapters the rather diffuse densities accumulated behind these. It is evident, therefore, that these diffuse densities follow these light nuclei much less than the densities at the other end of the molecule which are tightly bound by the larger nuclear charges of O and F. The magnitudes of the $K_A^{(AA)}$'s at either end of the molecule therefore correlate with the tightness of binding of density. At Be, the larger value of $K_A^{(AA)}$ as compared to Li indicates significant accumulation of charge in front of that nucleus. The larger deshielding of that nucleus as compared to Li must be partly responsible for this increased relaxation in electronic density.

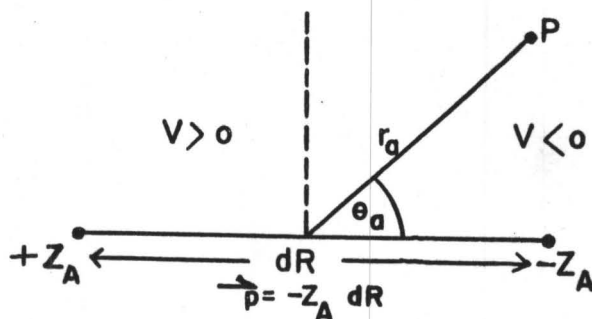
The above discussion can be summarized with the use

of the tabulated values of $K_A^{(D)}$ which appear in Table (5.3) and represent the total relaxation effect of overlap and atomic densities at nucleus A. A very significant revelation is that from the light end of the molecule this relaxation effect opposes nuclear motion increasingly as one goes from N to Li. The change in sign for $K_A^{(D)}$ occurs at B. This is the result of large negative atomic relaxation exceeding the overlap density relaxation. In all cases where $K_A^{(D)}$ is negative, i.e. at B, Be and Li, the sign of this contribution is due to the preponderance of atomic relaxation. Simultaneously, one has an increasing shielding of the other nucleus in the molecule. Thus at Li, the total force constant comes from the relaxation of nearly all atomic density, as the overlap is small at Li. At N_2 , overlap effects prevail over adverse atomic relaxations in order to decrease the large undershielding of the N nucleus. The increased shielding of the heavy nuclei in going from N_2 to LiF is consistent with ionic trends in the molecules. The decreasing magnitude of $K_A^{(D)}$ at C and B is a result of the diffuse densities (mostly from the 5σ orbital) behind these nuclei relaxing in opposition to nuclear motion. At Be and Li, similar relaxation which puts more density in the binding regions near these nuclei to where there had been depletion as seen from the $\Delta\rho$ diagrams for these, must occur. At the heavy nuclei, the group N,C,O behave

quite similarly. The net unshielded nuclear charge and the $K_A^{(D)}$'s are quite comparable. This is a result of decreasing overlap contributions and greater density following of nuclei as one goes to the heavier and thus more charged nucleus. The contributions at O and F in BeO and LiF do not behave in this manner. Deshielding of the light nuclei is less and as charge transfer has occurred to O and F, relaxation effects are smaller at these nuclei as a result of densities being more symmetrically situated with respect to these.

b) Densities and Nuclear Motion

The magnitude and sign of the various component contributions to the force constants can further be understood in terms of relaxation diagrams, representing the difference in atomic and overlap densities of the stretched and equilibrium molecules. The same approach can be used for contraction of nuclear configuration, the only difference being a reversal of signs in the appropriate expressions. The overall principles which characterize relaxations are the same. The use of a nuclear dipole $Z_A dR$ to help visualize these effects as discussed in section 5.7 depends on the potential $V(P)$ of such a dipole at a point P in space as seen from the following diagram:



$$V(P) = -\vec{p} \cdot \vec{\nabla}_a (1/r_a) = -Z_A dR \cos \theta_a / r_a^2$$

and therefore $\Delta E = Z_A (dR)^2 \int \frac{d\rho}{dR} \frac{\cos \theta_a}{r_a^2} d\tau$
in accord with Eq.(5.41).

In Figs.(5.3)-(5.6) there are given the atomic and overlap relaxation maps for densities centered on nucleus A. The heavy nucleus is always to the right of the light nucleus, and the latter is always to the left of the heavy nucleus. The nuclear dipoles are included in the diagrams to indicate the directions of nuclear motion.

In the group N_2 , CO, BF, it is evident that as one goes from nucleus C to nucleus B, more charge is removed from behind the nuclei and put into the bonding region. The effect is smallest, visually, for the nitrogen atom. This is in accord with the demonstration previously from ρ and $\Delta\rho$ diagrams that the density was most tightly bound to N. Thus at N, there is more density following the nucleus than at B and C. However, inasmuch as this following is incomplete, there is relaxation opposing the nuclear motion (the diagrams are all for bond extension). The smaller relaxation at N is both supported by the relaxation density diagram and the magnitude of $K_N^{(NN)}$. The net effect

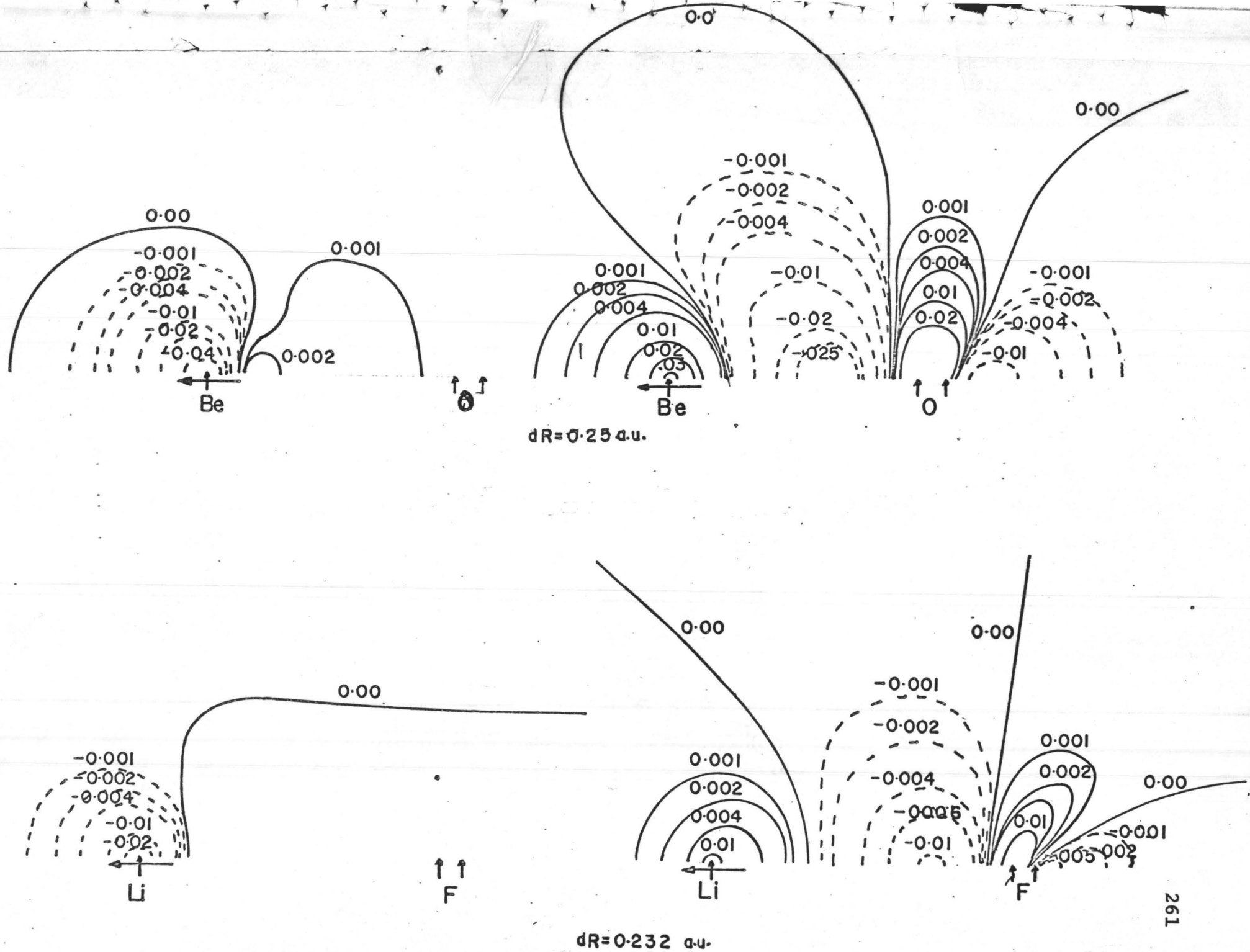
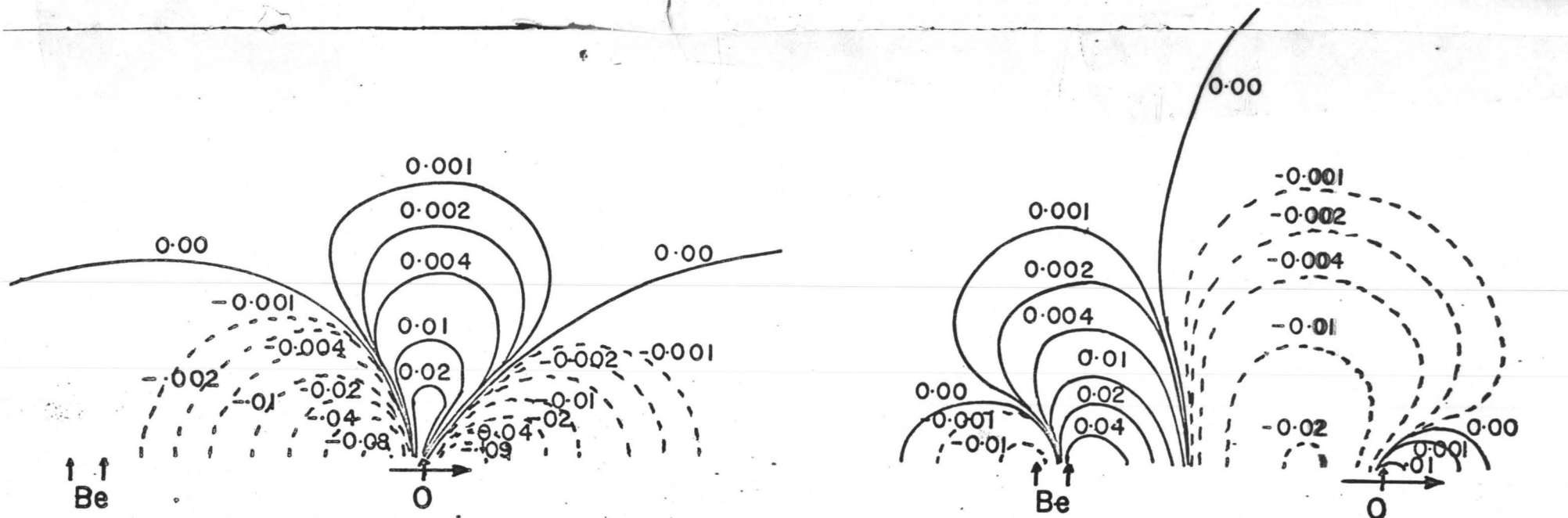
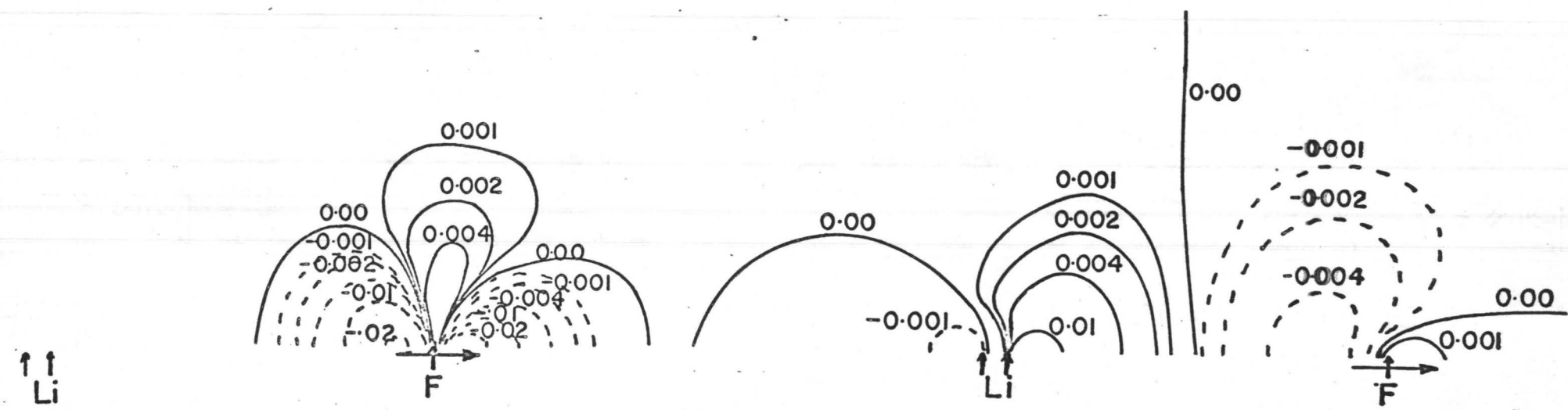


Fig. (5.5) Atomic, Overlap Relaxations



$dR = 0.25 \text{ au.}$



$dR = 0.232 \text{ au.}$

Fig. (5.6) Atomic, Overlap Relaxations

of the relaxation is an induced dipole moment in the electron density in the same direction as the nuclear dipole, thus increasing the dipole interaction and hence the energy of the system. This is equivalent to increasing the force constant. In the case of the nitrogen atom, there is a removal of charge from the $p\sigma$ region, in a geometrical fashion reminiscent of a $p\sigma$ orbital, and transference of this charge into the $p\pi$ region. In other words, extension of the configuration undoes the bonding process. In the molecule N_2 , there was charge depletion in the regions perpendicular to the bond axis, and charge accumulation along the bond axis. Thus we are witnessing the reversal to the valence states predicted before. As one goes through C, B, Be and Li, there is charge removal from behind the atom with a slow progression to symmetrical removal around the nucleus. This progression to symmetric removal of density reduces, therefore, the magnitude of the atomic relaxation. The density difference diagrams for these atomic densities are therefore indicative of progressive s-orbital type involvement in the relaxation. Thus, in the case of Be and Li, the small polarizations which occurred behind these nuclei are diminished in addition to overall removal around the nuclei and replenishing of the "hole" which was apparent in the $\Delta\rho$ maps for LiF and BeO in front of Li and Be. In the case of C and B, there

is also $p\sigma$ character involved in the density changes as seen from the geometrical shape of the contours. The dipolar interactions are strongest for C and B, as the electronic dipole which results from relaxation is larger and of the same sign as the nuclear dipole. The result is then an increasing hindering of nuclear motion as can also be seen from the magnitude of this effect via the $K_A^{(AA)}$'s in Table (5.3). From the magnitude of the contours, it becomes obvious that the relaxation process involves only small charge displacements, so that orbital following must be predominant at all times.

The atomic densities at the heavy nuclei demonstrate the increasing importance of p-type relaxation effects. In passing from N to O, and to F in N_2 , CO, BF, the removal of charge density from in front of and from behind the nuclei becomes more and more symmetrical, as portrayed by the diagrams. This correlates with the decreasing magnitude of $K_A^{(AA)}$ which always remains negative as slightly more charge is removed from behind. In other words, this counters the accumulation of charge behind the heavy nuclei during bond formation. The removal is nevertheless smaller than occurs at the other end of the molecule as a result of more tightly bound densities at the heavy end. The increase in p-orbital involvement in the relaxation is evident from the $p\sigma$ and $p\pi$ nodes coming closer to the nucleus as one comes

to F. The small $K_A^{(AA)}$ values for O and F in BeO and LiF are seen to arise from the mainly p-type relaxations which occurs at these. The relaxation effects have become quite symmetric about each nucleus, so that for F in LiF, the net electronic dipole is zero, and thus the effect on nuclear motion via dipole interaction becomes negligible. It seems, therefore, that as one increases charge transfer to the heavy nucleus in the order BF, BeO and LiF, as demonstrated by the $\Delta\rho$ maps in Chapter II, the relaxation effects decrease their influence on nuclear vibration. The $\Delta\rho$ maps indicate that this is the result of a symmetrical disposition of the transferred charge around the heavy nuclei which tends to move with these nuclei, as it is completely localized or nearly so in the case of BeO and less so in BF. The relaxation maps for the atomic densities along with the relative values of $K_A^{(AA)}$ support the tendency to symmetrical relaxations about the O and F nuclei. It is significant that in the case of the most ionic molecule LiF, the atomic relaxation at F actually helps nuclear motion, so that a little more charge leaves the bond region than from behind the nucleus. This is an indication of a decrease in the forward polarization of the transferred charge, rendering the density on F more symmetric and thus enhancing nuclear motion.

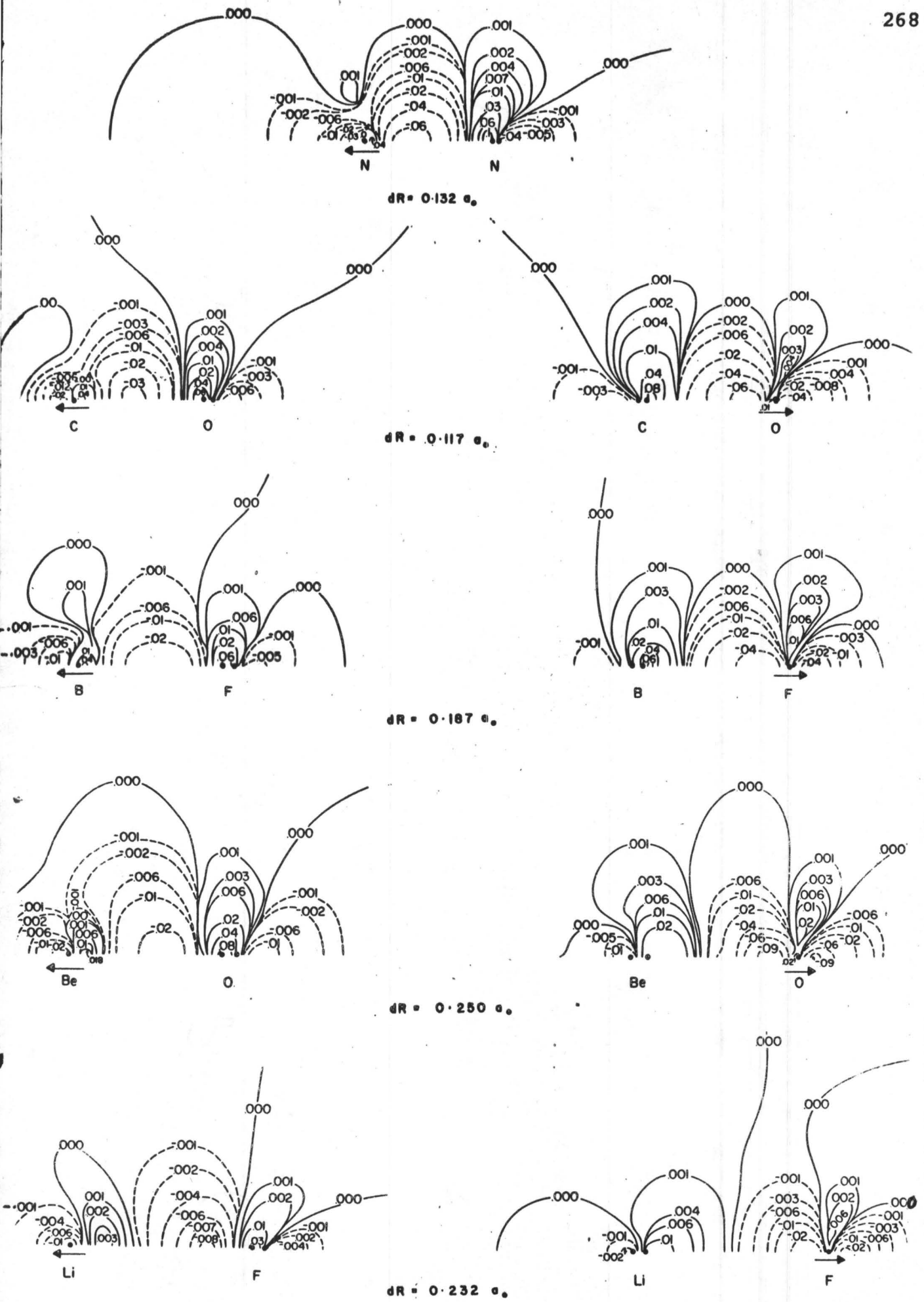
The overlap relaxation diagrams displayed in the Figs.

represent a relaxation which tends to facilitate nuclear motion. This is accomplished by large charge removals from the bonding (binding) region and increase of charge behind all the nuclei. At the heavy nuclei, the geometrical characteristics of the relaxation contours are suggestive of p-type density. At the light nuclei, especially Li and Be, one sees the restoration of s-type density around these nuclei, as opposed to the atomic relaxations where charge removal was put in evidence. It is apparent then that these overlap effects also include atomic density effects as noted in the force analysis where it was found that in the cases of LiF and BeO, overlap densities at the heavy nuclei were to be more appropriately considered as atomic densities. From the relaxation maps of the overlap densities, one sees that at the light nuclei the relaxation density encloses the nuclei with an evident increment in density which becomes less symmetrical as one progresses to B, C and N. In the case of Be and Li, the major part of the overlap contribution to the force constant comes from depletion of charge in the internuclear region, as a result of dilation of this density. For Li, this is small, as evidently the overlap density is strongly polarized towards the F nucleus. As one comes to N, the charge depletion has come near that nucleus and we thus have a large $K_N^{(AB)}$. In the case of the heavy nuclei, the overlap density increase about these nuclei is smaller than at the light nucleus. This is evidence

of the increasing contribution from p-type density to this relaxation, density which vanishes at the nucleus. Much of the magnitude of the $K_A^{(AB)}$'s comes from charge removal in the bond region. As this charge removal comes closer to the heavier nuclei by virtue of the density being tighter around these, the net effect is an increase in the repulsion of the nuclei from the bonding region via the dipolar interaction. This, therefore, offsets the decrease in s-character participation which would have otherwise increased the overlap density in the vicinity of these nuclei. The smaller overlap density changes at O in BeO and especially at F in LiF is further evidence that these densities largely follow the nuclei O and F, as if they were atomic densities centered on these. This then lends further support to our force partition in Chapter III, where the overlap forces were added to the atomic forces for these nuclei. The following of the nucleus by the overlap density is nearly perfect for the density at F as demonstrated by the nearly vanishing density changes from the relaxation diagram and the small value of $K_F^{(AB)}$ (0.57). We thus see that LiF is again approaching the limit of two separable densities centered on the nuclei Li and F.

It has become evident from the overlap density relaxation diagrams that appreciable changes occur in the

Fig. (5.7) Atomic+Overlap Relaxations



vicinity of the nuclei, so that much of this relaxation is to be associated with atomic densities. It is thus more appropriate to gauge the total effects. These are summarized in the relaxation maps in Fig.(5.7) corresponding to $K_A^{(D)}$, i.e. the sum of atomic and overlap contributions. As one goes through Li in LiF, Be in BeO, B in BF, C in CO, and N in N₂, one notices the appearance of a positive region in front of these nuclei which approaches these nuclei and finally envelops B, C and N. In all cases there is charge removal from behind the nuclei. At Be and Li, the restoration of density occurs in the region where there had been charge depletion typical of repulsion between two closed shells. At B, C and N, the restoration occurs around the nuclei, indicative of a decrease in the clustering phenomena around these nuclei as depicted by the profiles in Chapter II. Overlap contributions are seen to increase as one approaches N from Li. The preponderance of these overlap effects is made clear by these relaxation maps, thus corroborating the trends in $K_A^{(D)}$. At N₂, one has a net relaxation which facilitates nuclear motion because of large overlap density depletion in the bond region. At the other extreme, Li in LiF, the overlap changes are small. The atomic relaxation prevails in a direction opposing nuclear motion, as a result of decrease in backpolarization of the Li density. For the other nuclei, B, C and Be, the

overlap and atomic relaxations tend to cancel one another, the cancellation occurring nearly completely at B in BF. For this nucleus, the force constant arises from incomplete shielding of the F nucleus (see Table (5.3)).

At the heavy nuclei, the contours indicate that the total atomic and overlap relaxations become more localized as the molecule becomes more ionic. For O in BeO and F in LiF the independence of these two densities from the other nucleus in these molecules becomes quite evident. At all electronegative nuclei, there is removal of $p\sigma$ density and accumulation of $p\pi$ density. This charge rearrangement is therefore in exact opposition to the $\Delta\rho$ maps, so that by extending the nuclear configuration one is moving towards the more symmetrical electron distributions of the valence states. The charge removal is always larger from the binding region for the more covalent molecules CO and BF, but becomes more symmetrical in BeO and especially LiF. In fact, at F in LiF, $K_A^{(D)}$ is the smallest of all. The relaxation diagram demonstrates that nearly all the relaxation effect occurs for density centered on that nucleus, thus behaving as a real atomic density. The distinction between atomic and overlap densities is thus superfluous for this nucleus.

In summary, for the two limiting cases of covalent and ionic bonding, the dynamic properties of the electron

densities are very dissimilar. The covalent case, as exemplified by N_2 , is characterized by a very large deshielding of the nuclear charge. This was also manifested by the force analysis (See $F_A^{(Z-S)}$ in Table (5.3)). The electron density relaxes during nuclear vibrations in such a way as to aid the nuclear motion and thus reduce the net shielding contribution to the force constant. Much of this favourable relaxation comes from changes in the overlap density. This is partially reduced by the reversal of atomic polarizations behind the nuclei. In the ionic case, as portrayed by LiF , there are two contrasting behaviours exhibited by the electron density. At Li , there is complete shielding of the F nucleus, negligible overlap relaxation and accumulation of charge in front of the Li nucleus, thus impeding the "extending" motion of the Li nucleus. There is also tightening of the Li core, indicating that the atomic density is becoming still more ionic. At Li , then, most of the contribution to the force constant comes from a relaxation of the Li density which hinders nuclear motion. At F , there is a deshielding of the Li nucleus as expected for the ion Li^+ . There is, in addition, a contribution from the relaxation of density situated on the F nucleus, whereby charge is transferred from a $p\sigma$ -like orbital to a $p\pi$ orbital. This is then exactly opposite to the characteristics

Table 5.4
Orbital Contributions k_{iA} to Force Constant

	B	C	N	O	F
1σ	1.998	2.000	1.055	-0.007	0.068
2σ	0.035	0.060	1.000	2.003	2.004
3σ	2.234	1.966	1.764	2.036	2.134
4σ	1.087	1.425	-0.020	-1.431	-1.314
5σ	-0.079	-0.858	+0.313	0.927	0.420
1π	2.982	2.290	1.907	1.533	1.147
Totals	8.257	6.883	6.020	5.060	4.460
Totals from k_{iA}^{rel}	8.262	6.796	6.051	5.060	4.460

	Li	Be	O	F
1σ	1.999	2.011	-0.193	-0.085
2σ	0.226	0.106	2.001	2.066
3σ	1.605	1.606	1.446	0.570
4σ	1.384	0.951	-0.920	-0.419
1π	2.988	2.183	0.961	0.621
Totals	8.201	6.857	3.303	2.754
Totals from k_{iA}^{rel}	8.201	6.892	3.306	2.757

displayed by the $\Delta\rho$ map. As the density rearrangement is most symmetrical in comparison to all the other heavy nuclei, the effect on the force constant is therefore least in LiF. BeO behaves very much like LiF. CO and BF exhibit relaxations similar to N_2 . The presence of the 5σ orbital, which is partially very diffusely delocalized behind C and B, introduces large atomic relaxations of this diffuse density, which oppose nuclear motion. At O and F for these two molecules, overlap effects are dominant just as in N_2 .

5.10 Orbital Interpretation

A further breakdown of force constant contributions may be done orbital by orbital. We can define K_A^e as a sum of orbital components k_{iA} , where

$$k_{iA} = \frac{R^3}{2} n_i \int \frac{\partial(\phi_i^* \phi_i)}{\partial z'_a} \frac{\cos \theta_a}{r_a^2} d\tau$$

This partition was suggested in section (5.6) where it was shown that such a partition of the force constant is permissible. The numerical values of the k_{iA} 's reported in Table (5.4) were obtained from polynomial fits of the orbital forces as a function of internuclear distance. The agreement of the total k_{iA} 's with the totals of the atomic, overlap and shielding components is very satisfactory, thus confirming the consistency and accuracy of the method. All these numbers are reported together in Appendix 4.

In the first group N_2 , CO, BF, the 1σ orbital reflects the complete shielding from the two electrons

situated at the heavy nucleus. The 2σ orbital is essentially the same, the electrons being now localized at the lighter nucleus. The N_2 molecule is symmetric and thus has only one electron per orbital shielding the N nucleus. The polarizations of inner shells do not contribute visibly to the force constant. The 3σ orbital, which has the most density in the internuclear region as discussed previously in the force analysis, does not show much variation along the series and parallels the near homogeneity of the total force contribution for that orbital. The 4σ orbital demonstrates a transition at N_2 from a shielding to an antishielding or enhancement effect. Thus, the large backpolarizations of the atomic charge densities relax in such a manner as to oppose nuclear motion. One can define a net electronic force constant per orbital by averaging the contributions at both nuclei, i.e., the value of the expression $-\frac{1}{2}(Z_A^k{}_{iA} + Z_B^k{}_{iB})$. A simple calculation shows these to be: BF(+3.196), CO (+1.449), N_2 (+0.140). The net result is that the relaxation of the 4σ density accumulated behind the heavy nuclei enhances the force constant, an effect which seemingly decreases as the molecule becomes more covalent. It is evident that this is to some extent counterbalanced by the increase in nuclear contribution ($Z_A Z_B$) which is: BF(45), CO(48), N_2 (49). The 5σ orbital indicates the presence of the backpolarization on the light nuclei. Nevertheless, the influence of these is

not as dramatic as in the case of the 4σ orbital. The average contribution to the force constant, as estimated above, for this orbital is: BF(-1.693), CO(-1.134), N₂(-2.191), i.e. a shielding or decrease of the force constant. The 1π orbital force constant contributions parallel the forces for that same orbital, the separation in magnitude of the effective charges increasing as one goes to BF. This orbital resembles the 3σ orbital, as covalency is predominant in these two from the force analysis (equal overlap forces at both nuclei). The sum of their contributions make up between 60 and 70% of the total electronic force constant in N₂, CO, and BF.

The group LiF and BeO indicates increasing inner core polarization relaxations, but otherwise, the 1σ and 2σ orbital show the same behaviour as in the first series. The 3σ orbital shows little variation except at F. The small contribution at F is a result of the smaller relaxation of the $2s_F^2$ density as expected, in view of the larger nuclear charge of F which binds this density very tightly. In the force analysis, a smaller overlap contribution at F supported this contention. This is then probably another reason for this discontinuity. The contributions at the light nuclei Li and Be for this orbital reflect the shielding of the heavy nuclei by charge situated on these. The shielding is not as complete as in the forces. The

4σ orbital which is largely backpolarized at the heavy nucleus, demonstrates an antishielding effect, this being very pronounced at the oxygen in BeO. The force analysis showed that it was in this orbital much of the charge transfer occurred, the density change being greatest in BeO as compared to LiF. This backpolarized transferred charge is obviously relaxing against the nuclear motion, thus enhancing the force constant. The 1π orbital shows that the relaxation of the electron density at the heavy nuclei is not negligible and tends to facilitate nuclear motion by contribution to the reduction of the nuclear field gradient which makes up the force constant. At the electropositive nuclei, the contributions are less than what one would expect from point charges situated at the other end of the molecule, i.e. 4.0 at F and O, on the basis of an ionic model. This typical undershielding of the π densities was shown to be operative in the forces, and thus persists in the force constants.

The orbital contributions to force constants are of interest in correlating vibrational frequency shifts of certain groups, such as the carbonyl group $-C=O$, in different molecular environments. Force constants derived from frequencies in polyatomics are unfortunately often derived from potential fields which are in turn based on preconceived molecular models. Some caution is therefore

required in determinations of force constants as discussed recently by Machida and Overend⁽²²⁷⁾. Aside from this remark, general MO considerations⁽²²⁸⁾ assume invariant, nonpolar sigma networks and thus attribute variations in the carbonyl stretching frequency to changes in π -bond polarity. We have already commented that the 3σ and 1π orbitals contribute substantially to the force constant. Furthermore, upon loss of an electron from the 1π orbital, there is an increase in bond length by about 10% and a concomitant decrease in the force constant by about 48%.⁽⁷⁷⁾ Inasmuch as the 1π orbital is higher in energy than the 3σ orbital, it will be more easily perturbed by different environments. Thus, changes in the π -bond density will affect the force constant of the C=O group appreciably. As the bonding occurs principally via donation of the 5σ electrons, diffusely disposed to some extent behind the C nucleus, there arises the question what effect the bonding of these will have on the force constant. Stretching of the carbonyl group is usually described as an electron-demanding process⁽²²⁹⁾, i.e. transfer of charge into the C=O bond. On this basis, it is possible to explain the larger band intensities observed in metal carbonyls as compared to the intensities for the carbonyl group in organic molecules and even CO itself. Increased metal size and increased negative charge via substitution on the metal

enhances the carbonyl intensities. This can be explained if one assumes the 5σ density bonded behind the C nucleus relaxes in the same fashion as we discussed previously in CO, where it was found that the relaxation at C was going counter to the C motion or in the same direction as the O displacement. As this increases the force constant, this may well be one reason why the carbonyl force constant is not too different from that in CO (2040 cm^{-1} in $\text{Ni}(\text{CO})_4$ ⁽⁸⁴⁾ as compared to 2170 cm^{-1} in CO). Delocalization of π density from CO would have appreciably reduced the constant. In fact, our relaxation map as discussed in section 5.9 would seem to indicate that relaxation of density in the σ -region is larger than that in the π -region. Thus it seems that the assumption of invariant σ -density may be an oversimplification.

5.11 Semiempirical Considerations

There have been, in the past, certain general approximate relationships which have been useful in correlating force constants and other properties of molecules. One remarkable rule of diatomic molecular spectroscopy has been that if ω_e is the vibrational frequency in cm^{-1} , and R_e the equilibrium internuclear distance, then one has to surprising accuracy

$$R_e^2 \omega_e = \text{constant} \quad (5.44)$$

through all electronic states of one molecule⁽²³⁰⁾, Morse⁽²³¹⁾ showed the relation $\omega_e R_e^3 = \text{const.}$ can be derived from simple theoretical considerations. This last relationship has been shown to hold quite well for many nitrogen bonds⁽²³²⁾. The somewhat more accurate relation of Badger⁽¹⁹⁵⁾ is known to be much more universal. (See Eq.(5.46)). The first relationship (5.44) has been recently demonstrated to follow from the kinetic-energy form of the virial theorem by Parr and Borkman⁽¹⁹³⁾. Other recent work of Empedocles⁽¹⁹⁹⁾ has also stressed the utility of the kinetic energy form of the virial theorem for understanding potential functions and force constants in diatomic molecules. Parr and Borkman have shown that the relation follows from treating the valence electrons in the bond region (which can be obtained from overlap-population methods) as an electron gas, an assumption which implies that the electronic kinetic energy is of the form $T(R) = T_0 + T_2/R^2$. The force constant then follows from the virial relationship $k_2 = -1/R_e (dT/dR)_{R_e} = -2T_2/R_e^4$.

One does not have to invoke the electron gas model to obtain this R_e^{-4} dependence of the force constant. An instructive derivation is the following. The force equation is

$$dE/dR = \langle \psi | \partial H / \partial R | \psi \rangle / \langle \psi | \psi \rangle$$

In scaled coordinates such as elliptical coordinates, one has

$$\frac{dE}{dR} \langle \psi | \psi \rangle = \langle \psi | \frac{\partial H}{\partial R} | \psi \rangle = - \langle \psi(R, r') | \frac{2T(1, r')}{R^3} + \frac{V(1, r')}{R^2} | \psi(R, r') \rangle$$

where $r' = r/R$ and is thus made independent of R (see Chapter III). Differentiating again, one obtains

$$\begin{aligned} \langle \psi | \psi \rangle \frac{d^2 E}{dR^2} &= \langle \psi(R, r') | \frac{6T(1, r')}{R^4} + \frac{2V(1, r')}{R^3} | \psi(R, r') \rangle \\ &- \frac{\partial \psi}{\partial R} (R, r') | \frac{2T(1, r')}{R^3} + \frac{V(1, r')}{R^2} | \psi(R, r') \rangle + \frac{3N}{R} \langle \psi | \frac{\partial H}{\partial R} | \psi \rangle \end{aligned}$$

The last term arises from the explicit dependence of the volume on R :

$$\begin{aligned} \frac{d}{dR} \int \psi^* (R, r) \psi (R, r) d\tau &= \frac{d}{dR} \int \psi^* (R, r') \psi (R, r') R^{3N} d\tau' \\ &= \int \frac{d\rho(R, r')}{dR} d\tau' + \frac{3N}{R} \int \rho d\tau' \end{aligned}$$

But since $\langle \partial H / \partial R \rangle = 0$ at R_e , and from the virial theorem

$$-2 \langle \frac{T(1, r')}{R^2} \rangle = \langle \frac{V(1, r')}{R} \rangle$$

(see Eq. (4.16), (4.17), we can summarize the force constant expression

$$k_2 = \frac{d^2 E}{dR^2} = \frac{2}{R^4} \langle \psi(R, r') | T(1, r') | \psi(R, r') \rangle - \frac{2}{R} \langle \frac{\partial \psi}{\partial R} (R, r') | 2T+V | \psi(R, r') \rangle$$

where all integrals are done in scaled coordinates. The first term is then the counterpart of the rule of Eq. (5.44) and also

the assumption of Parr and Borkman. There is, nevertheless, an extra term, a relaxation term expressed in scaled coordinates. For the H_2 molecule, one can easily show that this term is -0.830 , whereas the force constant is 1.401 . This follows from the expression⁽²⁰⁷⁾

$$\langle \psi | \partial^2 H / \partial R^2 | \psi \rangle = \langle \psi | \frac{6T+2V}{R_e^2} | \psi \rangle = \frac{-2E}{R_e^2}$$

which are obtainable from the scaled coordinate expressions of T and V and use of the virial theorem $-2\langle T \rangle = \langle V \rangle$ and $E = T + V$. For N_2 , one can calculate the above expression to be of the order of 50 . Hence, extensive cancellation via the relaxation term must occur in order to reproduce the force constant value of 1.417 for N_2 . The electron gas model therefore does not follow easily from this rigorous derivation of the force constant expression, as it is difficult again to evaluate the relaxation term.

The force constants, which we have calculated by considering the charge densities and electropositive forces from these, include implicitly the very important effect of relaxation. The question then arises whether there are any regularities in the numerical values obtained which would seem to indicate the existence of some semiempirical relationship. If one averages the shielding and relaxation contributions, one can obtain a correlative expression for the force constants. Let us define

$$Z'_A Z'_B = \frac{1}{2} [Z'_A (Z'_B - K_A^{(BB)}) + Z'_B (Z'_A - K_B^{(AA)})]$$

$$M = \frac{1}{2} [Z'_A (K_A^{(AA)} + K_A^{(AB)}) + Z'_B (K_B^{(BB)} + K_B^{(BA)})]$$

The first expression represents an average shielding contribution for the whole molecule and M represents the average relaxation effect. The force constant can then be defined as

$$k_2 = \frac{2Z'_A Z'_B}{R^3} m \quad (5.45)$$

where m now takes the form $m = 1 - M/Z'_A Z'_B$.

This expression has close resemblance to Badger's rule which relates the force constant to the bond length in the fashion:

$$k_2 = 1.86 (R_e - d_{ij})^{-3} \quad (5.46)$$

where d_{ij} is fixed for bonds between atoms from rows i and j of the periodic table, but is not so appropriate for isoelectronics. The values of $Z'_A Z'_B$ and m are for the molecules as follows

	<u>N₂</u>	<u>CO</u>	<u>BF</u>	<u>BeO</u>	<u>LiF</u>
<u>Z'_A Z'_B</u>	20.195	15.531	12.363	8.612	4.100
<u>m</u>	0.329	0.458	0.306	0.562	0.580
k ₂ (calc)	1.503	1.493	0.553	0.639	0.191
k ₂ (exptl)	1.417	1.222	0.519	0.483	0.165

The slight anomaly for CO is a result of the predicted force constant being higher than the experimental value.

Using the experimental k_2 , m becomes 0.375, which is more in line with the values of N_2 and BF . A slightly larger $Z'_A Z'_B$ would also improve the correlation. The force constant for C_2 is 0.782. Whether this molecule would have a similar m as BeO and LiF , its isoelectronic analogues, cannot be answered definitely. The low value of the force constant and the change in bond type, p character at both ends of the molecule, may invalidate any possible correlation. Aside from this, the interesting observation is that a plot of k_2 vs. $2Z'_A Z'_B / R^3$ would be predicted to be nearly linear and probably going through the origin, corresponding to k_2 and $Z'_A Z'_B$ being zero. From the Hellmann-Feynman viewpoint, for extremely ionic molecules, one has under-shielding at one nucleus and over-shielding at the other, so that these two effects cancel in the averaging procedure, tending to make $Z'_A Z'_B$ approach zero or negative values. If one assumes the main shielding comes from the core electrons only, then $Z'_A Z'_B$ is for N_2 : 25; CO : 24; BF : 21; BeO : 12; LiF : 7. All these values are much larger than those reported above, so that it is evident that some shielding does occur by the valence electrons. Using these higher $Z'_A Z'_B$ values, Murrell⁽²⁰¹⁾ obtained a straight line, for the above plot, which did not go through the origin. It is perhaps not too irrelevant to point out that the last members of these two isoelectronic series are the rare

gas diatoms BeNe and HeNe. These hypothetical molecules represent a discontinuous change in bonding because of the high stability of closed shells, and could be considered to have zero force constants or nearly so as their interactions are of van der Waals type. One can expect, therefore, for these the shielding to be nearly complete, in accord with the existence of a zero on the correlation line. The objection of including these into the correlation scheme is of course the ambiguity in defining force constants for such molecules.

It is to be emphasized that the correlation can only be approximate as warranted by the ad hoc averaging of the various contributions at both nuclei. A rigorous correlation between any parameters and k_2 is difficult to justify a priori. The above correlation will have to be tested for more molecular series to see whether it is real and not artificial. The question of C_2 fitting into the group BeO and LiF will have to be answered by calculations as outlined in the previous sections. At the present writing, the exact physical meaning of the near constancy of \underline{m} in isoelectronic groups is not easily understood. Nevertheless, the regularities reflect the extent to which the repulsive forces between the nuclei of the bonded atoms are reduced by electronic shielding and electronic relaxation effects.

5.12 On Force Constant Models

The total electronic forces F_A^e , which at equilibrium necessarily equal Z_B , are in contrast to the total electronic force constant K_A^e which must be less than Z_B in magnitude since $k_2 = \frac{2Z_A}{R^3} (Z_B - K_A^e)$ must be greater than zero. This can be qualitatively understood from the general relaxation expression

$$K_A^{el} = \frac{R^3}{2} \int \frac{\partial \rho}{\partial z'_a} (\alpha, \vec{r}_a) \frac{\cos \theta_a}{r_a^2} d\tau$$

The differentiation of the density with respect to the parameters $(\frac{\partial \rho}{\partial z'_a} = \sum_i \frac{\partial \rho}{\partial \alpha_i} \frac{\partial \alpha_i}{\partial R})$ results partly in radial excitations of the density. For example, a 1s orbital centered on A will become promoted to a 2s orbital after the differentiation, as discussed in section 5.4. This removes charge farther away from nucleus A and thus reduces the shielding because of the geometrical nature of the force operator, which preferentially weighs densities close to the nucleus. As one goes to higher derivatives and thus higher order constants, the decrease in shielding becomes larger as noted by Hershbach and Laurie⁽¹⁹⁶⁾. (Shielding is defined by a positive K_A^e which thus reduces the force constant). This simple explanation is not the complete story as this does not take into account explicit variation of those parameters which are not necessarily scale parameters but account for changes in polarizations, charge

transfer, etc.^{a)}. Radial excitations, which correspond to scaling and thus changes in the molecular geometry similar to "breathing" modes, present an attractive approach as pursued by Empedocles⁽¹⁹⁹⁾. This permits one to easily calculate changes in the kinetic energy upon scale change, and then via the virial theorem, one can obtain the force constant. However, as Schwendeman⁽²⁰⁶⁾ has pointed out, the decrease in electronic shielding with higher derivatives is slow. This can be attributed to inner shell electrons which move rigidly with the nuclei during vibrations and provide a perfect partial shield for the nuclear repulsions. In addition to scale changes, changes in polarization will also occur. The total effects can best be ascertained from an analysis of how the forces in a molecule change upon vibration. These then include scale changes, polarizations and other relaxation effects. We have already seen how densities (in CO and BF) which are diffusely disposed behind nuclei indicate large relaxation effects which oppose the nuclear motion and therefore are an antishielding or enhancing contribution to the force constant. Thus, the problem of whether one should include "lone pairs" in ρ as spherical shells or whether they are sufficiently polarized so as to

a) Footnote: The distinction between scale changes and polarization changes is unreal. The gross effect is a scale change, i.e., either a net contraction or a net expansion of the total density. In terms of forces, it is the detailed disposition of the the charge which is important. Therefore, polarization changes and charge transfer effects are a more detailed description than scale changes.

warrant their exclusion from the electron density as for inner shells⁽²³³⁾, can only be solved by including explicit relaxation of these densities via a change in polarization.

On reexamining the various contributions to the force constant in the LiF molecule, it is evident the ionic model of two polarizable charge spheres is relevant to the discussion of this molecule. The small overlap contribution at Li to the force constant supports the view of this molecule being two separate charge densities. This point is further accentuated by the fact that the overlap force constant contribution at F can be considered, just as in the forces, to be part of the F density as seen from the relaxation maps. This same conclusion was drawn earlier from the $\Delta\rho$ map for LiF. On the other hand, the ionic polarization mechanisms, which are a result of the detailed quantum mechanical calculation, show features which are somewhat different from the usual assumptions of polarizable ions. One interesting feature is that the F nucleus is negligibly overshielded ($K_{\text{Li}}^{(\text{AB})} + K_{\text{Li}}^{(\text{BB})} = 9.18$, see Table (5.3)), and thus most of the force constant at Li comes from the restoration of charge in front of Li. In BeO, $K_{\text{Be}}^{(\text{AB})} + K_{\text{Be}}^{(\text{BB})} = 8.82$, so that the density at the O nucleus does not behave as a predicted shielding population of 10.00, i.e., Be^{++}O^- . The undershielding can be traced largely to the behaviour of the $p\pi$ electrons situated at

the heavy nuclei. As one goes from the forces to field gradients, it has been noted previously that the π -densities exhibit enhanced undershielding by virtue of the nature of the operators involved. As much of the force constant contribution at Li from π -electrons at F comes as a field gradient contribution, the undershielding in the force constant by this density is thus understandable. One can, therefore, see that predictions of the force constant from the ionic model based on two polarizable spheres Li^+ and F^- will be in difficulty if this undershielding is not taken into account. This same difficulty appeared in the interpretation of quadrupole coupling constants based on such a model. Force constants determined from the polarizable spheres model⁽⁸²⁾ show agreement with observed spectroscopic constants⁽²³⁴⁾ when only dipole polarizabilities are used. The introduction of quadrupolar and higher polarizabilities results in a polarization catastrophe in the standard ionic theory, in addition to destroying the original agreement. Recent improvements, such as the inclusion of deformation dipole potentials⁽²³⁵⁾ via the use of short-range polarizations in order to maintain induced dipoles small, reintroduce agreement with experimental constants but still do not completely eliminate the polarization catastrophe.

This dipole deformation model is basically equivalent to the shell model of solid state physics which gives

rather accurate account of the phonon dispersion curves in the alkali halides with physical reasonable values of the parameters⁽²³⁶⁾. The physical idea behind the shell model⁽²³⁷⁾ is that in an ion, those electrons far from the nucleus, being less tightly bound are more profoundly affected by the application of an electric field than the inner electrons. This intuitive view is supported by the work of Sternheimer⁽¹⁸⁰⁾ who showed that the polarizabilities of rare-gas configuration ions are due almost entirely to the outermost shells. Accordingly, the shell model incorporates these qualitative features. It is thus assumed that under the field of neighbouring ions, the shell retains its spherical charge distribution (because of the cubic symmetry of the alkali halide crystals so that one has no net forces and field gradients at equilibrium⁽²³⁸⁾), but moves with respect to the core. The resulting polarizability is kept finite by a harmonic restoring force between the core and the shell, thus also taking partly into account the repulsive effect between adjacent shells. In terms of our previous discussion, this corresponds to complete non-following of the nuclei by the valence electrons. Our relaxation maps suggest that this phenomenon, which would have been expected to be largest at F due to the weak binding of valence electrons in F⁻, is probably exaggerated by the shell model. It is true that there are more Li⁺ near

neighbours to contend with. On the other hand, the internuclear distance in the LiF crystal is now 3.81 a.u. as compared to 2.96 a.u. in the molecule, so that electrostatic effects are partially decreased. In view of the high symmetry of the lattice, we may surmise that relaxations will remain symmetrical about the fluorine ion and the force constant contribution at F will approach the field gradient produced by the Li^+ ion. At Li, x-ray crystallography indicates the density about this nucleus to be unsymmetrical⁽¹⁰⁰⁾, increasing in regions away from the nuclei. This is in accord with our $\Delta\rho$ map for LiF where polarization behind the Li core is evident. It is to be expected that relaxation effects of this core density will be again dominant, since in moving away from one F^- ion, there will be shell repulsion from the other ions behind it, thus helping the charge accumulation in the internuclear region in front of it. The undershielding by the F^- density is to be expected again although somewhat less. In the case of solid BeO, the undershielding of the O nucleus by the density centered on it is more serious. The introduction of effective charges less than the ionic charges at the heavy nuclei would seem to be a promising improvement. Such an effective charge has been introduced previously by Szigeti⁽²³⁹⁾ in order to include electronic polarizability along with lattice displacements. For LiF, the effective or Szigeti charge

is 0.83. This is an average of the charges at both ions, positive and negative. The large undershieldings of densities at F and O indicate that the effective charges should be still smaller than the usual Szigeti charges.

VI. SUMMARY AND CONCLUSION

All knowledge is based on a measure of personal participation. Michael Polanyi

The formation of a molecule is intimately connected with a change in the electron distribution. The binding energy is only a small part of the total electronic energy ($\sim 1\%$ for N_2). One would therefore predict that the formation of a molecule is the result of small perturbations on the atoms concerned. One might, furthermore, expect that the change in the electron distribution on formation of a molecule will also be small and one might hope that such changes would by and large be restricted to those regions where the interaction was strongest, that is in the regions between those atoms where the traditional chemical bonds are supposed to be localized. An appreciation of these effects is best ascertained from the density map (ρ) and density difference maps ($\Delta\rho$) of molecules. In particular, with the advent of Hartree-Fock calculations from which one can obtain accurate wavefunctions, a study based on a density approach has been pursued in this work. The existence of a theorem (Brillouin's) which puts bounds on the accuracy of one-electron properties calculated from these densities

renders this approach advantageous and makes possible a classical electrostatic interpretation based on the Hellmann-Feynman theorem.

In view of Brillouin's theorem, Hartree-Fock densities approach exact densities. These reveal significant features, particularly anisotropies of atoms in molecular environments. From the total density (ρ) one can define molecular diameters corresponding to a cutoff contour of 0.002 a.u. These diameters are in agreement with empirical molecular sizes. Determination of atomic radii in the nonbonded regions of the molecule, i.e. behind the nuclei, and comparison of these with the atomic radii of free atoms and ions give information on tightness of binding in the molecule as compared to the molecule. In the series N_2 , CO, BF it is found that electron density is very diffuse behind C and B. For CO this is in accord with its electron donor properties as exemplified by the existence of many carbonyl compounds. As the density behind the B nucleus is more diffuse than behind C, one is tempted to suggest that BF should be a still more potent electron donor. In view of the tendency of the B atom towards triple coordination, the existence of BF molecules doubly bridged to metal atoms via two B-metal bonds should be possible. Thus, another class of compounds similar to metal-carbonyls would be an interesting experi-

mental possibility. In the 12-electron series C_2 , BeO , LiF , the densities are much more tightly bound at the electro-positive elements, as a result of charge transferred to the other end of the molecule. The density difference maps ($\Delta\rho$) depict the rearrangement of the molecular density and thus provide one with a picture of the bond density. In the series N_2 , CO , BF , the bulk of binding is due to increased concentration of density in the internuclear region. Accumulation in the bond goes hand in hand with depopulation at the nuclei. Charge increase also occurs behind the nuclei. In the group BeO , LiF , there is extensive charge removal in regions behind the light nuclei and relocation of this density at the electronegative site in the molecule. This behaviour is characteristic of ionic bonding. The accumulation of density in the bonding region, which is equally shared in N_2 but more polarized towards F in BF , is characteristic of covalent bonding, BF being indicative of a gradual transition between these two types of bonding.

One can further partition the electron space via weight factors in order to correlate characteristics of the densities of different molecules. In particular, by the use of the Hellmann-Feynman theorem, a comparison of the contributions to the total force, from charge density in different spatial regions of the molecule, demonstrates the

manner in which a state of electrostatic equilibrium is reached is characteristic of the binding found in each of these molecules. The general nature of the variation in the spatial distribution of the charge density through these two series of molecules is evident from ρ and $\Delta\rho$ maps. A comparison of the force components with the limiting components of separated atoms accentuates the mechanism by which electrostatic equilibrium is attained in the molecule as opposed to the separated atoms. The comparison thus isolates those changes in the atomic distributions which are responsible for binding the nuclei in the molecule. From the force analysis, there emerge distinctive characteristics of covalent and ionic densities. In the covalent case, there is undershielding of the nuclei and the binding comes essentially from the shared overlap charge density. In the ionic case, there is overshielding of the heavy nucleus and charge depletion at the light nucleus. Using contributions to the forces based on a partitioning of the charge in the manner indicated by the $\Delta\rho$ diagrams, it is possible to approach the classical model of two polarizable ions Li^+, F^- for LiF . BeO is thus found to be intermediate between Be^+O^- and Be^{++}O^- .

Along with the $\Delta\rho$ maps, profiles of the density difference on the bond axis indicate increased concentration of density near nuclear positions. This "clustering" of

density occurs for atoms which have p electrons taking part in the bonding. It is, therefore, to be expected that any property which sensitively depends upon the electron density near the nucleus will exhibit a characteristic change when the atom is incorporated in a molecule. Hence, theoretical calculations of such properties should be based on molecular wavefunctions which properly describe the contractive effect. One molecular property strongly influenced by this effect is the field gradient at a nucleus, giving rise to nuclear quadrupole interactions. This interaction is simple as it is obtained from first order perturbation theory and thus gives direct information on the charge distribution in the ground state. The analysis of the field gradient contributions in the molecules LiF and BeO indicate that the Sternheimer antishielding model, which is the result of trying to extend the point charge model, predicts field gradients of incorrect sign at the heavy nuclei. The cause of this disagreement is the different polarizations of $p\sigma$ and $p\pi$ electrons at the negative ion, arising from the quantum mechanical effects of bonding. At the positive ion, field gradients are less than predicted by the Sternheimer theory as a result of the undershielding of π density situated at the negative ion. The undershielding occurs from polarization effects and the geometrical nature of π densities. Similarly, analysis of

field gradients in N_2 , CO, BF indicate that the Townes-Dailey theory used in the interpretation of nuclear quadrupole constants in covalent molecules, must be viewed with caution as a result of independent σ and π polarizations. These polarizations (quadrupole) strongly depend on the rearrangement of charge which occurs in bond formation, an effect displayed by the $\Delta\rho$ maps.

This 'cautionary tale' regarding the interpretation of experimental data in terms of simple models is further pursued in a calculation and analysis of force constants. By differentiating the Hellmann-Feynman force, one obtains an interpretive expression for the force constant. It has been shown in this work that much of the static part of the expression, namely field gradient contributions, cancel out with relaxation contributions if the density is expressed in space fixed coordinates, i.e., the Hellmann-Feynman procedure. By expanding the total density onto one nucleus (A), and calculating the change in forces at that nucleus as it undergoes a virtual displacement, the force constant is then the result of relaxation of the density, i.e., a dynamic effect. Contributions from density centered on nucleus (B) can be separated out rigorously as a field gradient and the remaining atomic and overlap densities at A are viewed as purely relaxation phenomena. This relaxation is depicted in terms of relaxation diagrams which are

correlated to the magnitude of the contributions from the atomic and overlap densities. All force constant contributions are calculated from polynomial fits of the corresponding forces. As in the forces and $\Delta\rho$ diagrams, covalent and ionic densities exhibit contrasting characteristics in their force constant contributions. The covalent molecules as exemplified by N_2 demonstrate the importance of overlap density relaxations which facilitate nuclear motion. These override atomic contributions which impede nuclear displacements by the flow of charge back into the bonding regions from nonbonded regions, i.e., behind the nuclei. The observation made is that densities situated diffusely behind a nucleus exhibit large relaxation effects countering nuclear motion, as such densities do not follow nuclei with which they are associated. Thus, at B in BF, atomic relaxation overrides overlap relaxation, the net effect being a hinderance of nuclear motion. Densities situated at heavy nuclei follow these nuclei more completely, as a result of larger nuclear electrostatic fields. In the ionic molecules - LiF being most representative of this type of bonding - much of the force constant contribution at the light nucleus (Li) comes from relaxation of the Li^+ density in the direction opposite to displacements of the Li nucleus. At the heavy nucleus (F), relaxation is symmetric about that

nucleus, thus contributing little to the force constant. The main contribution at F then arises from the field gradient produced by Li^+ . Of significance is the substantial undershielding of the heavy nucleus by density situated there. This effect is more severe in BeO , where, as a result, the representation of this molecule as Be^{++}O^- is rendered questionable.

In conclusion, we would like to remark on the appropriateness of the use of a classical approach to chemical binding as we have pursued. A theorem of Møller⁽²⁵⁶⁾ states that classical point particles may not have any spin. On the other hand, quantum mechanical particles are defined in terms of rather abstract properties of the linear manifold of their physical states. Such definitions accommodate the notion of spinning particles very naturally. In view of the theorem due to Hohenberg and Kohn⁽²⁵⁾, if we know the 3-dimensional charge density $\rho(\vec{r})$ of a specified state of a molecule, however complicated it may be, then we have all the information that we need to answer any question about any spin-independent property. The usefulness of the density approach is amplified by recent experiments⁽²⁵⁷⁾ from which it appears that the over-all electron configuration of a molecule is more important in determining its reactivity than the finer details such as spin or orbital angular momentum. The use of the Hellmann-Feynman theorem makes possible, therefore,

a classical electrostatic interpretation of these densities. From such interpretation, it becomes evident that exact calculations reveal significant features, particularly anisotropies of atoms in molecular environments. These features exert a strong influence on calculated molecular properties. The moral of our story, then, is that detailed calculation will often reveal important effects that simple models rule out in advance. One wonders whether we may one day be able to abandon all models - just store all our machine-recorded calculations based on fundamental laws and when needed, extract the specific information from memory tapes!

APPENDIX 1

Hartree-Fock Theory⁽²⁴⁰⁾

In an exact Hartree-Fock calculation, the single particle states are determined by a variational calculation where their wavefunctions are subject to an unrestricted variation, and are called unrestricted (UHF) Hartree-Fock wavefunctions. Such a program is very complicated and is not usually carried out. By expanding the unknown single particle states in a complete basis, the Hartree-Fock equations become an infinite set of non-linear equations in the expansion coefficients. Upon limiting the expansion to a finite number of terms, one solves this non-linear secular equation using an iteration procedure.⁽⁴⁷⁾ If the number of terms is large, as it should be for a good approximation, the problem is still considerable.

The Hartree-Fock equations are simplified by imposing symmetries on the Hartree-Fock potential, usually rotational inversion symmetry. The equations thus become a set of integro-differential equations which determine the radial part of the wavefunctions, the angular-spin part being determined from the imposed symmetry. These are then called restricted Hartree-Fock wavefunctions (RHF), or more appropriately, symmetry restricted functions.⁽²⁴¹⁾ The Hartree-Fock equations have in general very many solutions, since they constitute only a necessary condition for the minimization of the energy. Imposing symmetry conditions means that one restricts oneself to a part

of the possible solutions, namely those which have the given symmetry. The lowest energy minimum may not be contained in this part.⁽²⁴²⁾ This is the price to pay for the simplification of the problem.

The basic Hamiltonian of the system of N particles will be written $H = T + V$, where T is the kinetic energy, and V is a two-body interaction. Choosing N orthonormal functions ϕ_1, \dots, ϕ_N (which are elements of the one-particle Hilbert space denoted by \mathcal{H}), one can construct an operator h (acting in \mathcal{H}) defined by its matrix elements between any two states $|\alpha\rangle$ and $|\beta\rangle$ of \mathcal{H} (these states are antisymmetric products of the ϕ 's)

$$\langle \alpha | h | \beta \rangle \equiv \langle \alpha | T + W | \beta \rangle = \langle \alpha | T | \beta \rangle + \sum_{i=1}^N \langle \alpha | \phi_i | V | \beta \phi_i - \phi_i \beta \rangle \quad A1.1$$

It is easily shown⁽⁴⁷⁾ that h is invariant under any unitary transformation of the function ϕ_i so that it is determined by the N -dimensional subspace spanned by these functions. This space will be denoted by $\{\phi\}$ and the corresponding operators by $h\{\phi\}$ and $W\{\phi\}$.

The Hartree-Fock Hamiltonian h and the Hartree-Fock potential W are defined as operators of the above structure but where the ϕ_i 's are the N lowest energy solutions of the eigenvalue problem

$$h\{\psi\}\psi_i = [T + W\{\psi\}]\psi_i = \epsilon_i \psi_i \quad A1.2$$

The equations for $(i = 1, N)$ are called the Hartree-Fock equations. Their solutions are denoted by ψ_1, \dots, ψ_N and the space spanned by

these functions is labelled $\{\psi\}$. The Hartree-Fock Hamiltonian $h\{\psi\}$ is usually constructed by an iterative procedure. Starting with N orthogonal functions $\{\phi^{(1)}\}$, one constructs $h\{\phi^{(1)}\}$ according to A(1.1) and finds its eigenvalue $\epsilon_i^{(2)}$ and eigenfunctions $\phi_i^{(2)}$. From the N functions of lowest energy (more functions can be obtained than N if the basis set is larger than N) one constructs another $h\{\phi^{(2)}\}$ and repeats the previous procedure until consistency is achieved. The eigenfunctions ψ_i of the final, self-consistent operator $h\{\psi\}$ form a complete set of functions in \mathcal{H} and are called Hartree-Fock orbitals. The N functions of lowest energy are referred to as occupied orbitals.

Now let the states $|\beta\rangle$ differ from $|\alpha\rangle$ by replacing the functions $\psi_S (S \leq N)$ by $\phi_S^\sigma (\sigma > N)$ one at a time, i.e., we are considering only single excitations. Then one can easily show that the change in energy to first order is (243)

$$\delta E = \sum_{S=1}^N \sum_{\sigma=N+1}^{\infty} [\langle \phi_S^\sigma | H | \alpha \rangle + \langle \alpha | H | \phi_S^\sigma \rangle] \quad A1.3$$

For minimum energy, this first order variation which is the most important, implies in view of the Hermitian property of the Hamiltonian

$$\langle \phi_S^\sigma | H | \alpha \rangle = 0 \quad A1.4$$

This is precisely Brillouin's theorem for the energies. In terms of the orbitals, ϕ_S^σ corresponds to arbitrary variations $S\psi_i$ in first order. These variations must vanish for A(1.4) to hold. This condition is then the usual differential equation for self-consistent wavefunctions as obtained from a variational procedure. (244)

An immediate consequence of this is that in first order perturbation theory, the states $|\beta\rangle$ must be doubly substituted determinants $|\beta_{st}^{\sigma\tau}\rangle$ where the occupied orbitals s and t are replaced by the excited orbitals σ and τ respectively. It follows from this that the mean value of any one-electron operator F , which has no matrix elements $\langle\alpha|F|\beta_{st}^{\sigma\tau}\rangle$ for any σ and τ , differs from the Hartree-Fock value by second-order terms only, quadratic in the coefficients $C_{st}^{\sigma\tau}$ of the states $|\beta_{st}^{\sigma\tau}\rangle$ estimated for the first-order wavefunction. This is the counterpart of Brillouin's theorem for one-electron operators. This result applies only to UHF calculations.

The Hellmann-Feynman theorem follows by differentiating the expression for the energy

$$E = \langle\alpha|T|\alpha\rangle + \langle\alpha|V|\alpha\rangle = \langle\alpha|H|\alpha\rangle$$

so that

$$F_N = -\nabla E_N \equiv -\langle\alpha|\nabla_N H|\alpha\rangle - 2\langle\nabla_N \alpha|T|\alpha\rangle - 2\langle\nabla_N \alpha|V|\alpha\rangle$$

Now $\nabla_N |\alpha\rangle$ can be expanded in terms of the complete set of Hartree-Fock states $|\beta\rangle$ where $|\beta\rangle$ differs from $|\alpha\rangle$ by only one orbital which because of the antisymmetric property of $|\alpha\rangle$ may not be an orbital already in $|\alpha\rangle$. The expansion is expressible in terms of states which contain only one orbital different from those in $|\alpha\rangle$ as ∇_N is a one-electron operator. We then have, using the Hermitian properties of T and V ,

$$F_N = -\langle\alpha|\nabla_N H|\alpha\rangle - 2 \sum_{\beta \neq \alpha} [\langle\alpha|T|\beta\rangle + \langle\alpha|V|\beta\rangle] \quad A1.5$$

where the sum over β excludes α since the state $\nabla_N |\alpha\rangle$ is orthogonal to $|\alpha\rangle$ from the normalization condition $\nabla_N \langle\alpha|\alpha\rangle = 0$. We

can rewrite the last bracketed term as a one-electron operator by averaging V over the orbitals which are the same in $|\alpha\rangle$ and $|\beta\rangle$, as in A(1.1), i.e.,

$$F_N = -\langle \alpha | \nabla_N H | \alpha \rangle - 2 \sum_{\delta \neq \alpha} \sum_{i=1}^{N-1} [\langle \alpha | T | \beta \rangle + \langle \alpha \phi_i | V | \beta \phi_i - \phi_i \beta \rangle]_{A1.5'}$$

where now the sum goes only to $N - 1$, as a result of one orbital being different in $|\beta\rangle$. However, the bracketed term is formally identical to A(1.1) since in that equation the sum includes a self-energy term which is identically zero, corresponding to the interaction of the orbital ϕ_i with itself. Therefore the correction term to the classical expression for the force is the matrix elements $\sum_{\delta \neq \alpha} \langle \alpha | h | \beta \rangle$ which, by virtue of the self-consistent orbitals obeying equation A(1.2), must vanish. The final result is then the Hellmann-Feynman theorem for Hartree-Fock wavefunctions:

$$F_N = -\langle \alpha | \nabla_N H | \alpha \rangle \quad A1.6$$

We have already shown in the previous paragraph that the expectation value of F_N is correct to second order, as $\nabla_N H$ is a one-electron operator in the Hellmann-Feynman formulation (see chapter two). This also includes the case of electron densities, which are defined by the one electron operator $\delta(\vec{r})$, i.e., the delta function at the point \vec{r} in space.

In this thesis, we are dealing with molecules in their ground state, the symmetry of which is Σ^+ , and furthermore these are closed shell systems. For such systems, the RHF method is internally consistent with the UHF equations. A HF wavefunction should transform in the manner of an exact energy eigenstate. Open shell

systems with degenerate ground states do not have this property and thus do not satisfy Brillouin's theorem.⁽²⁴⁵⁾ Specifically, the Slater determinant for a state containing only doubly occupied orbitals is left invariant under unitary transformations.⁽²⁴⁶⁾ As the ground states considered in this present work are made up of doubly occupied orbitals, then their RHF wavefunctions will obey Brillouin's theorem.

APPENDIX 2

Field Gradients

The calculation of field gradients involves the average of the operator $(3\cos^2\theta-1)/r^3$ over atomic, overlap and shielding distributions. These are then one-center integrals for the atomic densities and two-center integrals for the remaining densities. The operator is singular at $r=0$. As all integrals are done by integrating over angular coordinates first, then an undefined integral occurs for spherically symmetric distributions because in a vanishing small volume τ ,

$$\int_{\tau \rightarrow 0} \left(\frac{3\cos^2\theta-1}{r^3} \right) e^{-\tau} \cdot 2\pi r^2 dr \sin\theta d\theta = 0/0 \quad \text{A2.1}$$

This difficulty does not arise for higher orbitals, since these contribute a factor $r^{2\ell}$ with $\ell > 0$, and then the integral is absolutely convergent. To circumvent this operational difficulty, the integral over all space is broken up into two parts, r from ϵ to ∞ , and then 0 to ϵ . The limit $\epsilon \rightarrow 0$ is performed after integrating over angular coordinates. For the last part we can express the integral as

$$\int_{\tau \rightarrow 0} \frac{\partial^2}{\partial z^2} (1/r) \rho d\tau = -\frac{4\pi}{3} \rho(0) \quad \text{A2.2}$$

where the equality is a result of Poisson's equation $\nabla^2(1/r) = -4\pi\delta(0)$. By symmetry, all three components of the Laplacean are equal for a spherical distribution so that the integral is then only 1/3 of the equation. The result can also be easily proven by use of

Green's theorem⁽²⁴⁷⁾ and integrating over two surfaces, one at ∞ and the other at $r = \epsilon$. The result is that

$$\int_{\text{true}} \left(\frac{3 \cos^2 \theta - 1}{r^3} \right) \rho d\tau = \int_{\substack{\tau > \frac{4\pi}{3} \epsilon^3 \\ \text{limit } \epsilon \rightarrow 0}} \left(\frac{3 \cos^2 \theta - 1}{r^3} \right) d\tau - \frac{4\pi}{3} \rho(0) \quad \text{A2.3}$$

The formulae given below are for Slater atomic orbitals of the form⁽²⁴⁸⁾

$$X(n, l, m) = (2\alpha)^{n+\frac{1}{2}} [(2n!)]^{\frac{1}{2}} r^{n-1} e^{-\alpha r} Y_l^m(\theta, \varphi) \quad \text{A2.4}$$

$$\text{where } Y_l^m(\theta, \varphi) = (2\pi)^{-\frac{1}{2}} \frac{e^{im\varphi}}{2^l l!} \left[\frac{(2l+1)(l-m)!}{2(l+m)!} \right]^{\frac{1}{2}} (-\sin\theta)^m \left(\frac{d}{d \cos\theta} \right)^{l+m} (\cos^2\theta - 1)^l$$

$$\text{For example } Y_0^0 = \frac{1}{\sqrt{4\pi}}, \quad Y_1^0 = \sqrt{\frac{3}{4\pi}} \cos\theta, \quad Y_1^{-1} = \sqrt{\frac{3}{8\pi}} \sin\theta e^{-i\varphi}, \quad Y_2^0 = \sqrt{\frac{5}{16\pi}} (3\cos^2\theta - 1)$$

$$Y_2^{-1} = \sqrt{\frac{15}{8\pi}} \sin\theta \cos\theta e^{-i\varphi}, \quad Y_3^0 = \sqrt{\frac{7}{16\pi}} (5\cos^3\theta - 3\cos\theta), \quad Y_3^{-1} = \sqrt{\frac{21}{64\pi}} \sin\theta (5\cos^2\theta - 1) e^{-i\varphi}$$

For computational facility the normalization factor N is defined as

$$N = (2\alpha)^{n_1+\frac{1}{2}} (2\beta)^{n_2+\frac{1}{2}} [(2n_1)]^{-\frac{1}{2}} [(2n_2)]^{-\frac{1}{2}} \quad \text{A2.5}$$

where α and β represent different exponents for atomic orbitals with quantum numbers n_1 and n_2 respectively. Angular integrals of the form

$$\int Y_l^{m*}(\theta, \varphi) Y_{l'}^{m'}(\theta, \varphi) Y_{l''}^{m''}(\theta, \varphi)$$

can be readily worked out from Slater's⁽²⁴⁹⁾ tables of $C^k(lm_1, l'm_1')$

Atomic Field Gradients

$$A(nlm, n'l'm') = 2 \int X(nlm) X(n'l'm') P_2(\cos\theta) / r^3 d\tau$$

We list only the nonzero elements.

$$A(1s, 3d\sigma) = \frac{2N}{(\alpha+\beta)^2} \sqrt{1/5}$$

$$A(2p\sigma, 2p\sigma) = \frac{16}{15} \frac{\alpha^{5/2} \beta^{5/2}}{(\alpha+\beta)^2}$$

$$A(2s, 3d\sigma) = \frac{4N}{(\alpha+\beta)^3} \sqrt{1/5}$$

$$A(3d\sigma, 3d\sigma) = \frac{12N}{(\alpha+\beta)^4} (2/7)$$

$$A(3s, 3d\sigma) = \frac{12N}{\alpha \beta} \sqrt{1/5}$$

$$A(4f\sigma, 4f\sigma) = \frac{2N(5!)}{(\alpha+\beta)^6} \sqrt{\frac{16}{225}}$$

$$A(2p\delta, 4f\delta) = \frac{12N}{(\alpha+\beta)^4} \sqrt{\frac{27}{175}}$$

$$A(4f\pi, 4f\pi) = \frac{2N(5!)}{(\alpha+\beta)^6} \sqrt{\frac{9}{225}}$$

$$A(2p\pi, 2p\pi) = -\frac{8}{15} \frac{\alpha^{5/2} \beta^{5/2}}{(\alpha+\beta)^2}$$

$$A(2p\pi, 4f\pi) = \frac{12N}{(\alpha+\beta)^4} \sqrt{\frac{18}{175}}$$

$$A(3d\pi, 3d\pi) = \frac{12N}{(\alpha+\beta)^4} \left(\frac{1}{7}\right)$$

Overlap Field Gradients

Overlap field gradients can be reduced to the general integral

$$J(k, l, m) = \int e^{-\alpha r_a} e^{-\beta r_b} \cos^k \theta_a r_a^{l-1} r_b^{m-1} dr \quad A2.6$$

by use of the relations $r_a \sin \theta_a = r_b \sin \theta_b$, $r_a \cos \theta_a = R - r_b \cos \theta_b$ (see fig. 3.2) One then expands functionals of r_b and θ_b by the Coulson-Barnett method: (250)

$$r_b^{m-1} e^{-\beta r_b} = \sum_{h=0}^{\infty} \frac{(2h+1)}{\sqrt{r_a R}} P_h(\cos \theta_a) J_{m,n}(\beta, r_a, R) \quad A2.7$$

where the J 's are products of imaginary Bessel functions $J_{n+1/2}$ and $K_{n+1/2}$. By the substitution $t = \beta r_a$, $\tau = \beta R$, $K = \alpha/\beta$, one has also

$$J(k, l, m) = \frac{4\pi}{\beta^{l+m+1}} \sum_{n=0}^{\infty} \frac{(2n+1)}{2\sqrt{\tau}} \left(\int_{-1}^{+1} P_n(u) u^k du \right) Z_{m,n,l+1/2}(K, \tau) \quad A2.8$$

Thus all integrals can be reduced to the functions $Z_{m,n,l+1/2}$ which are calculated by iterative procedures desented by Coulson and Barnett (250) for the integral representation:

$$Z_{m,n,l+1/2}(K, \tau) = \int_0^{\infty} \exp(-Kt) J_{m,n}(i, t; \tau) t^{l+1/2} dt \quad A2.9$$

Occasionally use of the following definitions will be made:

$$Z_{0,n,l+1/2} = G_{n,l+1/2} \quad ; \quad Z_{1,n,l+1/2} = P_{n,l+1/2}$$

The general definition of an overlap field gradient is then:

$$O(n, l, m, n', l', m') = 2 \int X_a(n, l, m) P_2 \left(\frac{\cos \theta_a}{r_a^3} \right) X_b(n', l', m') d\tau_a \quad A2.10$$

The expressions for the individual overlap elements are listed as follows.

$$O(1s, 1s) = \alpha^{3/2} \beta^{3/2} \cdot \frac{8}{5} \sqrt{\tau} [G_{1,-1+1/2} - G_{3,-1+1/2}]$$

$$O(2s, 2s) = \frac{\alpha^{5/2} \beta^{5/2}}{\beta^2 \sqrt{\tau}} \cdot 8 \cdot \left[-\frac{4\tau}{15} G_{1,0+1/2} + \frac{1}{3} G_{2,1+1/2} - \frac{2\tau}{5} G_{3,0+1/2} + \frac{\tau^2}{3} G_{2,-1+1/2} \right]$$

$$O(2p, 2p) = \frac{\alpha^{5/2} \beta^{5/2}}{\beta \sqrt{\tau}} \cdot 4 \cdot \left[R \left(\frac{4}{5} P_{1,-1+1/2} + \frac{6}{5} P_{3,-1+1/2} \right) - \frac{1}{\beta} \left(\frac{4}{15} P_{0,0+1/2} + \frac{22}{21} P_{2,0+1/2} + \frac{24}{35} P_{4,0+1/2} \right) \right]$$

$$O(1s, 2s) = \frac{\alpha^{3/2} \beta^{5/2}}{\beta \sqrt{3\tau}} \cdot 8 \cdot \left[G_{2,0+1/2} + \tau^2 G_{2,-2+1/2} - \frac{4\tau}{5} G_{1,-1+1/2} - \frac{6\tau}{5} G_{3,-1+1/2} \right]$$

$$O(1s, 2p) = \frac{\alpha^{3/2} \beta^{5/2}}{\sqrt{\tau}} \cdot \frac{8}{5} \left[R\tau (G_{1,-1+1/2} - G_{3,-1+1/2}) - \frac{1}{\beta} (2P_{1,-1+1/2} + 3P_{3,-1+1/2}) \right]$$

$$O(2s, 1s) = \frac{\alpha^{5/2} \beta^{3/2}}{\sqrt{3} \beta} \sqrt{\tau} \cdot \frac{8}{5} [G_{1,0+1/2} - G_{3,0+1/2}]$$

$$O(2s, 2p) = \frac{\alpha^{5/2} \beta^{5/2}}{\beta \sqrt{3\tau}} \cdot \frac{8}{5} \left[R\tau (G_{1,0+1/2} - G_{3,0+1/2}) - \frac{1}{\beta} (2P_{1,0+1/2} + 3P_{3,0+1/2}) \right]$$

$$O(2p, 1s) = \frac{\alpha^{5/2} \beta^{3/2}}{\beta \sqrt{\tau}} \cdot \frac{8}{5} [2P_{1,-1+1/2} + 3P_{3,-1+1/2}]$$

$$O(2p, 2s) = \frac{\alpha^{5/2} \beta^{5/2}}{\beta^2 \sqrt{3\tau}} \cdot \frac{8}{5} \left\{ 2 \left[G_{1,1+1/2} + \tau^2 G_{1,-1+1/2} - \frac{2\tau}{3} (G_{0,0+1/2} + 2G_{2,0+1/2}) \right] + 3 \left[G_{3,1+1/2} + \tau^2 G_{3,-1+1/2} - \frac{2\tau}{7} (3G_{2,0+1/2} + 4G_{4,0+1/2}) \right] \right\}$$

$$O(1s, 3s) = \frac{2N}{\beta^2 \sqrt{c}} Z_{3,2,-2+1/2}$$

$$O(3s, 1s) = \frac{2N}{\beta^2 \sqrt{c}} P_{2,0+1/2}$$

$$O(1s, 3d\sigma) = \frac{\sqrt{5}N}{2\beta^2 \sqrt{c}} \left[4Z_{3,2,-2+1/2} + \frac{4}{5}Z_{1,0,0+1/2} - \frac{20}{7}Z_{1,2,0+1/2} + \frac{72}{35}Z_{1,4,0+1/2} \right]$$

$$O(3d\sigma, 1s) = \frac{\sqrt{5}N}{2\beta^2 \sqrt{c}} \left[\frac{4}{5}Z_{1,0,0+1/2} + \frac{8}{7}Z_{1,2,0+1/2} + \frac{72}{35}Z_{1,4,0+1/2} \right]$$

$$O(1s, 4f\sigma) = \frac{\sqrt{7}N}{2\sqrt{c}} \left[\frac{R}{\beta^2} \left(4Z_{3,2,-2+1/2} + \frac{4}{3}Z_{1,0,0+1/2} - \frac{100}{21}Z_{1,2,0+1/2} \right. \right. \\ \left. \left. + \frac{24}{7}Z_{1,4,0+1/2} \right) - \frac{1}{\beta^3} \left(\frac{8}{5}Z_{3,1,-1+1/2} + \frac{12}{5}Z_{3,3,-1+1/2} \right. \right. \\ \left. \left. - \frac{4}{7}Z_{1,1,1+1/2} - \frac{4}{3}Z_{1,3,1+1/2} + \frac{40}{21}Z_{1,5,1+1/2} \right) \right]$$

$$O(4f\sigma, 1s) = \frac{\sqrt{7}N}{2\sqrt{c}} \frac{1}{\beta^3} \left[\frac{36}{35}Z_{1,1,1+1/2} + \frac{16}{15}Z_{1,3,1+1/2} + \frac{40}{21}Z_{1,5,1+1/2} \right]$$

$$O(2s, 3s) = \frac{2N}{\beta^3 \sqrt{c}} Z_{3,2,-1+1/2}$$

$$O(3s, 2s) = \frac{2N}{\beta^3 \sqrt{c}} Z_{2,2,0+1/2}$$

$$O(2s, 3d\sigma) = \frac{\sqrt{5}N}{2\sqrt{c}} \frac{1}{\beta^3} \left[4Z_{3,2,-1+1/2} + \frac{4}{5}Z_{1,0,1+1/2} - \frac{20}{7}Z_{1,2,1+1/2} + \frac{72}{35}Z_{1,4,1+1/2} \right]$$

$$O(3d\sigma, 2s) = \frac{\sqrt{5}N}{2\sqrt{c}} \frac{1}{\beta^3} \left[\frac{4}{5}Z_{2,0,0+1/2} + \frac{8}{7}Z_{2,2,0+1/2} + \frac{72}{35}Z_{2,4,0+1/2} \right]$$

$$O(2s, 4f\sigma) = \frac{\sqrt{7}N}{2\sqrt{c}} \left[\frac{R}{\beta^3} \left(4Z_{3,2,-1+1/2} + \frac{4}{3}Z_{1,0,1+1/2} - \frac{100}{21}Z_{1,2,1+1/2} \right. \right. \\ \left. \left. + \frac{24}{7}Z_{1,4,1+1/2} \right) - \frac{1}{\beta^4} \left(\frac{8}{5}Z_{3,1,0+1/2} + \frac{12}{5}Z_{3,3,0+1/2} - \frac{4}{7}Z_{1,5,2+1/2} \right. \right. \\ \left. \left. - \frac{4}{3}Z_{1,3,2+1/2} + \frac{40}{21}Z_{1,5,2+1/2} \right) \right]$$

$$O(4f\sigma, 2s) = \frac{\sqrt{7} N}{2\sqrt{c} \beta^4} \left[\frac{36}{35} Z_{2,1,1,+\frac{1}{2}} + \frac{16}{15} Z_{2,3,1+\frac{1}{2}} + \frac{40}{21} Z_{2,5,1+\frac{1}{2}} \right]$$

$$O(3s, 3s) = \frac{2N}{\beta^4 \sqrt{c}} Z_{3,2,0+\frac{1}{2}}$$

$$O(3s, 3d\sigma) = \frac{\sqrt{5} N}{2\sqrt{c} \beta^4} \left[4 Z_{3,2,0+\frac{1}{2}} + \frac{4}{5} Z_{1,0,2+\frac{1}{2}} - \frac{20}{7} Z_{1,2,2+\frac{1}{2}} + \frac{72}{35} Z_{1,4,2+\frac{1}{2}} \right]$$

$$O(3d\sigma, 3s) = \frac{\sqrt{5} N}{2\sqrt{c} \beta^4} \left[\frac{4}{5} Z_{3,0,0+\frac{1}{2}} + \frac{8}{7} Z_{3,2,0+\frac{1}{2}} + \frac{72}{35} Z_{3,4,0+\frac{1}{2}} \right]$$

$$O(3s, 4f\sigma) = \frac{\sqrt{7} N}{2\sqrt{c}} \left[\frac{R}{\beta^4} \left(4 Z_{3,2,0+\frac{1}{2}} + \frac{4}{3} Z_{1,0,2+\frac{1}{2}} - \frac{100}{21} Z_{1,2,2+\frac{1}{2}} \right. \right. \\ \left. \left. + \frac{24}{7} Z_{1,4,2+\frac{1}{2}} \right) - \frac{1}{\beta^5} \left(\frac{8}{5} Z_{3,1,1+\frac{1}{2}} + \frac{12}{15} Z_{3,3,1+\frac{1}{2}} - \frac{4}{7} Z_{1,1,3+\frac{1}{2}} \right. \right. \\ \left. \left. - \frac{4}{3} Z_{1,3,3+\frac{1}{2}} + \frac{40}{21} Z_{1,5,3+\frac{1}{2}} \right) \right]$$

$$O(4f\sigma, 3s) = \frac{\sqrt{7} N}{2\beta^5 \sqrt{c}} \left[\frac{36}{35} Z_{3,1,1+\frac{1}{2}} + \frac{16}{15} Z_{3,3,1+\frac{1}{2}} + \frac{40}{21} Z_{3,5,1+\frac{1}{2}} \right]$$

$$O(3s, 2p\sigma) = \frac{\sqrt{3} N}{\sqrt{c}} \left[\frac{2R}{\beta^2} Z_{1,2,0+\frac{1}{2}} - \frac{1}{\beta^3} \left(\frac{4}{5} Z_{1,1,1+\frac{1}{2}} + \frac{6}{5} Z_{1,3,1+\frac{1}{2}} \right) \right]$$

$$O(2p\sigma, 3s) = \frac{\sqrt{3} N}{\beta^3 \sqrt{c}} \left[\frac{4}{5} Z_{3,1,-1+\frac{1}{2}} + \frac{6}{5} Z_{3,3,-1+\frac{1}{2}} \right]$$

$$O(3d\sigma, 3d\sigma) = \frac{5N}{4\beta^4 \sqrt{c}} \left[\frac{8}{5} Z_{3,0,0+\frac{1}{2}} + \frac{16}{7} Z_{3,2,0+\frac{1}{2}} + \frac{144}{35} Z_{3,4,0+\frac{1}{2}} \right. \\ \left. - \frac{8}{7} Z_{1,0,2+\frac{1}{2}} + \frac{8}{7} Z_{1,2,2+\frac{1}{2}} - \frac{144}{77} Z_{1,4,2+\frac{1}{2}} + \frac{144}{77} Z_{1,6,2+\frac{1}{2}} \right]$$

$$O(3d\sigma, 2p\sigma) = \frac{\sqrt{15} N}{2\sqrt{c}} \left[\frac{R}{\beta^2} \left(\frac{4}{5} Z_{1,0,0+\frac{1}{2}} + \frac{8}{7} Z_{1,2,0+\frac{1}{2}} + \frac{72}{35} Z_{1,4,0+\frac{1}{2}} \right) \right. \\ \left. - \frac{1}{\beta^3} \left(\frac{44}{35} Z_{1,1,1+\frac{1}{2}} + \frac{8}{5} Z_{1,3,1+\frac{1}{2}} + \frac{8}{7} Z_{1,5,1+\frac{1}{2}} \right) \right]$$

$$O(2p\sigma, 3d\sigma) = \frac{\sqrt{15} N}{2\sqrt{e}} \frac{1}{\beta^3} \left[\frac{8}{5} Z_{3,1,1+1/2} + \frac{12}{5} Z_{3,3,-1+1/2} + \frac{12}{35} Z_{1,1,1+1/2} - \frac{4}{5} Z_{1,3,1+1/2} + \frac{8}{7} Z_{1,5,1+1/2} \right]$$

$$O(3d\sigma, 4f\sigma) = \frac{N\sqrt{35}}{4\sqrt{e}} \left[\frac{R}{\beta^4} \left(\frac{8}{5} Z_{3,0,0+1/2} + \frac{16}{7} Z_{3,2,0+1/2} + \frac{144}{35} Z_{3,4,0+1/2} + \frac{40}{21} Z_{1,0,2+1/2} + \frac{40}{21} Z_{1,2,2+1/2} - \frac{240}{77} Z_{1,4,2+1/2} + \frac{240}{77} Z_{1,6,2+1/2} - \frac{1}{\beta^5} \left(\frac{88}{35} Z_{3,1,1+1/2} + \frac{16}{5} Z_{3,3,1+1/2} + \frac{16}{7} Z_{3,5,1+1/2} - \frac{8}{7} Z_{1,1,3+1/2} - \frac{8}{33} Z_{1,3,3+1/2} - \frac{80}{273} Z_{1,5,3+1/2} + \frac{240}{143} Z_{1,7,3+1/2} \right) \right]$$

$$O(4f\sigma, 3d\sigma) = \frac{\sqrt{35} N}{4\sqrt{e}} \frac{1}{\beta^5} \left[\frac{72}{35} Z_{3,1,1+1/2} + \frac{32}{15} Z_{3,3,1+1/2} + \frac{80}{21} Z_{3,5,1+1/2} - \frac{24}{35} Z_{1,1,3+1/2} + \frac{136}{165} Z_{1,3,3+1/2} - \frac{496}{273} Z_{1,5,3+1/2} + \frac{240}{143} Z_{1,7,3+1/2} \right]$$

$$O(4f\sigma, 4f\sigma) = \frac{7N}{4\sqrt{e}} \left[\frac{R}{\beta^5} \left(\frac{72}{35} Z_{3,1,1+1/2} + \frac{32}{15} Z_{3,3,1+1/2} + \frac{80}{21} Z_{3,5,1+1/2} - \frac{8}{7} Z_{1,1,3+1/2} + \frac{136}{99} Z_{1,3,3+1/2} - \frac{5 \cdot 496}{3 \cdot 273} Z_{1,5,3+1/2} + \frac{400}{143} Z_{1,7,3+1/2} - \frac{1}{\beta^6} \left(\frac{24}{35} Z_{3,0,2+1/2} + \frac{16}{7} Z_{3,2,2+1/2} + \left(\frac{720}{77} - \frac{32}{5} \right) Z_{3,4,2+1/2} + \frac{160}{77} Z_{3,6,2+1/2} - \frac{8}{21} Z_{1,0,4+1/2} - \frac{40}{231} Z_{1,2,4+1/2} + 5 \left(\frac{136}{35} + \frac{96}{143} + \frac{360}{77} \right) Z_{1,4,4+1/2} - \frac{80}{231} Z_{1,6,4+1/2} + \frac{640}{429} Z_{1,8,4+1/2} \right) \right]$$

$$O(2p\sigma, 4f\sigma) = \frac{\sqrt{21} N}{2\sqrt{e}} \left[\frac{R}{\beta^3} \left(\frac{8}{5} Z_{3,1,-1+1/2} + \frac{12}{5} Z_{3,3,-1+1/2} - \frac{4}{7} Z_{1,1,1+1/2} - \frac{4}{3} Z_{1,3,1+1/2} + \frac{40}{21} Z_{1,5,1+1/2} \right) - \frac{1}{\beta^4} \left(\frac{8}{15} Z_{3,0,0+1/2} + \frac{44}{21} Z_{3,2,0+1/2} + \frac{48}{35} Z_{3,4,0+1/2} - \frac{4}{21} Z_{1,0,2+1/2} - \frac{20}{21} Z_{1,2,2+1/2} + \frac{8}{77} Z_{1,4,2+1/2} + \frac{80}{77} Z_{1,6,2+1/2} \right) \right]$$

$$O(4f\sigma, 2p\sigma) = \frac{\sqrt{21} N}{2\sqrt{e}} \left[\frac{R}{\beta^3} \left(\frac{36}{35} Z_{1,1,1+1/2} + \frac{16}{15} Z_{1,3,1+1/2} + \frac{40}{21} Z_{1,5,1+1/2} \right) - \frac{1}{\beta^4} \left(\frac{12}{35} Z_{3,0,2+1/2} + \frac{16}{7} Z_{3,2,2+1/2} + \left(\frac{720}{77} - \frac{32}{5} \right) Z_{3,4,2+1/2} + \frac{160}{77} Z_{3,6,2+1/2} - \frac{8}{21} Z_{1,0,4+1/2} - \frac{40}{231} Z_{1,2,4+1/2} + 5 \left(\frac{136}{35} + \frac{96}{143} + \frac{360}{77} \right) Z_{1,4,4+1/2} - \frac{80}{231} Z_{1,6,4+1/2} + \frac{640}{429} Z_{1,8,4+1/2} \right) \right]$$

$$+\frac{8}{7} Z_{1,2,2+1/2} + \frac{568}{358} Z_{1,4,2+1/2} + \frac{80}{77} Z_{1,6,2+1/2}]$$

$$O(2p\pi, 2p\pi) = \frac{3N}{2\sqrt{c}} \frac{1}{\beta^2} \left[-\frac{4}{15} Z_{1,0,0+1/2} + \frac{20}{21} Z_{1,2,0+1/2} - \frac{24}{35} Z_{1,4,0+1/2} \right]$$

$$O(2p\pi, 3d\pi) = \frac{\sqrt{45}N}{2\sqrt{c}} \left[\frac{R}{\beta^2} \left(-\frac{4}{15} Z_{1,0,0+1/2} + \frac{20}{21} Z_{1,2,0+1/2} - \frac{24}{35} Z_{1,4,0+1/2} \right) \right. \\ \left. - \frac{1}{\beta^3} \left(\frac{4}{35} Z_{1,1,1+1/2} + \frac{4}{15} Z_{1,3,1+1/2} - \frac{8}{21} Z_{1,5,1+1/2} \right) \right]$$

$$O(3d\pi, 2p\pi) = \frac{\sqrt{45}N}{2\sqrt{c}} \frac{1}{\beta^3} \left[\frac{4}{35} Z_{1,1,1+1/2} + \frac{4}{15} Z_{1,3,1+1/2} - \frac{8}{21} Z_{1,5,1+1/2} \right]$$

$$O(2p\pi, 4f\pi) = \sqrt{\frac{63}{32}} \frac{N}{\sqrt{c}} \frac{1}{\beta^4} \left[-\frac{16}{15} Z_{3,0,0+1/2} + \frac{80}{21} Z_{3,2,0+1/2} - \frac{96}{35} Z_{3,4,0+1/2} \right. \\ \left. + \frac{32}{21} Z_{1,0,2+1/2} - \frac{80}{21} Z_{1,2,2+1/2} + \frac{256}{77} Z_{1,4,2+1/2} - \frac{80}{77} Z_{1,6,2+1/2} \right]$$

$$O(4f\pi, 2p\pi) = \sqrt{\frac{63}{32}} \frac{N}{\sqrt{c}} \frac{1}{\beta^4} \left[\frac{16}{35} Z_{1,0,2+1/2} + \frac{32}{55} Z_{1,4,2+1/2} - \frac{80}{77} Z_{1,6,2+1/2} \right]$$

$$O(3d\pi, 3d\pi) = \frac{15N}{2\sqrt{c}} \left[\frac{R}{\beta^3} \left(\frac{4}{35} Z_{1,1,1+1/2} + \frac{4}{15} Z_{1,3,1+1/2} - \frac{8}{21} Z_{1,5,1+1/2} \right) \right. \\ \left. - \frac{1}{\beta^4} \left(\frac{4}{105} Z_{1,0,2+1/2} + \frac{4}{21} Z_{1,2,2+1/2} - \frac{8}{385} Z_{1,4,2+1/2} - \frac{16}{77} Z_{1,6,2+1/2} \right) \right]$$

$$O(4f\pi, 4f\pi) = \frac{21N}{16\sqrt{c}} \frac{1}{\beta^6} \left[\frac{64}{35} Z_{3,0,2+1/2} + \frac{128}{55} Z_{3,4,2+1/2} - \frac{320}{77} Z_{3,6,2+1/2} \right. \\ \left. - \frac{32}{21} Z_{1,0,4+1/2} + \frac{160}{77} Z_{1,2,4+1/2} + 5 \left(-\frac{256}{35} + \frac{24*38}{77} - \frac{15*48}{143} \right) Z_{1,4,4+1/2} \right. \\ \left. + 5 \left(\frac{16*38}{11*21} - \frac{64}{33} \right) Z_{1,6,4+1/2} - \frac{640}{429} Z_{1,8,4+1/2} \right]$$

$$O(3d\pi, 4f\pi) = \frac{\sqrt{15}\sqrt{21}N}{\sqrt{32}\sqrt{c}\beta^5} \left[\frac{16}{35} \sum_{3,1,1+\frac{1}{2}} + \frac{16}{15} \sum_{3,3,1+\frac{1}{2}} - \frac{32}{21} \sum_{3,5,1+\frac{1}{2}} \right. \\ \left. + \frac{160}{117} \sum_{1,5,3+\frac{1}{2}} - \frac{80}{143} \sum_{1,7,3+\frac{1}{2}} \right]$$

$$O(4f\pi, 3d\pi) = \frac{\sqrt{15}\sqrt{21}N}{\sqrt{32}\sqrt{c}} \left[\frac{R}{\beta^4} \left(\frac{16}{35} \sum_{1,0,2+\frac{1}{2}} + \frac{32}{55} \sum_{1,4,2+\frac{1}{2}} - \frac{80}{77} \sum_{1,6,2+\frac{1}{2}} \right) \right. \\ \left. - \frac{1}{\beta^5} \left(\frac{16}{35} \sum_{1,1,3+\frac{1}{2}} + \frac{128}{495} \sum_{1,3,3+\frac{1}{2}} + \left(\frac{184}{63} - \frac{40}{13} \right) \sum_{1,5,3+\frac{1}{2}} \right. \right. \\ \left. \left. - \frac{80}{143} \sum_{1,7,3+\frac{1}{2}} \right) \right]$$

Shielding Field Gradients

The integrals of the form

$$\int (\alpha, n_1, l_1, m) \begin{Bmatrix} \cos m \ell \\ \sin m \ell \end{Bmatrix} \frac{P_2(\cos \theta_B)}{r_B^3} (\beta, n_2, l_2, m) \begin{Bmatrix} \cos m \ell \\ \sin m \ell \end{Bmatrix} d\Omega$$

have been discussed by Pitze, Kern, and Lipscomb.⁽¹⁵⁴⁾ These

authors use the expansions for spherical harmonics as given by

Hobson⁽²⁵¹⁾

$$\frac{P_n^m(\cos \theta_t)}{r_t^{n+1}} = \frac{1}{R^n} \sum_{l=m}^{\infty} \binom{l+n}{n-m} \frac{r_a^l}{R^{l+1}} P_l^m(\cos \theta_a) \quad \text{if } r_a < R$$

A2.11

$$= \frac{(-1)^{n-m}}{R^n} \sum_{l=n}^{\infty} \binom{l-m}{n-m} \frac{R^l}{r_a^{l+1}} P_l^m(\cos \theta_a) \quad \text{if } r_a > R$$

There is a singularity at $r_a = R$ for cases involving $n-m \geq 2$. For

the field gradient operator, an additional factor of $-\frac{8\pi}{3} \rho(R)$

must be added to $(3\cos^2 \theta_B - 1)/r_B^3$ if angular integrations are

performed first as is the usual case. The integrals are all

reducible to the functional:

$$G(2, 0, n, l, \rho) = \binom{l+2}{2} \int_0^1 t^{n+l} \exp(-\rho t) dt + \binom{l}{2} \int_1^{\infty} t^{n-l-1} \exp(-\rho t) dt \quad \text{A2.12}$$

where $\rho = (\alpha + \beta)R$, $l_1 + l_2 > l > |l_1 - l_2|$, $n = n_1 + n_2$

The formulae for averages over orbital products are then defined

from

$$P(n, l, m_1; n_2, l_2, m_2) = 2 \int X_a(n, l, m_1) \frac{P_2(\cos \theta_t)}{r_t^3} X_a(n_2, l_2, m_2) d\Omega \quad \text{A2.13}$$

and are given by the following:

$$P(1s, 1s) = 2N \left[-\frac{1}{3} \exp(-\rho) + G(2, 0, 2, 0, \rho) \right]$$

$$P(1s, 2s) = 2NR \left[-\frac{1}{3} \exp(-\rho) + G(2, 0, 3, 0, \rho) \right]$$

$$P(1s, 3s) = 2NR^2 \left[-\frac{1}{3} \exp(-\rho) + G(2, 0, 4, 0, \rho) \right]$$

$$P(2s, 2s) = 2NR^2 \left[-\frac{1}{3} \exp(-\rho) + G(2, 0, 4, 0, \rho) \right]$$

$$P(2s, 3s) = 2NR^3 \left[-\frac{1}{3} \exp(-\rho) + G(2, 0, 5, 0, \rho) \right]$$

$$P(3s, 3s) = 2NR^4 \left[-\frac{1}{3} \exp(-\rho) + G(2, 0, 6, 0, \rho) \right]$$

$$P(1s, 2p\sigma) = \frac{2NR}{\sqrt{3}} \left[-\exp(-\rho) + G(2, 0, 3, 1, \rho) \right]$$

$$P(1s, 3d\sigma) = 2NR^2 \left[-\frac{\sqrt{5}}{3} \exp(-\rho) + \frac{1}{\sqrt{5}} G(2, 0, 4, 2, \rho) \right]$$

$$P(1s, 4f\sigma) = 2NR^3 \left[-\frac{\sqrt{7}}{3} \exp(-\rho) + \frac{1}{\sqrt{7}} G(2, 0, 5, 3, \rho) \right]$$

$$P(2s, 2p\sigma) = \frac{2NR^2}{\sqrt{3}} \left[-\exp(-\rho) + G(2, 0, 4, 1, \rho) \right]$$

$$P(2s, 3d\sigma) = 2NR^3 \left[-\frac{\sqrt{5}}{3} \exp(-\rho) + \frac{1}{\sqrt{5}} G(2, 0, 5, 2, \rho) \right]$$

$$P(2s, 4f\sigma) = 2NR^4 \left[-\frac{\sqrt{7}}{3} \exp(-\rho) + \frac{1}{\sqrt{7}} G(2, 0, 6, 3, \rho) \right]$$

$$P(3s, 2p\sigma) = \frac{2NR^3}{\sqrt{3}} \left[-\exp(-\rho) + G(2, 0, 5, 1, \rho) \right]$$

$$P(3s, 3d\sigma) = 2NR^4 \left[-\frac{\sqrt{5}}{3} \exp(-\rho) + \frac{1}{\sqrt{5}} G(2, 0, 6, 2, \rho) \right]$$

$$P(3s, 4f\sigma) = 2NR^5 \left[-\frac{\sqrt{7}}{3} \exp(-\rho) + \frac{1}{\sqrt{7}} G(2, 0, 7, 3, \rho) \right]$$

$$P(2p\sigma, 2p\sigma) = 2NR^2 \left[-\exp(-\rho) + G(2, 0, 4, 0, \rho) + \frac{2}{5} G(2, 0, 4, 2, \rho) \right]$$

$$P(2p\sigma, 3d\sigma) = 2NR^3 \left[-\frac{\sqrt{15}}{3} \exp(-\rho) + \sqrt{\frac{4}{15}} G(2, 0, 5, 1, \rho) + \sqrt{\frac{27}{245}} G(2, 0, 5, 3, \rho) \right]$$

$$P(2p\sigma, 4f\sigma) = 2NR^4 \left[-\frac{\sqrt{21}}{3} \exp(-\rho) + \sqrt{\frac{27}{145}} G(2, 0, 6, 2, \rho) + \sqrt{\frac{16}{189}} G(2, 0, 6, 4, \rho) \right]$$

$$P(3d\delta, 3d\delta) = 2NR^4 \left[-\frac{5}{3} \exp(-\rho) + G(2,0,6,0,\rho) + \frac{2}{7} G(2,0,6,2,\rho) + \sqrt{\frac{36}{441}} G(2,0,6,4,\rho) \right]$$

$$P(3d\delta, 4f\delta) = 2NR^5 \left[-\frac{\sqrt{35}}{3} \exp(-\rho) + \sqrt{\frac{9}{35}} G(2,0,7,1,\rho) + \sqrt{\frac{16}{315}} G(2,0,7,3,\rho) + \sqrt{\frac{1000}{15,246}} G(2,0,7,5,\rho) \right]$$

$$P(4f\delta, 4f\delta) = 2NR^6 \left[-\frac{7}{3} \exp(-\rho) + G(2,0,8,0,\rho) + \frac{4}{15} G(2,0,8,2,\rho) + \sqrt{\frac{36}{1089}} G(2,0,8,4,\rho) + \sqrt{\frac{40,000}{736,164}} G(2,0,8,6,\rho) \right]$$

$$P(2p\pi, 2p\pi) = 2NR^2 \left[G(2,0,4,0,\rho) - \frac{1}{5} G(2,0,4,2,\rho) \right]$$

$$P(2p\pi, 3d\pi) = 2NR^3 \left[\sqrt{\frac{3}{15}} G(2,0,5,1,\rho) - \sqrt{\frac{9}{245}} G(2,0,5,3,\rho) \right]$$

$$P(2p\pi, 4f\pi) = 2NR^4 \left[\sqrt{\frac{18}{175}} G(2,0,6,2,\rho) - \sqrt{\frac{6}{189}} G(2,0,6,4,\rho) \right]$$

$$P(3d\pi, 3d\pi) = 2NR^4 \left[G(2,0,6,0,\rho) + \frac{1}{7} G(2,0,6,2,\rho) - \sqrt{\frac{16}{441}} G(2,0,6,4,\rho) \right]$$

$$P(3d\pi, 4f\pi) = 2NR^5 \left[\sqrt{\frac{8}{35}} G(2,0,7,1,\rho) + \sqrt{\frac{2}{315}} G(2,0,7,3,\rho) - \sqrt{\frac{5000}{15,246}} G(2,0,7,5,\rho) \right]$$

$$P(4f\pi, 4f\pi) = 2NR^6 \left[G(2,0,8,0,\rho) + \frac{1}{5} G(2,0,8,2,\rho) + \sqrt{\frac{1}{1089}} G(2,0,8,4,\rho) - \sqrt{\frac{22,500}{736,164}} G(2,0,8,6,\rho) \right]$$

N₂

R	log	1σμ	2σg	2σμ	3σg	1πμ	T
1.85							
A	.00577	-.00259	.67835	.62151	2.21187	-1.94934	1.56557
O	.007284	-.001301	.55766	-.01264	.36402	-.14164	.77338
S	.31576	.31468	.28097	.07953	.16833	.198334	1.35760
T	.32881	.31079	1.51698	.68840	2.72886	-1.89265	3.69655
1.95							
A	.00440	-.00284	.59816	.55888	2.18759	-1.91545	1.43074
O	.004282	.00020		-.00060	.33217	-.12176	.69946
S	.26966	.26879	.24537	.07927	.15154	.18194	1.19657
T	.278342	.26615	1.32870	.63755	2.65594	-1.85527	3.32677
2.0132							
A	.00168	-.00284	.55419	.533326	2.18105	-1.89403	1.37338
O	.00310	.000644	.44645	-.00378	.30341	-.11134	.63848
S	.24508	.24434	.22496	.075126	.14319	.171675	1.10438
T	.24986	.24214	1.22560	.60467	2.62765	-1.833695	3.11623
2.05							
A	.00333	-.00280	.52557	.51568	2.17161	-1.88919	1.32420
O	.002599	.00079	.420027	-.00317	.30687	-.10482	.62230
S	.23214	.23146	.21437	.07377	.13715	.16744	1.05633
T	.23807	.22945	1.15997	.58628	2.60027	-1.82657	3.00283
2.15							
A	-.00490	-.00263	.46509	.47172	2.16023	-1.86877	1.22074
O	.001769	.00096	.36277	-.00588	.28561	-.09141	.55382
S	.20134	.20076	.18847	.06961	.12454	.15442	.93914
T	.19821	.19909	1.01633	.53545	2.55502	-1.80576	2.71370
2.45							
A	-.00726	-.00231	.29711	.33424	2.13883	-1.83858	.92203
O	.00046	.00088	.23074	-.00757	.23835	-.06169	.40117
S	.13604	.13583	.12974	.06283	.09564	.12250	.68258
T	.12924	.13440	.65759	.38950	2.47282	-1.77777	2.00578

C-O

R	1σ	2σ	3σ	4σ	5σ	1π	T
1.898							
AT	.00000	.03719	.27026	.11076	1.12011	-.53908	.99924
OV	.00015	.00163	.42437	.13627	.20260	-.01978	.74524
PE	.58523	.00000	.44811	.25417	.09179	.36532	1.74462
T	.58538	.03882	1.14274	.50120	1.41450	-.19354	3.48910
2.081							
AT	.00000	.02364	.19413	.07010	1.12513	-.47172	.94128
OV	.00000	.00059	.30812	.09984	.19236	-.01157	.58945
PE	.44397	.00000	.38140	.18701	.09384	.31497	1.48116
T	.44408	.02423	.88365	.35695	1.41133	-.16832	2.95192
2.132							
AT	.00000	.02096	.17855	.05874	1.12410	-.45475	.92760
OV	.00010	.00047	.28202	.09093	.19161	-.01491	.55022
PE	.41285	.00000	.36169	.17151	.09651	.30533	1.34790
T	.41296	.02143	.82226	.32118	1.41222	-.16433	2.82572
2.366							
AT	.00000	.01090	.12814	.01992	1.13123	-.39320	.89699
OV	.00005	.00032	.19098	.05569	.18616	-.01133	.42187
PE	.30208	.00000	.27012	.10813	.10214	.25609	1.03856
T	.30213	.01122	.58924	.18374	1.41953	-.14844	2.35742
2.600							
AT	.00000	.00614	.08904	.00296	1.14173	-.34365	.89622
OV	.00003	.00027	.12515	.02864	.17718	-.00911	.32216
PE	.22763	.00000	.20925	.06125	.09797	.21674	.81284
T	.22766	.00641	.42344	.09285	1.41688	-.13602	2.03122

O-C

R	1σ	2σ	3σ	4σ	5σ	1π	T
1.898							
AT	.01199	.00003	.68206	4.99030	.63099	-4.94843	1.36694
OV	.00011	.00008	.40224	.40206	.02031	-.236657	.58814
PE	.00000	.58617	.10438	.05933	.13756	.07613	.96357
T	.01210	.58628	1.18868	5.45169	.78886	-5.10896	2.91865
2.081							
AT	.00470	.00001	.53480	4.37190	.99448	-4.99048	.91541
OV	.00020	.00000	.29510	.33450	.02040	-.18370	.46650
PE	.00000	.44447	.06529	.06375	.11590	.05876	.74817
T	.00490	.44448	.89519	4.77015	1.13078	-5.11542	2.13008
2.132							
AT	.00334	.00001	.49498	4.18161	1.12632	-5.02990	.77635
OV	.00026	.00001	.26884	.31276	.01868	-.159285	.44127
PE	.00000	.41328	.05800	.06401	.11013	.05659	.70201
T	.0036	.41330	.82182	4.55838	1.25513	-5.13259	1.91964
2.366							
AT	.00069	.00000	.31820	3.19216	1.82472	-5.13071	.21127
OV	.00033	.00005	.18020	.23270	.035530	-.111583	.33723
PE	.00000	.30225	.03916	.07191	.08436	.04261	.54029
T	.00102	.30230	.53756	3.49676	1.94461	-5.19968	1.08257
2.600							
AT	-.00046	.00000	.19666	2.12349	2.54231	-5.26210	-.40010
OV	.00020	.00004	.11666	.16040	.07985	-.078643	.27851
PE	.00000	.22772	.02489	.08237	.06282	.3221	.43001
T	-.00026	.22776	.33821	2.36626	2.68498	-5.30853	.30842

B-F

R	1σ	2σ	3σ	4σ	5σ	1π	τ
2.00							
AT	.00000	.02889	.04017	.08474	.33030	-.08094	.40316
OV	.00010	.00567	.16804	.16061	.05529	-.005796	.38391
PE	.50005	.00004	.48558	.42260	.04136	.54298	1.99261
T	.50015	.03460	.69379	.66795	.42695	.45625	2.77969
2.354							
AT	.00000	.01290	.01753	.07046	.29180	-.04323	.34946
OV	-.00002	.00033	.07296	.12647	.03799	-.00187	.23586
PE	.30667	.00000	.32331	.27096	.03924	.39191	1.33209
T	.30665	.01323	.41380	.46789	.36903	.34681	1.91741
2.391							
AT	.00000	.01230	.01628	.06918	.28726	-.04100	.34402
OV	-.00018	.000123	.06802	.12386	.03603	-.000701	.22715
PE	.29265	.00000	.30815	.25791	.03956	.37925	1.27752
T	.29247	.01242	.39245	.45095	.36285	.33755	1.84869
2.770							
AT	.00000	.00614	.00792	.05302	.23258	-.02316	.27650
OV	.00002	-.00021	.03038	.09294	.02091	.002183	.14622
PE	.18822	.00000	.19506	.15629	.03797	.27169	.84923
T	.18824	.00593	.23336	.30225	.29146	.25071	1.27195
3.155							
AT	.00000	.00275	.00380	.03244	.18165	-.01335	.20729
OV	.00001	-.00034	.01304	.06390	.01343	.001801	.09184
PE	.12738	.00000	.13062	.09467	.04023	.19823	.59113
T	.12739	.00241	.14746	.19101	.23531	.18668	.89026

F-B

R	F-B						
2.00	1σ	2σ	3σ	4σ	5σ	1π	T
AT	.00095	.00037	.41203	10.06539	.23265	-10.14885	.56254
OV	.00028	.00179	.15164	.35837	-.00497	-.09525	.41186
PE	.00000	.50060	.02219	.02583	.08158	.01151	.64171
T	.00123	.50276	.58586	10.44959	.30926	-10.23259	1.61611
2.354							
AT	-.00081	.00005	.23046	9.15162	.51410	-10.34680	-.45138
OV	.00025	.00003	.07106	.28871	-.03420	-.04579	.28006
PE	.00000	.30724	.00673	.02235	.07231	.00536	.41399
T	-.00056	.30732	.30825	9.46268	.55221	-10.38723	.24267
2.391							
AT	-.00081	.00004	.21346	9.06558	.55476	-10.35879	-.52576
OV	.000232	-.00002	.06695	.28602	-.03793	-.04591	.269342
PE	.00000	.29320	.00619	.02275	.07141	.00507	.39862
T	-.00058	.29322	.28660	9.37435	.58824	-10.39963	.14220
2.770							
AT	-.00085	.00001	.09893	8.10835	1.09868	-10.51326	-1.20814
OV	.00011	-.00008	.03434	.24596	-.05220	-.03091	.19722
PE	.00000	.18847	.00261	.02641	.05949	.00259	.27957
T	-.00074	.18840	.13588	8.38072	1.10597	-10.54158	-.73135
3.155							
AT	-.00069	.00000	.04873	6.90604	2.09124	-10.60188	-1.55656
OV	.00007	-.00004	.01608	.18842	-.05262	-.01909	.13282
PE	.00000	.12749	.00101	.02817	.04586	.00129	.20382
T	-.00062	.12745	.06582	7.12263	2.08448	-10.61968	-1.21992

		BeO					
R		1 σ	2 σ	3 σ	4 σ	1 π	T
1.80							
AT	.00000	.03723	.05471	.12300	-.099820	.11512	
OV	-.00050	.05952	.09063	.20360	-.02202	.33123	
PE	.68664	.00385	.59959	.54488	.384999	2.21995	
T	.68614	.10060	.74493	.87148	.26315	2.66630	
2.100							
AT	.00000	.01030	.03190	.07721	-.079929	.03948	
OV	-.00009	.2167	.07847	.12920	-.01668	.21257	
PE	.43215	.00082	.41871	.34399	.312843	1.50851	
T	.43206	.03279	.52908	.55040	.21623	1.76056	
2.3500							
AT	.00000	.00372	.02025	.05877	-.068280	.01446	
OV	-.00001	.00908	.06097	.09165	-.00955	.15214	
PE	.30832	.00018	.30456	.24188	.261974	1.11691	
T	.30831	.01298	.38578	.39230	.18414	1.28351	
2.4377							
AT	.00000	.00262	.01714	.05384	-.064507	.00909	
OV	-.00001	.00669	.05548	.08750	-.00751	.14215	
PE	.27622	.00011	.27343	.21504	.246391	1.01119	
T	.27621	.00942	.34605	.35638	.17437	1.16243	
2.500							
AT	.00000	.00203	.01518	.05060	-.061847	.005963	
OV	-.00000	.00536	.05131	.08353	-.00621	.13399	
PE	.25607	.00007	.25371	.19802	.236033	.943903	
T	.25607	.00746	.32020	.33215	.167976	1.083856	
2.750							
AT	.00000	.00067	.00907	.03889	-.050864	-.00223	
OV	.00000	.00213	.03584	.06994	-.00224	.10567	
PE	.19238	.00001	.19077	.14200	.200300	.72546	
T	.19238	.00281	.23568	.25083	.14720	.82890	
3.100							
AT	.00000	-.00017	.00382	.02164	-.030587	-.00530	
OV	.00000	.00051	.01924	.04986	.00092	.07053	
PE	.13429	.00000	.13312	.08070	.164146	.51226	
T	.13429	.00034	.15618	.15220	.13448	.57749	

		OBe					
R		1 σ	2 σ	3 σ	4 σ	1 π	T
1.800							
AT	.00406	.01242	.28275	7.22842	-4.878916	2.64873	
OV	-.00090	.05697	.00094	.26175	-.22665	.09211	
PE	.00000	.64604	.03803	.04500	.014456	.74353	
T	.00316	.71543	.32172	7.53517	-5.09111	3.48437	
2.100							
AT	.00203	.00264	.21774	6.54814	-4.950153	1.82040	
OV	-.00018	.01414	.04843	.26334	-.12802	.19771	
PE	.00000	.41909	.01411	.02253	.014138	.46987	
T	.00185	.43587	.28028	6.83401	-5.06404	2.48798	
2.350							
AT	.00107	.00070	.14344	6.04728	-5.04021	1.15228	
OV	.00002	.00409	.04895	.24600	-.08849	.21057	
PE	.00000	.30322	.00753	.01910	.012094	.341944	
T	.00109	.30801	.19992	6.31238	-5.11661	1.70479	
2.4377							
AT	.00088	.00044	.12087	5.87420	-5.081354	.91504	
OV	.00005	.00266	.04660	.24111	-.07887	.21155	
PE	.00000	.27244	.00626	.01896	.011320	.30898	
T	.00093	.27554	.17373	6.13427	-5.14890	1.43557	
2.500							
AT	.00073	.00032	.10628	5.74901	-5.114242	.742098	
OV	.00006	.00196	.04458	.23793	-.07284	.21169	
PE	.00000	.25299	.00553	.01903	.010765	.288315	
T	.00079	.25527	.15639	6.00597	-5.176317	1.242103	
2.7500							
AT	.00028	.00009	.06051	5.19312	-5.290694	-.03669	
OV	.00008	.00056	.03390	.21661	-.05342	.19773	
PE	.00000	.19087	.00343	.02036	.008501	.22316	
T	.00036	.19152	.09784	5.43009	-5.33561	.38420	
3.100							
AT	-.00042	.00001	.02475	4.06049	-5.675925	-1.59110	
OV	.00007	.00008	.02025	.18625	-.03045	.17620	
PE	.00000	.13363	.00167	.02619	.004820	.16631	
T	-.00035	.13372	.04667	4.27293	-5.70156	-1.24859	

		LiF					
R		1σ	2σ	3σ	4σ	1π	T
2.45							
	AT	.00000	-.00148	-.00403	.00551	-.00244	-.00244
	OV	.00001	.02847	-.00400	.01014	.01181	.04643
	PE	.27201	.00288	.26468	.32884	.34376	1.21217
	T	.27202	.02987	.25665	.34449	.35313	1.25616
2.65							
	AT	.00000	-.00575	-.00223	.00569	-.00216	-.00445
	OV	.00000	.014706	.00241	.01579	.01145	.04436
	PE	.21495	.00109	.21290	.26494	.28680	.98068
	T	.21495	.01005	.21308	.28642	.29609	1.02059
2.7877							
	AT	.00000	-.00735	-.00146	.00568	-.00193	-.00506
	OV	.00000	.00945	.00401	.01752	.01076	.04174
	PE	.18465	.00057	.18415	.22176	.25457	.84570
	T	.18465	.00267	.18670	.24496	.26340	.88238
2.8877							
	AT	.00000	-.00810	-.00106	.00562	-.00176	-.00529
	OV	.00000	.00691	.00439	.01804	.01014	.03948
	PE	.16612	.00036	.16623	.19910	.23407	.96588
	T	.16612	-.00083	.16956	.22276	.24245	.80006
2.9877							
	AT	.00000	-.00849	-.00076	.00552	-.00160	-.00533
	OV	.00000	.00509	.00439	.01814	.00948	.03710
	PE	.14999	.00023	.15045	.17937	.21568	.69572
	T	.14999	-.00317	.15408	.20303	.22356	.72749
3.20							
	AT	.00000	-.00872	-.00035	.00524	-.00129	-.00512
	OV	.00000	.00274	.00378	.01734	.00803	.03189
	PE	.12208	.00009	.12281	.14518	.18245	.57261
	T	.12208	-.00589	.12624	.16776	.18919	.59938
3.55							
	AT	.00000	-.00807	-.00004	.00466	-.00089	-.00434
	OV	.00000	.00107	.00241	.01457	.00590	.02395
	PE	.08941	.00002	.09010	.10516	.14080	.42549
	T	.08941	-.00698	.09247	.12439	.14581	.44510

R	FLi					
	1 σ	2 σ	3 σ	4 σ	1 π	T
2.45						
AT	.00052	.01952	.02823	10.98191	-9.99868	1.03150
OV	.00002	.01883	-.00212	.05268	-.09123	-.02182
PE	.00000	.26033	.00627	.01023	-.00035	.27648
T	.00054	.29868	.03238	11.04482	-10.09026	1.28616
2.65						
AT	.00027	.00882	.02448	10.73317	-10.06150	.70524
OV	.00002	.00866	.00440	.06375	-.08713	-.01030
PE	.00000	.20880	.00276	.00577	-.00027	.21706
T	.00029	.22628	.03164	10.80269	-10.14890	.91200
2.7877						
AT	.00018	.00514	.02115	10.56170	-10.10407	.48410
OV	.00002	.00511	.00583	.06553	-.08193	-.00544
PE	.00000	.18052	.00160	.00409	-.00020	.18601
T	.00020	.19077	.02858	10.63132	-10.18620	.66467
2.8877						
AT	.00010	.00348	.01878	10.46209	-10.13342	.35103
OV	.00002	.00350	.00606	.06509	-.07762	-.00295
PE	.00000	.16296	.00110	.00327	-.00015	.16733
T	.00012	.16994	.02594	10.53045	-10.21104	.51541
2.9877						
AT	.00010	.00238	.01664	10.37268	-10.16122	.23058
OV	.00002	.00242	.00590	.06373	-.07316	-.00109
PE	.00000	.14753	.00076	.00268	-.00010	.15087
T	.00012	.15233	.02330	10.43909	-10.23448	.38036
3.20						
AT	.00002	.00107	.01287	10.21448	-10.21375	.01469
OV	.00001	.00112	.00498	.05906	-.06361	.00156
PE	.00000	.12057	.00037	.00190	-.00002	.12282
T	.00003	.12276	.01822	10.27544	-10.27738	.13907
3.55						
AT	-.00007	.00031	.00873	10.02966	-10.28036	-.24173
OV	.00001	.00034	.00321	.04951	.04934	.00373
PE	.00000	.08867	.00013	.00129	.00007	.09016
T	-.00006	.08932	.01207	10.08046	-10.32963	-.14784

APPENDIX 3

Forces

The forces reported in this section have been calculated using formulae presented in a thesis by W. H. Henneker.⁽²⁵²⁾ The overlap forces have been calculated by the Coulson-Barnett method described in Appendix 2 for the field gradients. Shielding forces follow from the auxiliary function method of Kotani et al.⁽²⁵³⁾

N₂

R	1 σ _g	1 σ _u	2 σ _g	2 σ _u	3 σ _g	1 π	T
1.850							
AT	.037350	.018216	-.079534	-.150992	-.414776	.111884	-.477852
OV	.005035	.003124	.534063	-.069377	.288052	.271680	1.032577
PE	.291944	.291097	.255011	.114989	.183027	.290918	1.426986
T	.334329	.312437	.709540	-.105380	.056303	.674482	1.981711
1.950							
AT	.036504	.017253	-.042610	-.181492	-.410143	.104709	-.475779
OV	.003094	.003475	.484924	-.044783	.282629	.245868	.975207
PE	.262819	.262086	.231090	.117978	.172504	.272441	1.318888
T	.302417	.282814	.673404	-.108297	.044990	.623018	1.818346
2.050							
AT	.035485	.017262	-.015683	-.180705	-.403498	.097697	-.449442
OV	.002015	.003248	.439470	-.040418	.277308	.222529	.904152
PE	.237870	.237253	.209893	.112464	.162669	.255906	1.216055
T	.275370	.257763	.633680	-.108659	.036479	.576132	1.670765
2.150							
AT	.033626	.017857	.010037	-.180529	-.391262	.091618	-.418653
OV	.001330	.002825	.393093	-.035318	.268151	.202170	.832251
PE	.216377	.215819	.191443	.108481	.152986	.240769	1.125875
T	.251333	.236501	.594573	-.107366	.029875	.534557	1.539473
2.450							
AT	.036186	.017919	.050418	-.177236	-.354100	.075449	-.351364
OV	.000509	.001828	.278800	-.025087	.247723	.151414	.655187
PE	.166609	.166378	.148167	.102198	.128712	.203239	.915303
T	.203304	.186125	.477385	-.100125	.022335	.430102	1.219126
2.0132							
AT	.03574	.01722	-.02566	-.17904	-.41998	.10058	-.47114
OV	.00235	.00338	.456781	-.04297	.290942	.230841	.94132
PE	.24662	.245960	.21732	.11366	.16850	.261355	1.25342
T	.28471	.26656	.64844	-.108349	.03946	.59278	1.72360
2.068							
AT	.03551	.01726	-.00993	-.18132	-.41304	.09717	-.45435
OV	.00187	.00319	.43066	-.03896	.28540	.21874	.90090
PE	.23375	.23316	.20632	.11202	.16277	.25291	1.20093
T	.27113	.25361	.62705	-.10826	.03513	.56882	1.64748

N₂

R	N ₂						
1.650	1 σ_g	1 σ_u	2 σ_g	2 σ_u	3 σ_g	ln	T
AT	.050698	.020415	-.189715	-.087665	-.467176	.128164	-.545279
OV	.012377	.002202	.644713	-.128814	.337852	.334199	1.202529
PE	.366346	.365249	.313540	.117883	.215652	.335348	1.714018
T	.429421	.387866	.768538	-.098596	.086328	.797711	2.371268
1.905							
AT	.036996	.017283	-.057838	-.177658	-.414192	.107913	-.487496
OV	.003760	.003539	.506872	-.049238	.286398	.257124	1.008455
PE	.275344	.274534	.241481	.119221	.177409	.280514	1.368503
T	.316100	.295356	.690515	-.107675	.049615	.645551	1.889462
2.110							
AT	.035249	.017387	.001613	-.183954	-.393736	.094200	-.429241
OV	.001575	.003027	.410083	-.035559	.269634	.210246	.859006
PE	.224565	.224028	.198637	.111455	.156422	.246651	1.161758
T	.261389	.244442	.610333	-.108058	.032320	.551097	1.591523
2.200							
AT	.035302	.017531	.019394	-.184266	-.385140	.088831	-.408348
OV	.001116	.002732	.371853	-.031274	.264318	.192731	.801476
PE	.206592	.206152	.183063	.108739	.148482	.233836	1.086864
T	.243010	.226415	.574310	-.106801	.027660	.515398	1.479992
2.239							
AT	.035446	.017609	.025737	-.183971	-.381362	.086614	-.399927
OV	.000685	.002588	.356248	-.029759	.262278	.185606	.777646
PE	.199462	.199063	.176848	.107688	.145238	.228620	1.056919
T	.235593	.219260	.558833	-.106042	.026154	.500840	1.434638

CO

R	CO						
1.80	1σ	2σ	3σ	4σ	5σ	1π	T
AT	.000002	.075374	-.266645	-.107668	-.568997	.057851	-.810083
OV	-.000304	.004026	.402504	.131379	.196442	.247563	.981610
PE	.617881	.000014	.550259	.347211	.113560	.551420	2.180345
T	.617579	.079414	.686118	.370922	-.258995	.856834	2.351872
1.898							
AT	.000000	.065017	-.207998	-.080372	-.552780	.054593	-.721540
OV	-.000119	.003234	.355696	.116338	.186926	.220886	.882961
PE	.555520	.000009	.502397	.308447	.113704	.520797	2.000874
T	.555401	.068260	.650095	.344413	-.252150	.796276	2.162295
2.015							
AT	.000000	.058987	-.152125	-.054049	-.533634	.050924	-.629897
OV	-.000023	.002518	.306645	.101099	.178593	.192480	.781312
PE	.492788	.000006	.449043	.265775	.115179	.487453	1.810244
T	.492765	.061511	.603563	.312825	-.239862	.730857	1.961659
2.132							
AT	.000000	.056576	-.108845	-.033517	-.513547	.047496	-.552837
OV	.000013	.001962	.263629	.087139	.173383	.167729	.693855
PE	.440131	.000004	.401221	.225901	.117999	.457196	1.642432
T	.440144	.058578	.556005	.279523	-.222165	.672421	1.784470
2.249							
AT	.000000	.056497	-.075804	-.018599	-.491212	.044214	-.484904
OV	.000023	.001557	.225676	.073668	.170926	.146133	.617983
PE	.395493	.000003	.359344	.188721	.121836	.429702	1.495099
T	.395516	.058057	.509216	.243790	-.198450	.620049	1.628178
2.366							
AT	.000000	.057093	-.050785	-.009646	-.465178	.041011	-.427505
OV	.000023	.001233	.192123	.060336	.170698	.127259	.551672
PE	.357343	.000002	.323155	.154299	.125867	.404639	1.365305
T	.357366	.058328	.464493	.204989	-.168613	.572909	1.489472
2.483							
AT	.000000	.057891	-.032182	-.006876	-.434782	.037901	-.378048
OV	.000021	.000993	.162567	.047436	.171748	.110757	.493522
PE	.324455	.000002	.292109	.123241	.128976	.381782	1.250565
T	.324476	.058886	.422494	.163801	-.134058	.530440	1.366039

OC

R	OC						
1.80	1σ	2σ	3σ	4σ	5σ	1π	T
AT	.077040	-.000075	.183871	-.721338	.131129	.151802	-.177571
OV	-.001660	.001362	.382745	.315304	-.154081	.242386	.786056
PE	.000003	.617029	.076763	.048827	.288465	.112691	1.143778
T	.075383	.618316	.643379	-.357207	.265513	.506879	1.752263
1.898							
AT	.073015	-.000032	.202450	-.689604	.132952	.144331	-.136888
OV	-.000802	.000958	.342318	.295715	-.147401	.218148	.708936
PE	.000001	.554969	.064982	.052559	.265795	.103581	1.041887
T	.072214	.555895	.609750	-.341330	.251346	.466060	1.613935
2.015							
AT	.070353	-.000011	.211361	-.653116	.128193	.136501	-.106719
OV	-.000252	.000646	.298503	.276350	-.134690	.191982	.632539
PE	.000000	.492440	.054614	.060410	.239034	.093237	.939735
T	.070101	.493075	.564478	-.316356	.232537	.421720	1.465555
2.132							
AT	.070101	-.000003	.210176	-.612895	.115299	.129660	-.087662
OV	.000014	.000442	.259093	.256807	-.116203	.168876	.569029
PE	.000000	.439913	.046852	.071231	.212440	.084023	.854459
T	.070105	.440352	.516121	-.284857	.211536	.382559	1.335816
2.249							
AT	.070136	.000000	.202351	-.566397	.093543	.123448	-.076919
OV	.000124	.000312	.223694	.234534	-.091702	.148390	.515352
PE	.000000	.395372	.040713	.084333	.186092	.075804	.782314
T	.070260	.395684	.466758	-.247530	.187933	.347642	1.220747
2.366							
AT	.070600	.000001	.189908	-.511998	.062543	.117639	-.071307
OV	.000165	.000221	.192076	.208101	-.061048	.130188	.469703
PE	.000000	.357267	.035609	.098699	.160454	.068381	.720410
T	.070765	.357489	.417593	-.205198	.161949	.316208	1.118806
2.483							
AT	.071305	.000001	.174524	-.450879	.023880	.112008	-.069161
OV	.000180	.000160	.164017	.177903	-.025547	.114004	.430717
PE	.000000	.324408	.031187	.113008	.136532	.061675	.666810
T	.071485	.324569	.369728	-.159968	.134865	.287687	1.028366

BF

R	BF						
2.0	1σ	2σ	3σ	4σ	5σ	1π	T
AT	.000001	.068541	-.095057	-.138501	-.253525	.015856	-.402685
OV	.000143	.009265	.119024	.134554	.017338	.114133	.394457
PE	.499966	.000075	.513803	.423149	.055724	.688490	2.181207
T	.500110	.077881	.537770	.419202	-.180463	.818479	2.172979
2.10							
AT	.000001	.062929	-.069522	-.113986	-.249501	.014311	-.355768
OV	.000113	.006864	.106068	.133213	.013176	.097543	.356977
PE	.453481	.000046	.462566	.381937	.054271	.645498	1.997799
T	.453595	.069839	.499112	.401164	-.182054	.757352	1.999008
2.1925							
AT	.000001	.059988	-.051602	-.094528	-.245387	.012957	-.318571
OV	.000091	.005146	.094419	.131846	.009590	.084167	.325259
PE	.416034	.000029	.421277	.347897	.052951	.608879	1.847067
T	.416126	.065163	.464094	.385215	-.182846	.706003	1.853755
2.391							
AT	.000001	.058765	-.026409	-.060663	-.235782	.010350	-.253738
OV	.000058	.002779	.071284	.127153	.002642	.061027	.264943
PE	.349831	.000011	.349596	.286216	.050919	.539105	1.575678
T	.349890	.061555	.394471	.352706	-.182221	.610482	1.586883
2.5775							
AT	.000001	.060003	-.013429	-.036163	-.225998	.008292	-.207294
OV	.000039	.001602	.053044	.120222	-.002898	.044941	.216950
PE	.301045	.000005	.298527	.239495	.050420	.482645	1.372137
T	.301085	.061610	.338142	.323554	-.178476	.535878	1.381793
2.770							
AT	.000000	.061440	-.006256	-.016438	-.215075	.006558	-.169771
OV	.000026	.000971	.038257	.110970	-.007433	.032747	.175538
PE	.260655	.000003	.257455	.199509	.051494	.431981	1.201097
T	.260681	.062414	.289456	.294041	-.171014	.471286	1.206864
2.9625							
AT	.000000	.061823	-.002581	-.001303	-.203348	.005175	-.140234
OV	.000018	.000623	.027239	.100295	-.010508	.023913	.141580
PE	.227883	.000001	.224789	.165222	.054373	.387900	1.060168
T	.227901	.062447	.249447	.264214	-.159483	.416988	1.061514

FB

R	FB						
2.00	1 σ	2 σ	3 σ	4 σ	5 σ	1 π	T
AT	.058877	-.000025	.242137	-.611168	.099279	.137498	-.073402
OV	.000721	.003031	.147092	.356710	-.114544	.110920	.503930
PE	.000001	.498451	.017221	.029320	.200499	.021022	.766514
T	.059599	.501457	.406450	-.225138	.185234	.269440	1.197042
2.10							
AT	.057638	.000004	.225465	-.578879	.106285	.129326	-.060160
OV	.000653	.001995	.132817	.345367	-.120844	.096808	.456796
PE	.000001	.452546	.013808	.028873	.192836	.017948	.706012
T	.058293	.454545	.372090	-.204639	.178277	.244082	1.102648
2.1925							
AT	.058106	.000013	.208876	-.550540	.111100	.122705	-.049740
OV	.000593	.001350	.119678	.335675	-.124560	.085141	.417877
PE	.000001	.415456	.011453	.029249	.185582	.015457	.657198
T	.05870	.416819	.340007	-.185616	.172122	.223303	1.025335
2.39							
AT	.056463	.000011	.173376	-.490869	.117487	.110516	-.033016
OV	.000467	.000599	.093168	.313602	-.128025	.064152	.343963
PE	.000001	.349694	.007903	.031359	.170041	.011151	.570149
T	.056931	.350304	.274447	-.145908	.159503	.185819	.881096
2.5775							
AT	.054256	.000008	.142674	-.436778	.119966	.100569	-.019305
OV	.000362	.000295	.071885	.290785	-.127423	.048754	.284658
PE	.000000	.301065	.005643	.034074	.155710	.008185	.504677
T	.054618	.301368	.220202	-.111919	.148253	.157508	.770030
2.770							
AT	.051340	.000005	.115166	-.384782	.119597	.091081	-.007593
OV	.000275	.000155	.054169	.266248	-.123590	.036484	.233741
PE	.000000	.260741	.003973	.037355	.140936	.005967	.448972
T	.051615	.260901	.173308	-.081179	.136943	.133532	.675120
2.9625							
AT	.047835	.000003	.092374	-.337559	.115899	.082165	.000717
OV	.000210	.000088	.040494	.241673	-.116422	.027192	.193235
PE	.000000	.227977	.002779	.041410	.125692	.004380	.402238
T	.048045	.228068	.135647	-.054476	.125169	.113737	.596190

R	BeO					
	1 σ	2 σ	3 σ	4 σ	1 π	T
1.800						
AT	.000003	-.069743	-.215726	-.296472	.029274	-.552664
OV	-.000420	.068801	.029883	.110946	.202829	.412039
PE	.617869	.003754	.612823	.536176	.532965	2.303587
T	.617452	.002812	.426980	.350650	.765068	2.162962
2.100						
AT	.000000	-.116052	-.107298	-.156163	.017159	-.362354
OV	-.000092	.029539	.055436	.095419	.136680	.316982
PE	.453710	.000830	.458510	.379685	.466331	1.759066
T	.453618	-.085683	.406648	.318941	.620170	1.713694
2.35						
AT	.000000	-.123410	-.057072	-.096924	.013106	-.264300
OV	-.000016	.012709	.056720	.092940	.103314	.265667
PE	.362239	.000186	.360603	.291820	.412167	1.427015
T	.362223	-.110515	.360251	.287836	.528587	1.428382
2.4377						
AT	.000000	-.123543	-.045348	-.082057	.012148	-.238800
OV	-.000007	.009279	.054073	.091874	.094056	.249275
PE	.336634	.000108	.333516	.267251	.394955	1.332464
T	.336627	-.114155	.342241	.277068	.501159	1.342939
2.500						
AT	.000000	-.123038	-.038395	-.072748	.011550	-.222631
OV	-.000002	.007381	.051637	.090969	.088027	.238012
PE	.320059	.000073	.316189	.251242	.383396	1.270959
T	.320057	-.115584	.329431	.269463	.482973	1.286340
2.75						
AT	.000000	-.117818	-.019212	-.042602	.009510	-.170122
OV	.000004	.002836	.039809	.085881	.067084	.195614
PE	.264503	.000015	.259488	.195239	.343041	1.062286
T	.264507	-.114967	.280085	.238518	.419635	1.087778
3.100						
AT	.000000	-.100226	-.006508	-.012160	.006728	-.112166
OV	.000005	.000621	.023710	.071365	.041828	.137529
PE	.208142	.000001	.204032	.124166	.303495	.839836
T	.208147	-.099604	.221234	.183371	.352051	.865199

R	OBe					
	1σ	2σ	3σ	4σ	1π	T
1.800						
AT	.039808	.000656	.194127	-.453507	.075246	-.143670
OV	-.001450	.039364	.032789	.232669	.172546	.475918
PE	.000005	.582245	.040222	.050778	.058999	.732249
T	.038363	.622265	.267138	-.170060	.306791	1.064497
2.100						
AT	.041386	.000433	.179699	-.473631	.085629	-.166484
OV	-.000385	.012098	.074021	.278210	.126734	.490678
PE	.000001	.441242	.016832	.027924	.041020	.527019
T	.041002	.453773	.270552	-.167497	.253383	.851213
2.35						
AT	.047463	.000107	.151296	-.461055	.085216	-.176973
OV	-.000036	.004047	.074910	.288371	.099222	.466514
PE	.000000	.357195	.009518	.025692	.032565	.424970
T	.047427	.361349	.235724	-.746992	.217003	.714511
2.4377						
AT	.049732	.000062	.140905	-.451042	.084195	-.176148
OV	.000017	.002718	.071403	.287202	.091149	.452489
PE	.000000	.332871	.008021	.026228	.030159	.397279
T	.049749	.335651	.220329	-.137612	.205503	.673620
2.500						
AT	.051176	.000042	.133609	-.442805	.083305	-.174673
OV	.000048	.002041	.068273	.285485	.085805	.441652
PE	.000000	.316977	.007141	.026861	.028549	.379528
T	.051224	.319060	.209023	-.130459	.197659	.646507
2.75						
AT	.056461	.000008	.105044	-.406727	.078756	-.166458
OV	.000089	.000629	.053429	.275399	.066781	.396327
PE	.000000	.262967	.004571	.031413	.022433	.321384
T	.056550	.263604	.163044	-.099915	.167970	.551253
3.100						
AT	.057733	.000000	.068648	-.359378	.069763	-.163234
OV	.000096	.000101	.033291	.260694	.042963	.337145
PE	.000000	.207439	.002360	.047458	.012640	.269897
T	.057829	.207540	.104299	-.051226	.125366	.443808

R	LiF					
	1 σ	2 σ	3 σ	4 σ	1 π	T
2.45						
AT	.000000	-.048161	-.025944	-.070690	.002182	-.142613
OV	.000006	.033916	-.008523	-.015341	.040179	.050237
PE	.333205	.003038	.325624	.376621	.510142	1.548630
T	.333211	-.011207	.291157	.290590	.552503	1.456254
2.65						
AT	.000000	-.050873	-.015537	-.050908	.002331	-.114987
OV	.000005	.018360	.000896	.000896	.035819	.055976
PE	.284806	.001243	.281188	.317193	.447378	1.331808
T	.284811	-.031270	.266547	.267181	.485528	1.272797
2.7877						
AT	.000000	-.050836	-.010922	-.041221	.002328	-.100651
OV	.000004	.012206	.003666	.007858	.032496	.056230
PE	.257365	.000678	.255175	.284214	.411159	1.208591
T	.257369	-.037952	.247919	.250851	.445983	1.164170
2.8877						
AT	.000000	-.050165	-.008467	-.035568	.002286	-.091914
OV	.000003	.009159	.004592	.0011377	.030077	.055208
PE	.239851	.000440	.238327	.263412	.387715	1.129745
T	.239854	-.040566	.234452	.239221	.420078	1.093039
2.9877						
AT	.000000	-.049156	-.006572	-.030800	.002223	-.084305
OV	.000002	.006935	.004950	.013901	.027723	.053511
PE	.224065	.000287	.223029	.244825	.366316	1.058522
T	.224067	-.041934	.221407	.227926	.396262	1.027728
3.20						
AT	.000000	-.046220	-.003858	-.022908	.002044	-.070942
OV	.000001	.003947	.004687	.016837	.023086	.048558
PE	.195321	.000119	.194911	.211353	.326532	.928236
T	.195322	-.042154	.195740	.205282	.351662	.905852
3.55						
AT	.000000	-.040395	-.001624	-.014252	.001719	-.054552
OV	.000001	.001677	.003312	.017302	.016823	.039115
PE	.158703	.000030	.158745	.169431	.273809	.760718
T	.158704	-.038688	.160433	.172481	.292351	.745281

R	FLi					
	1 σ	2 σ	3 σ	4 σ	1 π	T
2.45						
AT	.014176	.003171	.065850	-.155303	.075399	.003293
OV	.000037	.017097	.010958	.086243	.024018	.138353
PE	.000000	.320288	.008392	.014498	.002513	.345691
T	.014213	.340556	.085200	-.054562	.101930	.487337
2.65						
AT	.018598	.001724	.062892	-.149667	.061366	-.005087
OV	.000039	.008266	.014663	.091634	.022567	.137169
PE	.000000	.277752	.003984	.008718	.002448	.292902
T	.018637	.287742	.081539	-.049315	.086381	.424984
2.7877						
AT	.021042	.001110	.059091	-.142699	.053919	-.007537
OV	.000034	.005066	.014528	.091554	.021401	.132583
PE	.000000	.252530	.002426	.006412	.002338	.263706
T	.021076	.258706	.076045	-.044733	.077658	.388752
2.8877						
AT	.022112	.000810	.056067	-.136798	.049441	-.008368
OV	.000031	.003578	.013770	.090297	.020510	.128186
PE	.000000	.236100	.001714	.005258	.002238	.245310
T	.022143	.240488	.071551	-.041243	.072189	.365128
2.9877						
AT	.022049	.000585	.052774	-.130552	.045590	-.009554
OV	.000028	.002547	.012737	.088350	.019604	.123266
PE	.000000	.221108	.001224	.004404	.002128	.228864
T	.022077	.224240	.066735	-.037798	.067322	.342576
3.20						
AT	.023024	.000295	.045982	-.117112	.039070	-.008741
OV	.000018	.001269	.010261	.082750	.017681	.111979
PE	.000000	.193454	.000626	.003246	.001880	.199206
T	.023042	.195018	.056869	-.031116	.058631	.302444
3.55						
AT	.022419	.000096	.036460	-.096454	.031768	-.005711
OV	.000010	.000434	.006666	.071598	.014715	.093423
PE	.000000	.157732	.000240	.002336	.001492	.161800
T	.022430	.158260	.043366	-.022520	.047975	.249511

APPENDIX 4

In this section we present the orbital densities $\rho(A)$ at nucleus A, and also the total atomic, overlap and shielding values. Furthermore, listed are the coefficients F_1, F_2, F_3, F_4 obtained from a parametric polynomial fit for the electronic forces F_A , using the expression:

$$F_A = \sum_{n=1}^5 F_n^A \left(\frac{R-R_e}{R_e} \right)^{n-1} \quad A(4.1)$$

The factors F_1, F_2, F_3, F_4 are then obtained from the F_n^A 's by multiplication of these with R_e^n corresponding to the simpler expansion

$$F_A = \sum_{n=1}^5 F_n (R-R_e)^{n-1} \quad A(4.2)$$

$$N_2 \quad R_e = 2.068$$

	F_1	F_2	F_3	F_4	$\rho(A)$
log	0.27034	-0.23854	0.21583	-0.19840	98.20623
lou	0.25356	-0.22612	0.17636	-0.12142	98.31037
2og	0.62707	-0.39898	-0.03594	0.20472	4.68913
2ou	-0.10823	0.00443	0.05482	-0.02916	3.91519
3og	0.03512	-0.07089	0.11025	-0.03192	0.47054
1 π u	0.56871	-0.43135	0.22062	-0.12274	
Total	1.64657	-1.36145	0.74194	-0.29392	205.59145
A	-0.44977	0.27319	0.55584	-0.43237	205.91189
O	0.89630	-0.71083	-0.28559	0.40096	-0.33221
S	1.20165	-0.93064	0.42349	-0.21818	0.01177
Total	1.64818	-1.36828	0.69374	-0.24959	205.59145

C-O $R_e = 2.132$

	F_1	F_2	F_3	F_4	ρ (A)
1 σ	0.44014	-0.41280	0.29036	-0.19076	0.00000
2 σ	0.05866	-0.01234	0.07497	-0.16845	121.83605
3 σ	0.55598	-0.40570	0.03303	0.16876	1.37676
4 σ	0.27956	-0.29407	-0.09662	-0.06968	1.87429
5 σ	-0.22221	0.17713	0.22575	0.02084	1.98562
1 π	0.67241	-0.47269	0.22236	-0.08147	
Total	1.78454	-1.42047	0.74985	-0.32076	127.07272
A	-0.55179	0.61689	-0.41251	0.20419	127.27500
O	0.69387	-0.69449	0.41959	-0.24595	-0.22203
S	1.64249	-1.34298	0.74124	-0.27681	0.02019
Total	1.78457	-1.42058	0.74832	-0.31857	127.07272

	O-C				
	F ₁	F ₂	F ₃	F ₄	ρ (Å)
1 σ	0.06996	0.00144	0.02477	-0.07119	296.52552
2 σ	0.44036	-0.41339	0.29185	-0.19424	0.0011
3 σ	0.51615	-0.42015	-0.03845	0.17697	11.15704
4 σ	-0.28490	0.29542	0.22010	-0.08618	3.14568
5 σ	0.21152	-0.19127	-0.09523	0.00946	0.05992
1 π	0.38249	-0.31630	0.16101	-0.06540	
Total	1.33558	-1.04425	0.56405	-0.23058	310.88837
A	-0.08795	0.12047	-0.26920	0.38158	310.96380
O	0.56899	-0.49676	0.35860	-0.26697	-0.07866
S	0.85446	-0.66805	0.47649	-0.34422	0.00323
Total	1.33550	-1.04434	0.56589	-0.22961	310.88837

$$BF \quad R_e = 2.391$$

	F_1	F_2	F_3	F_4	$\rho(A)$
1σ	0.34987	-0.29234	0.18482	-0.10938	0.00000
2σ	0.06150	-0.00506	0.04769	-0.09625	69.11742
3σ	0.39447	-0.32684	0.13040	+0.02964	0.21947
4σ	0.35270	-0.15907	0.01929	-0.02182	0.67691
5σ	-0.18222	+0.01157	0.04398	+0.00820	1.68180
1π	0.61048	-0.43635	0.20939	-0.08068	
Total	1.58680	-1.20809	0.63557	-0.27029	71.69560
A	-0.25374	0.28184	-0.19712	0.12180	71.76445
O	0.26491	-0.27852	0.12120	-0.02892	-0.07694
S	1.57568	-1.21222	0.70842	-0.34922	0.00808
Total	1.58685	-1.20888	0.63255	-0.25634	71.69560

	FB				
	F_1	F_2	F_3	F_4	$\rho(A)$
1 σ	0.05682	-0.01001	-0.00940	0.00000	425.64772
2 σ	0.35027	-0.29324	0.18685	-0.11299	0.00016
3 σ	0.27445	-0.31226	0.10625	0.05824	20.52984
4 σ	-0.14591	0.19225	-0.04787	-0.03855	1.16622
5 σ	0.15950	-0.06144	0.00868	-0.00827	0.18475
1 π	+0.18582	-0.16786	0.09492	-0.05007	
Total	0.88095	-0.65256	0.33943	-0.14194	447.52869
A	-0.03281	0.07660	-0.03452	0.05568	447.57233
O	0.34383	-0.34143	0.14298	-0.05092	- 0.04626
S	0.57010	-0.38769	0.22456	-0.14671	0.00263
Total	0.88112	-0.65252	0.33302	-0.14195	447.52869

BeO $R_e = 2.50$

	F_1	F_2	F_3	F_4	$\rho(A)$
1 σ	0.32006	-0.25101	0.14655	-0.08895	0.00000
2 σ	-0.11558	-0.01356	0.08221	-0.09305	34.17555
3 σ	0.32943	-0.20559	0.02567	0.09048	0.22840
4 σ	0.26946	-0.12171	0.00255	-0.03178	0.47621
1 π	0.48297	-0.27937	0.12552	-0.04461	0.0
Total	1.28634	-0.87124	0.38251	-0.16790	34.88016
A	-0.22250	0.24715	-0.18552	0.16048	35.01991
O	0.23840	-0.17473	0.01807	-0.06197	-0.14789
S	1.27068	-0.95459	0.55625	-0.27049	0.00815
Total	1.28658	-0.88217	0.38880	-0.17198	34.88016

OBe

	F_1	F_2	F_3	F_4	$\rho(A)$
1σ	0.51224	0.02473	-0.01340	-0.02373	296.74173
2σ	0.31906	-0.25100	0.14910	-0.09581	0.00103
3σ	0.20902	0.18512	-0.01043	0.10843	13.41578
4σ	-0.13046	0.11673	0.03296	-0.03699	0.64266
1π	0.19766	-0.12295	0.02602	-0.03235	0.0
Total	0.64651	-0.41761	0.18425	-0.08046	310.80120
A	-0.17525	0.02265	0.08932	-0.09124	310.85436
O	0.44170	-0.17465	-0.07070	0.13692	-0.05462
S	0.37976	-0.227115	0.16923	-0.12662	0.00146
Total	0.65121	-0.42315	0.18785	-0.08094	310.80120

$$\text{LiF } R_e = 2.8877$$

	F_1	F_2	F_3	F_4	$\rho(\text{A})$
1 σ	0.23985	-0.16602	0.08653	-0.04202	0.00000
2 σ	-0.04059	-0.01873	0.06420	-0.08247	13.57171
3 σ	0.23447	-0.13333	0.01960	0.04648	0.07327
4 σ	0.23923	-0.11492	0.01596	0.01748	0.13204
1 π	0.42008	-0.24815	0.10427	-0.03996	
Total	1.09304	-0.68115	0.29055	-0.10049	13.77702
A	-0.09192	0.08112	-0.05572	0.04334	13.81026
O	0.05522	-0.01414	-0.03441	0.04422	-0.03561
S	1.12974	-0.74815	0.38069	-0.18805	0.00237
Total	1.09304	-0.68117	0.29055	-0.10049	13.77702

	FLi				
	F ₁	F ₂	F ₃	F ₄	ρ (Å)
1σ	0.02184	0.00702	-0.1795	0.01584	425.84175
2σ	0.24048	-0.17161	0.09915	-0.05925	0.01905
3σ	0.07150	-0.04736	-0.00936	0.04725	21.45627
4σ	-0.04124	0.03484	-0.00243	-0.02176	0.09467
1π	0.07219	-0.05161	0.03040	-0.01423	
Total	0.36477	-0.22872	0.09981	-0.03215	447.41174
A	-0.00868	-0.00814	0.02815	-0.02443	447.44678
O	0.12820	-0.04732	-0.02704	0.04994	-0.03513
S	0.24530	-0.17350	0.09793	-0.05674	0.00010
Total	0.36482	-0.66117	0.09914	-0.03123	447.41174

APPENDIX 5

Errors in Force Constant Calculations

The Hartree-Fock wavefunction $\psi^{(0)}$ gives results for the expectation values of one-electron operators that are correct through first order. This is a consequence of no orbital correction functions from $\psi^{(1)}$, the first order correction to the function--"One-electron clusters" we refer to as orbital correction functions (see chapter 1). In second order these expectation values will be affected by products of the first-order 2-electron clusters $U_{ij}^{(1)}$ and by the interaction of the second-order orbital correction functions $U_i^{(2)}$ with the unperturbed orbitals. No other second order functions make any contributions. (254)

Let F be a symmetric sum of one-electron operators $F = \sum_i f_i$.
Then $\langle F \rangle = \langle \Psi | F | \Psi \rangle / \langle \Psi | \Psi \rangle$

Keeping only second-order terms:

$$\langle F \rangle = \langle \psi^0 | F | \psi^0 \rangle [1 - \langle \psi^{(1)} | \psi^{(1)} \rangle] + \langle \psi^{(1)} | F | \psi^{(1)} \rangle + 2 \sum_i \langle u_i^{(2)} | f_i | \phi_i \rangle \quad \text{A5.1}$$

where the ϕ_i 's are the Hartree-Fock orbitals, $U_i^{(2)}$ the second-order corrections to these. Using the Hellmann-Feynman theorem, then one can write the change in correlation energy as a function of R

$$\frac{\partial E_c}{\partial R} = \left\{ \langle \psi^{(1)} | \frac{\partial H}{\partial R} | \psi^{(1)} \rangle - \langle \psi^{(1)} | \psi^{(1)} \rangle \langle \psi^{(0)} | \frac{\partial H}{\partial R} | \psi^{(0)} \rangle \right\} + 2 \sum_i \langle u_i^{(2)} | \frac{\partial H}{\partial R} | \phi_i \rangle$$

A5.2

The $U_i^{(2)}$ are suspected to have the same sign as the ϕ_i in

regions close to the nucleus.⁽²⁵⁴⁾ This has a natural physical interpretation. The Hartree-Fock energy contains too large a contribution from electrostatic repulsion. The formalism which leads to $\psi^{(1)}$ will tend to minimize this excess repulsion energy by spreading the charge density farther out in space than it should be. After the introduction of the correlation clusters U_{ij} , this charge density should relax. It is the orbital correction functions which produce this relaxation through an interference term $2\sum_i \phi_i U_i^{(2)}$ in the expression for the charge density. As a pair of correlating electrons at a fixed relative separation moves toward the nucleus, then cluster corrections become smaller. As U_{ij} implies an electron density spread out further from the nucleus than that of $\psi^{(0)}$, only $U_i^{(2)}$ will affect densities appreciably near the nuclei. It would then seem that the $U_i^{(2)}$'s will be important in the determination of one-electron properties in general. The phase properties of the corrections have been computed by Sinanoglu and Tuan⁽⁴¹⁾ and appear to be in agreement with the above proposals.

In view of the same phases between the $U_i^{(2)}$ and ϕ_i , then from (A5.2), assuming $\langle \psi^{(0)} | \frac{\partial H}{\partial R} | \psi^{(0)} \rangle = 0$ at $R_e(\text{HF})$, and since $\langle \psi^{(1)} | \frac{\partial H}{\partial R} | \psi^{(1)} \rangle$ will depend mainly on $U_i^{(2)}$ as discussed above, it is evident that around $R_e(\text{HF})$, the change in "correlation" energy ($E_{\text{HF}} - E_0$) will have the same sign as the force. This reasoning also follows from physical interpretation. At distances less than R_e , in approaching the united atom there is an increase in correlation energy. At distances larger than R_e , there is increase in correlation energy as a result of the short-

comings of the HF method based on single determinants for large distances. From these considerations we conclude that d^2E_c/dR^2 will be positive. McLean⁽²⁵⁵⁾ has observed a minimum in E_c vs R curves for diatomic molecules. These minima occur near $R_e(\text{exptl.})$, at values of R less than $R_e(\text{exptl.})$ for H_2 and LiF . Thus his results concur with the above considerations.

$$\begin{aligned} \text{Let } R_0 &= R_e(\text{exptl.}) & E_0 &= E(\text{exptl.}) \\ R_H &= R_e(\text{Hartree-Fock}) & E_H &= E(\text{Hartree-Fock}) \\ k_n^O &= \frac{2}{n!} d^n E_0 / dR^n & k_n^{HF} &= \frac{2}{n!} d^n E_H / dR^n \end{aligned}$$

Using a series expansion about R_0 :

$$E_0(R) = E_0(R_0) + \sum_{n=1}^{\infty} k_n^O (R - R_0)^n = E_H(R) - \epsilon^2 E_2(R) + \dots \quad A5.3$$

where $\epsilon^2 E_2$ is the contribution to second order from correlation effects. Expanding E_H about R_0 , one has from A5.3:

$$\epsilon^2 E_2(R) = E_H(R_0) - E_0(R_0) + \sum_{n=1}^{\infty} [(k_n^{HF})_{R_0} - k_n^O] (R - R_0)^n \quad A5.4$$

or expanding about R_H , then

$$\epsilon^2 E_2(R) = E_H(R_H) - E_0(R_0) + \sum_{n=1}^{\infty} [(k_n^{HF})_{R_H} (R - R_H)^n - k_n^O (R - R_0)^n] \quad A5.5$$

Differentiating both sides n times, and evaluating derivatives at R_0 :

$$(\epsilon^2 E_2^n)_{R_0} = -k_n^O + (k_n^{HF})_{R_H} + (n+1) (k_{n+1}^{HF})_{R_H} (R_0 - R_H) + 0 [(R_0 - R_H)^2] \quad A5.6$$

$$\text{From A5.4} \quad (\epsilon^2 E_2^n)_{R_0} = (k_n^{HF})_{R_0} - k_n^O \quad A5.4a$$

$$\text{or} \quad (k_n^{HF})_{R_0} = (k_n^{HF})_{R_H} + (n+1) (k_{n+1}^{HF})_{R_H} (R_0 - R_H) + \dots \quad A5.7$$

This expression therefore relates derivatives of the HF energy

evaluated at R_0 and R_H . If the energy E_H is a true HF energy, then we can expect

$$(k_n^{HF})_{R_0} = k_n^0 + \epsilon^2 k_n^2 \quad A5.4b$$

where $\epsilon^2 k_n^2$ is a second order correction. ($k_n^2 = E_2^n$)

From A5.7, since $k_3^0 < 0$, $k_3^{HF} \sim k_3^0$, $R_0 > R_H$, then

$$(k_2^{HF})_{R_0} < (k_2^{HF})_{R_H}$$

We have the result that the Hartree-Fock constant evaluated at R_0 is less than that evaluated at R_H provided $R_0 > R_H$. We must now establish bounds on this relation. From A5.4a:

$$(k_2^{HF})_{R_0} = k_2^0 + \epsilon^2 (d^2 E_2 / dR^2)_{R_0}$$

Now $E_2 = E_c$ to second order (see above discussion). Thus $d^2 E_2 / dR^2$ must be positive as E_c has a minimum near R_0 . Thus we have

$$k_2^0 < (k_2^{HF})_{R_0} < (k_2^{HF})_{R_H}$$

We conclude that for $R_0 > R_H$, the force constant for a Hartree-Fock potential energy curve evaluated at $R_0 = R_e$ (exptl.) will be closer to the true value than if evaluated at $R_H = R_e$ (HF). Furthermore, from A5.4b, the error in the constant should be of order ϵ^2 , resulting in a force constant slightly larger than the experimental value.

Bibliography

1. P. A. M. Dirac, Proc. Cambridge Phil. Soc. 26, 376 (1930); 27, 240 (1931)
K. Husimi, Proc. Phys. Math. Soc. Japan 22, 264 (1940).
2. A. J. Coleman, Rev. Mod. Phys. 35, 668 (1963).
3. P. O. Löwdin, Phys. Rev. 97, 1474, 1490, 1509 (1955).
4. H. C. Longuet-Higgins, Proc. Roy. Soc. (London) A235, 537 (1956).
5. D. W. Smith, S. J. Fogel, J. Chem. Phys. 43, 91 (1965).
6. D. W. Smith, Phys. Rev. 147, 896 (1966).
7. B. H. Chirgwin, Phys. Rev. 107, 1013 (1957).
8. A. Messiah, Quantum Mechanics, vol. 1, page 336; John Wiley, New York (1961).
9. R. P. Feynman, Phys. Rev. 56, 340 (1939); H. Hellmann, Einführung in die Quantenchemie; Fran. Deuticke, Leipzig (1937) page 285ff.
10. F. J. Dyson, A. Lenard, J. Math. Phys. 8, 423 (1967).
11. C. A. Coulson, R. P. Bell, Trans. Faraday Soc. 41, 141 (1945).
12. T. Berlin, J. Chem. Phys. 19, 208 (1951).
13. K. Fajans, Chem. Engng. News 27, 900 (1949).
14. R. F. W. Bader, J. Amer. Chem. Soc. 86, 5070 (1964), R. F. W. Bader, W. H. Henneker, J. Am. Chem. Soc. 87, 3063 (1965), J. Am. Chem. Soc. 88, 280 (1966).
15. T. Kato, Commun. Pure Appl. Math. 10, 151 (1957); Perturbation Theory of Linear Operators, Springer Verlag, Berlin (1966).
16. W. B. Brown, Disc. Faraday Soc. 40, 151 (1965).
17. I. Levine, J. Chem. Phys. 41, 2044 (1964).
18. B. Kirtman, M. L. Benston, J. Chem. Phys. 46, 472 (1967).
19. J. Schaeffer, R. Yaris, J. Chem. Phys. 46, 949 (1967).
20. J. N. Silverman, G. H. Brigman, Rev. Mod. Phys. 39, 228 (1967).
21. K. Frankowski, C. L. Pekeris, Phys. Rev. 146, 46 (1966).
22. P. A. M. Dirac, Phys. Rev. 139B, 684 (1965).
23. M. J. Lighthill, Introduction to Fourier Analysis and Generalized Functions, Cambridge Press (1958); J. S. Langer, S. Vosko, J. Phys. Chem. Solids 12, 196 (1959).
24. W. A. Bingel, Z. Naturforsch., 18a, 1249 (1963).
25. P. Hohenberg, W. Kohn, Phys. Rev. 136B, 864 (1964).
26. N. H. March, Advanc. Phys. 6, 1 (1957).
27. J. Friedel, Phil. Mag. 43, 153 (1952).
28. H. Primas, Int. J. Quant. Chem. 1, 493 (1967).
29. M. Bunge, Rev. Mod. Phys. 39, 463 (1967).
30. V. Fock, Izvest. Nauk SSSR, Ser. Fiz. 18, 161 (1954).
T. L. Allen, H. Skull, J. Chem. Phys. 35, 1644 (1961); J. Phys. Chem. 66, 281 (1962).
31. V. L. Bronch-Bruevich, S. V. Tyablikov, The Green Function Method in Statistical Mechanics; North Holland, Amsterdam (1962).
32. F. Hund, Z. Physik. 40, 742; 42, 93 (1927).
R. S. Mulliken, Phys. Rev. 32, 186 (1928).
33. J. E. Lennard-Jones, Trans. Faraday Soc. 25, 668 (1929).
34. O. Sinanoglú, Proc. Roy. Soc. (London) A260, 379 (1961).
35. J. I. Musher, Rev. Mod. Phys. 39, 203 (1967).
36. W. Brenig, Nucl. Phys. 4, 363 (1957).
K. Kumar, Nucl. Phys. 21, 99 (1960).
37. W. Kutzelnigg, V. H. Smith, J. Chem. Phys. 41, 896 (1964).
38. E. Wigner, Math. u. Naturw. Anz. Unzar. Akad. Wiss. 53, 477 (1935).
R. A. Silverman, Phys. Rev. 85, 227 (1952).
P. W. Langhaff, J. D. Lyons, R. P. Hurst, Phys. Rev. 148, 18 (1966).

39. H. Preus, Fortschr. Physik 10, 271 (1962) .
40. H. Primas, Modern Quantum Chemistry, vol II, edit. O. Sinanoglu, Academic Press (1965) .
41. O. Sinanoglu, D. F. Tuan, J. Chem. Phys. 38, 1740 (1963) .
O. Sinanoglu, J. Chem. Phys. 36, 706 (1962) .
42. L. Brillouin, Actualités Sci. Ind. 159, (1934) .
43. C. Møller, M. S. Plesset, Phys. Rev. 46, 618 (1934) .
44. M. Cohen, A. Dalgarno, Proc. Phys. Soc. (London) 77, 748 (1961) .
45. G. G. Hall, Phil. Mag. 6, 249 (1961) .
J. Goodisman, W. Klemperer, J. Chem. Phys. 38, 172 (1963) .
46. William N. Lipscomb et al., J. Am. Chem. Soc. 88, 2353, 2361, 2384 (1966) .
47. C. C. J. Roothaan, Rev. Mod. Phys. 32, 186 (1961) .
48. E. Clementi, J. Chem. Phys. 36, 33 (1962) .
49. W. Moffitt, Rept. Progr. Phys. 17, 173 (1954) .
50. M. G. Evans, Proc. Roy. Soc. (London) A207, 1 (1951) .
51. R. K. Nesbet, J. Chem. Phys. 43S, 30 (1965) .
52. P. O. Löwdin, H. Shull, Phys. Rev. 101, 1730 (1956) .
53. C. F. Bender, E. R. Davidson, J. Phys. Chem. 70, 2675 (1966); J. Chem. Phys. 47, 360 (1967) .
54. E. R. Davidson, J. Chem. Phys. 39, 875 (1963) .
55. R. F. W. Bader, W. H. Henneker, P. E. Cade, J. Chem. Phys. 46, 3341 (1967) .
R. F. W. Bader, I. T. Keaveny, P. E. Cade, to be published in J. Chem. Phys. vol. 47, (1967) .
56. B. J. Ransil, J. J. Sinai, J. Chem. Phys. 46, 3341 (1967) .
57. J. Lennard-Jones, J. A. Pople, Phil. Mag. 43, 581 (1952) .
58. P. E. Cade, W. M. Huo, J. Chem. Phys. 47, 614 (1967) .
59. P. E. Cade, K. D. Sales, A. C. Wahl, J. Chem. Phys. 44, 1973 (1966) .
60. W. M. Huo, J. Chem. Phys. 43, 624 (1965) .
61. A. D. McLean, M. Yoshimine, IBM Journal of Research, November 1967 .
E. Clementi, Supplement to IBM Journal of Research and Development, 9, 2 (1965) .
62. C. H. Townes, Handbuch der Physik, vol 38/1, Springer Verlag, Berlin (1958) .
63. C. H. Townes, B. P. Dailey, J. Chem. Phys. 20, 35 (1952) .
64. D. G. Hornig, Svensk. Kem. Tidskr. 67, 379 (1955) .
65. R. M. Sternheimer, Phys. Rev. 80, 102 (1950); 84, 244 (1951) .
66. R. Bersohn, R. G. Shulman, J. Chem. Phys. 45, 2298 (1966) .
67. L. Salem, J. Chem. Phys. 38, 1227 (1963) .
68. C. A. Coulson, A. H. Nielson, Disc. Faraday Soc. 35, 71 (1963) .
69. S. Peyerimhoff, R. J. Buenker, L. C. Allen, J. Chem. Phys. 45, 734 (1966) .
70. J. C. Slater, J. Chem. Phys. 1, 687 (1933) .
71. E. Clementi, J. Chem. Phys. 46, 3842 (1967) .
72. J. R. Platt, Handbuch der Physik, vol. 37/2, Springer Verlag, Berlin (1961) .
73. R. T. Birge, Nature, February 27, (1926) .
74. I. Langmuir, J. Am. Chem. Soc. 42, 274 (1920) .
75. W. Heitler, G. Herzberg, Naturwissenschaften 17, 673 (1929) .
76. D. W. Robinson, J. Phys. Chem. 69, 3359 (1965) .
77. G. Herzberg, Spectra of Diatomic Molecules, D. Van Nostrand Inc., N.Y. (1950) .
78. R. S. Mulliken, Rev. Mod. Phys. 4, 1 (1932) .
79. G. Verhaegen, W. G. Richards, J. Chem. Phys. 45, 1829 (1966) .
80. M. Yoshimine, J. Chem. Phys. 40, 2970 (1964) .
81. J. Trischka, H. Salwen, J. Chem. Phys. 31, 218 (1959) .
J. Goodisman, J. Chem. Phys. 38, 2597 (1963) .
82. E. S. Rittner, J. Chem. Phys. 19, 1030 (1951) .
83. M. Kaufman, L. Wharton, W. Klemperer, J. Chem. Phys. 43, 943 (1965) .
84. C. A. Coulson, Valence, Oxford Press (1961) .

85. M. A. Nusimovici, J. L. Birman, *Phys. Rev.* 156, 925 (1967).
86. L. Pauling, *The Nature of the Chemical Bond*, Cornell University Press (1960).
87. K. Ruedenberg, *Rev. Mod. Phys.* 34, 326 (1962).
88. (a) M. Roux, M. Cornille, L. Burnelle, *J. Chem. Phys.* 37, 933 (1962).
(b) S. Bratosz, R. Daudel, M. Roux, M. Allavena, *Rev. Mod. Phys.* 32, 412 (1960).
89. J. L. J. Rosenfeld, *Acta. Chem. Scand.* 18, 1719 (1964).
90. P. Manning, *Proc. Roy. Soc. (London)* A230, 415 (1955).
91. R. S. Mulliken, *J. Chem. Phys.* 23, 1833, 1841, 2338 (1958).
92. Krishnaji, V. Prakash, *Rev. Mod. Phys.* 38, 690 (1966).
93. J. O. Hirschfelder, C. F. Curtiss, R. B. Bird, *Molecular Theory of Gases and Liquids*, John Wiley, N. Y. (1954).
94. N. F. Ramsey, I. Ozier, P. Yi, A. Khosla, *J. Chem. Phys.* 46, 1530 (L) (1967).
95. T. H. Spurling, E.A. Mason, *J. Chem. Phys.* 46, 323 (1967).
96. A. D. McLean, M. Yoshimine, *J. Chem. Phys.* 46, 3682 (L) (1967).
97. A. Ron, O. Schnepf, *J. Chem. Phys.* 46, 3991 (1967).
98. C. S. Barrett, L. Meyer, J. Wasserman, *J. Chem. Phys.* 47, 740 (1967).
99. I. H. Hillier, S. A. Rice, *J. Chem. Phys.* 46, 3881 (1967).
100. J. Krieg, H. Witte, E. Wolfel, *Z. Phys. Chem.* 4, 36 (1955).
101. J. Lahiri, A. Mukherji, *Proc. Phys. Soc. (London)* 87, 913 (1966).
102. P. R. Smith, J. W. Richardson, *J. Phys. Chem.* 69, 3346 (1965).
103. P. R. Smith, J. W. Richardson, *J. Phys. Chem.* 71, 924 (1967).
104. E. R. Davidson, *J. Chem. Phys.* 46, 3320 (1967).
105. R. F. W. Bader, H. J. T. Preston, *Can. J. Chem.* 44, 1131 (1966).
106. A. C. Hurley, *Proc. Roy. Soc. (London)* A226, 170, 197 (1954).
107. R. F. W. Bader, *Can. J. Chem.* 38, 2117 (1960).
108. S. T. Epstein, A. C. Hurley, R. W. Wyatt, R. G. Parr, *J. Chem. Phys.* 47, 1275, (1967).
109. E. F. Hayes, R. G. Parr, *J. Chem. Phys.* 43, 1831 (1965).
110. S. T. Epstein, *J. Chem. Phys.* 45, 384 (1966).
111. R. E. Stanton, *J. Chem. Phys.* 44, 2368 (1963).
112. A. C. Hurley, *J. Chem. Phys.* 37, 447 (1962).
113. J. O. Hirschfelder, C. A. Coulson, *J. Chem. Phys.* 36, 941 (1962).
114. M. Geller, A. A. Frost, P. G. Lykos, *J. Chem. Phys.* 36, 2693 (1962).
115. D. Ebbing, H. Skull, *J. Chem. Phys.* 28, 866 (1958).
116. H. C. Longuet-Higgins, D. A. Brown, *J. Inorg. Nucl. Chem.* 1, 60 (1955).
117. R. L. Miller, P. G. Lykos, *J. Chem. Phys.* 37, 993 (1962).
118. L. Salem, E. B. Wilson, Jr., *J. Chem. Phys.* 36, 3421 (1962).
119. R. M. Sternheimer, *Phys. Rev.* 96, 951 (1954).
120. R. E. Stanton, *J. Chem. Phys.* 36, 1298 (1962).
121. L. C. Allen, *Phys. Rev.* 118, 167 (1960).
122. R. Yaris, *J. Chem. Phys.* 39, 863 (1963).
123. C. A. Coulson, A. C. Hurley, *J. Chem. Phys.* 37, 448 (1962).
124. M. L. Benston, Thesis, University of Washington (1964).
125. A. L. Wasserman, *J. Chem. Phys.* 40, 1812 (1964).
126. P. O. Löwdin, *J. Mol. Spectry* 3, 46 (1957).
127. T. Koopmans, *Physica* 1, 104 (1933).
128. R. S. Mulliken, *Phys. Rev.* 56, 778 (1939).
129. D. Peters, *J. Chem. Phys.* 44, 3473 (1966).
130. R. S. Mulliken, *J. Chem. Phys.* 1, 492 (1933); *Phys. Rev.* 46, 549 (1934).
131. W. L. Clinton, W. C. Hamilton, *Rev. Mod. Phys.* 32, 422 (1960).
132. A. C. Hurley - in *Molecular Orbitals in Chemistry, Physics, and Biology*, P. O. Löwdin and B. Pullman, Eds., Academic Press, N. Y. (1964), page 161.

133. R. S. Mulliken, J. Phys. Chem. 56, 295 (1950).
134. R. S. Mulliken - in Quantum Theory of Atoms, Molecules and Solids, P. O. Löwdin Ed., Academic Press, N. Y. (1966) page 1.
135. R. S. Mulliken, J. Chem. Phys. 3, 564 (1935).
136. M. Kasha, Disc. Faraday Soc. 9, 14 (1950).
M. I. Al-Johoury, D. W. Turner, J. Chem. Soc. 5141 (1963), 616 (1965).
137. W. M. Huo, K. F. Freed, W. Klemperer, J. Chem. Phys. 46, 3557 (1967).
138. B. J. Ransil, Rev. Mod. Phys. 32, 239, 245 (1960).
139. H. Shull, J. Appl. Phys. Suppl. 33, 290 (1962).
140. H. Shull, J. Am Chem. Soc. 82, 1287 (1960).
141. W. Moffitt, Proc. Roy. Soc. (London) A196, 524 (1949).
142. C. W. Kern, M. Karplus, J. Chem. Phys. 40, 1374 (1964).
143. L. C. Allen, J. Chem. Phys. 34, 1156 (1961).
144. H. J. Kolker, M. Karplus, J. Chem. Phys. 36, 960 (1962).
145. T. P. Das, E. L. Hahn, Nuclear Quadrupole Resonance Spectroscopy, Academic Press, N. Y. (1958).
146. B. P. Dailey, Disc. Faraday Soc. 19, 255 (1955).
147. H. M. Foley, R. M. Sternheimer, D. Tycko, Phys. Rev. 93, 734 (1954).
148. J. Van Kranendonk, Physica 20, 781 (1954).
149. E. G. Wikner, W. E. Blumberg, E. L. Hahn, Phys. Rev. 118, 631 (1960).
150. T. P. Das, M. Karplus, J. Chem. Phys. 30, 848 (1959).
151. T. P. Das, M. Karplus, J. Chem. Phys. 42, 2885 (1965).
152. H. W. De Wijn, J. Chem. Phys. 44, 810 (1966).
153. B. S. Gourary, F. J. Adrian, Solid State Physics, vol. 10, Academic Press, N. Y. (1960) page 246.
154. R. M. Pitzer, C. W. Kern, W. N. Lipscomb, J. Chem. Phys. 37, 267 (1962).
155. E. G. Wikner, T. P. Das, Phys. Rev. 109, 360 (1958).
156. A. Dalgarno, Advanc. Phys. 11, 281 (1962).
157. T. P. Das, R. Bersohn, Phys. Rev. 102, 733 (1956).
158. A. J. Freeman, R. E. Watson, Treatise on Magnetism, edit. G. Rado, H. Shull; Academic Press, N. Y. (1965), vol. 11A, page 167.
159. R. M. Sternheimer, Phys. Rev. 146, 140 (1966).
160. V. M. Evdomikov, Opt. Spectry. 22, 287 (1967).
161. R. Braunstein, T. W. Trischka, Phys. Rev. 98, 1092 (1955).
162. J. C. Browne, F. A. Matsen, Phys. Rev. 135A, 1227 (1964).
163. S. E. Veazey, W. Gordy, Phys. Rev. 138A, 1303 (1965).
164. J. D. Lyons, P. W. Langhoff, R. P. Hurst, Phys. Rev. 151, 60 (1966).
165. R. L. Matcha, to be published in J. Chem. Phys.
166. R. M. Sternheimer, Phys. Rev. 115, 1198 (1959).
167. G. Burns, E. Wikner, Phys. Rev. 121, 155 (1961).
168. T. Taylor, T. P. Das, Phys. Rev. 133, A1327 (1964).
169. H. J. Zeiger, D. I. Bolef, Phys. Rev. 85, 788 (1952).
170. T. Tokichiro, J. Chem. Phys. 47, 109 (1967).
171. A. D. Buckingham, Trans. Faraday Soc. 58, 1277 (1962).
172. G. C. Benson, M. E. Van der Hoff, J. Chem. Phys. 22, 469 (1954).
173. K. Yoshida, T. Moriya, J. Phys. Soc. (Japan) 11, 33 (1956).

174. A. J. Freeman, R. E. Watson, *Phys. Rev.* 127, 2058 (1962).
175. W. Gordy, *Disc. Faraday Soc.* 19, 14 (1955).
176. W. J. Orville-Thomas, *Quart. Rev. (London)* 11, 162 (1957).
177. E. A. C. Lucken, *Physical Methods in Heterocyclic Chemistry*, ed. A. R. Katritzky, 2, 89 (1963).
178. N. F. Ramsey, *Molecular Beams*, Oxford Press, (1956).
179. R. Barnes, W. V. Smith, *Phys. Rev.* 93, 95 (1954).
180. R. M. Sternheimer, *Phys. Rev.* 95, 736 (1954).
181. E. H. Hygh, T. P. Das, *Phys. Rev.* 143, 453 (1966).
182. F. A. Cotton, C. B. Harris, *Proc. Natl. Acad. Sci.* 56, 12 (1966).
183. D. W. Davies, *Theory of Electric and Magnetic Properties of Molecules*, John Wiley and Sons, N. Y. (1966), page 193.
184. R. S. Mulliken, *J. Chimie Phys.* 46, 497 (1948).
185. J. W. Richardson, *J. Chem. Phys.* 35, 1836 (1961).
186. H. W. de Wijn, *J. Chem. Phys.* 45, 3318 (1966).
187. E. Clementi, H. Clementi, *J. Chem. Phys.* 36, 2824 (1962).
J. A. Pople, G. A. Segal, *J. Chem. Phys.* 43, 136 (1965).
188. W. Adam, A. Grimison, *Theoret. Chim. Acta* 7, 342 (1967).
189. E. Schempp, P. J. Bray, *J. Chem. Phys.* 46, 1190 (1967).
190. H. D. Cohen, C. C. J. Roothaan, *J. Chem. Phys.* 43, 534 (1965).
191. J. C. Polanyi, *J. Chem. Phys.* 31, 1338 (1959).
192. A. D. Liehr, *Z. Naturforschg.* 13a, 311 (1958).
W. E. Donath, *J. Chem. Phys.* 42, 118 (1965).
193. R. F. Borkman, R. G. Parr, to be published in *J. Chem. Phys.*
194. G. Herzberg, *Infrared and Raman Spectra*, D. Van Nostrand Co. (1945).
195. R. M. Badger, *J. Chem. Phys.* 2, 128 (1934); 3, 710 (1935).
196. D. R. Herschbach, V. W. Laurie, *J. Chem. Phys.* 35, 458 (1961).
H. S. Hohnston, *J. Am. Chem. Soc.* 86, 1643 (1964).
J. W. Linnett, *Quart. Rev. (London)*, 1, 73 (1947).
197. Y. P. Varshni, *Rev. Mod. Phys.* 29, 664 (1957).
G. R. Somayajulu, *J. Chem. Phys.* 34, 1449 (1960).
198. F. O. Ellison, *J. Chem. Phys.* 42, 369 (1965).
D. M. Bishop, M. Randic, *J. Chem. Phys.* 44, 2480 (1966).
199. C. H. Douglas Clark, *Trans. Faraday Soc.* 37, 299 (1941).
W. Clinton, *J. Chem. Phys.* 33, 1603 (1960).
P. Empedocles, *J. Chem. Phys.* 46, 4474 (1967).
200. J. Goodisman, *J. Chem. Phys.* 39, 2397 (1963).
201. W. Byers Brown, *Proc. Cambridge Phil. Soc.* 54, 251 (1958);
J. Chem. Phys. 37, 461 (1961).
J. N. Murrell, *J. Mol. Spectry.* 4, 446 (1960).
G. G. Hall, D. Rees, *Theoret. Chim. Acta* 1, 448 (1963).
202. J. R. Platt, *J. Chem. Phys.* 18, 932 (1950).
G. G. Hall, D. Rees, *Mol. Phys.* 5, 279 (1962).
T. F. Moran, L. Friedman, *J. Chem. Phys.* 40, 860 (1964).
203. L. Pauling, *Proc. Roy. Soc. (London)* A114, 181 (1927).
204. L. Salem, *Ann. de Phys.* 8, 169 (1963); ref. 67.
205. P. Phillipson, *J. Chem. Phys.* 39, 3010 (1963).
206. R. H. Schwendeman, *J. Chem. Phys.* 44, 556, 2115 (1966).
207. M. L. Benston, B. Kirtman, *J. Chem. Phys.* 44, 119, 126 (1966).
208. H. O. Pritchard, H. A. Skinner, *J. Chem. Soc.* 1951, 945.
209. M. Born, K. Huang, *Dynamical Theory of Crystal Lattices*, Oxford Press 1954, appendix 6.

210. T. Caves, M. Karplus, J. Chem. Phys. 45, 1670 (1966).
V. W. Weiss, W. H. Flygare, J. Chem. Phys. 45, 3475 (1966).
211. I. M. Mills, Mol. Phys. 1, 99, 107 (1958); 4, 57 (1961).
212. W. Byers Brown, E. Steiner, J. Chem. Phys. 37, 461 (1962).
213. J. D. Jackson, Classical Electrodynamics, John Wiley, N. Y. (1961).
214. W. G. Mc Dugle Jr., T. L. Brown, J. Am. Chem. Soc. 89, 3111 (1967).
215. R. F. W. Bader, Can. J. Chem. 42, 1822 (1964).
216. W. L. Clinton, J. Chem. Phys. 33, 633 (1960).
217. T. L. Brown, J. C. Puckett, J. Chem. Phys. 44, 2238 (1966).
218. R. F. W. Bader, Mol. Phys. 3, 137 (1960).
219. A. D. McLean, J. Chem. Phys. 40, 2775 (1964).
220. C. L. Beckel, J. Chem. Phys. 33, 1885 (1960).
221. J. Pliva, S. Toman, F. Jenc, J. Mol. Spectry. 16, 24 (1965).
222. S. Fraga, B. J. Ransil, J. Chem. Phys. 35, 669 (1961).
223. H. C. White, Phys. Rev. 112, 1092 (1958).
224. W. D. Jones, J. Mol. Spectry. 10, 131 (1963).
225. A. D. Liehr, Can. J. Phys. 35, 1123 (1957).
226. J. L. Magee, J. Chem. Phys. 8, 687 (1940).
S. Datz, R. W. Minturn, J. Chem. Phys. 41, 1153 (1964).
227. K. Machida, J. Overend, J. Chem. Phys. 46, 3512 (1967).
228. S. Bratosz, S. Besnainous, J. Chem. Phys. 34, 1142 (1961).
S. Forsen, Spectrochim. Acta 18, 595 (1962).
229. R. M. Wing, D. C. Crocker, Inorg. Chem. 6, 289 (1967).
230. R. T. Birge, Phys. Rev. 25, 240 (1925).
R. Mecke, Z. Physik 32, 823 (1925).
231. P. M. Morse, Phys. Rev. 34, 57 (1929).
232. J. C. Decius, J. Chem. Phys. 45, 1069 (1966).
233. L. Salem, M. Alexander, J. Chem. Phys. 39, 2994 (1963).
234. W. Klemperer, W. G. Norris, A. Bücher, J. Chem. Phys. 33, 1535 (1960).
235. M. P. Tosi, M. Doyama, Phys. Rev. 160, 716 (1967).
236. A. D. B. Woods, W. Cochran, B. N. Brockhouse, Phys. Rev. 119, 980 (1960).
237. B. G. Dick, A. W. Overhauser, Phys. Rev. 112, 91 (1958).
J. C. Slater, Quantum Theory of Molecules and Solids, vol. 3, McGraw-Hill, N. Y. (1967), page 221.
238. M. Tinkham, Group Theory and Quantum Mechanics, McGraw-Hill (1964), page 68.
239. B. Szigeti, Proc. Roy. Soc. (London), A204, 51 (1950).
240. M. Bouten, P. Van Leuwen, Physica 34, 461 (1967).
241. R. K. Nesbet, Proc. Roy. Soc. (London) A230, 312 (1955).
242. T. A. Kaplan, W. H. Kleiner, Phys. Rev. 156A, 1 (1967).
243. V. Fock, Z. Physik 61, 126 (1930).
244. J. C. Slater, Phys. Rev. 34, 1293 (1929).
245. W. M. Huo, J. Chem. Phys. 45, 1554 (1966).
246. W. A. Goddard, Phys. Rev. 157A, 81 (1967).
247. P. Franklin, Methods of Advanced Calculus, McGraw-Hill (1944), page 319.
248. A. C. Wahl, P. E. Cade, C. C. J. Roothaan, J. Chem. Phys. 41, 2578 (1964).

249. J. C. Slater, Quantum Theory of Atomic Structure, vol II, Appendix 20-2, McGraw-Hill (1960) .
250. M. P. Barnett, C. A. Coulson, Phil. Trans. Roy. Soc. (London) 243A, 221 (1951) .
251. E. W. Hobson, Theory of Spherical and Ellipsoidal Harmonics, Chelsea Publishing Co., N. Y. (1955) .
252. W. H. Henneker, Thesis, McMaster University, Hamilton (1968) .
253. M. Kotani, A. Amemiya, E. Ishiguro, T. Kumura, Table of Molecular Integrals, Maruzen Co, Tokyo (1955) .
254. R. E. Stanton, J. Chem. Phys. 42, 2353 (1965) .
255. A. D. McLean, J. Chem. Phys. 40, 243 (L) (1964) .
256. C. Møller, The Theory of Relativity, Oxford Press (1952), page 173 .
257. E. R. Fisher, M. McCarty, J. Chem. Phys. 45, 781 (1966) .